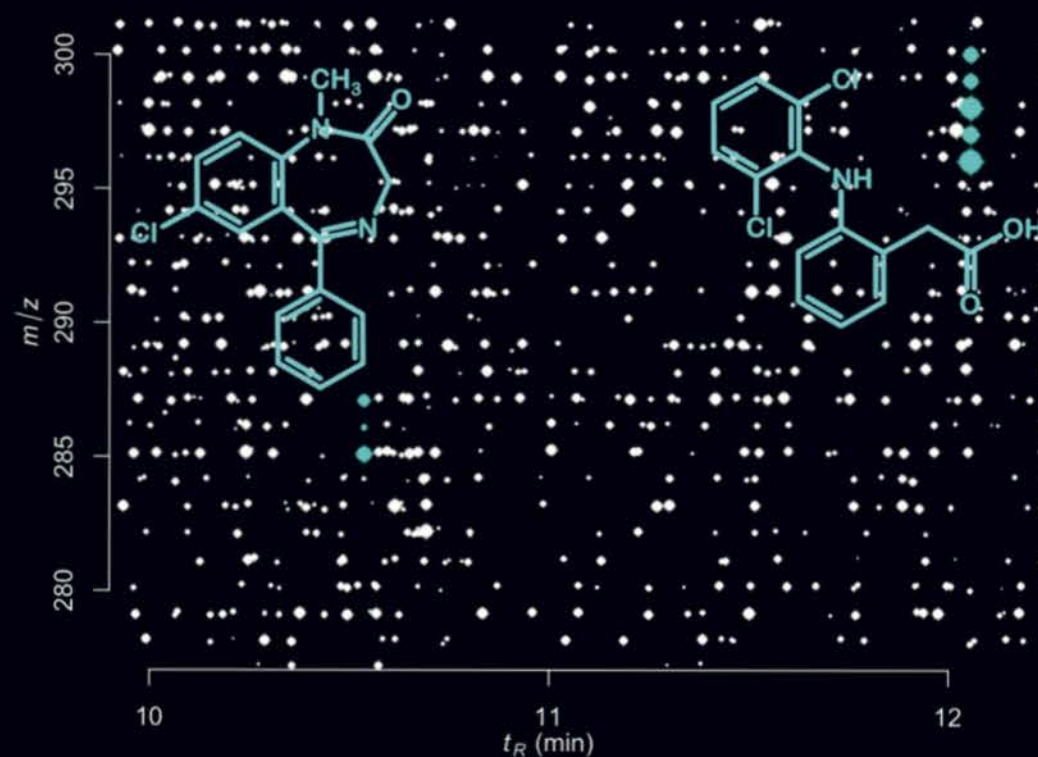


# Screening and Quantification of Pharmaceutical Residues in Aquatic Environments using High-Resolution Mass Spectrometry



LEENDERT VERGEYNST

Screening and Quantification of Pharmaceutical Residues in  
Aquatic Environments using High-Resolution Mass Spectrometry

Ir. Leendert Vergelynst

2014

ISBN 978-9-0598976-3-2



9

789059

897632



FACULTEIT BIO-INGENIEURSWETENSCHAPPEN



Promotor: Prof. dr. ir. Kristof Demeestere  
Research group EnVOC  
Department of Sustainable Organic Chemistry and Technology  
Faculty of Bioscience Engineering  
Ghent University

Dean: Prof. dr. ir. Guido Van Huylenbroeck

Rector: Prof. dr. Anne De Paepe

ir. Leendert Vergeynst

Screening and Quantification of  
Pharmaceutical Residues in  
Aquatic Environments using  
High-Resolution Mass Spectrometry

Thesis submitted in fulfillment of the requirements for the degree of  
Doctor (PhD) of Applied Biological Sciences: Environmental  
Technology



Dutch translation of the title: Screenen en kwantificeren van geneesmiddelenresidu's in water met hoge-resolutie massaspectrometrie

Cover: *Constellations of diazepam and diclofenac* by Leendert Vergeynst

Printed: University Press, [info@universitypress.be](mailto:info@universitypress.be)

Vergeynst Leendert, 2014, Screening and Quantification of Pharmaceutical Residues in Aquatic Environments using High-Resolution Mass Spectrometry

ISBN-number: 978-90-5989-763-2

The author and the promoters give the authorization to consult and to copy parts of this work for personal use only. Every other use is subject to the copyright laws. Permission to reproduce any material contained in this work should be obtained from the author.

*There is a crack in everything. That's how the light gets in.*

*Leonard Cohen*



# Woord vooraf

Heel wat *krakken* hebben dit werk verlicht, belicht en opgelicht.

Kristof, bedankt voor de diepgaande discussies die we samen voerden om steeds weer de kers op de taart te zetten. Naast een wetenschappelijke leidraad, was je een uitmuntend leraar. Ik heb geleerd dat wetenschap, naast toewijding en inventiviteit, ook een relevant kader en een doordachte afwerking vergt.

Onderzoeksgroep EnVOC, de beste collega's. Jullie wil ik bedanken voor alle momenten wanneer de student in ons zegevierde. Ik denk hierbij vooral aan de nieuwste olympische discipline *office ball vóór 16u30*, café Koepuur om 16u30, en de Overpoort tot 4u30.

Patrick en Lies, gouden medaille in marathon LC-MS injecties. Ik ben de tel kwijt geraakt, maar samen hebben jullie vast (een paar?) duizend analyses op de teller staan.

Maarten, Hanne, Sim, Ariane, Wieter en zoveel andere vrienden, 't is zalig om jullie erbij te hebben. Bedankt voor de leuke activiteiten, weekendjes en avontuurlijke reizen.

Leescomité Lidewei en Laura, de kans is klein dat jullie nu van mijn wetenschappelijk gewauwel verlost zijn. Graag wil ik jullie bedanken voor alle morele en literaire bijdragen aan dit werk.

De familie Vergeynstjes, vijf op één rij, en altijd paraat om een tandje bij te steken. Een kwarteeuw leren en proberen, dat vraagt heel wat boterhammen, verse groenten en fruit, en vooral veel liefde. Mama en papa, dank je wel voor al die kansen.

Laura, m'n lief, jij bent mijn belangrijkste ontdekking. Al moest ik daarvoor de wereld rond, langs de *King's Trail*, via de *Lofoten*, en met de boot (vliegtuig gemist) samen naar huis. 't Zal steeds opnieuw meer dan de moeite waard zijn.

Leendert, december 2014

# Table of Contents

<b>Abbreviation index</b>	<b>ix</b>
<b>Introduction</b>	<b>1</b>
<b>Research objectives</b>	<b>5</b>
<b>Acknowledgements</b>	<b>9</b>
<b>1 Pharmaceuticals as emerging micropollutants in the environment</b>	<b>11</b>
1.1 The complex biochemical characteristics of pharmaceuticals	13
1.2 Sources and pathways to the environment . . . . .	15
1.2.1 Human consumption . . . . .	17
1.2.2 Pharmaceutical manufacturing facilities . . . . .	18
1.2.3 Agricultural and veterinary applications . . . . .	18
1.2.4 Wastewater treatment plants . . . . .	19
1.3 Occurrence, fate and toxicity in the environment . . . . .	21
1.4 Drinking water and the risk for human health . . . . .	26
1.5 Conclusions . . . . .	28

<b>2</b>	<b>Liquid-chromatography - high-resolution mass spectrometry for multi-residue analysis of organic micropollutants in aquatic environments</b>	<b>31</b>
2.1	Introduction . . . . .	32
2.2	Basic principles of high-resolution mass spectrometry . .	34
2.2.1	Interpreting the mass spectrum and visualizing chromatograms in HRMS . . . . .	35
2.2.2	High-resolution mass analyzers . . . . .	38
2.2.3	Hybrid instruments . . . . .	41
2.3	General aspects of multi-residue HRMS analysis . . . . .	42
2.4	Selective and accurate mass measurement in HRMS . . .	48
2.4.1	Measuring mass in the presence of isobaric interferences . . . . .	48
2.4.2	Instrumental characteristics and mass calibration	51
2.5	Achievements in LC-HRMS screening . . . . .	55
2.5.1	Suspect versus non-target screening . . . . .	55
2.5.2	Identification refinement and confirmation . . . . .	64
2.5.3	Evaluation of the screening performance . . . . .	67
2.6	Quantitative aspects of LC-HRMS . . . . .	68
2.6.1	Quantification in the presence of isobaric interferences . . . . .	68
2.6.2	Analytical performance of validated LC-HRMS methods . . . . .	69
2.7	Tandem and high-resolution mass spectrometry . . . . .	73
2.8	Conclusions and future challenges . . . . .	76

<b>3</b>	<b>Quality assessment and quantification of pharmaceuticals in wastewater using solid-phase extraction - HPLC - magnetic sector mass spectrometry</b>	<b>79</b>
3.1	Introduction . . . . .	80
3.2	Experimental section . . . . .	82
3.2.1	Chemicals and materials . . . . .	82
3.2.2	Sampling and WWTP description . . . . .	82
3.2.3	Sample pretreatment and solid-phase extraction .	85
3.2.4	Instrumental analysis . . . . .	86
3.2.4.1	HPLC separation . . . . .	86
3.2.4.2	Selective ion detection . . . . .	87
3.2.4.3	Response normalization and instrumental validation . . . . .	89
3.2.4.4	Method validation and determination of the SPE recovery and matrix effects . .	92
3.2.5	First tier environmental risk assessment . . . . .	95
3.3	Results and discussion . . . . .	96
3.3.1	Method development and optimization . . . . .	96
3.3.1.1	Instrumental analysis . . . . .	96
3.3.1.2	Optimization of the solid-phase extraction procedure . . . . .	97
3.3.2	Method validation and quality assessment . . . . .	99
3.3.2.1	The process efficiency unravelled: extraction recovery and matrix effects .	99
3.3.2.2	Variability analysis . . . . .	109
3.3.3	Application in 2 WWTPs . . . . .	111



3.3.3.1	Concentrations and potential associated environmental risks . . . . .	111
3.3.3.2	Loads and elimination . . . . .	115
3.4	Conclusions . . . . .	117
<b>4</b>	<b>Accurate mass measurement, selective quantification and determination of detection limits</b>	<b>119</b>
4.1	Introduction . . . . .	120
4.2	Experimental section . . . . .	122
4.2.1	Chemicals . . . . .	122
4.2.2	Sampling and sample pretreatment . . . . .	122
4.2.3	Instrumentation . . . . .	123
4.2.4	Centroiding algorithms, accurate mass determination and measuring the full width at half maximum . . . . .	125
4.2.5	Software and statistical analyses . . . . .	128
4.3	Results and discussion . . . . .	129
4.3.1	Accurate mass determination . . . . .	129
4.3.2	Optimizing the mass window width . . . . .	132
4.3.2.1	Centroid or profile data and relative (ppm) or absolute (mDa) units for the construction of XICs? . . . . .	135
4.3.2.2	Sensitivity versus selectivity . . . . .	138
4.3.3	Calculation of the decision limit and detection capability . . . . .	142
4.4	Conclusions . . . . .	148

**5 Suspect screening and quantification of pharmaceuticals in drinking and surface water using large-volume injection - UHPLC - Time-Of-Flight mass spectrometry** 151

5.1 Introduction . . . . . 152

5.2 Experimental section . . . . . 153

    5.2.1 Chemicals . . . . . 153

    5.2.2 Sampling and sample pretreatment . . . . . 155

    5.2.3 Instrumental analysis . . . . . 155

    5.2.4 Development of the suspect screening methodology 157

        5.2.4.1 Investigation of the relation between the accurate mass error and the ion's signal intensity . . . . . 157

        5.2.4.2 Retention time and fragments for confirmation . . . . . 158

    5.2.5 Validation strategy for target quantification . . . 158

        5.2.5.1 Instrumental validation . . . . . 159

        5.2.5.2 Calibration and quantification . . . . . 160

        5.2.5.3 Method validation . . . . . 160

5.3 Results and discussion . . . . . 161

    5.3.1 Large-volume injection ultra-high performance liquid chromatography . . . . . 161

    5.3.2 Development of the signal intensity-dependent suspect screening model . . . . . 163

    5.3.3 Validation for target quantification . . . . . 166

        5.3.3.1 Instrumental validation . . . . . 166

        5.3.3.2 Method validation . . . . . 172

    5.3.4 Application in surface and drinking water . . . . 183

*Table of Contents*

5.3.4.1	Application of the suspect screening methodology . . . . .	183
5.3.4.2	Evaluation of the screening performance	187
5.3.4.3	Target quantification . . . . .	189
5.3.5	Evaluation of large-volume injection UHPLC and HRMS for rapid screening and quantification: pros and cons . . . . .	190
5.4	Conclusions . . . . .	193
<b>6</b>	<b>Balancing the false negative and positive rates for suspect screening in wastewater using solid-phase extraction and Orbitrap mass spectrometry</b>	<b>195</b>
6.1	Introduction . . . . .	196
6.2	Material and methods . . . . .	198
6.2.1	Chemicals . . . . .	198
6.2.2	Sampling, sample pretreatment and solid-phase extraction . . . . .	199
6.2.3	Instrumental analysis . . . . .	199
6.2.4	Suspect screening . . . . .	200
6.2.4.1	Suspect library . . . . .	200
6.2.4.2	Non-target peak picking . . . . .	202
6.2.4.3	Method development based on a training dataset . . . . .	204
6.2.4.4	Multivariate discrimination of noise and peaks . . . . .	205
6.2.4.5	Applied computational techniques . . .	208
6.3	Results and discussion . . . . .	208

6.3.1	Qualitative evaluation of the analytical method (set A) . . . . .	208
6.3.2	Development of the suspect screening . . . . .	209
6.3.2.1	Componentization: automated grouping of mono isotopic ions and their isotopes . . . . .	210
6.3.2.2	Multivariate hypothesis testing for a holistic screening approach . . . . .	212
6.3.2.3	Including a peak/noise filter in the holistic screening approach . . . . .	215
6.3.3	Evaluation of the suspect screening performance based on artificial suspects (set A) . . . . .	219
6.3.3.1	Screening limits of identification . . . . .	219
6.3.3.2	False positive versus false negative rate	221
6.3.3.3	Specificity of carbon and heteroatom isotopes . . . . .	223
6.3.4	Application of the suspect screening (set A + B)	226
6.4	Conclusions . . . . .	229
<b>7</b>	<b>General discussion, conclusions and perspectives</b>	<b>231</b>
7.1	Multi-residue analysis of pharmaceuticals in aquatic environments . . . . .	233
7.1.1	Sample collection and storage . . . . .	234
7.1.2	Sample pretreatment by solid-phase extraction versus large-volume injection . . . . .	236
7.1.3	Quantitative and qualitative analysis with full- spectrum HRMS . . . . .	240

*Table of Contents*

7.1.3.1	Selective quantification . . . . .	241
7.1.3.2	Qualitative analysis and suspect screening	242
7.1.4	Quantitative and qualitative validation of multi-residue methods . . . . .	247
7.1.4.1	Precise determination of the analytical process efficiency . . . . .	248
7.1.4.2	Determination of decision/detection limits	249
7.1.4.3	Response linearity . . . . .	250
7.1.4.4	Mass measurement uncertainty . . . . .	251
7.2	Occurrence of pharmaceuticals in wastewater and surface water . . . . .	253
7.3	Perspectives for screening-to-quantification of environmentally relevant contaminants . . . . .	255
	<b>Summary</b>	<b>261</b>
	<b>Samenvatting</b>	<b>267</b>
	<b>Addenda</b>	<b>273</b>
	<b>Bibliography</b>	<b>285</b>
	<b>Curriculum Vitae</b>	<b>323</b>

# Abbreviation index

a.u.	absolute units
AGC	automatic gain control
ANOVA	analysis of variance
APD	automated peak detection
API	atmospheric pressure ionization
CAS	conventional active sludge
$CC\alpha$	decision limit
$CC\alpha_{adjusted}$	adjusted decision limit
$CC\beta$	detection capability
CEC	cation exchange capacity
CWT	continuous wavelet transform
$D_{ow}$	octanol-water distribution coefficient
EC	environmental concentration
$EC_{50}$	half-maximal effect concentration

*Abbreviation index*

EDA	effect directed analysis
EDTA	ethylenediaminetetraacetic acid
ERA	environmental risk assessment
ESI	electrospray ionization
ESIV	equivalent sample injection volume
EU	European Union
FDR	false discovery rate
FNR	false negative rate
FPR	false positive rate
FWHM	full width at half maximum
GC	gas chromatography
HE	high collision energy
HPLC	high performance liquid chromatography
HRMS	high-resolution mass spectrometer
IDL	instrumental detection limit
IP	identification point
$K_{ow}$	octanol-water partition coefficient
LC	liquid chromatography
LE	low collision energy

LOEC	lowest observed effect concentration
LOI	limit of identification
LVI	large-volume injection
$m/z$	mass-to-charge
MBR	membrane bioreactor
MDL	method detection limit
ME	matrix effect
MEC	measured environmental concentration
MID	multiple ion detection
MQL	method quantification limit
MS	mass spectrometer
NMR	nuclear magnetic resonance
NPA	normalized peak area
PA	peak area
PE	process efficiency
PEG	polyethylene glycol
$pK_a$	acid dissociation constant
PNEC	predicted no-effect concentration
QqQ	triple quadrupole



*Abbreviation index*

QSPR	quantitative structure-property relationship
RE	recovery
RF	response factor
ROI	region of interest
RQ	risk quotient
RSD	relative standard deviation
S/N	signal-to-noise
SD	standard deviation
SIM	selected ion monitoring
SPE	solid-phase extraction
SSRE	sum of squares of the relative errors
TIC	total ion chromatogram
TOF	Time-of-Flight
TP	transformation product
$t_R$	retention time
UHPLC	ultra-high performance liquid chromatography
UQL	upper quantification limit
US EPA	United States Environmental Protection Agency
WWTP	wastewater treatment plant
XIC	extracted ion chromatogram

# Introduction

Where water is, life flourishes. Clean water is one of human's first needs and was natural for a very long time in history. However, technological revolutions have driven human population to the boundaries of sustainability (Rockström *et al.*, 2009). One of the consequences is water pollution with organic and inorganic compounds and, since the growing interest in organic chemistry in the 19<sup>th</sup> century, with persistent chemicals. Existing measures on the European level to prevent pollution of water resources with persistent chemicals focus on 45 priority substances, which are listed in the Water Framework Directive (2013/39/EU, European Union, 2013). These priority contaminants include polycyclic aromatic hydrocarbons, biocides, pesticides, flame retardants and metals. However, many other aquatic micropollutants emerge and receive increasing attention.

Two decades of advances in environmental analytical chemistry have resulted in the discovery of an increasing number of anthropogenic emerging organic contaminants such as pharmaceuticals, pesticides, sunscreen/ultraviolet filters, artificial sweeteners, brominated flame-retardants, perfluorinated compounds, benzotriazoles, benzothiazoles, plasticizers, surfactants and disinfection byproducts (Kümmerer,

2009a,b; Richardson, 2012; Richardson & Ternes, 2011, 2009, 2014). These contaminants are most probably not isolated cases; rather they are expected to be the tip of the iceberg. The awareness grows that even more unknown contaminants, such as transformation products, are dispersed in the aquatic environment (Hug *et al.*, 2014; Schymanski & Singer, 2014).

This continuous burden on the environment of bio-recalcitrant micropollutants being often poorly removed in wastewater treatment plants (WWTPs) and with an intrinsic ability to interfere with organisms concerns the scientific community. Although for most organic contaminants the environmental fate is not well understood and ecotoxicological knowledge is lacking, some contaminants have shown to cause (eco)toxic effects in aquatic organisms at very low environmentally relevant concentrations, namely microgram down to subnanogram per liter. For example, endocrine-disrupting effects have been related to estrogens, steroids, surfactants and phthalates (Thomas *et al.*, 2001; Weiss *et al.*, 2011; Metcalfe *et al.*, 2013). Behavioral changes and other toxic effects have been observed for psychiatric drugs and the anti-inflammatory drug diclofenac in fish (Hoeger *et al.*, 2005; Brodin *et al.*, 2013) and for antidepressants in marine snail (Fong & Molnar, 2013). Additionally, the presence of antibiotics has been related to an increased presence of resistance genes in bacteria in wastewater and the environment (Hoa *et al.*, 2011; Gao *et al.*, 2012; Rizzo *et al.*, 2013). These potential (eco)toxic effects can be a threat for the good ecological status of water bodies and for healthy drinking water.

The focus in this dissertation is on a special group of micropollutants, namely pharmaceuticals. At date, about 3000 pharmaceuticals are

produced and consumed to treat and prevent diseases (Richardson & Ternes, 2011) and paradoxically, these chemicals are now seen as emerging pollutants which might have toxic effects in our environment. The occurrence, fate and (eco)toxicity of pharmaceuticals in the environment is concisely overviewed in Chapter 1.

Analysis of trace concentrations of contaminants such as pharmaceutical residues is very challenging but prerequisite for studying and monitoring their environmental fate and occurrence. Therefore, the interest in methods for multi-residue analysis of this variety of micropollutants in all kinds of environmental samples is growing. Analysis typically involves different steps including sample collection, storage, pretreatment, separation and detection. Each of these steps must be adequately performed because various processes such as sorptive losses or instability of analytes can affect the results. Sample pretreatment often consists of extraction steps such as solid-phase extraction (SPE) or liquid-liquid extraction for enrichment and purification. The aim is to concentrate the compounds of interest in order to be able to detect trace concentrations in complex matrices. For the subsequent separation, both gas chromatography (GC) and liquid chromatography (LC) can be employed. Whereas GC is appropriate for apolar volatile compounds, LC is suited for more polar, less volatile and thermolabile compounds, such as pharmaceuticals and many other water contaminants. For the final compound detection, mass spectrometry (MS) is the preferred technique for selective and sensitive analysis. Each of the mentioned steps must be thoroughly optimized and evaluated, which is often challenging, especially in the

light of multi-residue analysis when chemically different compounds are of interest.

The state-of-the-art for target analysis of polar water contaminants, such as pharmaceuticals, is SPE followed by (ultra)-high performance liquid chromatography (UHPLC) and tandem mass spectrometry (MS/MS). As such, trace levels of analytes can be confirmed and quantified down to the subnanogram per liter level (Barceló & Petrović, 2007). Most of the current knowledge about micropollutants in the environment is based on this targeted technique, which enables to measure a predefined set of known target compounds. Many potential relevant, but unknown contaminants might thus be overlooked.

However, since the early 2000's, new and advanced high-resolution mass spectrometry (HRMS) technologies became a viable alternative. With these instruments, wide MS spectra are continuously acquired over the entire chromatogram allowing a quasi untargeted analysis, without the requirement to define a priori which specific compounds should be measured. The full-spectrum HRMS approach has therefore the potential to both identify and quantify a virtually unlimited number of analytes based on accurate mass measurement and offers the ability for screening towards new (un)known contaminants (Petrović *et al.*, 2006; Lommen *et al.*, 2007; Nielen *et al.*, 2007; Ibáñez *et al.*, 2009; Krauss *et al.*, 2010; Díaz *et al.*, 2011; Müller *et al.*, 2011; Hernández *et al.*, 2011; Chitescu *et al.*, 2012; Masiá *et al.*, 2013). The basic principles of HRMS and the achievements of full-spectrum HRMS for screening and quantification of emerging organic micropollutants in the aquatic environment are reviewed in Chapter 2.

# Research objectives

Developing HRMS-based analytical methodologies as steppingstones of an innovative screening-to-quantification workflow is the general aim throughout the experimental parts of this dissertation. Different techniques using double focussing magnetic sector, Time-of-Flight, and Orbitrap HRMS are applied and their applicability is investigated for the analysis of pharmaceuticals in drinking water, surface water and (biologically treated) wastewater.

The opportunity for untargeted analysis with full-spectrum HRMS is the trigger for this screening-to-quantification workflow. The final idea is to first screen the chromatograms for the presence of large lists of suspect contaminants, named suspect screening. This is possible because in HRMS wide mass spectra are acquired over the whole chromatogram. No analytical standards are a priori required for screening because analytes can be indicatively identified based on their accurately measured molecular mass. As such, analytical standards are only required to confirm the detected compounds. Subsequently, the

validation for target quantification can be focussed on the confirmed analytes.

To accomplish this general aim, the screening-to-quantification workflow must be inverted. First, an analytical method based on HRMS must be developed and a good performance of compounds having different chemical characteristics must be assured. Therefore, the method must be optimized and validated in a targeted quantitative approach for a predefined set of target pharmaceuticals. Second, screening techniques, which fit in the screening-to-quantification workflow, must be developed, implemented and evaluated for the developed full-spectrum HRMS method. The different research topics in this dissertation are visually connected in Figure 1.

The first specific goal, elaborated in Chapter 3, is to obtain a validated method for target analysis of 43 selected pharmaceuticals in (treated) wastewater based on state-of-the-art SPE as sample enrichment and purification technique. Therefore, high performance liquid chromatography (HPLC) coupled to a double-focussing magnetic sector HRMS operated in target mode is used for selective mass measurement. The quality of the quantitative measurement results is assessed in order to identify and eliminate source of quantification variability and the applicability range of SPE in multi-residue analysis is investigated.

As a second goal, in Chapters 4 and 5, a screening-to-quantification strategy is developed and validated for 69 pharmaceuticals in drinking water and surface water. The analytical method is based on large-volume injection (LVI) ultra-high performance liquid chromatography

(UHPLC) and full-spectrum Time-of-Flight (TOF) HRMS. In Chapter 4, the specific nature of full-spectrum HRMS is investigated to formulate guidelines for accurate mass measurement, selective quantification and validation of multi-residue analysis using full-spectrum HRMS. Subsequently, in Chapter 5, the suspect screening, taking into account the accurate mass of the mono isotopic ions of the suspect compounds, and quantitative validation results are presented. In addition, the use of LVI as replacement of the SPE step is investigated.

Third, in Chapter 6, the suspect screening concept presented in Chapter 5 is extended taking into account also the isotopic pattern in order to improve the identification success and reduce both the number of false negative and false positive findings. For this study, the SPE method presented in Chapter 3 was combined with a UHPLC and full-spectrum Orbitrap high-resolution mass spectrometer (HRMS) and applied for 77 pharmaceuticals in treated wastewater.

As proof of concept, the developed methods have been applied on different water matrices: drinking water and surface water (Chapter 5), and influent and effluent of WWTPs (Chapters 3 and 6). The screening and quantitative results revealed one of the first occurrence data and concentrations of pharmaceuticals in the Belgian aquatic environment and allowed to calculate removal efficiencies in WWTPs.

General conclusions and discussion about the outcomes of this work, guidelines and future research perspectives for the whole screening-to-quantification approach using HRMS are formulated in Chapter 7.



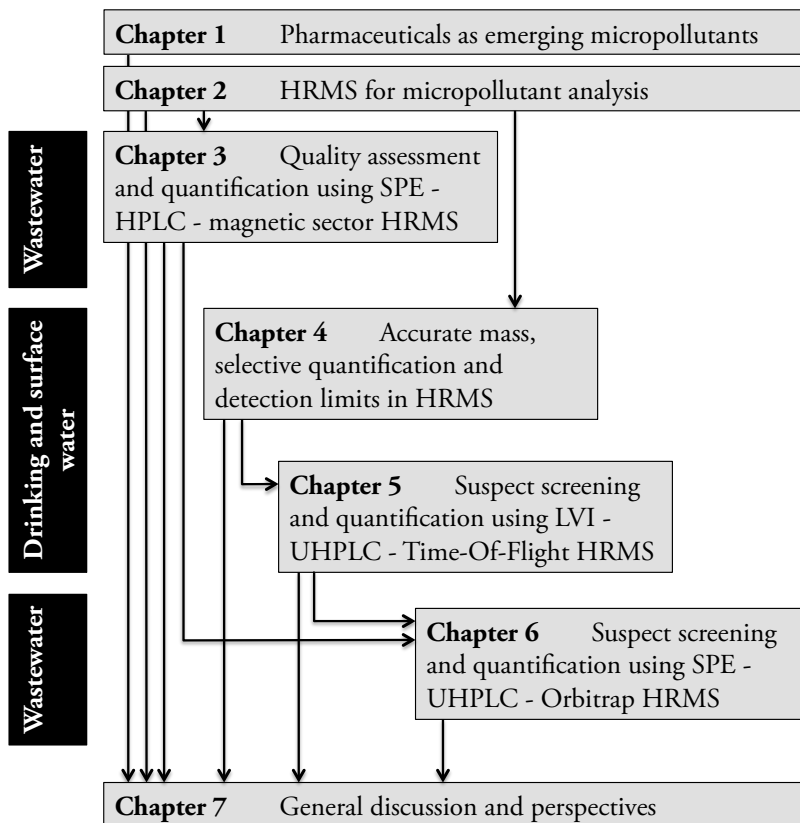


Figure 1 Schematic outline of the research topics in this dissertation.

# Acknowledgements

The authors acknowledge Pieter Joos, Els Van Meenen and Paul Ackermans from Water-Link, Antwerpse Waterwerken Walem, Belgium for their support; as well as Joris Roels and Marleen Peerean from Aquafin, Belgium, for their support during sample collection and for providing data on the WWTP characteristics.

We thank Waters for the use of the UPLC system and the Xevo G2 QTOF mass spectrometer, the Flemish Government for the mass spectrometry facilities (AmberLAB), and the financial support (AUGE/11/016) from the Hercules Foundation of the Flemish Government for the UHPLC-Q-Exactive mass spectrometry equipment. The computational resources (Stevin Supercomputer Infrastructure) and services used in this work were provided by the VSC (Flemish Supercomputer Center), funded by Ghent University, the Hercules Foundation, and the Flemish Government – department EWI. The Special Research Fund BOF 11/STA/027 of the Ghent University is acknowledged for their financial support.



# 1

## Pharmaceuticals as emerging micropollutants in the environment

Pharmaceuticals are a particular group of emerging micropollutants. They are mainly used for human and veterinary applications and to a smaller scale in agriculture. These chemicals are in most cases designed with the intention of performing a biological effect (Halling-Sørensen *et al.*, 1998). They must be able to pass biological membranes while at the same time be persistent in order to avoid inactivation before having a curing effect. Paradoxically, these properties are responsible for their potential toxic effects and bioaccumulation in aquatic and terrestrial ecosystems (Fent *et al.*, 2006).

Advances in analytical chemistry from 1980 to 2000 allowed observation

of pharmaceuticals in the  $\text{ngl}^{-1}$  to  $\mu\text{gl}^{-1}$  range in the aquatic environment (Halling-Sørensen *et al.*, 1998; Daughton & Ternes, 1999; Jørgenson & Halling-Sørensen, 2000; Heberer, 2002). This led to an increasing awareness of their potential effects over the past 15 years. Even though the study of pharmaceutical residues is a fairly new topic, a vast amount of research has already been published worldwide (e.g. Europe (Zuccato *et al.*, 2010; Morasch *et al.*, 2010; Gros *et al.*, 2012; Samaras *et al.*, 2013), America (Crouse *et al.*, 2012; Hedgespeth *et al.*, 2012), Australia (Watkinson *et al.*, 2009), Asia (Yiruhan *et al.*, 2010), Africa (K'oreje *et al.*, 2012)). Figure 1.1 illustrates the impressive increase of studies on the occurrence of pharmaceuticals in waste-, surface- and groundwater in the years 2000 to 2010.

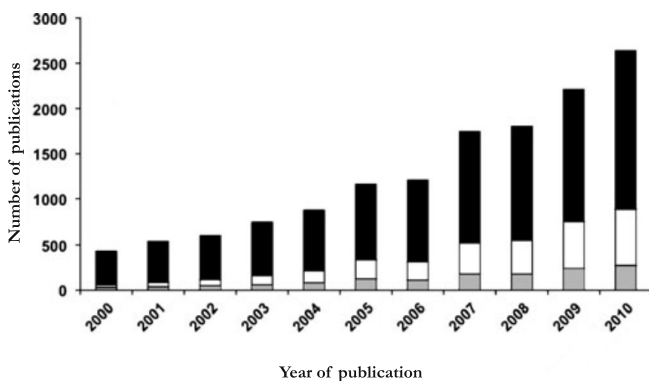


**Figure 1.1** The number of publications about the occurrence of pharmaceuticals in waste (white)-, surface (black)- and groundwater (gray) increased over the period of 2000 to 2010. Figure from Fatta-Kassinos *et al.* (2011).

In this introduction, the aim is to give a general overview of the current knowledge about the environmental occurrence, fate and

ecotoxicology of pharmaceuticals based on review articles published from 1998 to 2014.

## **1.1 The complex biochemical characteristics of pharmaceuticals**

Pharmaceuticals are special chemicals. They are designed for a specific action in the organism, are engineered with complex chemical structures, and their size, lipophilicity and charge must in first instance allow their permeation through biological membranes. Subsequently, they must concentrate in the target organs, persist until mode of action, and finally be removed from the body.

Most pharmaceuticals are relatively small molecules with a molecular weight between 200 and 1000 Da, allowing their fast permeation through biological membranes (Fatta-Kassinos *et al.*, 2011).

The lipophilicity of pharmaceuticals (and by extent chemicals) is the most used property to predict their partitioning in biological systems. Van der Waals' interactions, such as hydrogen bonding and London dispersion forces are the underlying intermolecular interactions (Fatta-Kassinos *et al.*, 2011). The octanol-water partition coefficient ( $K_{ow}$ ) is commonly used to describe the lipophilicity and indicates thus the tendency to partition into biological matrices (i.e. lipids). Pharmaceuticals have  $K_{ow}$  values in a broad range: iodated contrast media for example are typically very hydrophilic allowing their rapid removal from the body (e.g., iohexol,  $\log K_{ow} -3.1$ , Schriks *et al.*, 2010) whereas the antidepressant fluoxetine is a very lipophilic

pharmaceutical, which allows them to partition into fatty organs such as the nervous system ( $\log K_{ow}$  4.1, Minguez *et al.*, 2014).

Heteroatoms (N and S) and functional groups (e.g. carboxyl) in pharmaceuticals makes them ionizable. Dependent on the solution pH, they can be neutral, have (multiple) positive or negative charges, or be zwitterionic. The predominant speciation as a function of pH is described by acid dissociation constants ( $pK_a$ s). For example, the fluoroquinolone antibiotic ciprofloxacin has 4 ionizable moieties with 3.32, 5.59, 6.14 and 8.85 as  $pK_a$  values (Van Doorslaer *et al.*, 2014a). In antibiotics, these charges play a role in the transport through charged bacterial cell membranes.

Many pharmaceuticals are metabolized as the organism attempts to convert lipophilic compounds into more easily excreted polar residues. This bioconversion into one or more metabolites can occur throughout phase I (oxidation, reduction or hydrolysis) and phase II (conjugation) reactions (Santos *et al.*, 2010). However, often, only partial metabolism occurs and a large fraction of the active pharmaceutical can be excreted unaltered or only slightly transformed via urine and faeces (Heberer, 2002). Excretion factors of the unaltered pharmaceutical strongly differ depending on the compound from almost 0% (e.g. carbamazepine) to 100% (e.g. iohexol) (ter Laak *et al.*, 2010; Celle-Jeanton *et al.*, 2014).

Pharmaceuticals have thus a broad range of chemical characteristics from hydrophilic to lipophilic, can be neutral, cationic, anionic or zwitterionic, and undergo often only partial biotransformation. It is the combination of these characteristics that gives them their functionality, but at the same time, makes their environmental fate complex. For

example, the  $K_{ow}$  has also been used a lot in environmental science to describe the fate of pollutants (e.g. neutral industrial chemicals and pesticides): to predict sorption onto organic matter, sediment or soil, and to estimate bioconcentration factors for aquatic life (Fatta-Kassinos *et al.*, 2011). The hydrophilics tend to partition to aqueous phases whereas the lipophilics partition more into biota, organic matter and soil. In addition, pH, ionic strength, and cation exchange capacity (CEC) in soil, sediments or sludge can influence to a large extent the sorption capacity when electrostatic interactions play a role. As a result, on the one hand, charged chemicals become more hydrophilic as compared to their neutral form. On the other hand, charged moieties in pharmaceuticals can contribute to their partitioning behavior. Therefore, pH dependent  $K_{ow}$  values, labeled often as  $D_{ow}$ ,  $P_{ow}$ ,  $P_{app}$  or  $D$ , are considered to be more relevant for ionizable compounds. Their bio-recalcitrant nature makes pharmaceuticals and their metabolites persistent in the environment, and phase II metabolites may transform back to their parent compound, i.e. deconjugation (Celiz *et al.*, 2009).

## **1.2 Sources and pathways to the environment**

Pharmaceuticals are used in various life sciences and the origin of pharmaceutical pollution in the environment has been traced back to 3 main sources: human consumption, agricultural, veterinary and aquaculture applications, and pharmaceutical manufacturing facilities (Halling-Sørensen *et al.*, 1998; Jørgenson & Halling-Sørensen, 2000; Heberer, 2002; Kümmerer, 2009a; Santos *et al.*, 2010; Lapworth



*et al.*, 2012). Aquatic or solid waste streams of these sources can directly pollute the environment with pharmaceuticals or their related transformation products. However, often, intermediate barriers intended for purification or decontamination of these waste streams such as wastewater treatment plants (WWTPs) and leachate from landfill disposal are pathways to, in first instance, surface water. In addition, run-off and percolation from agricultural soils fertilized with WWTP sludge or with manure can be a very diffuse pathway to the environment. In second instance, surface water can percolate and contaminate groundwater. These sources and pathways are schematically connected in Figure 1.2.

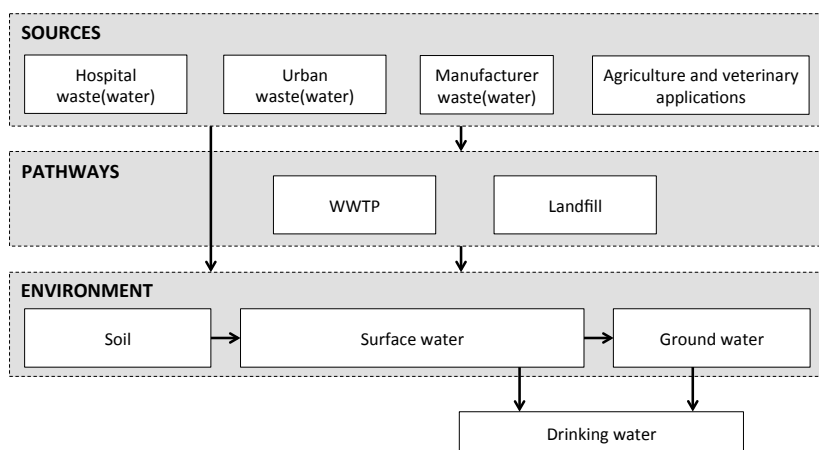


**Figure 1.2** Sources and pathways of pharmaceuticals to and in the environment.

### **1.2.1 Human consumption**

In terms of sources, human consumption has typically been divided into inpatient hospital care and outpatient ambulatory care. Via urine and faeces, pharmaceuticals and their residues end up in the wastewater. Higher total concentrations of pharmaceuticals are typically found in hospital wastewater than in urban wastewater. However, Le Corre *et al.* (2012) estimated that hospitals contributed to only 1 to 9 % of the total load of pharmaceuticals in combined hospital and urban wastewater, but among the different therapeutic groups, the contribution of hospital effluents entering the receiving WWTP varied in a wide range (Santos *et al.*, 2013). Anti-inflammatory drugs, analgesics and antibiotics are amongst the groups with highest loads coming from hospitals (> 50 %), whereas the load of antihypertensives, psychiatric drugs or lipid regulators could be mainly attributed to ambulatory care (> 90 %).

Next to consumed pharmaceuticals, overdue or excess pharmaceuticals are sometimes incorrectly disposed with the solid waste or flushed via toilet or sink (they should be returned to a pharmacy) and can end up in landfills or in wastewater. Only 4 % of the questioned households in a UK survey disposed unused drugs via sink or toilet (mainly liquid medicine), while 71 % of the households discard them with solid waste (Bound & Voulvoulis, 2005; Tong *et al.*, 2011). Reports also indicate incorrect disposal in pharmacies and in health care facilities (Tong *et al.*, 2011; Mankes & Silver, 2013).

## 1.2.2 Pharmaceutical manufacturing facilities

Wastewater of manufacturing facilities of pharmaceuticals have been identified as sometimes very concentrated sources of pharmaceutical pollution. Chinese, Taiwanese, Indian and Korean bulk drug producers seem to discharge the highest concentrations up to  $30 \text{ mg l}^{-1}$ . Extreme situations with average daily loads of 10 and 46 kg pharmaceuticals were measured in wastewater flows from Korean and Indian pharmaceutical producers, respectively (Sim *et al.*, 2010; Larsson *et al.*, 2007). However, also factories in the USA, Germany, Switzerland and Denmark have been traced back as polluters leading to concentrations up to the  $\mu\text{g l}^{-1}$  level in the environment (Cardoso *et al.*, 2014). Significant pollution from manufacturing facilities is thus not restricted to Asian countries, but also occurs in the Western world.

## 1.2.3 Agricultural and veterinary applications

Antibiotics are among the most widely administered pharmaceuticals for agricultural and veterinary applications (Sarmah *et al.*, 2006; Kümmerer, 2009a). In veterinary and aquaculture, antibiotics are used for prevention or therapy of infections, to improve feed efficiency, and, although forbidden in Europe, to promote the growth of animals. In addition, antibiotics such as streptomycins are used in bee-keeping and mixtures of streptomycins and oxytetracycline are used to control bacterial diseases in plants (Kümmerer, 2009a). Veterinary medicine, as in humans, are excreted via urine and faeces, which is mostly used as manure for agriculture (Heberer, 2002).

## 1.2.4 Wastewater treatment plants

Wastewater treatment plants (WWTPs) are often seen as a key pathway for pharmaceutical residues to the aquatic environment. Concentrations of pharmaceutical residues in WWTP influent range from the  $\text{ng l}^{-1}$  to almost  $\text{mg l}^{-1}$  level (Verlicchi *et al.*, 2012). For some pharmaceuticals with the highest concentrations in wastewater, the concentrations in WWTP effluent are reduced by a factor of about 10 (e.g. analgesic, anti-inflammatory and antibiotic drugs). However, for many pharmaceuticals (e.g.  $\beta$ -blockers, psychiatric drugs, lipid regulators, antihypertensives) the effluent concentrations for both conventional active sludge (CAS) and membrane bioreactor (MBR) systems are not reduced (Figure 1.3). For pharmaceuticals of all classes, removal efficiencies calculated from the data in Figure 1.3 ranged from almost complete removal ( $> 99.9\%$ ) to almost no removal (about  $0\%$ ). For some compounds, concentrations in the effluent were even higher than in the filtered influent, which might be explained by deconjugation or by desorption from solids entering the WWTP (and thus not measured in the influent water) (Verlicchi *et al.*, 2012).

In conventional WWTPs, sorption and biodegradation are two main removal pathways. Rather lipophilic or charged pharmaceuticals tend to sorb onto sludge in WWTPs and are as such at least partially removed via excess sludge. This sludge might be anaerobically digested, incinerated, landfilled or used as a fertilizer in agriculture (not in Belgium). For both sorption and biodegradation, removal ranging from 0 to almost 100% for pharmaceuticals of all classes has been calculated, and often this variable behavior is not well understood.

**A** Analgesics/anti-inflammatories **B** Antibiotics **C** Antidiabetics **D** Antifungal **E** Antihypertensives **F** Barbiturates  
**G** beta-blockers **H** Diuretics **I** Lipid regulators **J** Psychiatric drugs **K** Receptor antagonists **L** Hormones  
**M** beta agonists **N** Antineoplastics **O** Topical products **P** Antiseptics **Q** Contrast media

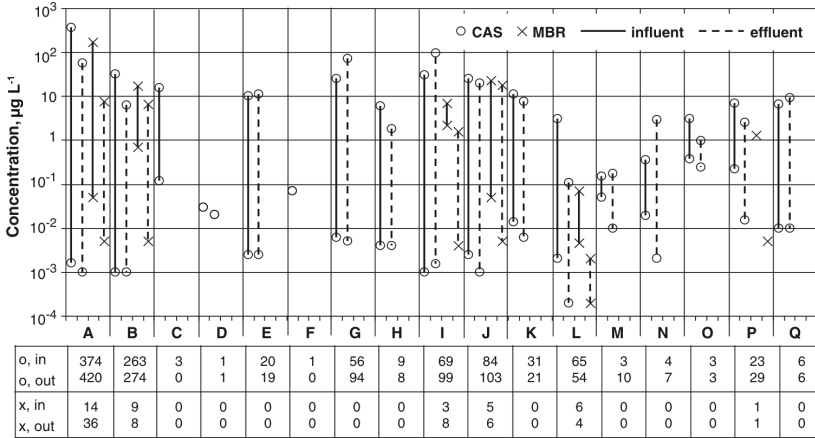


**Figure 1.3** Comparison between the concentration ranges for 17 classes of pharmaceuticals in the influent (solid lines) and effluent water (dashed lines) of CAS (○) and MBR (×) WWTPs. The table reports the number of collected data per class. Figure from Verlicchi *et al.* (2012).

Verlicchi *et al.* (2012) and Miège *et al.* (2008) concluded that the different chemical characteristics of pharmaceuticals and the variety in operational conditions of WWTPs, such as aerobic, anaerobic or anoxic reactors, sludge retention time, hydraulic retention time, pH and water temperature, might cause the variable fate of pharmaceuticals in WWTPs.

In addition, WWTPs are intended mainly for the removal of dissolved and suspended organic matter and the removal of nutrients such as nitrogen and phosphorus. Although pharmaceuticals are also organic chemicals, their concentrations might be too low for sufficient biodegradation or they can be too persistent and thus not biodegradable. More research is thus needed to upgrade existing

wastewater treatment technology and eventually implement advanced post-treatment technologies (Rivera-Utrilla *et al.*, 2013; Eggen *et al.*, 2014).

### **1.3 Occurrence, fate and toxicity in the environment**

A variety of pharmaceuticals from different therapeutical classes has been detected in the aquatic environment (Figure 1.4). An EU-wide survey by Loos *et al.* (2009) reported maximal concentrations ranging from about  $200 \text{ ng l}^{-1}$  up to  $30 \mu\text{g l}^{-1}$  for 9 selected pharmaceuticals in more than 100 rivers from 27 European countries (Table 1.1). Concentrations higher than  $100 \text{ ng l}^{-1}$  were measured in at least 10 % of the rivers for ibuprofen, carbamazepine, sulfamethoxazole and caffeine.

As in WWTPs, the fate of pharmaceuticals in the environment is complex. In rivers, they might sorb onto suspended solids or onto sediments (Figure 1.5), and undergo biotransformation and photolysis (Yamamoto *et al.*, 2009; Wang & Lin, 2014). River attenuation rates of pharmaceuticals showed a very wide range with half-life times from 1.6 to 34 h for 34 pharmaceuticals (Acuña *et al.*, 2014). These half-life times showed to be very variable with relative standard deviations  $> 50\%$  for 28 out of the 34 pharmaceuticals. Despite pharmaceuticals seem to be (slowly) removed in the environment, they remain ubiquitously present due to their continuous release, and are therefore often labeled as pseudo-persistent (Hernando *et al.*, 2006).

**Table 1.1** Maximum and 10% highest measured concentrations ( $\text{ng l}^{-1}$ ) in more than 100 European rivers (Loos *et al.*, 2009) and examples of pharmaceuticals for which RQs  $> 1$  have been reported for river waters in Europe.

Pharmaceutical	10 % high- est	maxi- mum	Ref. reporting RQs $> 1$
<i>Analgesic/anti-inflammatory drugs</i>			
Acetylsalicylic acid	-	-	Grung <i>et al.</i> (2008)
Diclofenac	43	247	Hernando <i>et al.</i> (2006)
Ibuprofen	220	31 323	Grung <i>et al.</i> (2008); Hernando <i>et al.</i> (2006); Vazquez-Roig <i>et al.</i> (2012)
Ketoprofen	17	239	Hernando <i>et al.</i> (2006)
Mefenamic acid	-	-	Jones <i>et al.</i> (2002)
Naproxen	47	2027	Hernando <i>et al.</i> (2006)
Paracetamol	-	-	Grung <i>et al.</i> (2008); Jones <i>et al.</i> (2002); Carlsson <i>et al.</i> (2006)
<i>Antibiotics</i>			
Amoxicillin	-	-	Jones <i>et al.</i> (2002)
Azithromycin	-	-	Valcárcel <i>et al.</i> (2011)
Ciprofloxacin	-	-	Vazquez-Roig <i>et al.</i> (2012); Ferrari <i>et al.</i> (2004); Grung <i>et al.</i> (2008)
Clarithromycin	-	-	Isidori <i>et al.</i> (2005); Valcárcel <i>et al.</i> (2011)
Lincomycin	-	-	Isidori <i>et al.</i> (2005)
Sulfamethoxazole	104	4072	Ferrari <i>et al.</i> (2004); Valcárcel <i>et al.</i> (2011)
Trimethopim	-	-	Valcárcel <i>et al.</i> (2011)
Ofloxacin	-	-	Vazquez-Roig <i>et al.</i> (2012); Ferrari <i>et al.</i> (2004); Grung <i>et al.</i> (2008)
Oxytetracycline	-	-	Jones <i>et al.</i> (2002)
<i>Anti-epileptic</i>			
Carbamazepine	308	11 561	Ferrari <i>et al.</i> (2004); Hernando <i>et al.</i> (2006)
<i><math>\beta</math>-blocker</i>			
Propranolol	-	-	Ferrari <i>et al.</i> (2004)
<i>Fibrate</i>			
Bezafibrate	56	1235	
Gemfibrozil	17	970	
<i>Hormones</i>			
17 $\beta$ -estradiol	$<5$	$<5$	Carlsson <i>et al.</i> (2006)
Estriol	-	-	Carlsson <i>et al.</i> (2006)
17 $\alpha$ -ethinylestradiol	$<5$	$<5$	Carlsson <i>et al.</i> (2006)
<i>Stimulant</i>			
Caffeine	542	39 813	Valcárcel <i>et al.</i> (2011)

- Not measured by Loos *et al.* (2009).

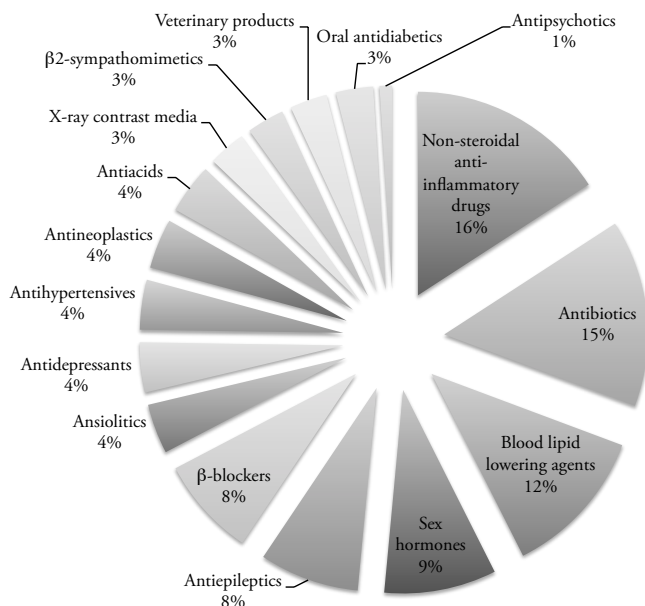


**Figure 1.4** Therapeutic classes detected in the environment, expressed in relative percentage. Data collected from 134 articles published between 1997 and 2009. Figure from Santos *et al.* (2010).

Pharmaceuticals are developed to permeate biological membranes and can thus also bioconcentrate in aquatic life. Measured concentrations in animals and in plants range from the low  $\text{ng g}^{-1}$  to about  $100 \text{ ng g}^{-1}$  depending on the species and environmental concentrations (Zenker *et al.*, 2014; Van Doorslaer *et al.*, 2014a). For example, Wille *et al.* (2011b) reported concentration of 1-11  $\text{ng/g}$  for carbamazepine, 30-63  $\text{ng/g}$  for propranolol and 14-288  $\text{ng/g}$  for salicylic acid in mollusks in the Belgian marine environment.

Although observed concentrations in the environment are for most of the pharmaceuticals below the acute toxicity lowest observed effect



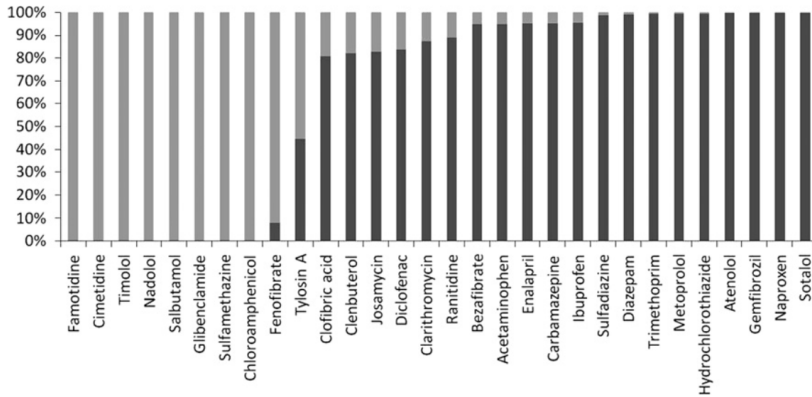


**Figure 1.5** In river water, pharmaceuticals can be completely sorbed onto suspended solids (gray), partitioned between the water phase (black) and suspended solids or remain completely in the water phase. Figure from Silva *et al.* (2011).

concentrations (LOECs), concentration levels in wastewater-influenced surface waters approaching chronic toxicity LOECs have been observed recently for some specific pharmaceuticals such as carbamazepine, clofibric acid, diclofenac, fluoxetine, propranolol, salicylic acid and oxazepam (Richardson & Ternes, 2011; Brodin *et al.*, 2013). Ecological risk assessment (ERA) has been used as a tool to evaluate the risk associated to the potential effects of pollutants in the environment. In environmental risk assessment (ERA), measured or predicted environmental concentrations (ECs) are compared to predicted no-effect concentrations (PNECs), which are derived from ecotoxicity data and corrected by a uncertainty factors to extrapolate experimental data on a limited number of species to the actual environment (European Medicine Agency, 2005). A risk quotient (RQ), calculated as  $\frac{EC}{PNEC}$ , exceeding 1 indicates that there is a risk and that more research is

required to better evaluate the effects on the ecosystem. RQs > 1 have been reported for pharmaceuticals from several therapeutic classes such as analgesic/anti-inflammatory drugs, antibiotics, anti-epileptics,  $\beta$ -blockers, hormones and stimulants (Table 1.1).

An interesting and thorough ecotoxicological risk evaluation has been conducted by Segura *et al.* (2009) who evaluated the ecological significance of the presence of the antibiotics sulfamethoxazole (sulfonamide) and ofloxacin (fluoroquinolone) in the environment. Therefore, they combined literature occurrence data (measured concentrations) with ecotoxicological data from different species (Figure 1.6). They observed that < 1% of LOEC values and < 0.1% of half-maximal effect concentration ( $EC_{50}$ ) values were lower than the highest 10% of the concentrations of sulfamethoxazole and ofloxacin in the aquatic environment. Thus, the ecotoxicological significance of the occurrence of sulfamethoxazole and ofloxacin in environmental waters is low, however, cannot be neglected. According to the authors, even a weak overlap between environmental concentration values and ecotoxicological data could have detrimental effects on the most sensitive species such as bacteria or algae. Because antibiotics are constantly being released into surface waters, microbiota are constantly exposed to these compounds. In addition, harmful effects can be more important in small streams affected by urban or agricultural discharges, because of their reduced dilution capacity. Given that large populations of bacteria are being exposed to a selective pressure of antibiotics, environmental waters and especially wastewaters, having even higher concentrations, become ideal settings for the assembly and exchange of mobile genes

encoding for resistance in bacteria (O'Brien, 2002; Kümmerer, 2009b). Such evaluations of the ecological significance of micropollutants based on the current available data should be performed more frequently and would help to direct future research towards the most relevant toxicants.

The environmental impact of mixtures of pharmaceuticals (and eventually other micropollutants) in the environment is less clear. However, it has been demonstrated that a mixture of paracetamol, carbamazepine, gemfibrozil and venlafaxine in the low  $\mu\text{g l}^{-1}$  range had a significant impact on fish-embryo development in the short term (Galus *et al.*, 2013). The chronic impact of drugs (i.e., ecological and evolutionary), either individually or as mixtures, remains unknown (Petrie *et al.*, 2013).

## 1.4 Drinking water and the risk for human health

Surface and groundwaters are used for drinking water production (Figure 1.2) and pharmaceuticals have been measured in finished drinking water at concentrations from the low  $\text{ng l}^{-1}$  to about  $100 \text{ng l}^{-1}$  (Stackelberg *et al.*, 2004; Benotti *et al.*, 2009; Valcárcel *et al.*, 2011; Padhye *et al.*, 2014). These concentrations are very low and from human risk assessment no immediate risk could be concluded (Schwab *et al.*, 2005; de Jongh *et al.*, 2012). However, according to Touraud *et al.* (2011), no consensus among the scientific community exists on what risk pharmaceuticals and endocrine disruptors pose to human health. For example, the antibiotic sulfamethoxazole in a mixture

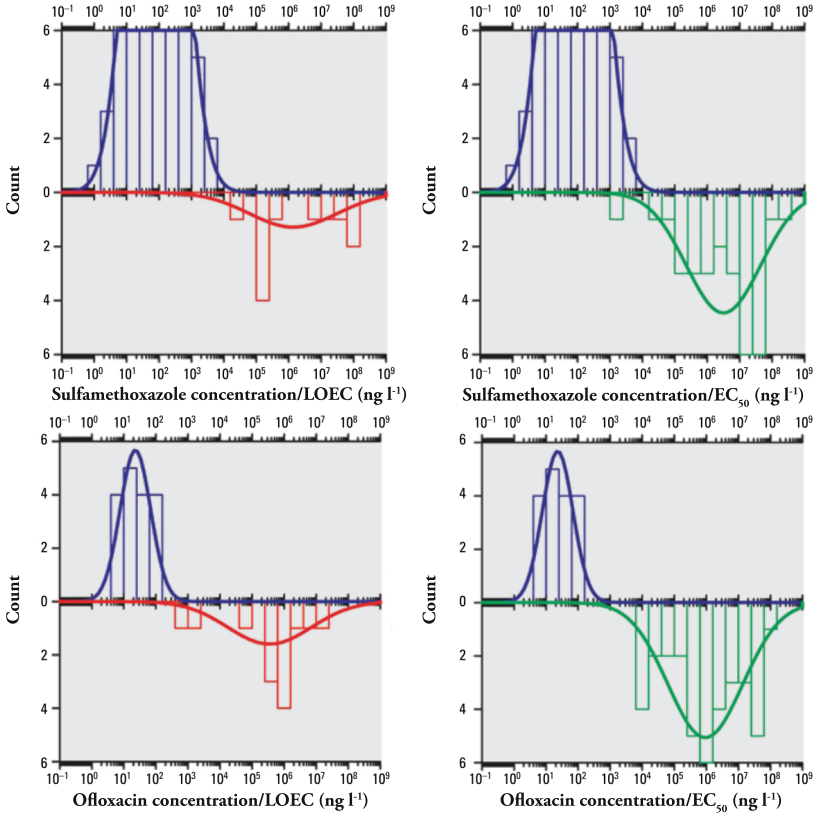


**Figure 1.6** Density histogram (blue bars) and density function (blue line) of sulfamethoxazole and ofloxacin concentration in surface waters compared with density histogram and density function of LOEC (left panels, red) and EC<sub>50</sub> (right panels, green) values for several aquatic species. Figure from Segura *et al.* (2009).

with 12 other pharmaceuticals could potentially inhibit the growth of human embryonic kidney cells at  $\text{ng l}^{-1}$  level (Pal *et al.*, 2014). In addition, iodated contrast media have been identified in drinking water as one of the precursors for the formation of highly genotoxic and cytotoxic iodo-trihalomethanes and iodo-acids, being disinfection byproducts of chlorination and chloramination (Duirk *et al.*, 2011). There are indications that low levels of micropollutants in drinking water could be a threat for human health. More research is thus required.

## 1.5 Conclusions

Pharmaceutical residues from human and veterinary applications are continuously released in the environment with WWTPs as major pathway. The highest concentrations (up to  $\mu\text{g l}^{-1}$  and even  $\text{mg l}^{-1}$ ) are measured in wastewater and treated wastewater; lower concentrations (up to about  $10 \mu\text{g l}^{-1}$ ) are observed in surface waters, and the lowest concentrations are measured in ground and drinking water (up to  $100 \text{ng l}^{-1}$ ). In all these environments, their fate and removal is very variable and not well understood. The diversity in chemical characteristics of pharmaceuticals seems to explain at least partially their complex environmental fate. Over the past 15 years, it has been realized that pharmaceuticals are ubiquitously present in the aquatic environment and the awareness of their potential ecotoxic and human health effects has grown. In addition, there are indications that the toxicity of mixtures is underestimated and that antibiotics in the

environment might induce the selection of resistance to antibiotics in bacteria.

Also the European Union (EU) and United States Environmental Protection Agency (US EPA) recognized the worrisome occurrence, fate and (eco)toxicity of pharmaceutical residues. The US EPA included the antibiotic erythromycin and 9 hormones, including 17 $\alpha$ -ethinylestradiol, in the Candidate Contaminant List 3 (CCL3, United States Environmental Protection Agency, 2009) and the EU has recently updated the Water Framework Directive with a Watch List for micropollutants including the analgesic diclofenac and the hormones 17 $\beta$ -estradiol and 17 $\alpha$ -ethinylestradiol (Water Framework Directive 2013/39/EU, European Union, 2013).

To assure a good chemical status of water, increasing efforts should go to measuring as prerequisite for studying the occurrence, fate and risks of these organic micropollutants passing between wastewater, surface water, groundwater and drinking water. Therefore, developing innovative analytical methods is the aim in this research.



# 2

## Liquid-chromatography - high-resolution mass spectrometry for multi-residue analysis of organic micropollutants in aquatic environments

*Redrafted from:*

*L. Vergeynst, H. Van Langenhove & K. Demeestere. Trends in liquid chromatography - high-resolution mass spectrometry for multi-residue analysis of organic micropollutants in aquatic environments. Submitted to Trends in Analytical Chemistry.*



## 2.1 Introduction

In the demanding targeted multi-residue analysis of organic micropollutants in water, tandem mass spectrometry (MS/MS) coupled to (ultra) high performance liquid chromatography (UHPLC) has shown its merits and is the most used technique nowadays. However, new analytical opportunities rose with the development of modern Time-Of-Flight (TOF) and Orbitrap high-resolution mass spectrometry (HRMS) providing ultimate sensitivity and identification capabilities over the full-spectrum in an untargeted analysis. A variety of multi-residue LC-HRMS methods have been developed over the last decade for the analysis of organic contaminants in environmental waters such as drinking water, groundwater, surface water including seawater and fresh water, and (biologically treated) wastewater. The majority of these methods were developed for the analysis of pharmaceuticals (Petrović *et al.*, 2006; Gómez *et al.*, 2007; Farré *et al.*, 2008; Lavén *et al.*, 2009; Gómez *et al.*, 2010; Nurmi & Pellinen, 2011; Wille *et al.*, 2011a; Cahill *et al.*, 2012; Ferrer & Thurman, 2012; Martín *et al.*, 2012; Wode *et al.*, 2012; Diaz *et al.*, 2013), pesticides (Ferrer & Thurman, 2007; Gómez *et al.*, 2010; Nurmi & Pellinen, 2011; Wille *et al.*, 2011a; Cahill *et al.*, 2012; Wode *et al.*, 2012; Diaz *et al.*, 2013), drugs of abuse (González-Mariño *et al.*, 2012; Martínez Bueno *et al.*, 2012; Bijlsma *et al.*, 2013; Fedorova *et al.*, 2013), and their known degradation products. The interest to analyze these classes of anthropogenic micropollutants using full-spectrum HRMS might be related to the large number of substances and degradation products (e.g. only a fraction of the more than 3000 pharmaceuticals have been investigated in environmental studies so

far (Richardson & Ternes, 2011)), which are continuously released to the environment originating from a variety of anthropogenic activities (Lapworth *et al.*, 2012) (e.g. industrial and domestic wastewater, landfills, agriculture, aquaculture, livestock breeding). Other classes of targeted micropollutants are endocrine-disrupting substances (Wang *et al.*, 2012), benzothiazoles and benzotriazoles (van Leerdam *et al.*, 2009), surfactants (Lara-Martín *et al.*, 2011), sweeteners (Ferrer & Thurman, 2010) and flame-retardants (Wode *et al.*, 2012).

This critical review covers the achievements in HRMS for qualitative and quantitative full-spectrum analysis of emerging organic micropollutants in the aquatic environment over the period of 2003 to the first half of 2014. It is investigated how and what kinds of information can be ultimately obtained from complex full-spectrum HRMS chromatograms. Five key topics are postulated and used as steppingstones to give a better insight in the specific nature and state-of-the-art of HRMS and to formulate challenges for future research. In Sections 2.2 and 2.3, basic principles of HRMS and analytical aspects related to sample pretreatment and liquid-chromatography are discussed, respectively. These aspects must reflect the multi-residue concept of HRMS, which means that a broad variety of analytes with different chemical characteristics must perform well throughout the whole analysis. Insights in the nature of HRMS and the related mass measurement selectivity and mass accuracy are reviewed in Section 2.4. Building on the unique ability of HRMS to identify analytes from the measured accurate mass, the newest trend in HRMS is screening towards suspect or unknown contaminants. This enhanced the identification

of emerging organic contaminants in the aquatic environment. The achievements of these screening studies are overviewed in Section 2.5 and opportunities for screening towards relevant contaminants from an environmental point of view are formulated. In Section 2.6, quantitative aspects of HRMS and the relationship between resolving power and quantitative selectivity are reviewed. Section 2.7 discusses the performance of current HRMS with the state-of-the-art MS/MS as a benchmark.

For this review, a total of 27 validated HRMS methods from 22 publications aiming quantitative target analysis of emerging pollutants in environmental waters were found in open literature (Table 2.1). These validated methods provided sufficient data, including several validation parameters such as linearity, instrumental and method detection limits, recoveries and matrix effects for a thorough discussion in Sections 2.3 and 2.6. In order to overview the recent trends in screening (Section 2.5), a total of 14 multi-residue screening techniques using HRMS (mainly in the aquatic environment) were found in open literature (Tables 2.2 and 2.3). Sections 2.4 and 2.7 are based on literature data on HRMS mainly from environmental science but also from other related disciplines such as food analysis.

## **2.2 Basic principles of high-resolution mass spectrometry**

Mass spectrometry is the last step in an analytical sequence and is typically preceded by a chromatographic separation, such as liquid

chromatography (LC), of the compounds of interest. The basic principle of mass spectrometry (MS) is to generate ions from these compounds by a suitable ionization method, to separate these ions by their mass-to-charge ( $m/z$ ) ratio, and to detect them qualitatively and quantitatively by their respective  $m/z$  and abundance (Gross, 2011). As such, a mass spectrum is acquired at each datapoint of the chromatogram.

For LC-MS coupling and the ionization of nonvolatile compounds, electrospray ionization (ESI) is the most prominent atmospheric pressure ionization (API) technique (Gross, 2011). ESI leads to the formation of, in most cases, protonated  $[M+H]^+$  or deprotonated  $[M-H]^-$  ions with a single positive or negative charge, respectively. In that case, the measured  $m/z$  values are equivalent to the exact molecular mass plus or minus the mass of a proton.

### **2.2.1 Interpreting the mass spectrum and visualizing chromatograms in HRMS**

In full-spectrum HRMS, wide mass spectra providing high mass resolving power are acquired over the whole chromatogram. Two neighboring mass peaks are assumed to be sufficiently separated when the valley separating their maxima has decreased to 10% of their intensity. Hence, this is known as the 10% valley definition of resolving power,  $R_{10\%} = \frac{m/z}{\Delta m/z}$  (Figure 2.1). The 10% valley conditions are fulfilled if the peak width at 5% relative height equals the mass difference of the corresponding ions, because then the 5% contribution of each peak adds up to 10% (Gross, 2011). However, the definition in terms of the full width at half maximum (FWHM), with  $R_{FWHM} =$

$\frac{m/z}{FWHM}$ , became widespread especially for TOF and Orbitrap MS. With Gaussian peak shapes, the ratio of  $R_{FWHM}$  to  $R_{10\%}$  is 1.8. For near-baseline separation of two adjacent masses, ions should thus differ by at least twice the FWHM in mass (Xia *et al.*, 2011). Consequently, increasing the resolving power is a key factor in HRMS allowing better differentiation of ions of interest from background ions and endogenous compounds (i.e. mass measurement selectivity). As a result, researchers have deployed instruments providing increasing resolving power from 5000 FWHM with the first TOF MS (Petrović *et al.*, 2006) up to 140 000 FWHM with the newest Orbitrap MS (Moschet *et al.*, 2013).

The importance of sufficient mass resolution is that accurate and precise  $m/z$  measurements become possible, as such allowing improved identification capabilities as compared to low-resolution MS. The term accurate mass refers to the measured mass of an analyte and is the value which corresponds to the center of a mass peak. The process to find the center of a mass peak requires a centroiding algorithm, which convert raw profile spectra to centroid spectra by attributing an accurate mass to the mass peaks. As such, spectrum peaks are replaced by sticks. For proper accurate mass measurement, the mass error, which is the absolute (Equation 2.1a, in mDa) or relative (Equation 2.1b, in ppm) difference between the measured accurate mass and the calculated exact

mass of an analyte, should be as low as reasonably possible and mass errors  $< 5$  ppm are often within the acceptable range.

$$\text{absolute mass error} = (m/z_{\text{experimental}} - m/z_{\text{exact}}) \cdot 10^3 \text{ mDa} \quad (2.1a)$$

$$\text{relative mass error} = \frac{m/z_{\text{experimental}} - m/z_{\text{exact}}}{m/z_{\text{exact}}} \cdot 10^6 \text{ ppm} \quad (2.1b)$$

Mass measurement uncertainty in terms of mass accuracy (i.e. average mass error) and mass precision (i.e. standard deviation on the mass error) is based on calculating the mass error of analytes (Brenton & Godfrey, 2010). Both, mass accuracy and precision are essential for proper accurate mass measurements and pinpointing different causes of mass measurement uncertainty can lead to improvement (Section 2.4).

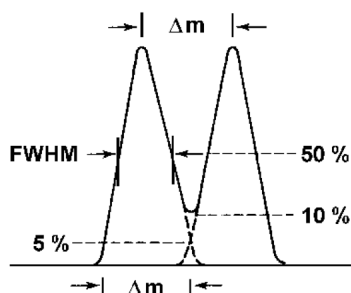


**Figure 2.1** The 10% valley and FWHM definitions of resolution. Figure from Gross (2011).

To visualize chromatograms from HRMS data, either a total ion chromatogram (TIC) or extracted ion chromatograms (XICs) can be plotted. A TIC is constructed by summation of all the measured peak intensities in the mass spectrum as a function of retention time and gives a general impression of the acquired chromatogram. Plotting the signals

observed in a narrow mass range (i.e. mass window width) around the exact mass of the ions of interest results in a more useful XIC. In full-spectrum HRMS an untargeted analysis is performed, which means that neither the mass nor retention time of the compounds of interest is a priori required to perform the analysis. However, for the quantification of the compounds, a targeted data processing procedure is followed by constructing a XIC around the exact mass at the experimentally (with analytical standards) determined retention time. XICs allow selective identification, peak integration and quantification of compounds of known  $m/z$  from the complex LC-HRMS data, which is further discussed in Section 2.6.

## 2.2.2 High-resolution mass analyzers

The first MS used a single magnetic sector to separate ions at unit resolution (Gross, 2011). Later, the introduction of double-focusing sector instruments, with in addition an electrostatic sector, allowed improved resolving power and mass accuracy. In recent years, there has been a strong tendency to substitute sector instruments by Time-of-Flight (TOF) or Orbitrap instruments (Gross, 2011).

In double-focussing sector instruments, deflection of a continuous ion beam, generated during ionization and subsequently accelerated in an electric field, is the basic principle for mass separation. In the magnetic sector, masses are separated by momentum due to Lorentz force. The magnetic field strength is set as such that only a target mass follows the central trajectory of the magnet. In the electrostatic sector, the aim is a reduction of the kinetic energy distribution of the ions. The combination

of a magnetic sector and an electric sector is able to focus ions onto a single point (i.e. the ion-multiplier detector), although these ions had (slightly) different directions and (slightly) different kinetic energies at the ion source (Figure 2.2). This process is called double focusing and can improve the resolving power of a magnetic sector instrument more than ten times (Gross, 2011).

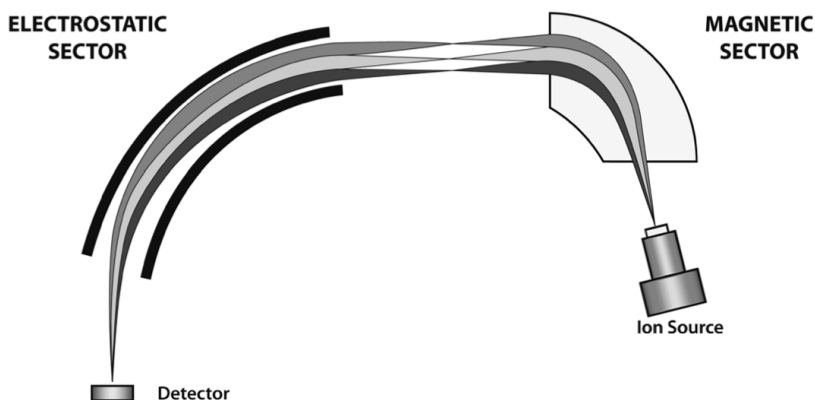


**Figure 2.2** The operating principles of a double focusing sector mass analyzer. Figure reproduced from Hart-Smith & Blanksby (2012).

In TOF instruments, ions are accelerated in an electric field and injected into a flight tube (Figure 2.3). Provided all the ions start their journey at the same time or at least within a sufficiently short time interval and with the same kinetic energy, the lighter (with higher velocity) ions will arrive earlier at the detector than the heavier ions (with lower velocity). The  $m/z$  of the detected ions is calculated from their flight time. In TOF MS, the ions should emerge from a pulsed ion source which is realized by pulsing ion packages orthogonally out of a continuous beam generated by the ionization source (Gross, 2011).



TOF mass analyzers can employ an ion mirror and they operate by sending ions toward this electrostatic mirror, which reflects the ions toward a detector. In addition to compensating for differences in ion kinetic energies, the use of an ion mirror has the additional advantage of increasing the total flight distance without having to significantly increase the size of the mass spectrometer. These improvements have led to increased mass resolving power (Hart-Smith & Blanksby, 2012).

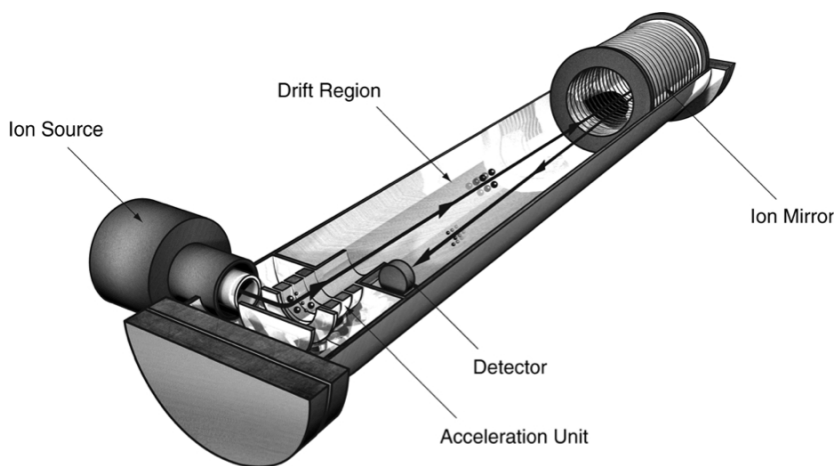


**Figure 2.3** An illustration of the basic components of an orthogonal acceleration TOF mass analyzer with ion mirror. Figure from Hart-Smith & Blanksby (2012).

In Orbitrap MS, ions generated by an ionization source are first accumulated and stored in a bent quadrupole, called C-trap. When sufficient ions are trapped, they are injected in the actual orbitrap. There, ions are moving in spirals around a spindle-like-shaped central electrode that creates an axial field gradient (Figure 2.4). The electrostatic attraction towards the central electrode is compensated by a centrifugal force that arises from the tangential velocity of ions. An

outer electrode is split in half by an insulating ceramic ring. The axially moving ions induce a current which is detected via a differential amplifier between the two halves of the outer orbitrap electrode. The  $m/z$  of different ions in the orbitrap can be determined from their respective frequencies of oscillation after a Fourier transform (Gross, 2011).

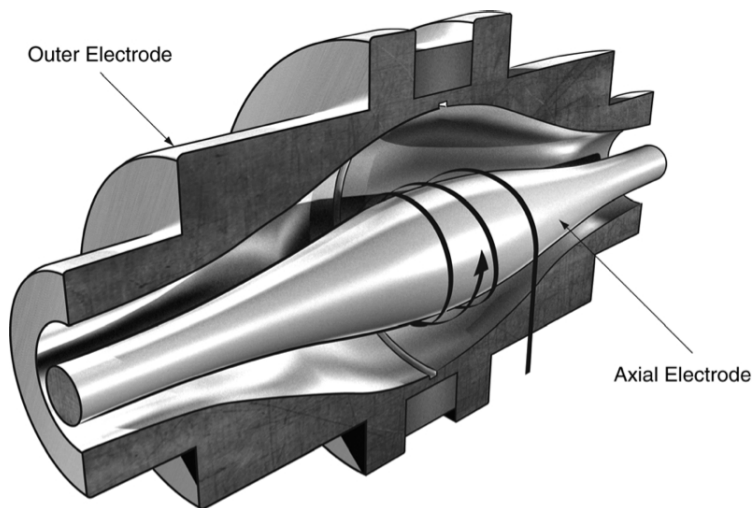


**Figure 2.4** An illustration of the basic components of an Orbitrap mass analyzer. The black arrow represents an illustrative ion path. Figure from Hart-Smith & Blanksby (2012).

### 2.2.3 Hybrid instruments

MS instrumentation may be constructed by combining different types of mass analyzers and ion-guiding devices in a single so-called hybrid instrument (Gross, 2011). The driving force to do so is the desire to obtain mass spectrometers that unite the advantageous properties of different mass analyzers. For example, HRMS can be preceded by a quadrupole, which allows to preselect a target ion mass at unit resolution

for further fragmentation. Subsequent analysis of the product ions in the HRMS analyzer allows accurate mass measurement of fragment ions. As such, in addition to full-spectrum MS, MS/HRMS and all ion fragmentation/HRMS are possible measurement modes. In MS/HRMS, a target ion is selected, fragmented and subsequently analyzed with the HRMS, whereas in all ion fragmentation/HRMS all ions generated by the ionizations source are fragmented and analyzed with the HRMS.

## 2.3 General aspects of multi-residue HRMS analysis

An important aspect of full-spectrum HRMS is that it allows the simultaneous measurement of a variety of analytes over a broad  $m/z$  range. However, the whole analytical procedure, starting from sampling, over sample storage, sample pretreatment, until the LC-HRMS analysis, must reflect the multi-residue concept. A variety of substances having very different physical-chemical characteristics must perform well throughout the whole analytical procedure.

Among the 27 validated HRMS methods in Table 2.1, solid-phase extraction (SPE) was amended in 25 methods (including 4 methods applying online-SPE) as sample preconcentration and purification technique. One author used a polydimethylsiloxane passive sampling device (Wille *et al.*, 2011a) in seawater. Although most authors aimed to develop sample enrichment techniques such as SPE for a broad range of substances, some compounds are still preconcentrated selectively and achieving acceptable recoveries for all compounds is challenging in multi-

residue applications (Busetti *et al.*, 2012). For examples, recoveries lower than 20% were reported by different authors (e.g., Lavén *et al.*, 2009; Nurmi & Pellinen, 2011). Therefore, different SPE cartridge materials for sorption based on hydrophilic/lipophilic interactions and ion exchange have been combined to achieve sufficient enrichment for a broader range of compounds (Kern *et al.*, 2009). As an alternative, Martínez Bueno *et al.* (2012) applied almost no sample pretreatment and a direct large-volume injection (LVI) of 100 µl of surface water onto the LC column was performed thereby omitting selective preconcentration.

For reversed phase separation, both HPLC and UHPLC have been coupled to TOF or Orbitrap HRMS. In most of the cases water with methanol/acetonitrile as organic modifier and formic/acetic acid or their ammonium buffers as acidifiers were used (2 authors used ammonium buffers as basic additives (Martínez Bueno *et al.*, 2012; Nurmi & Pellinen, 2011)) for ESI in positive ion mode (Table 2.1). For ESI negative ion mode, the same solvents were applied and in one case small amounts (0.05% (v/v), Nurmi & Pellinen, 2011) of acetic acid was added. Although UHPLC separation has been amended in about half of the studies in order to provide a high chromatographic resolution, HPLC is still widely applied and can be preferential when multiple MS modes are alternated (e.g. full-spectrum MS, MS/HRMS and all ion fragmentation/HRMS) in order to provide sufficient data points across the chromatographic peak.

Finally, also the interface, which is ESI for all the reviewed HRMS methods listed in Tables 2.1, 2.2 and 2.3, must be compatible. In particular for screening, Moschet *et al.* (2013) and Hug *et al.* (2014)

verified whether the analytes are amendable for the used ionization technique in order to improve the screening performance. They concluded that it is not fully understood which compounds are ionizable in ESI positive or negative ion mode and highlighted the need for general quantitative structure-property relationship (QSPR) approaches to predict ionization behaviour or ionization efficiencies for chemically different compounds.

**Table 2.1** Analytical characteristics of 27 validated LC-HRMS methods for target analysis of organic micropollutants in environmental waters.

Target substances	Matrix and applied volumes	Sample pretreatment	Recovery (%) <sup>a</sup>	LC (inj. vol. in µl), HRMS instrument, ionization mode, resolving power	Mass window width for XICs <sup>b</sup>	Linear range <sup>c</sup>	Reference
29 pharmaceuticals	500 ml river water, 100 ml WWTP influent and 200 ml effluent water	filtration, SPE (Oasis HLB), 1 ml extract	n.a.	UHPLC (10), QTOF (Waters Micro TOF), ESI <sup>+</sup> &-	20 mDa (centroid)	500 000	Petrović <i>et al.</i>
20 pharmaceuticals	100 ml hospital wastewater	filtration, SPE (Oasis HLB), 1 ml extract	n.a.	HPLC (20), TOF (Agilent 1100 series TOF), ESI <sup>+</sup> , 9500 FWHM at 922 Da	10 mDa (centroid)	100	Gómez <i>et al.</i> (2007) <sup>e</sup>
101 pesticides and degradation products	100 ml surface water	SPE (Oasis HLB), 0.3 ml extract	n.a.	HPLC (50), TOF (Agilent MSD TOF), ESI <sup>+</sup> , 9500 FWHM at 922 Da	50 mDa	100	Ferrer & Thurman (2007) <sup>f</sup>
9 nitrosamines	500 ml WWTP influent and effluent water	filtration, SPE (Oasis HLB-Bakerbond Carbon), 1 ml extract	PE: 0-133	HPLC (20), linear ion trap Orbitrap (Thermo LTQ Orbitrap), ESI <sup>+</sup> , 25 000-40 000 FWHM	10 ppm (SIM HRMS)	100	Krauss & Holender (2008) <sup>g</sup>
32 pharmaceuticals	500 ml river and drinking water, 200 ml WWTP effluent and 100 ml influent water	filtration, SPE (Oasis HLB), 1 ml extract	n.a.	UHPLC (10), QTOF (Waters QTOF Premier), ESI <sup>+</sup> &-	20 mDa (centroid)	20 000	Farré <i>et al.</i> (2008) <sup>h</sup>
6 benzotriazoles and benzothiazoles	4 11 drinking water and surface water	sand filtration, SPE (Oasis HLB), 1 ml extract	n.a.	HPLC (20), linear ion trap Orbitrap (Thermo LTQ Orbitrap), ESI <sup>+</sup> , 30 000 FWHM	7 ppm	100	van Leer-dam <i>et al.</i> (2009) <sup>i</sup>
15 pharmaceuticals	50 ml WWTP effluent and 25 ml influent water	filtration, SPE (Oasis MCX and MAX), 500 µl extract	RE: 11-141	UHPLC (5), QTOF (Waters QTOF Premier), ESI <sup>+</sup> &-	30 mDa	600-2600	Lavén <i>et al.</i> (2009) <sup>j</sup>
3 sweeteners	200 ml wastewater	SPE (Oasis HLB), 500 µl extract	PE: 53-90	HPLC (50), TOF (Agilent 6220 MSD TOF), ESI <sup>+</sup> , 15 000 FWHM at 922 Da	100 mDa (profile)	10-100	Ferrer & Thurman (2010) <sup>k</sup>

Table 2.1 (continued)

Target substances	Matrix and applied volumes	Sample pretreatment	Recovery (%) <sup>a</sup>	LC (inj. vol. in $\mu$ l), HRMS instrument, ionization mode, resolving power	Mass window width for XICs <sup>b</sup>	Linear range <sup>c</sup>	Reference
300 pesticides, 87 pharmaceuticals and 56 surfactants and metabolites	400 ml river water, 200 ml WWTP effluent water	filtration, SPE (Oasis HLB), 1 ml extract	PE: 22-127	UHPLC (20), QTOF (Agilent 6530 series), ESI <sup>+</sup> &-; 19 500 FWHM at 922 Da	n.a.	25-500	Gómez <i>et al.</i> (2010) <sup>1</sup>
68 pesticides and 16 pharmaceuticals	1000 ml WWTP influent, effluent and sea water	filtration, SPE (Oasis HLB), 1 ml extract	PE: 43-117	HPLC (10), TOF (Waters LCT Premier TOF), ESI <sup>+</sup> &-; 6000 FWHM	50 mDa	n.a.	Lara-Martin <i>et al.</i> (2011) <sup>m</sup>
17 pharmaceuticals and 13 pesticides	200 ml wastewater	filtration, SPE (Oasis MCX and Strate-X), 400 $\mu$ l extract	RE: 2-183	UHPLC (5), TOF (Waters LCT Premier TOF), ESI <sup>+</sup> &-; > 11 000 FWHM	60 mDa (centroid)	30-500	Nurmi & Pellinen (2011) <sup>n</sup>
4 pesticides and 5 pharmaceuticals	sea water	polydimethylsiloxane passive sampler, 200 $\mu$ l extract	PE: 88-102	UHPLC (10), Orbitrap (Thermo Exactive), ESI, 50 000 FWHM at 400 Da	10 ppm	10 000	Wille <i>et al.</i> (2011a) <sup>o</sup>
100 pharmaceuticals and transformation products	500 ml wastewater	filtration, SPE (Oasis HLB), 500 $\mu$ l extract	PE: 79-96	HPLC (10), linear ion trap Orbitrap (Thermo LTQ Orbitrap), ESI <sup>-</sup> , 30 000 FWHM at 400 Da	4 mDa (profile)	100-200	Cabill <i>et al.</i> (2012) <sup>p</sup>
24 drugs of abuse and metabolites	200 ml drinking and surface water	SPE (Oasis HLB), 500 $\mu$ l extract	n.a.	HPLC (40), QTOF (Agilent 6540 series), ESI <sup>+</sup> &-; 30 000 FWHM at 1522 Da	50 mDa	20	Ferrer & Thurnman (2012) <sup>q</sup>
24 drugs of abuse and metabolites	200 ml WWTP influent and 500 ml effluent water	filtration, SPE (Oasis MCX), 1 ml extract	n.a.	HPLC (10), QTOF (Agilent 6520 series), ESI <sup>+</sup> &-; 9500/22 000 FWHM at 113/980 Da in full-spectrum MS, 4750/11 000 FWHM at 113/980 Da in MS/MS	10 mDa at 9500-22 000 FWHM/20 mDa at 4750-11 000 FWHM	10-100	González-Marino <i>et al.</i> (2012) <sup>r</sup>

Table 2.1 (continued)

Target substances	Matrix and applied volumes	Sample pretreatment	Recovery (%) <sup>a</sup>	LC (inj. vol. in µl), HRMS instrument, ionization mode, resolving power	Mass window width for XICs <sup>b</sup>	Linear range <sup>c</sup>	Reference
5 antidiabetic pharmaceuticals	250 ml drinking, river and WWTP effluent water	filtration, SPE (Chromabond Tetracycline), 1 ml extract	PE: 16-87	HPLC (20), QTOF (Agilent 6520 series), ESI <sup>+</sup> &- <sup>+</sup> , 10000/20000 FWHM at 118/1520 Da	n.a. (SIM HRMS)	100	Martín <i>et al.</i> (2012) <sup>s</sup>
10 drugs of abuse and metabolites	100 µl river water	no preconcentration	n.a.	HPLC (100), QTOF (AB SCIEX TripleTOF 5600), ESI <sup>+</sup> , 20000 FWHM at 609 Da	20 mDa	200	Martínez Bueno <i>et al.</i> (2012) <sup>t</sup>
21 endocrine-disrupting substances and metabolites	1 l drinking water and 1 l river water	filtration, SPE (Oasis HLB), 500 µl extract	PE: 46-134	UHPLC (10), QTOF (Waters Synapt G2), ESI <sup>+</sup> &-	50 mDa	5000	Wang <i>et al.</i> (2012) <sup>u</sup>
5 industrial chemicals and metabolites, 3 flame retardants, 40 pesticides and metabolites	1 ml drinking water, 1 ml (1/2 diluted) surface water, 1 ml (1/5 diluted) wastewater	filtration, online-SPE (C18 column), 1 ml inj. v.	n.a.	UHPLC, Orbitrap (Thermo Exactive), ESI <sup>+</sup> &- <sup>+</sup> , 25000 FWHM	10 ppm	15 - 40	Wode <i>et al.</i> (2012) <sup>v</sup>
24 drugs of abuse and metabolites	100 ml WWTP influent and 200 ml effluent water	filtration, SPE (Oasis HLB), 500 µl extract	PE: 45-120	HPLC (20), linear ion trap Orbitrap (Thermo LTQ Orbitrap), ESI <sup>+</sup> , 30000 FWHM at 400 Da	10 ppm	325	Bijlsma <i>et al.</i> (2013) <sup>w</sup>
150 organic contaminants including pharmaceuticals and pesticides	100 ml surface, ground and WWTP effluent water	centrifugation, SPE (Oasis HLB), 1 ml extract	n.a.	UHPLC (50), QTOF (Waters QTOF Premier), ESI <sup>+</sup> &- <sup>+</sup> , 10000 FWHM at 556 Da	20 mDa (centroid)	n.a.	Díaz <i>et al.</i> (2013) <sup>x</sup>
27 drugs of abuse and metabolites	1 ml WWTP influent water	filtration, online-SPE (C18 column), 1 ml inj. v.	n.a.	HPLC, Q-Orbitrap (Thermo Q-Exactive), ESI <sup>+</sup> , 70000 FWHM at 400 Da	10 ppm	200	Fedorova <i>et al.</i> (2013) <sup>y</sup>

<sup>a</sup> If reported, the SPE recovery (RE) is given, otherwise the overall process efficiency (PE) including SPE recovery and matrix effects is given.

<sup>b</sup> The use of profile or centroid data if specified between brackets. <sup>c</sup> The instrumental linear working range is given as a factor, i.e. the highest concentration divided by the lowest concentration of the linear working range. <sup>d-y</sup> These labels refer to the references in Figures 2.10 and 2.11. n.a. Data not available.



## 2.4 Selective and accurate mass measurement in HRMS

### 2.4.1 Measuring mass in the presence of isobaric interferences

In HRMS, enhancing the resolving power increases the mass measurement selectivity and thus reduces the chance that ions are (partially) unresolved from other ions. In the case two adjacent masses differ less than twice the FWHM in mass, their signals merge, and the accurate mass will shift towards the interference. This phenomenon has been illustrated by Kellmann *et al.* (2009). In Figure 2.5, it is shown how increasing the resolving power from 10 000 to 100 000 FWHM revealed the presence of two co-eluting substances. At 10 000 FWHM, the measured mass of the merged peaks corresponds to the intensity-weighted mass average (Kaufmann & Butcher, 2006) resulting in mass errors up to 94 ppm, whereas, at 100 000 FWHM, mass errors not higher than 1.3 ppm were obtained.

The selectivity, which is thus of utmost importance especially for complex samples, results from the combination of HRMS and LC selectivity, and has been assessed in different ways. A first approach is by analysing the same sample(s) at different resolution settings (e.g. 10 000, 20 000, 50 000, 70 000 and 100 000 FWHM, Kellmann *et al.*, 2009; van der Heeft *et al.*, 2009; Xia *et al.*, 2011; Kaufmann & Walker, 2013). As such, isobaric interferences unresolved at low resolution can be resolved at higher resolution and the effect on the mass error can be investigated (e.g. Figure 2.5). The overall selectivity can be assessed

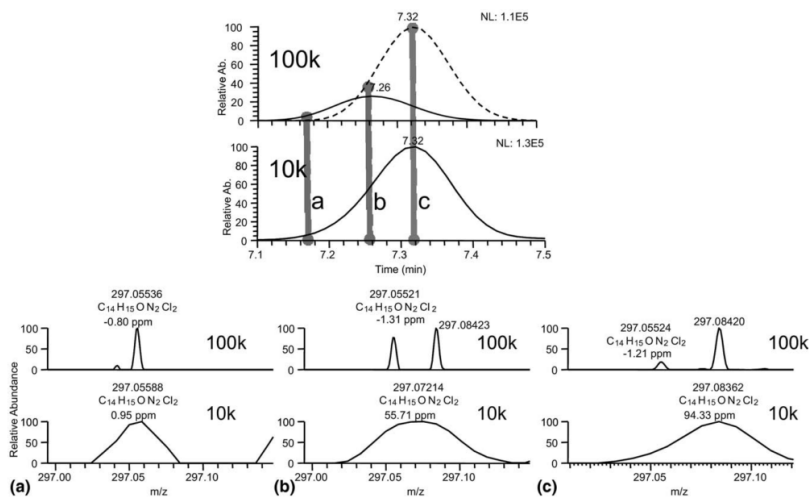


**Figure 2.5** Effect of resolving power on assigned mass accuracy of two co-eluting analytes imazalil ( $[M+H]^+$  297.05560 Da,  $C_{14}H_{14}Cl_2N_2O$ ,  $t_R = 7.26$  min) and flunixin ( $[M+H]^+$  297.08454 Da,  $C_{14}H_{11}F_3N_2O_2$ ,  $t_R = 7.32$  min). Upper figure: extracted ion chromatograms ( $\pm 5$  ppm around the exact mass of each of the ions at 100 000 FWHM and  $\pm 100$  ppm at 10 000 FWHM, respectively). Bottom figures: mass profiles at two resolving power settings 10 000 FWHM (10 k) and 100 000 FWHM (100 k) of 3 different scans (a-c). Figure from Kellmann *et al.* (2009).

by counting the number of isobaric peaks appearing in the XICs. For example, the number of isobaric peaks reduced by a factor of 1.4-2.2 when analysing samples at 20 000 instead of 10 000 FWHM (Xia *et al.*, 2011).

A second approach consists in the continuous post-column infusion of analytes of interest during the analysis of real matrix samples (Kaufmann & Walker, 2013). Plotting the measured mass of the analytes as a function of the retention time (so called mass traces, exemplified in Figure 2.6) allows studying the deviation of the accurate mass and the effect of isobaric interferences on the mass accuracy (and

thus the mass measurement selectivity) over the whole chromatogram at different resolution settings (Kaufmann & Walker, 2013). In Figure 2.6, it can be seen that the mass accuracy is severely affected ( $> 5$  to 80 ppm) in some regions of the chromatogram when using a resolving power of 10 000 FWHM, whereas very accurate mass measurements ( $< 1$  ppm mass error) are obtained in other regions. In that case, enhancing the resolving power to 50 000 FWHM (Figure 2.6) reduced the mass error to  $< 1$  ppm over the whole chromatogram.

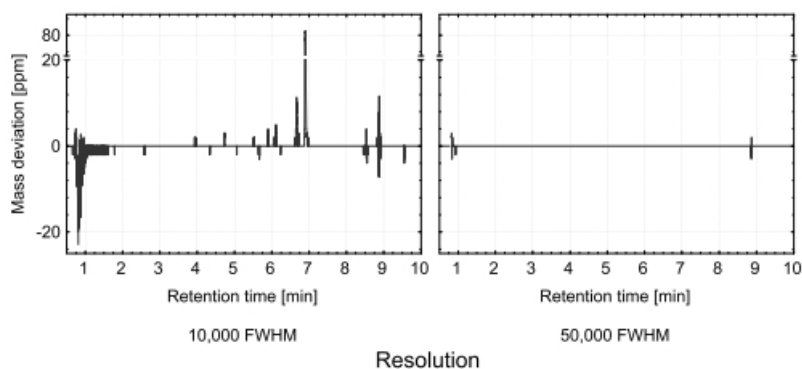


**Figure 2.6** Mass trace of ciprofloxacin in liver (using lock mass) at two resolving power settings (10 000 and 50 000 FWHM). A very strong mass shift is observed at 6.9 min, where the signal for ciprofloxacin shifts about 80 ppm (10 000 FWHM). A resolving power of 50 000 FWHM is capable of virtually eliminating any isobaric interferences ( $< 1$  ppm mass shift). Figure from Kaufmann & Walker (2013)

Even when using the highest resolving power, isobaric interferences can occur, and thus it is important to process the acquired data as such that the effect of possible interferences is minimized. With respect to accurate mass measurement, different authors reported an improved mass precision thanks to improved centroiding algorithms. First, in general, centroiding algorithms can more precisely determine

the accurate mass from narrower mass peaks (i.e. increased resolving power) (Blom, 2001; Marshall & Hendrickson, 2008; Kellmann *et al.*, 2009; van der Heeft *et al.*, 2009). Second, it has been emphasized that centroiding algorithms should be able to precisely centroid low and high signal intensity peaks and deconvolute partially unresolved peaks in the mass spectrum (Botitsi & Garbis, 2011). By deconvolution, unresolved mass peaks are decomposed into the underlying mass peaks. Deconvolution resolving power is the degree to which nearly isobaric mass peaks can be distinguished (deconvolved), and is defined as the FWHM divided by the resolvable mass difference ( $\Delta m/z$ ) between two mass peaks:  $\frac{FWHM}{\Delta m/z}$  (Sokkalingam *et al.*, 2014). This dimensionless variable normalizes analyzer resolution, and above a value of  $\pm 1$ , overlapping peaks become indistinguishable. Conventional centroiding algorithms have thus a maximal deconvolution resolving power of 1. However, a recently developed spectral deconvolution centroiding algorithm named PeakInvestigator has shown the capability to deconvolve overlapping peaks (Figure 2.7) and a deconvolution resolving power ranging from about 2 to 4 was reported for merged mass peaks having intensity ratios of 0.15 to 1, respectively (Sokkalingam *et al.*, 2014).

## **2.4.2 Instrumental characteristics and mass calibration**

With respect to instrumental characteristics, for both TOF and Orbitrap mass analyzers, the dynamic range for mass accuracy is limited on the one side statistically by too few ions detected or a too low signal-to-noise (S/N) ratio, and on the other side by peak position shifts due

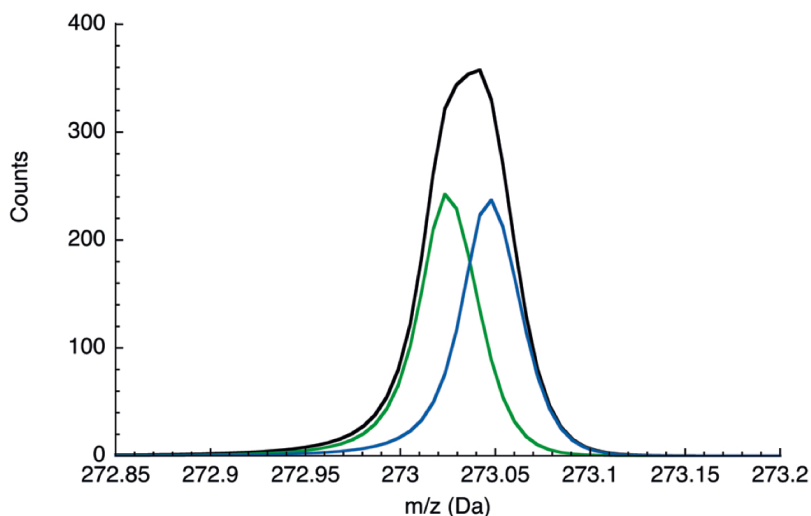


**Figure 2.7** At a resolving power of 5000 FWHM,  $C_{10}H_{14}N_2O_2Br_1$  (green) and  $C_8H_{17}O_6S_2$  (blue) are not resolved resulting in the black peak (mass error of 45 ppm and -38 ppm versus the first and second compound, respectively). PeakInvestigator is able to deconvolve these nearly isobaric peaks of equal abundance (i.e. signal intensity ratio of 1) resulting in the green (mass error 0.8 ppm) and blue (mass error 1.1 ppm) peaks. Figure reproduced from Sokkalingam *et al.* (2014).

to too many ions (Makarov *et al.*, 2006). For TOF and Orbitrap MS, a decreased mass precision at low ion abundance has been observed (Blom, 2001; Wolff *et al.*, 2003; Makarov *et al.*, 2006). For Orbitrap MS, this was only at S/N ratios approaching 3 and could be mainly related to the presence of noise (Makarov *et al.*, 2006). However, for TOF MS, mass imprecision has also been related to a statistically too low number of ions detected and the minimum concentrations at which mass errors are lower than 5 ppm, is typically found to be 10 times higher than those calculated at a signal-to-noise ratio of 3 (Calbiani *et al.*, 2006). Therefore, for TOF MS, some authors considered the mass measurement

uncertainty in the evaluation of the limits of detection; e.g. they defined the limits of detection as the minimum concentration providing a mass error  $< 3$  ppm and a signal-to-noise ratio  $> 3$  (Calbiani *et al.*, 2006; Gómez *et al.*, 2007). For distorted or saturated mass peaks having high signal intensity, mass errors up to 40 ppm have been reported (Petrović *et al.*, 2006; González-Mariño *et al.*, 2012). Although the issue of limited dynamic range can be avoided in some cases (e.g. the mass can be measured from spectra having a lower signal intensity in the chromatographic peak tails or diluted samples can be reanalyzed (Petrović *et al.*, 2006; González-Mariño *et al.*, 2012)), this factor is rather instrument related and more advanced HRMS showed to provide improved accurate mass dynamic ranges of about a factor 1000 and 5000 for TOF and Orbitrap MS, respectively (González-Mariño *et al.*, 2012; Makarov *et al.*, 2006). In addition, for Orbitrap MS, mass shifts can occur due to Coulombic interactions with other ions present at high abundance (Gorshkov *et al.*, 2012). Allowing fewer ions to enter the C-trap and Orbitrap analyzer has been suggested to improve the mass accuracy (Gorshkov *et al.*, 2012).

With respect to mass calibration, both external (i.e. prior to analysis) and internal (i.e. during analysis) mass calibration have been frequently applied. Improper external mass calibration can lead to large systematic erroneous mass measurements. For example, mass errors up to 12 ppm were systematically measured for ions with mass lower than the external mass calibration range (van Leerdam *et al.*, 2009; Krauss & Hollender, 2008). Therefore, the external mass calibration range must at least include the mass range of interest. For example, a mixture

of sodium hydroxide/formic acid diluted in acetonitrile/water, which leads to the formation of different adducts, can be used for external mass calibration over a wide range from 50 to 1000 Da in electrospray positive and negative ionization (Masiá *et al.*, 2013). Different other mixtures (e.g. polyethylene glycol) have been reported (Web *et al.*, 2004).

Drift of the external calibration over time has been reported, leading to systematic errors (up to 2 and 5 ppm after 8 days and 5 hours, respectively (van der Heeft *et al.*, 2009; Fedorova *et al.*, 2013). Therefore, using lock masses for internal mass correction of each acquired spectrum is recommended. Lock mass signals can be obtained by post-column lock mass addition (Lapworth *et al.*, 2012; Nurmi *et al.*, 2012) or by using a switching dual ionization source providing alternating lock mass ions and the LC eluent (Blom, 2001; Cahill *et al.*, 2012). Other strategies might be to apply post-acquisition mass correction using the measured target ions as reference (van der Heeft *et al.*, 2009) or to search for common LC-MS contaminants, being present in the whole chromatogram (e.g. diisooctyl phthalate  $C_{24}H_{38}O_4$  for ESI positive mode, Ferrer & Thurman, 2007). No common contaminant was found as lock mass for ESI negative mode. For Orbitrap MS, combined internal and external calibration is typically at least twice as accurate as only external calibration (van der Heeft *et al.*, 2009).

## **2.5 Achievements in LC-HRMS screening**

In 2006, Petrović & Barceló (2006), Sancho *et al.* (2006), and Lacorte & Fernández-Alba (2006) overviewed the first achievements in screening of environmental samples based on both accurate mass and fragment ions for confirmation. They concluded that achieving acceptable mass errors – better than 5 ppm – for identification at environmental trace levels seemed to be challenging using TOF instruments providing a resolving power in the range of 5000 to 10 000 FWHM. In addition, elucidating unknown compounds showed to be a complex matter taking into account the accurate mass, the isotopic pattern and fragment spectra.

### **2.5.1 Suspect versus non-target screening**

In 2010, Krauss *et al.* (2010) distinguished two predominant workflows that were applied in literature for multi-residue screening of micropollutants using HRMS (Figure 2.8). First, in suspect screening, suspect compounds are suggested a priori. For the identification of the compounds, their intrinsic exact mass and isotopic pattern are a priori known. Apart from that, retention time can be predicted and fragment ions can be matched with predicted spectra. Second, no a priori information is presumed in non-target screening and molecular formulae and chemical structures must be suggested from the measured accurate mass, isotopic pattern and fragment ions. Basically, these workflows diverge from the a priori knowledge of molecular formulae and structures. Screening typically leads to indicative identification



of analytes. Finally, for unequivocal confirmation and eventually also quantification (Section 2.6) reference standards are required.

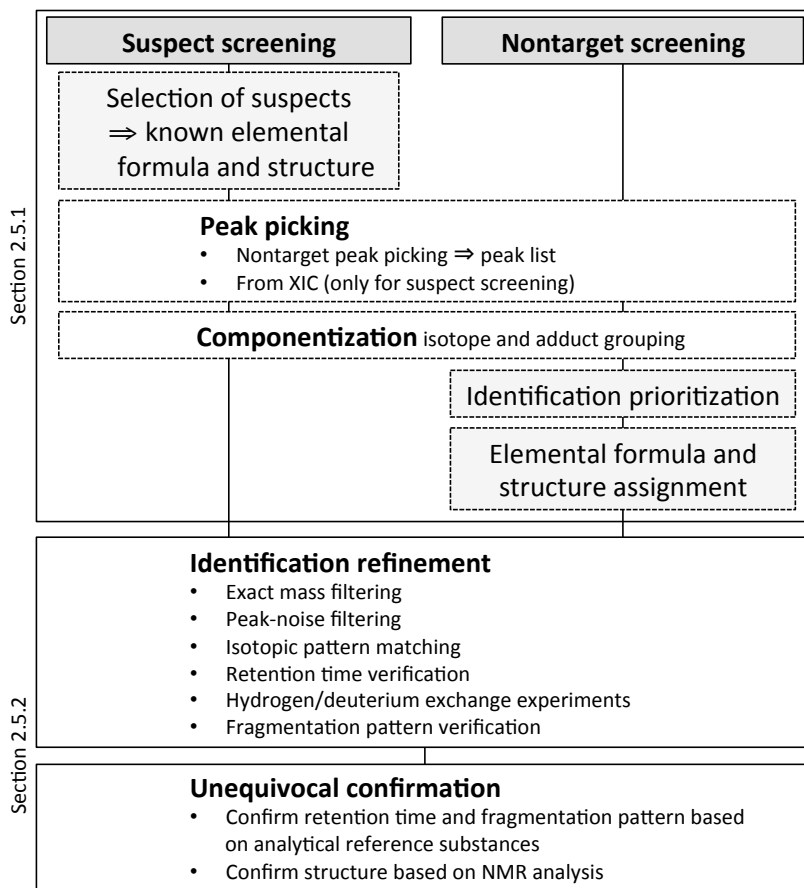


**Figure 2.8** Schematic workflow for suspect and non-target screening starting with peak picking and componentization, over different identification refinement strategies to finally unequivocal confirmation. The scheme includes the variety of strategies that have been applied in different suspect (Table 2.2) and non-target (Table 2.3) screening studies.

With respect to 8 suspect screening studies summarized in Table 2.2, surface water, wastewater and wastewater treatment plant (WWTP) effluent have been screened towards a set of suspects varying from about 40 (K'oreje *et al.*, 2012) up to almost 2000 (Kern *et al.*, 2009; Hug *et al.*, 2014) chemicals. In the majority of these studies, the suspects were anthropogenic contaminants, which are known to occur in the aquatic environment (e.g. several pharmaceuticals, personal care products, pesticides and their transformation products (TPs), and different classes of chemicals such as surfactants having homologous series). A recent trend is that potential water contaminants are selected based on the local supply or use of pharmaceuticals and industrial chemicals (K'oreje *et al.*, 2012; Hug *et al.*, 2014) or based on predicted or known transformation products of pharmaceuticals and pesticides (Kern *et al.*, 2009; Li *et al.*, 2013). As HRMS instrument, TOF or Orbitrap instruments were used in most of the studies, except by K'oreje *et al.* (2012) who used a magnetic sector HRMS.

The complexity of the applied screening techniques increased over the last years and a variety of algorithms have been written to automate the screening procedure. In general, the first step is to construct extracted ion chromatograms around the exact mass of the suspects (Ibáñez *et al.*, 2008; Martínez Bueno *et al.*, 2012; Nurmi *et al.*, 2012) or to perform a non-target peak picking on the chromatograms (Kern *et al.*, 2009; Hug *et al.*, 2014; Li *et al.*, 2013; Moschet *et al.*, 2013; Schymanski & Singer, 2014). The latter requires a powerful algorithm, which is able to find all the peaks in a chromatogram, but has the advantage that it lists the  $m/z$  and retention time combination of all the found peaks in an easily searchable peak list.

**Table 2.2** Characteristics of 8 suspect screening LC-HRMS methods.

Matrix	Analytical technique	Peak picking and componentization	Suspect screening list	Exact mass filter	Peak-noise filter	Isotopic pattern	$t_R$ prediction	H/D exchange	Fragments	Tentatively identified compounds	Confirmed compounds	Reference
wastewater	SPE-UHPLC-ESI-QTOF MS	XIC	±500 pesticides, pharmaceuticals, drugs of abuse and TPs	5 ppm	x	x	x	x	4 pesticide, 3 pharmaceuticals, 2 drugs of abuse and TP			Ibañez <i>et al.</i> (2008)
surface water	SPE-HPLC-ESI-LTQ-Orbitrap MS	nontarget peak picking	1794 predicted or known TPs of 52 pesticides and pharmaceuticals	5 ppm	x	x	x	x	19 pesticide and pharmaceutical TPs		12 TPs	Kern <i>et al.</i> (2009)
WW/TP effluent	SPE-UHPLC-ESI-TOF MS	XIC	147 pharmaceuticals and 54 metabolites	5 mDa	x	x			25 pharmaceuticals		4 pharmaceuticals	Nurmi <i>et al.</i> (2012)
surface water	SPE-HPLC-ESI-magnetic sector MS	XIC	43 pharmaceuticals locally supplied	5 ppm	x				12 pharmaceuticals		10 pharmaceuticals	K'oreje <i>et al.</i> (2012)
surface water	LVI-HPLC-ESI-QTOF MS	XIC	1200 pharmaceuticals and personal care products	5 ppm				x	5 pharmaceuticals			Martínez Bueno <i>et al.</i> (2012)

**Table 2.2** (continued)

Matrix	Analytical technique	Peak picking and componentization	Suspect screening list	Exact mass filter	Peak-noise filter	Isotopic pattern	$t_R$ prediction	H/D exchange	Fragments	Tentatively identified compounds	Confirmed compounds	Reference
surface water	SPE- HPLC- ESI-Q- Orbitrap MS	nontarget peak picking	140 pesticides and TPs having $\log K_{ow} < 5$ (water relevant substances) and at least one heteroatom (ESI amendable)	5 ppm	x	x	x	x	x	19 pesticides and 11 TPs (not taking into account predicted MS/HRMS fragments)	13 pesticides and 5 TPs	Moschet <i>et al.</i> (2013)
WWTP effluent	SPE- HPLC- ESI-LTQ- Orbitrap MS	nontarget peak picking	1706 LC-MS and ESI amendable compounds produced or used in local industry + 325 chemicals reported to occur in surface water	7 ppm	x	x	x	x	x	13 compounds	1 UV filter, 4 industrial chemicals, 1 pharmaceutical	Hug <i>et al.</i> (2014)
WWTP effluent	SPE- HPLC- ESI-LTQ- Orbitrap MS	nontarget peak picking, isotope and adduct grouping	394 compounds from 15 classes of homologous series (eg. linear alkylbenzyl sulfonates, sulfophenyl alkyl carboxylic acids, etc.)	3.5 ppm	x	x	x	x	x	69 compounds related to 11 classes of homologous series		Schymanski & Singer (2014)

n.a. Data not available.

The newest trend in screening aims finding and identifying non-target unknown compounds. In 4 studies, matrices such as WWTP effluent, process water, groundwater and landfill leachate have been screened for the presence of unknown contaminants (Table 2.3). Two non-target screening studies in river sediment were also incorporated in Table 2.3 because of their interesting methodological approach (Terzic & Ahel, 2011; Weiss *et al.*, 2011).

In general, these non-target screening techniques start with peak picking: a manual (Terzic & Ahel, 2011) or, in most cases, automated search for peaks, i.e. non-target peak picking (Godejohann *et al.*, 2011; Müller *et al.*, 2011; Terzic & Ahel, 2011; Weiss *et al.*, 2011; Schymanski & Singer, 2014), in the chromatograms. Subsequently, componentization aims isotope and adduct grouping resulting in thousands (about 1000 to 10 000) of unidentified analytes. Unless identifying the most intense peaks (Godejohann *et al.*, 2011; Terzic & Ahel, 2011; Schymanski & Singer, 2014), in this workflow, incorporating identification prioritization strategies has shown the ability to select the most relevant unidentified analytes from an environmental point of view. Pattern searching of analytes with temporal, spatial, or process-based relationships has shown to be an effective approach to reduce the number of analytes of interest. As such, Müller *et al.* (2011) prioritized by Venn diagram analysis those analytes relevant for drinking water or for the waterworks (Figure 2.9). This resulted in the assignment of 21 molecular formulae, from which 12 pharmaceuticals could be unequivocally identified. Another promising approach was the combined use of bioassays and LC-HRMS by Weiss *et al.* (2011) in an effect directed analysis (EDA) for the prioritization of substances

showing ecotoxicological activity. They selected 59 analytes showing (anti-) androgenic activity in river sediment extracts leading to the unequivocal identification of 8 contaminants. Considering the vast amount of unidentified analytes in non-target analysis, more research should focus to prioritize the most relevant analytes for identification. As such, the demanding identification efforts may be restricted to the most relevant analytes. This comprises proposing elemental formulae based on accurate mass and heuristic rules (e.g. restriction of element numbers, hydrogen or heteroatom/carbon element ratios) (Godfrey & Brenton, 2012), and database searching for possible chemical structures.

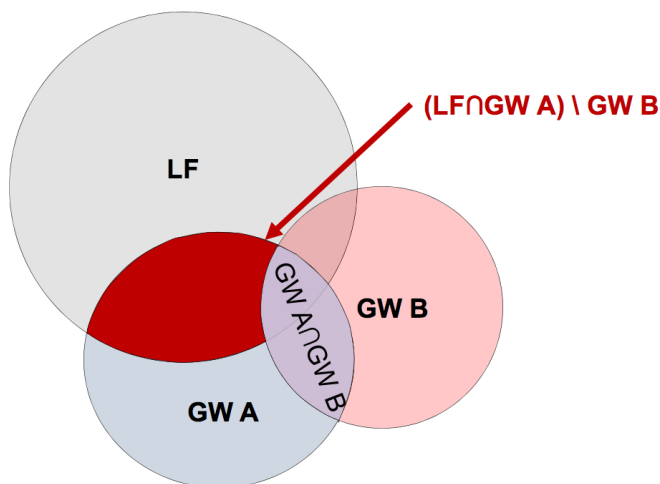


**Figure 2.9** Illustration of a Venn diagram for determining substances relevant for the waterworks. These compounds had to be present in landfill leachate (LF) and in groundwater well A (GW A) but not in GW B. Figure reproduced from Müller *et al.* (2011).

**Table 2.3** Characteristics of 6 non-target screening LC-HRMS methods.

Matrix	Analytical technique	Peak picking and component-tization	Identification and prioritization strategy for nontarget screening	Exact mass filter	Peak-noise filter	Isotopic pattern $t_R$ prediction	H/D exchange	Fragments	Tentatively identified compounds	Confirmed compounds	Reference
landfill leachate, groundwater, process water	SPE- HPLC- QTOF MS	peak picking, isotope and adduct grouping	Venn diagram analysis in order to select substances relevant for drinking water or the waterworks	n.a.	x	x	x		12 pharmaceuticals, 1 pesticide, 1 benzothiazole, 7 unknown molecular formulae	12 pharmaceuticals	Miller <i>et al.</i> (2011)
WW/TP effluent	SPE- HPLC- LTQ- Orbitrap MS	peak picking, isotope and adduct grouping	30 most intense peaks	5 ppm	x	x	x	9 formulae assigned	1 benzothiazole	1 benzothiazole	Schymanski & Singer (2014)
WW/TP effluent	SPE- HPLC- TOF MS / time-slice- SPE- NMR <sup>a</sup>	peak picking, adduct grouping	identification of the most concentrated compounds from the NMR spectra	n.a.	x			22 compounds tentatively identified based on accurate mass and NMR	6 pesticides, 1 UV filter and 1 food additive	6 pesticides, 1 UV filter and 1 food additive	Godejohann <i>et al.</i> (2011)
WW/TP effluent	SPE- HPLC- LTQ- Orbitrap MS	peak picking and isotope grouping	peaks having distinct isotopic pattern including <sup>37</sup> Cl, <sup>81</sup> Br, <sup>15</sup> N or <sup>34</sup> S and peaks with intensity > threshold	7 ppm	x	x	x	14 compounds	1 pharmaceutical, 1 pesticide TP and 3 industrial chemicals	1 pharmaceutical, 1 pesticide TP and 3 industrial chemicals	Hug <i>et al.</i> (2014)

**Table 2.3** (continued)

Matrix	Analytical technique	Peak picking and componentization	Identification and componentization strategy for nontarget screening	Exact mass filter	Peak-noise filter	Isotopic pattern	$t_R$ prediction	H/D exchange	Fragments	Tentatively identified compounds	Confirmed compounds	Reference
river sediment	extraction-fractionation-UHPLC-QTOF MS	manual search of major peaks	major peaks (> 10 % of full scale intensity)	5 mDa	x	x	x	x	x	8 pharmaceuticals, 3 TPs, 32 compounds related to homologous series (8 polypropylene glycols, 11 alkyl dimethyl benzyl ammonium compounds, 5 linear alkylbenzene sulfonates, 8 fatty acids)	8 pharmaceuticals	Terzic & Ahef (2011)
river sediment	extraction-fractionation-HPLC-LIQ-Orbitrap MS	non-target peak picking	EDA towards (anti-) androgenic activity	3 ppm	x	x	x	x	x	59 accurate masses tentatively identified	3 musks, 2 organophosphates, 2 steroids, 1 oxygenated polycyclic aromatic hydrocarbon	Weiss <i>et al.</i> (2011)

<sup>a</sup> In time-slice-SPE-NMR, briefly, different LC fractions are collected on SPE cartridges and subsequently eluted and analyzed with NMR. n.a. Data not available.



## 2.5.2 Identification refinement and confirmation

In both suspect and non-target screening, six different techniques have been tested and applied for identification refinement (Figure 2.8). Although the concept of identification for each of these techniques has been proven, it is not always clear how they should be optimally applied and combined with each other in order not to oversee truly present contaminants and at the same time omit false positives.

First, intrinsic to HRMS, an exact mass filter is applied. Only analytes (mono isotopic ion) having an accurate mass within a predefined mass error tolerance are retained. The applied mass error tolerance ranged from 3.5 to 10 ppm but was 5 ppm in most studies (Tables 2.2 and 2.3).

Second, several peak-noise differentiation strategies such as signal-to-noise (Moschet *et al.*, 2013), signal intensity (Kern *et al.*, 2009; Moschet *et al.*, 2013) and peak shape (Hug *et al.*, 2014; Moschet *et al.*, 2013) filters have been applied in order reduce the number of (noise) peaks that are unlikely to be related to analytes. In addition, blank subtraction was applied to eliminate compounds that do not originate from the sample (Kern *et al.*, 2009; Gerssen *et al.*, 2011; Hug *et al.*, 2014; Li *et al.*, 2013; Moschet *et al.*, 2013; Schymanski & Singer, 2014). Next to removing noise peaks, the risk exists that true peaks are omitted (i.e. false negatives). For example, Moschet *et al.* (2013) could reduce the number of initially picked peaks by 85 % using different peak filters. However, this resulted in 23 % false negatives. Differentiating noise from

true peaks without omitting too many true peaks seems a challenging task.

Third, isotopes are frequently used as diagnostic ions in order to enhance the identification confidence. Some authors performed a visual inspection of the isotopic pattern (Hug *et al.*, 2014) or compared the measured and theoretical isotope exact masses and/or ratios (Ibáñez *et al.*, 2008; Kern *et al.*, 2009; Nurmi *et al.*, 2012; Li *et al.*, 2013; Moschet *et al.*, 2013; Schymanski & Singer, 2014). Although various isotope matching methodologies have been applied, Cl- or Br-containing compounds seem to be quite easily distinct thanks to their specific and abundant isotopic pattern.

Fourth, predicting the retention time based on octanol-water partition coefficients ( $K_{ow}$ ) (Kern *et al.*, 2009; Nurmi *et al.*, 2012) or using linear solvation energy relationships (Hug *et al.*, 2014) has shown to improve the identification success. However, the application of these models can be problematic for ionic compounds because these substances showed unpredictable lower retention (Hug *et al.*, 2014).

Fifth, recently, two authors introduced hydrogen/deuterium (H/D) exchange experiments for the identification of non-target compounds by using deuterated LC solvents (Müller *et al.*, 2011; Hug *et al.*, 2014). As such, during chromatography, deuterium replaces exchangeable hydrogens in the analytes and their mass will shift by 1 unit per deuterium. Comparing the number of exchanged hydrogens with the predicted number of exchangeable hydrogens can lead to improved structure elucidation.

Sixth, several authors considered the occurrence of at least one fragment ion as additional identification criterion. This could be a fragment originating from in-source fragmentation, all ion fragmentation/HRMS or data dependent MS/HRMS. At least four strategies have been applied in order to interpret the fragmentation spectra: (i) comparison to in-house (Ibáñez *et al.*, 2008) or commercial spectra (Martínez Bueno *et al.*, 2012) or to fragments reported in literature (Ibáñez *et al.*, 2008; Moschet *et al.*, 2013); (ii) reconciliation of the measured fragments to substructures of the precursor ion (Schymanski & Singer, 2014); (iii) comparison to fragments of similar compounds (Kern *et al.*, 2009; Gerssen *et al.*, 2011; Hug *et al.*, 2014); (iv) and comparison to predicted fragments (Moschet *et al.*, 2013).

In a final step, unequivocal confirmation can be reached through obtaining and analysing analytical references of the indicatively identified analytes. As such, the retention time and fragmentation spectrum can be experimentally confirmed. In the case all mentioned techniques are not successful or no reference substances are available (e.g. for transformation products), nuclear magnetic resonance (NMR) spectroscopy is required to reveal the chemical structure of analytes in combination with the information obtained from LC-HRMS (Godejohann *et al.*, 2011; Richardson & Ternes, 2014). However, NMR requires intensive sample enrichment and pretreatment.

In suspect screening, the identified and confirmed substances were mainly pesticides, pharmaceuticals, their transformation products and some industrial chemicals (Table 2.2). Although some pesticides and pharmaceuticals were also found by non-target screening, many other

chemicals including benzothiazoles, musks, steroids, organophosphates, UV filters, food additives and industrial chemicals were confirmed (Table 2.3).

### **2.5.3 Evaluation of the screening performance**

In order to establish the reliability of screening, recently, Moschet *et al.* (2013) evaluated the identification success rate of their suspect screening methodology for a variety of pesticides in surface water. This was achieved through a hypothetical screening of artificially enriched samples with known contaminants at different concentrations. As such, false negatives and false positives could be observed and their frequency was determined. A false negative rate (i.e. fraction of the analytes not retained by the screening but detected by a target approach) and false positive rate (i.e. false positive count divided by the number of suspects in the screening library averaged over the analyzed samples) of about 30 % and 2.3 %, respectively, were reported.

In the whole identification train, the false negative rate should be as low as possible and, at the same time, not too many false positives must be retained (Moschet *et al.*, 2013). Therefore, identification criteria should be set not too stringent (to avoid false negatives) and at the same time sufficiently stringent (to avoid false positives). More research is needed to reveal the relationship between the false negative and false positive rate and how both can be minimized. From the study of Moschet *et al.* (2013), the false negative and false positive rates seem to be inversely related, thus an optimal trade-off must be found.

## 2.6 Quantitative aspects of LC-HRMS

In full-spectrum TOF and Orbitrap HRMS, quantification has been mainly performed from the measured signal of the mono isotopic ion of the ionized analytes. However, recently, some authors also employed selected ion monitoring (SIM) in which the molecular ion is preselected using a quadrupole or linear ion trap during a predefined time window (Krauss & Hollender, 2008; Fedorova *et al.*, 2013). In that case, a MS/HRMS experiment is performed and the quantification ion was the selected molecular ion or one of its fragment ions.

### 2.6.1 Quantification in the presence of isobaric interferences

In Section 2.4.1, it has been shown that the signals of a mass peak unresolved from an isobaric interference merge. As such, not only the mass shifts towards the interference but also their signals add up, resulting in overestimation of the signal intensity. The latter can be seen from the intensity scale in the XICs in Figure 2.5: the height of the resolved peak ( $t_R$  7.32 min) at 100 000 FWHM is  $1.1 \times 10^5$ , whereas it increases to  $1.3 \times 10^5$  due to the presence of an unresolved isobaric ion when the resolving power is reduced to 10 000 FWHM.

For the construction of XICs, different researchers applied different mass window widths varying over a wide range from 7 to 10 ppm or from 4 to 100 mDa for the validated HRMS studies in Table 2.1. Narrow mass windows seem to increase the selectivity (Section 2.4, Kaufmann & Butcher, 2006) but on the other hand the method sensitivity might be

affected (Kaufmann *et al.*, 2007; Kellmann *et al.*, 2009). To this respect, especially the use of centroid data (by centroiding, sticks replace the mass peaks in the mass spectrum) can lead to signal interruption or the complete disappearance of the signal when the accurate mass of an ion is shifted out of the XIC mass window (Kaufmann & Butcher, 2006). This can be due to isobaric interferences or other causes of mass error discussed in Section 2.4.1. Therefore, using profile data seems to be preferential for quantitative purposes. Although the use of centroid or profile mode is not always specified for the validated methods in Table 2.1, centroid data is often used. The reason might be that centroid data were chosen because this typically requires less storage capacity.

Overall, although selectivity will benefit from increased resolving power of both the chromatographic separation and the mass spectrometry (Kaufmann *et al.*, 2007; Kellmann *et al.*, 2009), it is not fully understood to which extent selectivity and sensitivity vary as a function of the mass window width.

### **2.6.2 Analytical performance of validated LC-HRMS methods**

With respect to the instrumental performance of TOF and Orbitrap instruments, linear working ranges of 1 to 2.5 orders of magnitude were reported for most of the validated HRMS methods (Table 2.1). Both instruments showed quasi-similar instrumental detection limits (IDLs) ranging for the majority of the compounds from 1 to 100 pg on column (Figure 2.10).

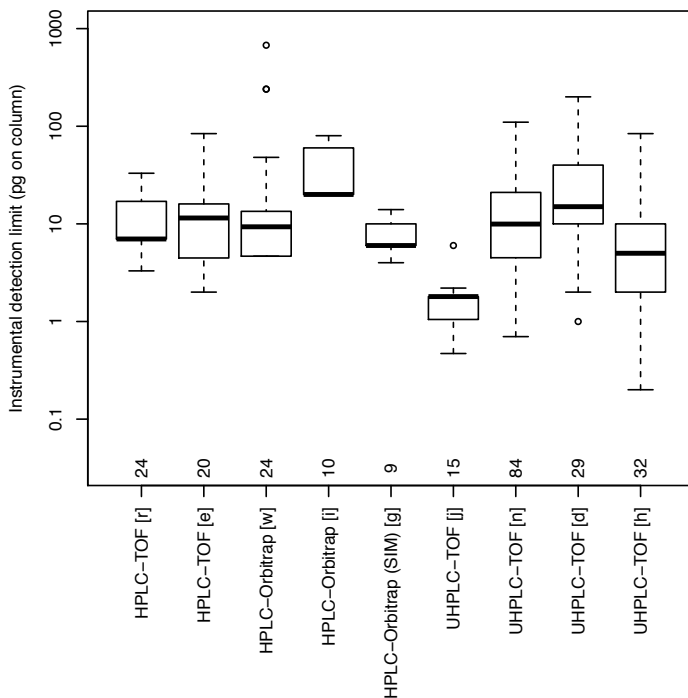


**Figure 2.10** Boxplots of the IDLs for different combinations of HPLC/UHPLC and TOF/Orbitrap HRMS of validated methods. The number of compounds included is given below each boxplot. The references [e-w] are given in Table 2.1

Regarding the method performance of the 27 validated HRMS methods summarized in Table 2.1, overall, method detection limits (MDLs) over a wide range from  $< 0.1 \text{ ng l}^{-1}$  to almost  $10 \mu\text{g l}^{-1}$  were reported. The reported MDLs are presented in Figure 2.11 per type of water matrix (drinking water, surface water, WWTP effluent and wastewater) and ordered by what can be introduced as increasing equivalent sample injection volume (ESIV). The ESIV is defined here

as the preconcentration factor of the sample pretreatment multiplied by the injection volume. The ESIV ranged from 100  $\mu\text{l}$  in the case of LVI to 20 000  $\mu\text{l}$  in the case large volumes of 1 l were concentrated by SPE. For drinking and surface water, a clear trend can be observed and lower MDLs are generally reached for increased ESIVs. For WWTP effluent water and wastewater, a less pronounced trend is observed with less decreasing MDLs for the same increase in ESIV. The latter is reflected in the matrix effects. Matrix effects are the signal enhancing or suppressing effect a matrix has on the peak area of an analyte as compared to a pure solvent. Whereas minor matrix effects, ranging from 80 to 120 %, were reported for the majority of the compounds in drinking and surface water, severe matrix effects (< 50 %) were reported for wastewater, especially when the ESIV raised above 2500  $\mu\text{l}$ . At the same time, authors analysing larger ESIVs tend to employ HRMS providing increased resolving power (from 5000 up to 70 000 FWHM). Therefore, although IDLs were for all instruments in the range of 1 to 100 pg on column (Figure 2.10), higher resolving power and thus increased selectivity allows in general targeting lower analyte concentrations in more complex matrices or, at the same time, increased resolving power allows larger ESIVs. For example, Fedorova *et al.* (2013) obtained relatively low method detection limits for 27 drugs of abuse in wastewater ranging from 0.5 to 50  $\text{ng l}^{-1}$  and matrix effects from 50 to 150 % for most of the compounds using a relative low ESIV of 1000  $\mu\text{l}$  with online SPE-UHPLC-Orbitrap HRMS operated at a high resolving power of 70 000 FWHM.



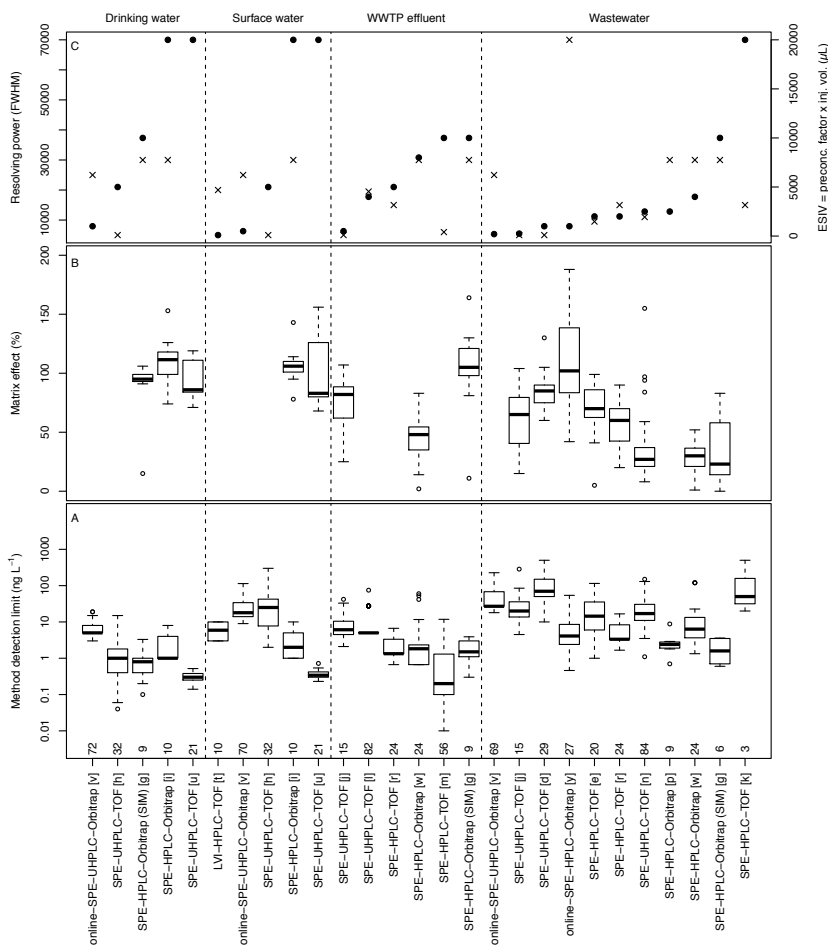


**Figure 2.11** Method detection limits (panel A) presented per type of water matrix and ordered by increasing equivalent sample volume (ESIV, ● in panel C) for the validated methods in Table 2.1. For each method, the number of compounds included in the boxplot (bottom of panel A), matrix effects (panel B) and resolving power (× in panel C) are presented. The references [d-y] are given in Table 2.1.

Different authors (Ibáñez *et al.*, 2008; Krauss & Hollender, 2008; Hogenboom *et al.*, 2009; Hernández *et al.*, 2012; Zedda & Zwiener, 2012) concluded that combined reliable qualitative analysis and subsequent quantification in one instrument has emerged with the most recent TOF and Orbitrap HRMS. However, some particular issues should not be overlooked and need more investigation. First, matrix effects are a known drawback related to ESI in LC-MS and similar matrix effects have been observed for ESI-MS/MS and ESI-HRMS (Fedorova *et al.*, 2013). However, in particular for full-spectrum Orbitrap MS, enhanced matrix suppression has been reported. This phenomenon, which is not fully understood yet, has been called post-interface matrix suppression and results in suppression or the complete loss of the signal of target ions (Kaufmann *et al.*, 2010b; Fedorova *et al.*, 2013). Second, although a resolving power starting from 5000 FWHM has been referred to as HRMS, an increased resolving power is clearly beneficial due to its improved selectivity and ability to detect lower analyte levels in more complex matrices. Techniques to assess the selectivity, as discussed in Section 2.4.1, must be employed more frequently in order to establish the minimal required resolving power for different types of matrices.

## **2.7 Tandem and high-resolution mass spectrometry**

The advantages of full-spectrum HRMS, as compared to MS/MS, have been praised for different reasons. First, exact molecular mass, which is accurately measured in HRMS, is universal and easily calculable. Therefore, setting up a HRMS method does in se not rely on the a priori

availability of reference standards whereas in MS/MS compound specific transitions must be experimentally defined (Kaufmann & Walker, 2012b). In addition, in HRMS a wide spectrum can be measured over the entire chromatogram, allowing the selective determination of a virtually unlimited number of analytes (Petrović *et al.*, 2006; Lommen *et al.*, 2007; Nielen *et al.*, 2007; Ibáñez *et al.*, 2009; Krauss *et al.*, 2010; Díaz *et al.*, 2011; Müller *et al.*, 2011; Hernández *et al.*, 2011; Chitescu *et al.*, 2012; Masiá *et al.*, 2013). In contrast, in MS/MS the specific transitions are only measured in a time-window around the experimentally determined retention time of the analytes. Second, the high resolving power in HRMS allows accurate mass measurement with high confidence to the ppm-level, hereby facilitating the identification of analytes based on accurate mass. As a result, HRMS and tandem MS/HRMS has been praised for its added value for confirmatory purposes. According to the Commission Decision 2002/657/EC (European Union, 2002), at a resolving power of at least 20 000 FWHM, precursor (HRMS) and fragment ions (MS/HRMS) value 2 and 2.5 identification points (IPs), respectively. This contrasts with 1 and 1.5 IPs for low-resolution precursor (MS) and fragment ions (MS/MS), respectively. As such, in HRMS 1 precursor and only 1 fragment ion is sufficient (= 4.5 IPs) to reach at least 4 identification points for unequivocal confirmation, whereas 1 precursor plus 2 fragment ions (= 4 IPs) are required in low-resolution MS. Third, post-run analysis of the acquired spectra is possible (Section 2.5) without having to set up additional instrumental runs. Screening the acquired spectra can thus lead to the identification of non-targeted compounds with the restriction that their mass falls within the acquired

mass range and that the compounds are amenable to the applied analytical techniques, as discussed in Section 2.3.

A fundamental question for the combined use of quantitative and qualitative HRMS is from when on HRMS outperforms – from a qualitative and quantitative point of view – tandem MS/MS, which is considered as the state-of-the-art MS detection and quantification technique (2002/657/EC, European Union, 2002). After all, as stated in the Section 2.4, HRMS has the potential for an increasingly better selectivity over the whole spectrum upon increasing the resolving power whereas the selectivity in MS/MS is limited by specific transitions over a predefined retention time window. For example, Farré *et al.* (2008) reported overestimated concentrations for some pharmaceuticals in wastewater using MS/MS as compared to HRMS. This could be related to the presence of interferences that were well resolved using a TOF instrument (5000 FWHM). Kaufmann *et al.* (2010a) calculated that similar selectivity can be expected at a resolving power of at least 50 000 FWHM as compared to MS/MS (1 transition) acquisition for pharmaceuticals in food matrices. However, from experiments with 27 drugs in wastewater samples, Fedorova *et al.* (2013) still observed slightly more interferences for MS/MS versus HRMS (70 000 FWHM) when monitoring 1 transition. However, a clearly better specificity for MS/MS was observed when 2 transitions are monitored. Although in many studies the earliest HRMS (mainly TOF) showed to be less sensitive in terms of detection limits than MS/MS (Farré *et al.*, 2008; Masiá *et al.*, 2013), Ferrer *et al.* (2008) elucidated that TOF sensitivity would be superior over MS/MS sensitivity when more than 300 analytes

are monitored in one run. This was explained by the fact that analysing more analytes in MS/MS requires the use of shorter dwell times (i.e. the time that is spent for the acquisition of an ion), whereas in HRMS such limitations do almost not apply. Recently, quasi-comparable performance characteristics including sensitivity, linearity, accuracy and precision have been reached for LC-Orbitrap HRMS (50 000-70 000 FWHM) and LC-MS/MS in multi-residue approaches (Kaufmann *et al.*, 2012; Fedorova *et al.*, 2013). There was one exception, namely with respect to matrix effects. Full spectrum Orbitrap-HRMS seemed to be affected by the previously discussed post-interface matrix suppression (Section 5.2), which is not present in quadrupole MS/MS. Research results from the combined use of HRMS and MS/MS are needed in order to provide fair comparisons of both MS technologies and to find out how much resolving power is equivalent to one or multiple MS/MS transitions for the definition of IP's.

## 2.8 Conclusions and future challenges

High mass resolving power is the key factor for selectivity in HRMS and allows the simultaneous accurate mass (qualitative) measurement and quantification in one instrument. Therefore, analysts should realize that sufficient selectivity, which results from the combined mass and chromatographic selectivity, is of utmost importance and must be thoroughly assessed for each matrix of interest. To do so, mass shifts of the analyzed target compounds and the presence of many isobaric peaks in XICs are a good indication for insufficient selectivity and can indicate that also the quantitative accuracy might be affected.

Therefore, qualitative and quantitative analysis are interrelated and should not always be seen apart from each other. In general, a resolving power of at least 50 000 to 70 000 FWHM seems to reach equivalent mass selectivity as provided by one MS/MS transition.

With HRMS, the possibility for full-spectrum screening towards suspect or unknown micropollutants has launched a revolution in environmental analytics to accelerate the identification of more and more environmental relevant contaminants. However, several analytical challenges are formulated in this review. First, the whole analytical procedure must reflect the multi-residue concept because a variety of substances having very different physical-chemical characteristics must perform well. Second, even at the highest resolving power, isobaric interferences can occur. Therefore, for ultimate mass accuracy, advanced centroiding algorithms for accurate mass determination in the presence of isobaric interferences must be implemented. Third, a gamut of suspect screening algorithms has shown the ability to reveal the presence of large lists of suspects. Hence, the future challenge is not to oversee truly present contaminants (i.e. low false negative rate) and to obtain not too many false positive hits. Fourth, non-target screening strategies have been invented and allowed the identification of unknown contaminants. Here, prioritization is a key factor in order to direct the demanding identification procedures towards the most relevant – from an environmental point of view – unidentified analytes.



# 3

## Quality assessment and quantification of pharmaceuticals in wastewater using solid-phase extraction - HPLC - magnetic sector mass spectrometry

*Redrafted from:*

*L. Vergeynst, A. Haeck, P. De Wispelaere, H. Van Langenhove & K. Demeestere (2015). Multi-residue analysis of pharmaceuticals in wastewater by liquid chromatography - magnetic sector mass spectrometry: Method quality assessment and application in a Belgian case study. Chemosphere 119: S2-S8.*



## 3.1 Introduction

Wastewater treatment plants (WWTP) have been pointed out as the main contamination pathway for pharmaceuticals to the environment (Section 1.2). For a broad range of pharmaceuticals often only partial removal is achieved in biological treatment processes (Michael *et al.*, 2013; Petrie *et al.*, 2013).

Measuring trace amounts of these micropollutants, as prerequisite for studying their occurrence and fate, is challenging because wastewater typically contain interferences causing matrix effects. In addition, in order to be able to measure sufficiently low concentrations, a preconcentration step is required.

Therefore, the objectives in this chapter are twofold. First, the goal is to develop and optimize a solid-phase extraction (SPE) preconcentration and clean-up technique followed by double-focusing sector HRMS for selective mass measurement hyphenated with HPLC by electrospray ionization (ESI) for quantitative trace analysis of 43 selected pharmaceuticals in influent and effluent water of WWTPs. Hereby, particular focus goes to the analytical performance, method validation, quality assessment and variability analysis, the latter being only scarcely discussed in multi-residue analysis. Although this type of HRMS has shown its merits in the analysis of micropollutants like dioxins and furans (Hernández *et al.*, 2012), and of oxygenated polycyclic aromatic hydrocarbons in airborne matrices (Walgraeve *et al.*, 2012), its use in multi-residue water analysis is very scarce. Recently, sector HRMS hyphenated to high performance liquid

chromatography (HPLC) by ESI has been used a first time for qualitative screening towards pharmaceuticals in surface water (K'oreje *et al.*, 2012), but so far, no reports are available describing its application in quantitative water analysis.

The second goal is to study the occurrence of the selected pharmaceuticals in influent and effluent waters of a parallel conventional active sludge (CAS) system - membrane bioreactor (MBR) and a second CAS WWTP in Belgium. This study brings forward one of the first concentration data of pharmaceuticals in wastewater in Belgium, and allows to perform a first tier environmental risk assessment for the Belgian river affected by the second CAS-WWTP. Finally, loads are calculated to determine removal efficiencies in both WWTP technologies.

For this study, twenty-five pharmaceuticals were selected from three studies (Cooper *et al.*, 2008; Coutu *et al.*, 2012; Kumar & Xagorarakis, 2010) dealing with prioritization of emerging contaminants. This selection was extended with 8 quinolone antibiotics because of their bio-recalcitrance in WWTPs (Jia *et al.*, 2012), and with 10 antiviral drugs belonging to the most hazardous pharmaceuticals based on predicted toxicity towards fish, daphnia and algae (Sanderson *et al.*, 2004) but only measured in the environment in a limited number of studies (Ghosh *et al.*, 2010; K'oreje *et al.*, 2012; Prasse *et al.*, 2010).

## 3.2 Experimental section

### 3.2.1 Chemicals and materials

The 43 pharmaceuticals selected in this study, their therapeutic usage, and their analytical standard suppliers are listed in Table A.1. Individual stock solutions of the pharmaceuticals were prepared on weight basis to a final concentration of about  $1 \text{ mg ml}^{-1}$  (solvents in Table A.1). A standard mix of the pharmaceuticals was prepared at a concentration of  $2 \text{ mg ml}^{-1}$  in 10:90 methanol/water. Standard and matrix-matched calibration curves were prepared by serial dilution of the standard mix in 10:90 methanol/water, and in influent and effluent water, respectively.

LC-MS grade methanol and LC-MS grade water (VWR Belgium), LC-MS grade acetonitrile (Biosolve, The Netherlands), formic acid (> 96 %), ammonium acetate (> 99.99 %) and  $\text{Na}_2\text{EDTA}\cdot 2\text{H}_2\text{O}$  (Sigma-Aldrich, Belgium) were purchased. Deionized water was produced using Aquadem ion exchanger cartridges (Werner, Germany).

### 3.2.2 Sampling and WWTP description

For the method development and validation (Section 3.3.2), influent and effluent grab samples were collected in prerinsed amber glass bottles at the WWTP of Lede, Belgium. For the method application (Section 3.3.3), influent and effluent 24 h time integrated samples were collected in a parallel CAS-MBR WWTP (WWTP1) and a CAS WWTP (WWTP2) using an automatic sampler (50 ml sample each 20 min, Sigma 900 and ISCO 4700, Elscolab, Belgium) during

4 and 6 days, respectively, resulting in a total of 10 influent and 18 effluent samples. Effluent samples were collected 24 hours after their corresponding influent sample. Figure 3.1 presents a schematic overview with indication of the sampling points, and Table 3.1 summarizes the sampling period, number of samples, precipitation data, and the main physical and chemical characteristics of both WWTPs.

Formic acid was added to the samples (pH 3) to prevent microbial activity during sample storage (at 4°C in the dark for  $\leq 4$  days) prior to extraction.

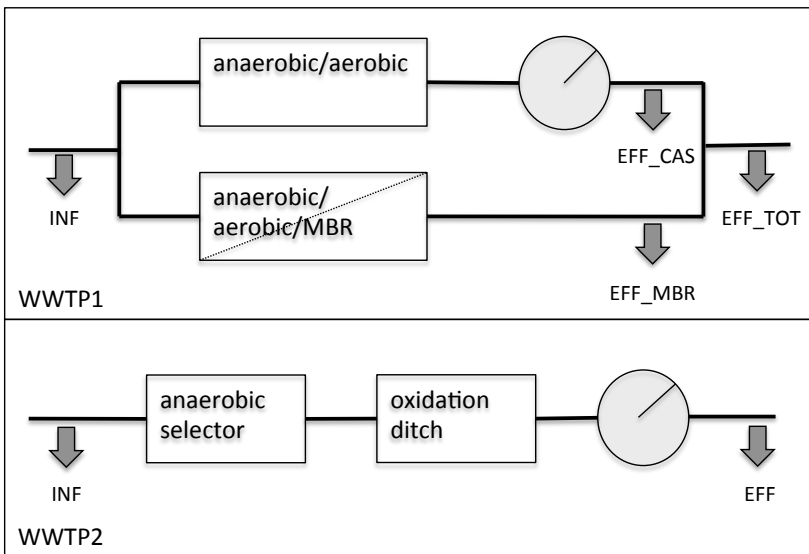


**Figure 3.1** Scheme representing the design and sampling points (arrows) of WWTP1 and WWTP2 (INF: influent, EFF: effluent, CAS: conventional active sludge, MBR: membrane bioreactor, TOT: total).

**Table 3.1** Physical and chemical characteristics of WWTP1 and WWTP2 during the sampling period.

Parameter	WWTP1, Schilde, Belgium				WWTP2, Aalst, Belgium	
	Influent CAS+MBR	Effluent CAS	Effluent MBR	Effluent CAS+MBR	Influent	Effluent
Sampling period and duration		March 2013, 4 days			August 2013, 6 days	
Inhabitant equivalents (I.E.)						100000
Hydraulic retention time (h)		9	6			28
Sludge retention time (d)		6	not applicable			22
Number of samples	4	4	4	4	6	6
Daily flow rate ( $\text{m}^3 \cdot \text{d}^{-1}$ )	12 775±1082	5544±1036	7231±68	12 775±1082	20 846±8153	20 846±8153
Chemical oxygen demand (COD) ( $\text{mgO}_2/\text{l}$ )	186±5	37±3	23±4	26±5	407±192	33±4
Total nitrogen ( $\text{mgN}/\text{l}$ )	31±2	21±1	6±2	15±1	47±7	7.7±1.0
Total phosphorus ( $\text{mgP}/\text{l}$ )	3.8±0.2	0.2±0.0	0.6±0.3	0.4±0.1	6.0±1.0	0.6±0.2
Suspended solids ( $\text{mg l}^{-1}$ )	110±56	6.0±2.2	4.0±0.0	4.0±0.0	163±42; day 1-3: day 4-6: 277±93	7.9±4.0
pH	7.4±0.1	7.4±0.5	7.6±0.1	7.6±0.1	7.6±0.1	7.7±0.1
Precipitation in Ukkel, Belgium (mm)		no precipitation			day 4: 0.1; day 5: 14; day 6: 0.4	

### 3.2.3 Sample pretreatment and solid-phase extraction

The optimized sample pretreatment and SPE protocol was as follows. Before SPE extraction, the pH of the samples was adjusted to  $7.0 \pm 0.1$  by addition of a 5 M NaOH and 10% formic acid solution. The samples were filtered first through a  $1.0\ \mu\text{m}$  GF/B Whatman glass fiber filter (VWR, Belgium), and then through a  $0.45\ \mu\text{m}$  Whatman nylon membrane (VWR, Belgium). 2 ml of a 5 wt%  $\text{Na}_2$ -ethylenediaminetetraacetic acid (EDTA) solution were added per 100 ml of sample. By adding EDTA, soluble metals are bound to the chelating agent, increasing the extraction efficiency of tetracycline and fluoroquinolone antibiotics (Gros *et al.*, 2009; Kasprzyk-Hordern *et al.*, 2007).

Oasis HLB SPE cartridges (6 ml, 200 mg sorbent) were placed on a VacMaster-10 and the vacuum was controlled maintaining a flow rate of approximately  $5\ \text{ml}\ \text{min}^{-1}$ . First, the cartridges were conditioned with 6 ml of methanol and 6 ml of deionized water. Then, 100 ml effluent or 50 ml influent sample were loaded on the cartridge. Subsequently, the cartridge was washed with 4 times 6 ml of deionized water. After drying the cartridges for 5 min, elution was performed using 5 ml of methanol and the eluents were collected in silanized glass tubes. The glass tubes were silanized by rinsing first with 5% dichlorodimethylsilane (Alfa Aesar, Belgium) in toluene, then twice with toluene, and finally thrice with methanol. The glass tubes were placed in a TurboVap and the eluent was evaporated under nitrogen stream until complete dryness. The walls of the tubes were rinsed twice with methanol in order to

prevent sorption of the analytes. Reconstitution was performed with 1 ml of 10:90 methanol/water. Then, the tubes were vortexed for 20 s and centrifuged for 5 min at 1000 rounds per min. Finally, the extract was distributed over 2 vials for ESI positive (+ 0.1 % formic acid) and negative analysis.

## 3.2.4 Instrumental analysis

### 3.2.4.1 HPLC separation

Chromatographic separation of the analytes was achieved using a Surveyor HPLC system (Thermo Finnigan) equipped with a Phenomenex Luna C18(2) 150 × 2.0 mm column (3 μm particle size) and operating at 35 °C. The sample injection volume was 10 μl. The mobile phase was a mixture of (A) methanol and (B) water, both with 0.1 % formic acid, and a mixture of (C) acetonitrile and (D) water for analysis in ESI positive and negative ion mode, respectively. The optimized gradient was as follows. For analysis in ESI positive ion mode, the mobile phase was (A) methanol and (B) water, both with 0.1 % formic acid. After 1 min isocratic at 10 % A, the gradient increased linearly to 20, 80 and 100 % A after 2, 35 and 40 min, respectively, followed by 10 min isocratic at 100 % A. Column equilibration was performed for 10 min at 10 % A making a total analysis time of 60 min. For analysis in ESI negative ion mode, the mobile phase was (C) acetonitrile and (D) water. After 1 min isocratic at 40 % C, the gradient increased linearly to 100 % C after 25 min, followed by 10 min isocratic at 100 % C. Column equilibration was performed for 10 min at 40 % C making a total analysis time of 45 min. The mobile phase flow rate was 170 μl min<sup>-1</sup>, from

which  $40 \mu\text{l min}^{-1}$  was combined with a  $10 \mu\text{l min}^{-1}$  reference solution for internal mass calibration, resulting in a flow rate of  $50 \mu\text{l min}^{-1}$  going to the ESI source.

#### **3.2.4.2 Selective ion detection**

The double focusing magnetic sector MAT95XP-TRAP HRMS (Thermo Finnigan, Bremen, Germany) was equipped with an ESI source and operated in multiple ion detection (MID) mode for selective target analysis at a resolving power of 10 000 (10% valley definition).

The ESI capillary temperature (200, 225, 250, 275 and 300 °C) and sheath gas (3 and 4 bar) flow rate conditions were optimized from duplicate injections of analytical standards ( $2 \text{mg l}^{-1}$ ) operating the MS in unit-resolution full-spectrum mode. In the ESI positive and negative ion mode, 4 bar, and 300 °C and 275 °C, respectively, showed increased peak areas and a good compromise for all the compounds. The final ESI parameters were as follows. The spray voltage was 3 kV. Nitrogen was used as sheath gas and optimized at 4 bar. The optimized capillary temperature was set at 300 °C and 275 °C for ESI positive and negative ion mode, respectively. Daily automatic tuning of the electric potentials of capillary, tube lens, skimmer, octapole and source lenses were performed for optimum sensitivity.

In the MID mode, the chromatographic analysis is divided in multiple retention time windows. In each of them, a defined MID window is analyzed (in which the highest mass is maximum 1.2 times the lowest mass) and the mass of the target ions and the ions for internal calibration are consecutively measured. In a MID cycle, the



accelerating voltage,  $V$ , is set to its maximum value (ca. 5 kV), and the strength of the magnetic field,  $B$ , is set to the value corresponding to 1 mass unit lower than the mass of the lightest ion to be measured. After that, the accelerating voltage is reduced stepwise, in order to obtain a consecutive pass of the masses of the target ions. To obtain the best signal-to-noise (S/N) ratio and at least 10 data points per chromatographic peak, the measuring time for each ion was set as close as possible to the maximum of 500 ms. This resulted into a MID cycle time of 0.9-2.8 s. To assure a maximal measuring time for each ion, and given the restriction of the MID window, 3 and 1 distinct runs in the ESI positive and negative ion mode were required, respectively, in order to be able to measure the 43 compounds. The MID windows are presented in Table 3.2.

For internal mass calibration, the ions from a reference solution provide each MID cycle with a specific lock and calibration mass (Table 3.2). In each MID cycle, the instrument automatically carries out an electric mass calibration by using these two reference masses as calibration points. In the positive ion mode, the reference solution was a  $3 \text{ mg l}^{-1}$  mixture of polyethylene glycol with average mass of 200, 300 and  $400 \text{ g mol}^{-1}$  (Acros Organics, Belgium) in methanol with 0.1% formic acid (Table 3.3). In the negative ion mode, a mixture of polyethylene glycol (PEG) with average mass of  $200 \text{ g mol}^{-1}$  ( $150 \text{ mg l}^{-1}$ ), ketoprofen ( $8 \text{ mg l}^{-1}$ ), and 4-hydroxy-2,3-dimethoxybenzoic acid ( $8 \text{ mg l}^{-1}$ ) in 1:1 acetonitrile/water with 25 mM ammonium acetate was used as a reference solution (Table 3.3).

The presented HPLC-HRMS method providing a resolving power of 10 000 (10 % valley definition, equivalent to about 20 000 FWHM) allows identification of analytes based on accurate mass (i.e. MID measurement) and retention time. Since no fragments and their ion ratios are monitored, unequivocal identification according to the Commission Decision 2002/657/EC (European Union, 2002) was not obtained.

### **3.2.4.3 Response normalization and instrumental validation**

In order to account for the inter- and intraday variability of the response of the MS detector, the obtained peak areas (PAs) of the analytes in each analytical run were normalized for the response of the detector. For each of the 4 MID methods, the response factor (RF) of the instrument was determined in each analytical run from the average signal intensity of a selected ion from the reference solution (Table 3.2). For each compound, the normalized peak area (NPA) was then calculated from Equation 3.1.

$$NPA = \frac{PA}{RF} \quad (3.1)$$

The linearity and stability of the detector was investigated by a four-points calibration curve (20-100-500-2000  $\mu\text{g l}^{-1}$ ). Intraday precision was determined by acquiring three calibration curves at the same day and by calculating the relative standard deviation (RSD) on each concentration level ( $n = 3$ ). Interday repeatability was determined as the RSD from injections of analytical standards (100  $\mu\text{g l}^{-1}$ ) on 5 different days in a time frame of 14 days ( $n = 5$ ). Weighted regression analysis ( $1/x^2$  weighting) using a statistical F-test for lack of fit (European Union,

**Table 3-2** Target pharmaceuticals and monitored ions for mass calibration with molecular formula, retention time, monitored ions, and used MTD window for MTD method 1 to 3 (ESI positive) and 4 (ESI negative).

Compound	Molecular formula	$t_R$ (min)	$[M\pm H]^\pm$	$[M(^{13}C/^{37}C)\pm H]^\pm$	MTD window (min)	Lock and calibration ions
<i>MTD method 1 (ESI positive)</i>						
Lamivudine	$C_8H_{11}N_3O_3S$	2.87	230.0594	-	0.00-5.45	195-239
Acyclovir	$C_8H_{11}N_5O_3$	4.67	226.0935	-	0.00-5.45	195-239
Metronidazole	$C_6H_9N_3O_3$	8.53	172.0717	-	5.45-10.05	151-195
Paracetamol	$C_8H_9NO_2$	8.96	152.0706	153.0740	5.45-10.05	151-195
Tetracycline	$C_{22}H_{24}N_2O_8$	11.31	445.1605	-	10.05-12.35	415-459
Oxytetracycline	$C_{22}H_{24}N_2O_9$	11.62	461.1555	-	10.05-12.35	415-459
Sarafloxacin	$C_{20}H_{17}F_2N_3O_3$	13.08	386.1311	-	12.35-14.75	371-415
Gatifloxacin	$C_{19}H_{22}FN_3O_4$	13.81	376.1667	-	12.35-14.75	371-415
Moxifloxacin	$C_{21}H_{24}FN_3O_4$	15.68	402.1824	-	14.75-16.80	371-415
Risperidone	$C_{23}H_{27}FN_4O_2$	15.74	411.2191	-	14.75-16.80	371-415
Rimantadine	$C_{12}H_{21}N$	17.55	180.1747	181.1780	16.80-18.80	151-195
Oseltamivir ethylester	$C_{16}H_{28}N_3O_4$	19.60	313.2122	314.2155	18.80-22.24	283-327 <sup>a</sup>
Paroxetine	$C_{19}H_{20}F_1NO_3$	23.37	330.1500	331.1534	22.24-25.00	327-371
Fluoxetine	$C_{17}H_{18}F_3NO$	25.72	310.1413	311.1447	25.00-29.14	283-327
Alprazolam	$C_{17}H_{13}ClN_4$	31.52	309.0902	311.0872	29.14-35.00	283-327
Diolofenac	$C_{14}H_{11}Cl_2NO_2$	39.65	296.0240	298.0210	35.00-45.00	283-327
<i>MTD method 2 (ESI positive)</i>						
Amoxicillin	$C_{16}H_{19}N_3O_5S$	5.98	366.1118	367.1152	0.00-8.54	327-371
Levofloxacin	$C_{18}H_{20}FN_3O_4$	10.34	362.1511	-	8.54-12.90	327-371
Ciprofloxacin	$C_{17}H_{18}FN_3O_3$	11.25	332.1405	-	8.54-12.90	327-371
Enrofloxacin	$C_{19}H_{22}FN_3O_3$	11.62	360.1718	-	8.54-12.90	327-371
Zidovudine	$C_{10}H_{13}N_5O_4$	14.17	268.1040	-	12.90-19.84	239-283 <sup>a</sup>
Sulfamethoxazole	$C_{10}H_{11}N_3O_3S$	15.39	254.0544	-	12.90-19.84	239-283 <sup>a</sup>
Venlafaxine	$C_{17}H_{27}N_1O_2$	16.86	278.2115	-	12.90-19.84	239-283 <sup>a</sup>

Table 3.2 (continued)

Compound	Molecular formula	$t_R$ (min)	$[M \pm H]^\pm$	$[M(^{13}C/^{37}C) \pm H]^\pm$	MID window (min)	Lock and calibration ions
Nevirapine	$C_{15}H_{14}N_4O$	21.96	267.1240	-	19.84-30.18	239-283 <sup>a</sup>
Amitriptyline	$C_{20}H_{23}N_1$	24.05	278.1903	-	19.84-30.18	239-283 <sup>a</sup>
Flumequine	$C_{14}H_{12}FNO_3$	27.70	262.0874	-	19.84-30.18	239-283 <sup>a</sup>
Temazepam	$C_{16}H_{13}ClN_2O_2$	32.65	301.0738	303.0709	30.18-36.11	283-327
Efavirenz	$C_{14}H_9ClF_3NO_2$	39.56	316.0347	318.0317	36.11-45.00	283-327
<i>MID method 3 (ESI positive)</i>						
Trimethoprim	$C_{14}H_{18}N_4O_3$	9.09	291.1452	292.1485	5.00-9.80	283-327
Amantadine	$C_{10}H_{17}N$	10.38	152.1434	153.1467	9.80-11.32	151-195
Osetamivir acid	$C_{14}H_{24}N_2O_4$	12.26	285.1809	-	11.32-19.00	283-327 <sup>a</sup>
Sulfamethazine	$C_{12}H_{14}N_4O_2S$	13.04	279.0910	-	11.32-19.00	283-327 <sup>a</sup>
Sulfadoxin	$C_{12}H_{14}N_4O_4S$	16.42	311.0809	-	11.32-19.00	283-327 <sup>a</sup>
Besifloxacin	$C_{19}H_{21}Cl_1FN_3O_3$	20.26	394.1328	395.1362+396.1299	19.00-23.97	317-415
Nalidixic acid	$C_{12}H_{12}N_2O_3$	26.58	233.0921	-	23.97-30.63	195-239
Carbamazepine	$C_{15}H_{12}N_2O$	28.39	237.1022	-	23.97-30.63	195-239
Diazepam	$C_{16}H_{13}ClN_2O$	34.86	285.0789	287.0760	30.63-37.28	283-327
Indomethacin	$C_{19}H_{16}ClNO_4$	39.60	358.0841	359.0874+360.0811	37.28-42.17	327-371
Pleconaril	$C_{18}H_{18}F_3N_3O_3$	44.74	382.1373	383.1407	42.17-50.00	371-415
<i>MID method 4 (ESI negative)</i>						
Chloramphenicol	$C_{11}H_{12}Cl_2N_2O_5$	4.69	321.0051	323.0021	0.00-7.98	297-341
Naproxen	$C_{14}H_{14}O_3$	11.27	229.0870	-	7.98-17.92	197-253 <sup>a</sup>
Ibuprofen	$C_{13}H_{18}O_2$	15.98	205.1234	-	7.98-17.92	197-253 <sup>a</sup>
Irgasan	$C_{12}H_7Cl_3O_2$	19.85	286.9439	288.9409	17.92-23.00	253-297

<sup>a</sup> Used for response normalization (RF).

**Table 3.3** Monitored ions for mass calibration with molecular formula and exact mass.

Compound	Molecular formula	[M±H] <sup>±</sup>
<i>Monitored ions for mass calibration (ESI positive)</i>		
PEG	HO(C <sub>2</sub> H <sub>4</sub> O) <sub>4</sub> H	151.0965
PEG	HO(C <sub>2</sub> H <sub>4</sub> O) <sub>5</sub> H	195.1227
PEG	HO(C <sub>2</sub> H <sub>4</sub> O) <sub>6</sub> H	239.1489
PEG	HO(C <sub>2</sub> H <sub>4</sub> O) <sub>7</sub> H	283.1751
PEG	HO(C <sub>2</sub> H <sub>4</sub> O) <sub>8</sub> H	327.2013
PEG	HO(C <sub>2</sub> H <sub>4</sub> O) <sub>9</sub> H	371.2276
PEG	HO(C <sub>2</sub> H <sub>4</sub> O) <sub>10</sub> H	415.2538
PEG	HO(C <sub>2</sub> H <sub>4</sub> O) <sub>11</sub> H	459.2800
PEG	HO(C <sub>2</sub> H <sub>4</sub> O) <sub>12</sub> H	503.3062
<i>Monitored ions for mass calibration (ESI negative)</i>		
4-hydroxy-2,3-dimethoxybenzoic acid	C <sub>9</sub> H <sub>10</sub> O <sub>5</sub>	197.0456
Ketoprofen	C <sub>16</sub> H <sub>14</sub> O <sub>3</sub>	253.0870
Acetic acid - PEG cluster	C <sub>2</sub> H <sub>4</sub> O <sub>2</sub> + HO(C <sub>2</sub> H <sub>4</sub> O) <sub>5</sub> H	195.1227
Acetic acid - PEG cluster	C <sub>2</sub> H <sub>4</sub> O <sub>2</sub> + HO(C <sub>2</sub> H <sub>4</sub> O) <sub>6</sub> H	239.1489

2002, Commission Decision 2002/657/EC) were used to verify the linearity of the detector response. The instrumental detection limits (IDLs) were defined on the basis of a S/N ratio of 3 and were estimated from the analysis of standard solutions.

#### 3.2.4.4 Method validation and determination of the SPE recovery and matrix effects

Influent and effluent water spiked with standards before (pre) and after (post) SPE extraction (standard addition method) as well as non-spiked samples were analyzed as schematically represented in Figure 3.2. For the pre-spiked samples, the validation range was 40 to 5000 ng l<sup>-1</sup> or 200 to 25 000 ng l<sup>-1</sup> for influent, and 20 to 2500 ng l<sup>-1</sup> or 100 to 12 500 ng l<sup>-1</sup> for effluent water, depending on the instrumental detection limit for the considered compound. The procedure was repeated on three different

days and matrix-matched calibration curves were constructed from the pre-spiked samples ( $n = 4$  concentration levels  $\times$  3 repetitions).

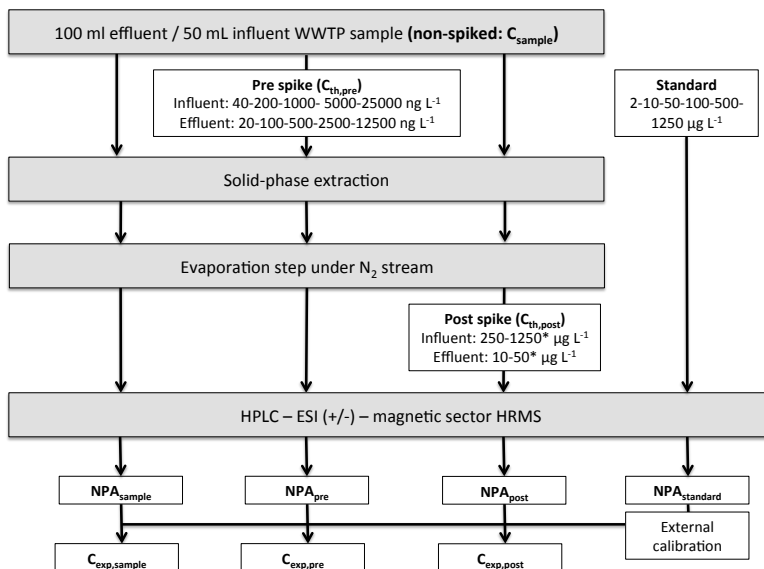


**Figure 3.2** Comprehensive scheme representing the procedure for method validation using pre-, post- and non-spiked WWTP influent and effluent samples, and for differentiation between matrix effects and SPE recoveries. \* The post-spiking levels were chosen depending on the instrumental detection limit for each compound.

The method interday repeatability (RSD, %) was determined from the triplicate SPE extraction and analysis of the pre-spiked samples, and method detection limits (MDLs) and method quantification limits (MQLs) were estimated from an average ( $n = 3$ ) S/N ratio of 3 and 10, respectively.

The methodology proposed by Matuszewski *et al.* (2003) was applied for the determination of the recovery (RE), matrix effect

(ME), and the overall 'process efficiency (PE)'. Recovery refers to the extraction efficiency of the SPE procedure (SPE extraction, drying and reconstitution) and has theoretically a value between 0 and 100%. A ME of 1 (i.e. 100%) is obtained when no matrix effects are present; and  $ME > 100\%$  and  $< 100\%$  represent signal enhancement and suppression, respectively. The overall 'process efficiency' refers to the combined effect of the recovery and matrix effects. For the determination of PE, the experimentally determined concentrations of the pre-spiked samples ( $C_{exp,pre}$ ), calculated using external calibration, were plotted as a function of the theoretical pre-spiked concentrations ( $C_{th,pre}$ ). The slope of this curve, determined by  $1/x^2$  weighted least squares regression, equals the PE (Equation 3.2a). ME and RE were determined using Equations 3.2b and 3.2c ( $C_{exp,sample}$  and  $C_{exp,post}$  represent the measured concentrations in the non-spiked and post-spiked samples, respectively). Finally, Equation 3.2d shows how the concentration present in non-spiked (or new) samples ( $C_{sample}$ ) is calculated from  $C_{exp,sample}$  by applying the PE after external calibration.

$$C_{exp,pre} = PE \cdot C_{th,pre} + C_{exp,sample} \quad (3.2a)$$

$$C_{exp,pre} = ME \cdot C_{th,post} + C_{exp,sample} \quad (3.2b)$$

$$PE = RE \cdot ME \quad (3.2c)$$

$$C_{exp,sample} = PE \cdot C_{sample} \quad (3.2d)$$

The standard deviation on the PE ( $\sigma_{PE}$ ) was determined by the R 2.14.1 software ([www.r-project.org](http://www.r-project.org)) using Equation 3.3a, and the

standard deviation on the ME ( $\sigma_{ME}$ ) was calculated applying the propagation of variance theory (Equation 3.3b).

$$\sigma_{PE} = \sqrt{\frac{1}{n-2} \sum_{i=1}^n e_i \cdot w_i^2} \quad (3.3a)$$

$$\sigma_{ME} = \frac{1}{C_{th,post}} \sqrt{\sigma_{C_{exp,post}}^2 + \sigma_{C_{exp,sample}}^2} \quad (3.3b)$$

where  $w_i$  is the applied weight and equals to  $1/x_i^2$ , with  $x_i$  the  $i^{th}$  concentration, and  $e_i$  is the difference between the calibration curve and the  $i^{th}$   $C_{exp,pre}$ .

### 3.2.5 First tier environmental risk assessment

The effluent of WWTP2 is discharged into a creek and subsequently into the river Dender, Belgium, for which flow data are available. The environmental risk posed by the discharged pharmaceuticals was assessed by means of the risk quotient (RQ), being the ratio between the measured environmental concentration (MEC) and the predicted no-effect concentration (PNEC). Since no river water was analyzed, quasi-MECs of the compounds quantified in the effluent were estimated according to Grung *et al.* (2008) by considering a dilution factor of 41, calculated from the average effluent flow of WWTP2 (Table 3.1) and the dry weather flow of the river Dender of about  $10 \text{ m}^3 \text{ s}^{-1}$  (Waterbouwkundig Laboratorium Belgium, 2013). PNEC values were based on ecotoxicity data and calculated according to the European Medicine Agency (2005, EMEA/CHMP/SWP/4447/00 guideline).



## 3.3 Results and discussion

### 3.3.1 Method development and optimization

#### 3.3.1.1 Instrumental analysis

First, the chromatographic conditions for both the ESI positive and negative ion mode were optimized using  $2\text{ mg l}^{-1}$  analytical standards and operating the MS in unit-resolution full-spectrum mode. Methanol and acetonitrile were tested as organic modifier with formic acid (0.1 %) initially only in the aqueous phase. In ESI positive ion mode, methanol showed clearly improved peak areas (factor 1.3 to 6.5) for most of the compounds, except for acyclovir (factor 0.4). When using acetonitrile as organic modifier, intense acetonitrile clusters were found in the spectra especially for the quinolone antibiotics, which may explain at least partially the reduced peak areas under this condition. Moreover, addition of 0.1 % formic acid in both phases improved the peak areas for most of the compounds (up to a factor 4.4) except for the quinolones, which showed reduced peak areas (ranging from a factor 0.27 to 0.96). Therefore, addition of 0.1 % formic acid showed to be a good compromise. In ESI negative ion mode, acetonitrile without additives was the organic modifier of choice because both methanol and additives such as formic acid caused corona discharge at the ESI spray tip. The optimal gradients showed satisfactory peak separation allowing the development of the retention time windows for the MID methods.

Finally, for the compounds measurable in both ESI positive and negative ion mode, the most sensitive mode was chosen, and MID windows were constructed as presented in Table 3.2. The linearity and

stability of the detector were investigated and the results for the RSDs are given in Table 3.4. Weighted regression analysis ( $1/x^2$  weighting) using a statistical F-test for lack of fit pointed out that a quadratic calibration curve fitted significantly better the calibration data for 14 out of the 43 compounds ( $p < 0.05$ ). Therefore, quadratic calibration curves were used for all the compounds. Intraday precision of the NPA was better than 20 and 10 % for 90 % of the compounds at the lowest and the highest tested concentration level (20 and 2000  $\mu\text{g l}^{-1}$ ), respectively. Interday repeatability (100  $\mu\text{g l}^{-1}$ ) of the NPA was better than 30 % RSD for 90 % of the compounds, showing the need for daily external calibration.

### **3.3.1.2 Optimization of the solid-phase extraction procedure**

For the optimization of the SPE, a total of 6 parameters of the SPE extraction protocol were varied and the optimal conditions (bold, Table 3.5) were selected. The SPE optimization experiments were performed on WWTP effluent samples pre-spiked (standard addition) at an environmental relevant concentration level of 100  $\text{ng l}^{-1}$ .

The effects of the different conditions on the process efficiency (PE) and the precision (RSD on  $\text{NPA}_{pre}$ ,  $n = 3$ ) were assessed for the 16 compounds measured with the MID 1 method (the effect of the loading volume was investigated for all 43 compounds). The most remarkable effects are discussed, taking into consideration that a compromise on the final conditions has to be reached because often no condition was optimal for all analytes. Washing the SPE cartridge after sample loading with 24 ml of water enhanced the PE for 12 out of the 16 compounds. On

the other hand, washing the cartridge with 12 ml of 2.5 % of methanol in water increased clearly the RSD of the measurements, indicating a decreased precision of the SPE extraction.

Silanized glass tubes for the evaporation of the extract showed increased PEs for 12 of the 16 compounds whereas the use of polystyrene tubes clearly reduced the precision: the RSDs increased from on average  $14\pm 9\%$  to  $69\pm 16\%$ . For the elution step, ethyl acetate resulted in lower PEs and increased RSDs for the 16 compounds. Elution with 5 ml instead of 10 ml methanol resulted in a small decrease of the PE (maximal 20 %) for 12 of the 16 compounds, however the precision improved with RSDs decreasing from  $19\pm 7\%$  to  $9\pm 8\%$ . No important trends were seen for the pH of the sample and for the effect of temperature during the extract evaporation. Increasing the loading volume from 50 ml to 250 ml and 500 ml reduced the PE for almost all the compounds. A loading volume of 100 ml resulted in a reduction of the PE with a median value of 5 %. For influent samples, in order to protect the HPLC column for a too high load (precipitates were present in the extract when 100 ml influent was loaded onto the cartridge), 50 ml sample volume was selected.

Thus, in the final SPE procedure 100 and 50 ml of influent and effluent samples, respectively, at pH 7 are loaded onto Oasis HLB cartridges, subsequently washed with 24 ml of water, and finally eluted in 5 ml of methanol. The evaporation of the extract is performed in silanized glass tubes at 25 °C.

### 3.3.2 Method validation and quality assessment

MDLs were lower than  $100 \text{ ng l}^{-1}$  for 27 and 34 out of the 43 target pharmaceuticals for influent and effluent, respectively. Even at the lowest detectable concentration, the RSD on the peak area was better than 20 % for 90 % of the compounds in both types of wastewater (Tables 3.6 and 3.7). The PE for most of the compounds ranged from 60 to 140 % (European Union, 2009, SANCO/10684/2009 guideline), except for acyclovir, amoxicillin, chloramphenicol, fluoxetine, lamivudine, oxytetracycline, paracetamol, paroxetine, pleconaril, temazepam and triclosan in one of both matrices.

#### 3.3.2.1 The process efficiency unravelled: extraction recovery and matrix effects

The decomposition of PE into RE and ME (Equations 3.2a to 3.2d and Figure 3.3) allows to differentiate whether PE values differing from 100 % result from low SPE recovery and/or matrix signal suppression/enhancement. For influent and effluent water, the recovery was higher than 80 % for 37 and 34 out of the 43 compounds, respectively. Figure 3.4 shows that low recoveries can occur for very polar or hydrophilic compounds such as acyclovir, amoxicillin and lamivudine ( $\log K_{ow}$  from -1.59 to 0.06) and for very lipophilic compounds such as pleconaril ( $\log K_{ow} > 5$ ). On the other hand, tetracycline, oxytetracycline, zidovudine and metronidazole have  $\log K_{ow} < 0$  but SPE recoveries  $> 95\%$  indicating that also other parameters than  $K_{ow}$ , such as charge or other specific interactions, can affect the analyte behaviour during Oasis HLB SPE. For example,

**Table 3.4** Instrumental precision: intraday repeatability ( $n = 3$ ) and interday repeatability ( $n = 5$ ) as % RSD at different concentration levels ( $\mu\text{g l}^{-1}$ ).

Analyte	Intraday RSD				Interday RSD $100 \mu\text{g l}^{-1}$
	20	100	500	2000	
Acyclovir	19	10	1	16	23
Alprazolam	8	2	1	2	23
Amantadine	9	6	7	7	18
Amitriptyline	39	5	3	10	25
Amoxicillin	14	8	9	12	19
Besifloxacin	13	4	2	2	29
Carbamazepine	3	9	3	2	19
Chloramphenicol	18	2	2	2	49
Ciprofloxacin	11	3	8	2	21
Diazepam	10	11	1	2	19
Diclofenac	12	2	1	1	20
Efavirenz	5	4	4	6	15
Enrofloxacin	15	7	6	8	24
Flumequine	6	4	3	6	28
Fluoxetine	10	4	5	4	21
Gatifloxacin	13	14	9	10	13
Ibuprofen	5	5	7	6	17
Indomethacin	4	3	5	3	20
Lamivudine	9	3	2	1	23
Levofloxacin	20	13	6	9	23
Metronidazole	4	9	11	10	35
Moxifloxacin	3	10	2	7	15
Nalidixic acid	16	6	2	3	15
Naproxen	6	8	4	2	3
Nevirapine	42	23	5	2	22
Oseltamivir acid	8	6	2	5	14
Oseltamivir ethylester	5	4	2	4	21
Oxytetracycline	3	14	7	4	28
Paracetamol	5	4	6	6	24
Paroxetine	6	10	11	8	22
Pleconaril	6	1	2	3	22
Rimantadine	9	10	5	7	26
Risperidone	11	6	10	4	52
Sarafloxacin	6	14	5	2	14
Sulfadoxin	9	1	4	6	26
Sulfamethazine	26	17	2	6	19
Sulfamethoxazole	10	0	3	5	26
Temazepam	23	13	3	6	31
Tetracycline	8	11	6	8	18
Triclosan	4	8	6	8	14
Trimethoprim	15	8	3	5	23
Venlafaxine	13	1	2	1	18
Zidovudine	10	5	11	8	23

**Table 3.5** Overview of the different parameters varied during SPE optimization. The optimal condition for each parameter is highlighted in bold.

Washing volume (water)	Material of tube for drying	Elution solvent	Temperature during drying	sample pH	Volume of sample
no wash - 12 ml - 12 ml with 2.5% MeOH - <b>24 ml</b>	NS glass	10 ml MeOH	25 °C	7	100 ml
24 ml	NS glass - <b>S glass</b> - PS	10 ml MeOH	25 °C	7	100 ml
24 ml	S glass	10 ml MeOH - 10 ml ethylAc - 5 ml MeOH + 5 ml ethylAc - <b>5 ml MeOH</b>	25 °C	7	100 mL
24 ml	S glass	5 ml MeOH	<b>25 °C</b> - 40 °C	7	100 ml
24 ml	S glass	5 ml MeOH	40 °C	<b>7</b> - 3	100 ml
24 ml	S glass	5 ml MeOH	25 °C	7	<b>50 (Inf)</b> - 100 ( <b>Eff</b> ) - 250-500 ml

NS: not-silanized

S: silanized

PE: polystyrene

MeOH: methanol

ethylacetate: ethylAc

**Table 3.6** Parameters of the method validation indicating the performance of the analytical method for the analysis of the 43 pharmaceuticals in WWTP influent.

Analyte (quality label)	% RSD ( $n = 3$ ) at different spiking levels ( $\text{ng l}^{-1}$ )					MDL ( $\text{ng l}^{-1}$ , $n = 3$ )	MQL ( $\text{ng l}^{-1}$ , $n = 3$ )	% PE $\pm\sigma$	$C_{\text{sample}}$ ( $\text{ng l}^{-1}$ , $n = 3$ )
	40	200	1000	5000	25 000				
Acyclovir (B)	n.a.	n.d.	n.d.	n.d.	n.d.	> 25 000	> 25 000	0.4 $\pm$ 0.1	n.d.
Alprazolam (A)	4	16	17	3	n.a.	18	60	84 $\pm$ 3	n.d.
Amandatine (A)	12	17	26	5	n.a.	0.5	1.8	97 $\pm$ 5	1.3 $\pm$ 0.3
Amitriptyline (A)	6	13	7	4	n.a.	10	35	93 $\pm$ 3	40 $\pm$ 2
Amoxicillin (B)	n.a.	n.d.	n.d.	n.d.	n.d.	> 25 000	> 25 000	13 $\pm$ 10	n.d.
Besifloxacin (A)	n.a.	5	15	13	6	60	201	99 $\pm$ 4	n.d.
Carbamazepine (A)	4	6	15	2	n.a.	39	129	99 $\pm$ 4	305 $\pm$ 41
Chloramphenicol (A)	11	11	9	6	n.a.	13	44	62 $\pm$ 2	n.d.
Ciprofloxacin (A)	n.a.	6	5	7	5	75	250	90 $\pm$ 3	342 $\pm$ 12
Diazepam (A)	10	8	11	3	n.a.	5.7	19	97 $\pm$ 3	n.d.
Diclofenac (A)	5	12	11	8	n.a.	35	118	87 $\pm$ 4	316 $\pm$ 16
Efavirenz (A)	n.a.	5	7	6	10	126	419	81 $\pm$ 4	n.d.
Enrofloxacin (A)	n.a.	4	6	10	3	76	252	96 $\pm$ 4	n.d.
Flumequine (A)	n.a.	23	14	4	8	159	529	108 $\pm$ 7	n.d.
Fluoxetine (A)	n.a.	6	13	23	11	8.6	29	69 $\pm$ 4	17 $\pm$ 2
Gatifloxacin (A)	n.a.	8	9	9	4	52	175	98 $\pm$ 4	n.d.
Ibuprofen (A)	n.a.	16	9	5	5	312	1051	90 $\pm$ 6	1039 $\pm$ 399
Indomethacin (A)	n.a.	14	12	8	10	81	269	87 $\pm$ 5	n.d.
Lamivudine (B)	n.a.	15	28	27	10	58	192	48 $\pm$ 4	n.d.
Levofloxacin (A)	n.a.	5	11	9	3	57	189	100 $\pm$ 4	413 $\pm$ 41
Metronidazole (A)	n.a.	18	20	28	6	25	84	82 $\pm$ 6	24 $\pm$ 4
Moxifloxacin (A)	n.a.	18	10	20	2	35	118	83 $\pm$ 5	317 $\pm$ 41
Nalidixic acid (A)	n.a.	19	14	14	11	198	661	109 $\pm$ 7	n.d.
Naproxen (A)	n.a.	13	14	5	4	689	2295	85 $\pm$ 4	1555 $\pm$ 285

**Table 3.6** (continued)

Analyte (quality label)	% RSD ( $n = 3$ ) at different spiking levels ( $\text{ng l}^{-1}$ )						MDL ( $\text{ng l}^{-1}$ , $n = 3$ )	MQL ( $\text{ng l}^{-1}$ , $n = 3$ )	% PE $\pm\sigma$	$C_{\text{sample}}$ ( $\text{ng l}^{-1}$ , $n = 3$ )
	40	200	1000	5000	25000					
Nevirapine (A)	n.d.	21	8	10	n.a.	220	732	99 $\pm$ 5	n.d.	
Oseltamivir acid (A)	n.a.	8	18	20	6	437	1457	101 $\pm$ 5	n.d.	
Oseltamivir ethylester (A)	n.a.	4	38	16	8	88	294	70 $\pm$ 7	57 $\pm$ 9	
Oxytetracycline (A)	n.a.	n.d.	47	9	5	592	1974	81 $\pm$ 7	n.d.	
Paracetamol (B)	n.a.	3	7	14	4	1217	4057	26 $\pm$ 27	385 868 $\pm$ 409 023	
Paroxetine (A)	n.a.	13	26	4	8	202	674	74 $\pm$ 5	n.d.	
Pleconaril (B)	n.a.	n.d.	n.d.	n.d.	n.d.	> 25 000	> 25 000	13 $\pm$ 7	n.d.	
Rimantadine (A)	11	15	27	14	n.d.	1.4	4.5	75 $\pm$ 5	n.d.	
Risperidone (A)	n.a.	8	11	13	3	44	147	100 $\pm$ 6	n.d.	
Sarafloxacin (A)	n.a.	9	8	7	1	41	137	90 $\pm$ 4	n.d.	
Sulfadoxin (A)	n.a.	10	17	18	5	17	55	91 $\pm$ 4	n.d.	
Sulfamethazine (A)	n.d.	27	14	7	n.a.	73	243	79 $\pm$ 7	n.d.	
Sulfamethoxazole (A)	20	5	8	8	n.a.	50	168	84 $\pm$ 4	n.d.	
Temazepam (B)	n.a.	6	12	7	10	61	203	354 $\pm$ 16	n.d.	
Tetracycline (A)	n.a.	9	4	12	5	295	985	122 $\pm$ 5	1371 $\pm$ 200	
Triclosan (A)	n.a.	1	8	2	3	350	1167	62 $\pm$ 1	n.d.	
Trimethoprim (A)	n.a.	11	16	17	3	28	93	101 $\pm$ 5	111 $\pm$ 8	
Venlafaxine (A)	5	10	9	6	n.a.	13	44	94 $\pm$ 4	454 $\pm$ 18	
Zidovudine (A)	n.a.	13	13	12	11	142	473	85 $\pm$ 3	n.d.	

n.d.: not detected (< MDL)

n.a.: data not available



**Table 3.7** Parameters of the method validation indicating the performance of the analytical method for the analysis of the 43 pharmaceuticals in WWTP effluent.

Analyte (quality label)	% RSD ( $n = 3$ ) at different spiking levels ( $\text{ng l}^{-1}$ )						MDL ( $\text{ng l}^{-1}$ , $n = 3$ )	MQL ( $\text{ng l}^{-1}$ , $n = 3$ )	% PE $\pm\sigma$	$C_{\text{sample}}$ ( $\text{ng l}^{-1}$ , $n = 3$ )
	20	100	500	2500	12500	43				
Acyclovir (B)	n.a.	n.d.	n.d.	n.d.	n.d.	43	9572	31906	0.22 $\pm$ 0.04	n.d.
Alprazolam (A)	3	4	2	1	1	n.a.	6.6	22	84 $\pm$ 1	12 $\pm$ 3
Amandatine (A)	2	2	8	1	1	n.a.	2.4	8.1	87 $\pm$ 1	n.d.
Amtripyline (A)	5	16	7	4	4	n.a.	8.1	27	81 $\pm$ 4	31 $\pm$ 2
Amoxicillin (B)	n.a.	n.d.	n.d.	n.d.	n.d.	17	9023	30076	5 $\pm$ 1	n.d.
Besifloxacin (A)	n.a.	29	22	8	8	3	38	128	80 $\pm$ 6	n.d.
Carbamazepine (B)	2	7	6	2	2	n.a.	97	323	66 $\pm$ 21	3208 $\pm$ 1085
Chloramphenicol (B)	6	12	1	7	7	n.a.	11	36	38 $\pm$ 1	n.d.
Ciprofloxacin (A)	n.a.	24	21	4	4	2	31	102	84 $\pm$ 7	45 $\pm$ 8
Diazepam (A)	9	9	5	3	3	n.a.	3.1	10	92 $\pm$ 2	6.1 $\pm$ 0.4
Diclofenac (A)	3	11	9	4	4	n.a.	17	57	72 $\pm$ 4	1011 $\pm$ 64
Efavirenz (A)	n.a.	2	13	8	8	6	40	132	70 $\pm$ 3	n.d.
Enrofloxacin (A)	n.a.	13	18	4	4	4	50	166	84 $\pm$ 6	n.d.
Flumequine (A)	n.a.	7	11	8	8	3	59	195	102 $\pm$ 3	n.d.
Fluoxetine (B)	n.a.	8	34	6	6	5	11	37	57 $\pm$ 4	n.d.
Gatifloxacin (A)	n.a.	9	6	5	5	3	23	76	88 $\pm$ 5	n.d.
Ibuprofen (A)	n.a.	n.d.	6	8	8	7	140	466	97 $\pm$ 3	n.d.
Indomethacin (A)	n.a.	12	7	7	7	8	80	267	72 $\pm$ 2	n.d.
Lamivudine (B)	n.a.	5	7	3	3	16	55	184	23 $\pm$ 2	n.d.
Levofloxacin (A)	n.a.	10	15	3	3	3	20	68	88 $\pm$ 5	45 $\pm$ 9
Metronidazole (A)	n.a.	5	4	3	3	4	12	40	93 $\pm$ 3	n.d.
Moxifloxacin (A)	n.a.	15	7	4	4	4	11	35	77 $\pm$ 8	281 $\pm$ 71
Nalidixic acid (A)	n.a.	17	26	12	12	16	86	287	73 $\pm$ 5	n.d.
Naproxen (A)	n.a.	n.d.	11	4	4	4	345	1149	90 $\pm$ 3	n.d.

Table 3.7 (continued)

Analyte (quality label)	% RSD ( $n = 3$ ) at different spiking levels ( $\text{ng l}^{-1}$ )					MDL ( $\text{ng l}^{-1}$ , $n = 3$ )	MQL ( $\text{ng l}^{-1}$ , $n = 3$ )	% PE $\pm\sigma$	$C_{\text{sample}}$ ( $\text{ng l}^{-1}$ , $n = 3$ )
	20	100	500	2500	12500				
Nevirapine (A)	n.d.	9	3	4	n.a.	77	256	97 $\pm$ 3	n.d.
Oseltamivir acid (A)	n.a.	n.d.	14	11	2	106	354	90 $\pm$ 7	n.d.
Oseltamivir ethylester (A)	n.a.	6	6	1	3	6.9	23	87 $\pm$ 2	n.d.
Oxytetracycline (B)	n.a.	n.d.	n.d.	17	3	1119	3731	49 $\pm$ 11	n.d.
Paracetamol (A)	n.a.	13	4	4	1	60	200	87 $\pm$ 2	n.d.
Paroxetine (B)	n.a.	21	21	7	2	74	248	59 $\pm$ 5	n.d.
Pleconaril (B)	n.a.	n.d.	n.d.	12	20	1319	4397	14 $\pm$ 3	n.d.
Rimantadine (A)	4	9	2	9	n.a.	0.43	1.4	82 $\pm$ 3	n.d.
Risperidone (A)	n.a.	9	18	9	4	39	129	65 $\pm$ 6	n.d.
Sarafloxacin (A)	n.a.	14	11	6	4	25	83	76 $\pm$ 7	n.d.
Sulfadoxin (A)	n.a.	2	2	12	1	18	61	77 $\pm$ 2	n.d.
Sulfamethazine (A)	n.d.	4	9	3	n.a.	46	154	75 $\pm$ 3	n.d.
Sulfamethoxazole (A)	7	4	6	2	n.a.	26	86	77 $\pm$ 2	54 $\pm$ 6
Temazepam (B)	n.a.	1	10	7	5	6.0	20	160 $\pm$ 5	n.d.
Tetracycline (A)	n.a.	n.d.	6	5	1	161	538	109 $\pm$ 4	n.d.
Triclosan (B)	n.a.	n.d.	14	18	7	203	675	55 $\pm$ 5	n.d.
Trimethoprim (A)	n.a.	3	6	7	2	59	197	94 $\pm$ 2	34 $\pm$ 2
Venlafaxine (A)	4	6	4	5	n.a.	2.7	9.1	98 $\pm$ 4	744 $\pm$ 109
Zidovudine (A)	n.a.	7	5	2	2	28	92	86 $\pm$ 2	n.d.

n.d.: not detected (< MDL)

n.a.: data not available

Prasse *et al.* (2010) obtained recoveries between 76% and 116% for acyclovir and lamivudine when using a hydroxylated polystyrene-divinylbenzene polymer at pH 8 (Isolute ENV+). Matrix effects were < 80% and > 120%, respectively, for 20 and 3 compounds in effluent, and for 11 and 2 compounds in influent, showing their importance in PE for ESI analysis of complex waters.

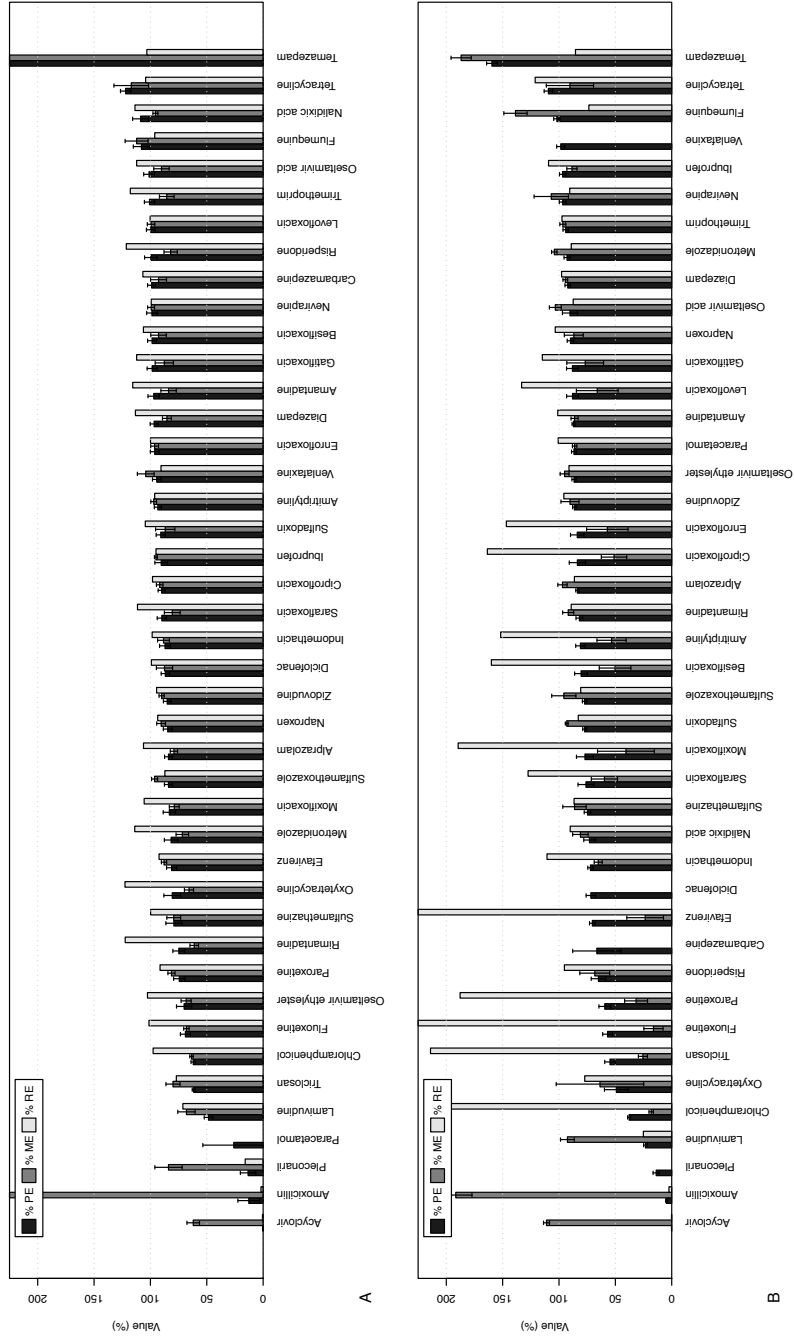


**Figure 3.3** Decomposition of the process efficiency (PE) in matrix effects (ME) and SPE recovery (RE) for (A) WWTP influent and (B) effluent water. The error bars represent 1 standard deviation. The compounds are ordered by increasing PE.

It should be denoted that the precision on the estimated RE and ME for 18 and 6 compounds, respectively, was higher than 20% RSD in effluent, whereas this was only the case for 1 compound in influent. The reason can mainly be accounted to the lower post-spiking concentration applied for the validation of the effluent. A more in-depth variability analysis is performed in Section 3.3.2.2.

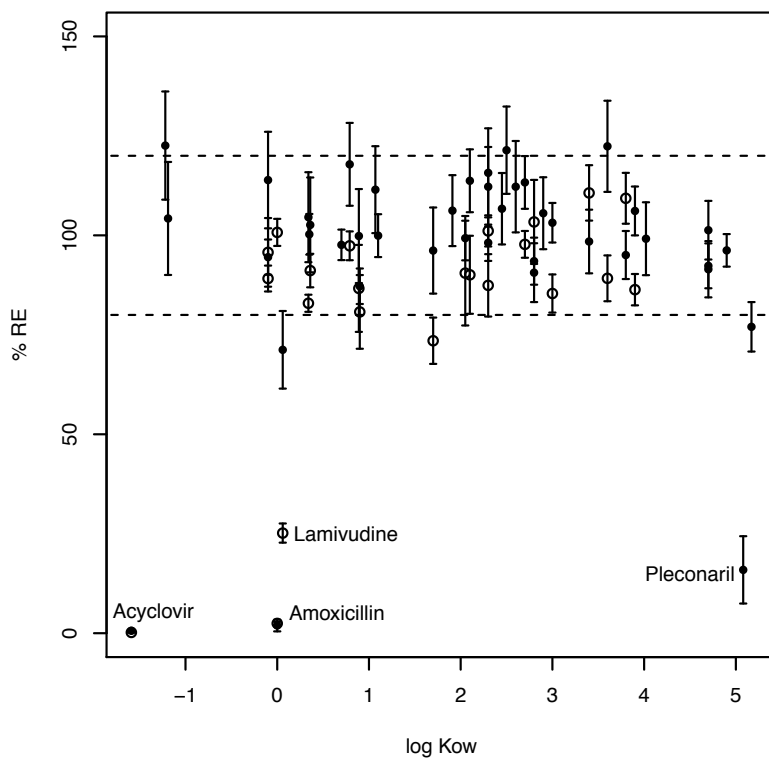


**Figure 3.4** SPE recoveries (RE) in the 80-120% range were obtained for all the analytes for (●) influent and (○) effluent water, except for some polar ( $\log K_{ow} \leq 0$ ) and apolar ( $\log K_{ow} \geq 5$ ) analytes. Only RE values with standard deviation  $< 20\%$  are plotted.

### **3.3.2.2 Variability analysis**

Validating an analytical method for compounds being ubiquitously present in environmental matrices such as wastewater can be problematic regarding at least two aspects.

The first aspect is related to the determination of the MDL/MQL values. Some compounds were clearly present ( $S/N$  ratios  $\gg 10$ ) in the non-spiked validation samples at elevated concentrations (e.g.  $> 1 \mu\text{g l}^{-1}$  for ibuprofen, naproxen, paracetamol and tetracycline in influent). Validating the method for such compounds at lower concentrations is not possible using the standard addition (pre-spiking) technique because truly blank matrix samples are hard to find. As such, extrapolation to a  $S/N$  level of 3 and 10 is required for the estimation of the MDL and MQL, respectively, and therefore the uncertainty on these values is expected to be high.

The second aspect is related to the precise determination of PE. The concentration of the spiking level must be high enough (Section 3.3.2.1) to obtain a PE with precision better than 20% RSD. For example, although the method was repeatable for paracetamol in influent and for carbamazepine in effluent water (precision on peak area  $< 14\%$  and  $7\%$  RSD, respectively), very elevated RSDs were obtained for the determination of the PE (105% and 36% RSD, respectively) due to their high concentration in the non-spiked validation sample, being much higher than the highest spiking level. This RSD propagates and results in high SDs for the calculated concentration in the sample (e.g.  $386 \pm 409 \mu\text{g l}^{-1}$  for paracetamol in influent and  $3 \pm 1 \mu\text{g l}^{-1}$  for

carbamazepine in effluent). Considering the observed RSDs, the highest spiking concentration should at least be 3 to 5 times higher than the concentration in the non-spiked sample – which is, however, not a priori known – to enable a precise ( $\text{RSD} < 20\%$ ) PE determination. For example, the PE of venlafaxine in effluent was precisely  $98(4)\%$  determined and the highest spiking level ( $2.5 \mu\text{g l}^{-1}$ ) was 3.6 times higher than the concentration in the non-spiked sample ( $0.7 \pm 0.1 \mu\text{g l}^{-1}$ ;  $\text{RSD} < 15\%$ ).

These bottlenecks in method validation have to be taken into account when interpreting data and their variability. When applying the validated method to measure and calculate concentrations in influent and effluent samples (Section 3.3.3), three sources of variability have to be considered: (i) the HPLC-MS instrumental variability, (ii) the variability during SPE and (iii) the variability on the PE. The HPLC-MS and SPE variability are included and documented by the interday repeatability ( $\%$  RSD on peak area) as presented in Tables 3.6 and 3.7. When calculating concentrations from the obtained peak areas by external calibration, the PE values are used as correction factor and therefore, also their variability is important for data interpretation. To account for this, we propose the use of a quality labeling system. Compounds having a  $\text{RSD} < 20\%$  on a PE value ranging between 60 and 140% (European Union, 2009, SANCO/10684/2009 guideline) are labelled as class A, being referred to as ‘quantitative compounds’. Other compounds, whose results have larger variability and should be interpreted as ‘indicative’, are labelled as class B. A total of 37 (6) and

33 (10) of the 43 compounds were labelled as class A (B) for influent and effluent water, respectively.

### 3.3.3 Application in 2 WWTPs

#### 3.3.3.1 Concentrations and potential associated environmental risks

A total of 22 pharmaceuticals, belonging to the anti-inflammatory drugs, antiviral drugs, psychoactive drugs (antidepressants, tranquilizers, anti-epileptics), and antibiotics were detected (identification based on MID measurement and retention time) at least once in the influent or effluent of one of both WWTPs. Measured concentrations and detection/quantification frequencies in both matrices are presented as boxplots in Figure 3.5. Average concentrations are presented in Table 3.8 and 3.9. The discussion is mainly based on the 17 detected class A compounds.

Four anti-inflammatory drugs were detected in all influent samples and occurred at the highest concentrations ( $500 \text{ ng l}^{-1}$  to  $> 50 \text{ } \mu\text{g l}^{-1}$ ) amongst all measured pharmaceuticals. On the other hand, their effluent concentrations were in most of the cases below MDL (except for diclofenac). Four antiviral drugs were detected at least once. Amantadine was quantified in all influent and effluent samples and measured concentrations ranged from  $50 \text{ ng l}^{-1}$  to  $1 \text{ } \mu\text{g l}^{-1}$ . Ghosh *et al.* (2010) reported comparable influent concentrations ( $200\text{-}600 \text{ ng l}^{-1}$ ) for amantadine in WWTPs in Japan. A total of 3 antidepressants (venlafaxine, risperidone, and amitriptyline) and 2 tranquilizers (alprazolam and temazepam) were found at concentrations varying



**Table 3.8** Average influent and effluent concentrations ( $\text{ng l}^{-1}$ ), mass balance and removal efficiencies for the pharmaceuticals detected in WWTP1.

Substance	Influent CAS+MBR <sup>a</sup> (n=4)	Effluent CAS <sup>a</sup> (n=4)	Effluent MBR <sub>a</sub> (n=4)	Effluent TOT <sup>a</sup> (n=4)	Mass balance <sup>b</sup>	% removal CAS <sup>c</sup>	% removal MBR <sup>c</sup>
Amanatadine	44±8(4)	54±5(4)	53±4(4)	55±6(4)	1.0±0.1(4)	-22	-20
Amitriptyline	b.l.q.	n.d.	b.l.q.	n.d.			
Carbamazepine (B)	462±72(4)	460±32(4)	468±42(4)	481±40(4)	1.0±0.1(4)	2	-1
Ciprofloxacin	278±(1)	120±(1)	121±19(3)	107±4(3)	0.8±(1)	-24	-10
Diclofenac	507±82(4)	623±59(4)	559±78(4)	542±73(4)	0.9±0.1(4)	>98	>98
Ibuprofen	5711±513(4)	b.l.q.	n.d.	n.d.			
Levofloxacin	n.d.	b.l.q.	b.l.q.	b.l.q.			
Metronidazole	b.l.q.	b.l.q.	b.l.q.	b.l.q.			
Moxifloxacin	149±17(3)	62±26(4)	66±29(4)	62±39(4)	1.0±0.4(4)	62	56
Naproxen	4110±(1)	b.l.q.	n.d.	n.d.			
Paracetamol (B)	67 107±8026(4)	n.d.	n.d.	b.l.q.		>99.9	>99.9
Paroxetine (B)	n.d.	b.l.q.	n.d.	b.l.q.			
Rimantadine	b.l.q.	b.l.q.	2±(1)	b.l.q.			
Sulfamethoxazole	245±15(4)	133±5(3)	124±16(4)	121±2(3)	1.0±0.1(3)	50	49
Trimethoprim	158±17(4)	n.d.	n.d.	n.d.		>62	>62
Venlafaxine	219±22(4)	208±22(4)	213±21(4)	205±17(4)	1.0±0.1(4)	5	3

<sup>a</sup> Concentration ( $\text{ng l}^{-1}$ ) ± standard deviation (number of quantifications).

<sup>b</sup> The mass balance over the effluent loads is calculated for each day, and the average of the  $\frac{TOT}{MBR+CAS}$  ratios and its standard deviation (number of data points) are given.

<sup>c</sup> Removal efficiencies are only calculated if the quantification frequency for the influent is > 50 %.

n.d. = not detected (< MDL)

b.l.q. = below limit of quantification (between MDL and MQL).

**Table 3.9** Average influent and effluent concentrations ( $\text{ng l}^{-1}$ ) and removal efficiencies for the pharmaceuticals detected in WWTP2.

Substance	Influent <sup>a</sup> (n=6)	Effluent <sup>a</sup> (n=6)	% removal <sup>b</sup>
Alprazolam	n.d.	23±1(2)	
Amantadine	326±394(6)	592±325(6)	-109
Amitriptyline	83±59(4)	n.d.	>90
Carbamazepine (B)	708±69(6)	741±83(6)	-17
Ciprofloxacin	978±380(6)	104±(1)	>97
Diclofenac	1450±366(6)	1391±163(6)	-2
Ibuprofen	7847±1239(6)	b.l.q.	>98
Lamivudine (B)	507±80(5)	n.d.	>89
Levofloxacin	335±112(6)	70±(1)	>94
Metronidazole	86±1(2)	b.l.q.	
Moxifloxacin	688±197(6)	1253±1628(6)	75(day1-3); -161(day4-6)
Naproxen	2374±76(2)	n.d.	
Oseltamivir ethylester	b.l.q.	n.d.	
Paracetamol (B)	56 172±9430(6)	n.d.	>99.9
Risperidone	364±28(6)	154±12(3)	64
Sulfamethoxazole	429±39(6)	250±90(6)	32
Temazepam (B)	b.l.q.	104±16(6)	
Tetracycline	1658±807(6)	n.d.	>90
Trimethoprim	228±32(6)	n.d.	>79
Venlafaxine	403±38(6)	365±58(6)	-3

<sup>a</sup> Concentration ( $\text{ng l}^{-1}$ ) ± standard deviation (number of quantifications).

<sup>b</sup> Removal efficiencies are only calculated if the quantification frequency for the influent is > 50 %.

n.d. = not detected (< MDL)

b.l.q. = below limit of quantification (between MDL and MQL).

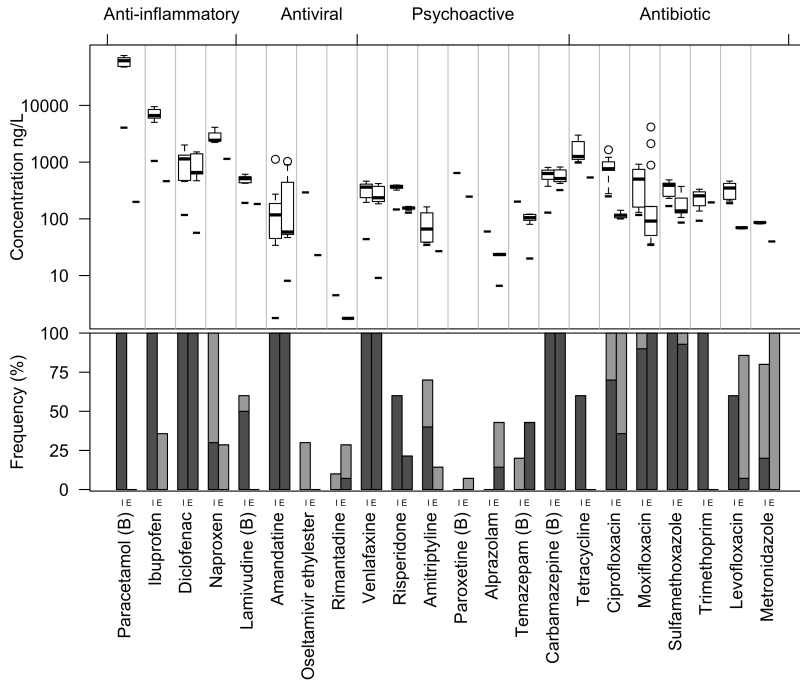


**Figure 3.5** Boxplots of the measured influent (I) and effluent (E) concentrations and the detection (gray) / quantification (black) frequencies based on all measured data for both WWTPs. The compounds are ordered by therapeutic class and the MQL values are indicated (–) in the box plots.

from 40 to 450 ng l<sup>-1</sup> in influent and from 20 to 420 ng l<sup>-1</sup> in effluent. According to the authors' knowledge, no other studies quantified risperidone in WWTPs. Paroxetine was detected in effluent below MQL. Carbamazepine, an anti-epileptic drug, was found at concentrations between 430 and 820 ng l<sup>-1</sup> in both influent and effluent. Finally, seven antibiotics were measured at concentrations (37-4200 ng l<sup>-1</sup>) similar as recently reviewed by Verlicchi *et al.* (2012).

Reported PNEC values and calculated environmental RQs of the compounds quantified in the WWTP2 effluent are presented in Table 3.10. No ecotoxicological data were found in open literature for alprazolam, amantadine and risperidone. According to the frequently applied risk classification (Hernando *et al.*, 2006), diclofenac and venlafaxine showed ‘high’ risk ( $RQ > 1$ ) to the environment, while the fluoroquinolone antibiotics ciprofloxacin and moxifloxacin indicated medium environmental risk ( $0.1 < RQ < 1$ ). Comparable ‘high’ risk was concluded in other studies for diclofenac (Hernando *et al.*, 2006).

### 3.3.3.2 Loads and elimination

The measured concentrations (Tables 3.8 and 3.9) and the wastewater flows (Table 3.1) are multiplied to calculate pharmaceutical loads ( $\text{g d}^{-1}$ ) and removal efficiencies. Comparing both WWTPs and the CAS versus MBR processes in WWTP1 only marginal differences are noticed. Regardless the technology (MBR or CAS), removal efficiencies better than 98% were observed for the most prevalent compounds belonging to the anti-inflammatory drugs (ibuprofen and paracetamol). In WWTP2, removal efficiencies were also  $> 90\%$  for amitriptyline, ciprofloxacin, lamivudine, levofloxacin and tetracycline. On the other hand, compounds such as carbamazepine, diclofenac and venlafaxine were clearly persistent ( $< 5\%$  removal). Moxifloxacin, risperidone and sulfamethoxazole were removed with efficiencies between 32 and 75%. Amantadine had a total effluent load higher than the influent load (‘negative’ removal) in both WWTPs, which was possibly due to desorption from suspended solids present in the influent ( $\log K_{ow}$

**Table 3.10** PNECs (literature data), quasi-MECs and RQs (mean and maximal values) for the quantified pharmaceuticals discharged from WWTP2 into the river Dender, Belgium.

Substance	Most sensitive taxon (acute/ chronic ecotoxicity data)	PNEC (ng l <sup>-1</sup> )	Quasi-MEC (ng l <sup>-1</sup> )		RQ		Risk level
			Mean	Max	Mean	Max	
Carbamazepine (B)	crustacean (chronic)	250 (Ferrari <i>et al.</i> , 2004)	18	20	7.10 <sup>-2</sup>	8.10 <sup>-2</sup>	low
Ciprofloxacin	algae (acute)	5 (Grung <i>et al.</i> , 2008)	- <sup>d</sup>	3	- <sup>d</sup>	5.10 <sup>-1</sup>	medium
Diclofenac	fish (subchronic)	5 (Hoeger <i>et al.</i> , 2005)	34	37	7	7	high
Levofloxacin	bacteria (acute)	60 (Kümmerer & Henninger, 2003)	- <sup>d</sup>	2	- <sup>d</sup>	3.10 <sup>-2</sup>	low
Moxifloxacin	algae (acute)	780 <sup>a</sup> (Van Doorslaer <i>et al.</i> , 2014b)	31	102	4.10 <sup>-2</sup>	1.10 <sup>-1</sup>	medium
Sulfamethoxazole	algae (chronic)	18 (Grung <i>et al.</i> , 2008)	6	9	5.10 <sup>-2</sup>	8.10 <sup>-2</sup>	low
Temazepam (B)	not reported	4300 <sup>b</sup> (van der Aa <i>et al.</i> , 2013)	3	3	6.10 <sup>-4</sup>	7.10 <sup>-4</sup>	low
Venlafaxine	mollusc	0.313 <sup>c</sup> (Fong & Hoy, 2012)	9	10	28	33	high

<sup>a</sup> The concentration resulting in 50% effect (EC<sub>50</sub>) for the green micro-alga *P. subcapitata*, taking into account an assessment factor of 1000 according to the EMEA guidelines.

<sup>b</sup> PNEC value of oxazepam is used because both are benzodiazepines having similar metabolic pathways.

<sup>c</sup> PNEC replaced by the lowest observed effect concentration (LOEC) for freshwater snails.

<sup>d</sup> Only one data point available ( $n = 1$ ).

2.44 (Ghosh *et al.*, 2010)) rather than deconjugation (< 3.6 % human excretion as acetylamantadine (Bras *et al.*, 1998)). Similarly, for moxifloxacin (log  $K_{ow}$  2.49 (Dorival-García *et al.*, 2012)) higher effluent concentrations were measured in WWTP2 after rainfall events (day 4-6, Table 3.1) resulting in 'negative' removal (-160 %). Since moxifloxacin had removal efficiencies of 56-62 % (WWTP1) and 75 % (day 1-3, WWTP2) during dry weather conditions, desorption from the higher input of suspended solids after rainfall events probably caused the high effluent concentrations.

A mass balance was made over the loads of the combined and individual MBR and CAS effluents of WWTP1 (Table 3.8). No treatment processes occurred between these sampling points and therefore  $\frac{TOT}{CAS + MBR}$  is expected to be 1. This verification was possible for 7 compounds and the ratios were in the range of 0.8 to 1.2 for all the compounds on the different days, except for moxifloxacin (0.6 to 1.5). These results support the quality and applicability of the analytical method.

### 3.4 Conclusions

A novel method using SPE and HPLC coupled to magnetic sector HRMS, which has been applied here for the first time in quantitative water analysis, has been developed for the analysis of 43 pharmaceuticals in WWTP influent and effluent. Apart from prioritized pharmaceuticals, also drugs like antivirals are included, which have been considered only in a very limited number of environmental

studies. Method quality assessment and variability analysis showed some scarcely reported bottlenecks in validating a multi-residue method for compounds present at relatively high levels in non-spiked validation samples. True blank samples are hard to find for some pharmaceuticals, and the highest spiking concentration should be at least 3 to 5 times higher than that in the non-spiked sample for a precise determination of the process efficiency. In order to consider these bottlenecks when interpreting data obtained with the validated method, a quality labeling system is proposed taking into account both the process efficiency and its variability.

The method application revealed – to the author’s knowledge – one of the first data on the occurrence, loads and removal efficiencies of 22 pharmaceuticals in a parallel CAS-MBR and a CAS WWTP in Belgium. The presence of scarcely measured antiviral drugs, such as amantadine ( $50 \text{ ng l}^{-1}$  to  $1 \mu\text{g l}^{-1}$ ) and lamivudine ( $400$  to  $600 \text{ ng l}^{-1}$ ), and the antidepressant risperidone ( $150$  to  $400 \text{ ng l}^{-1}$ ) has been shown, and a first tier environmental risk assessment of the discharged pharmaceuticals indicated that the anti-inflammatory drug diclofenac ( $450 \text{ ng l}^{-1}$  to  $1.8 \mu\text{g l}^{-1}$ ) and the antidepressant venlafaxine ( $180$  to  $460 \text{ ng l}^{-1}$ ) posed a potential ‘high’ risk to the receiving river Dender, Belgium. No ecotoxicological data were found in open literature for alprazolam, amantadine and risperidone, which established the need for more research in order to better assess the risk of pharmaceutical residues in the environment.

# 4

## Accurate mass measurement, selective quantification and determination of detection limits

*Redrafted from:*

*L. Vergeynst, H. Van Langenhove, P. Joos & K. Demeestere (2013).  
Accurate mass determination, quantification and determination of  
detection limits in liquid chromatography - high-resolution Time-Of-  
Flight mass spectrometry: Challenges and practical solutions. Analytica  
Chimica Acta, 789:74–82.*



## 4.1 Introduction

Uniform guidelines for the data processing and validation of qualitative and quantitative multi-residue analysis using full-spectrum HRMS are scarce. Moreover, recent applications of HRMS instruments showed that a proper post-acquisition data processing and validation might be challenging in multi-residue screening and quantification (Kaufmann, 2009; Kaufmann & Butcher, 2006). Three points of interest with respect to accurate mass measurement, selective quantification and the determination of detection limits need specific attention and are investigated in this chapter.

A first challenge is the determination of the accurate mass of a detected trace. Different methodologies using either profile or centroid data can be followed to determine accurate masses. So far, the performance of the different methodologies has not been compared.

Proper quantification is a second challenge. For peak integration, extracted ion chromatograms (XICs) are constructed out of the total ion chromatogram (TIC) by defining a mass tolerance around the exact ion mass of the analytes (i.e. mass window width). Different researchers applied different mass window widths and tend to apply narrower mass windows to increase selectivity (Kaufmann & Butcher, 2006) thereby also affecting the methods sensitivity (Kaufmann *et al.*, 2007; Kellmann *et al.*, 2009). Although selectivity will benefit from increased resolving power of both the chromatographic separation and the mass spectrometry (Kaufmann *et al.*, 2007; Kellmann *et al.*, 2009),

it is not fully understood to what extent selectivity and sensitivity vary in function of the mass window width.

Validation of analytical methods using high-resolution mass spectrometers (HRMSs) is a third challenge, especially regarding the determination of detection and quantification limits (Van Loco *et al.*, 2007; Antignac *et al.*, 2003). The widespread concepts for their determination, such as those based on the determination of signal-to-noise (S/N) ratios, have shown in some cases not to be applicable for HRMS data (Kaufmann, 2009). Using narrow mass windows can lead to the situation where no or almost no noise can be detected anymore leading to questionable S/N ratios.

These three issues are investigated based on results obtained from a Time-of-Flight (TOF) HRMS for full-spectrum analysis on a set of 17 pharmaceuticals with masses in the wide  $m/z$  range (152-916 Da). The major bottlenecks and possible solutions are discussed. In particular, the mass accuracy and its variability as a function of ion signal intensity of different algorithms for the determination of accurate mass are investigated. Second, the effect of the mass window width on the sensitivity and selectivity is assessed for quantitative analysis in order to conclude an optimal mass window width. Third, a widely applicable strategy for the determination of decision limits and detection capabilities was developed, and the decision limits and detection capabilities for the 17 pharmaceuticals in surface water were determined as a proof of concept.

## 4.2 Experimental section

### 4.2.1 Chemicals

The set of 17 pharmaceutical standards and their respective suppliers are listed in Table A.2. Methanol, acetonitrile and formic acid were purchased from Biosolve (Valkenswaard, the Netherlands) and NaOH from Merck (Damstadt, Germany). Deionized water was produced using Q-Gard2 cartridges in a MilliQ-water system (Millipore, USA).

Individual stock solutions (storage at 4°C in the dark) of the pharmaceuticals were prepared on weight basis and dissolved in 10 ml of solvent (used solvents are listed in Table A.2) to a final concentration of 1 mg ml<sup>-1</sup>. Daily, a standard mix of the pharmaceuticals was prepared at a concentration of 10 µg l<sup>-1</sup> in deionized water and subsequent serial diluted to a final concentration of 5, 1, 0.5, 0.1, 0.05 and 0.01 µg l<sup>-1</sup> in deionized and surface water.

Spiked deionized water samples are used for the first and the second research question on accurate mass determination and the width of the mass windows. Spiked surface water samples are used for the proof of concept of the developed strategy for the determination of decision limits and detection capabilities.

### 4.2.2 Sampling and sample pretreatment

Surface water was collected in prerinsed amber glass bottles on the Maas (Namêche, Belgium) and stored at 4°C in the dark. Prior to standard addition, the surface water was filtered through 1.5 µm glass

microfiber filters (934-AH, Whatman). Subsequently, 0.1 % and 0.02 % (v/v) formic acid was added for analysis in electrospray ionization (ESI) positive and negative ion mode, respectively, which improved the chromatographic peak shapes.

### **4.2.3 Instrumentation**

The analysis were performed using the Waters Acquity ultra-high performance liquid chromatography (UHPLC) system (Waters, Milford, USA) equipped with autosampler (CT2777 Sample Manager, Waters, Milford, USA) with 250  $\mu$ l loop for large-volume injection (LVI) and coupled to a Xevo G2 QTOF mass spectrometer (MS) with an orthogonal ESI probe (Waters Corporation, Manchester, U.K.). Chromatographic separation was achieved with an Acquity UHPLC HSS T3 150 x 2.1 mm column with 1.8  $\mu$ m particle size supplied by Waters (Milford, USA) operated at 50 °C.

For analysis in ESI positive ion mode, the mobile phase used was (A) water/acetonitrile 98:2 (v/v) with 0.1 % formic acid and (B) acetonitrile with 0.1 % formic acid. In ESI negative ion mode, the mobile phase used was (A) water/acetonitrile 98:2 (v/v) with 0.01 % formic acid and (B) acetonitrile. The elution gradient for both modes started with 1 min isocratic at 3 % B at a flow rate of 450  $\mu$ l min<sup>-1</sup>, then increased linearly to 98 % B in 11 min. Then the flow rate was increased to 600  $\mu$ l min<sup>-1</sup> and the gradient was kept isocratic at 98 % B for 2 min and subsequently decreased to 3 % B in 2 min and finally, back to initial conditions in 3 min. The total time for the chromatographic analysis was 19 min. The first 1.6 min of the eluent was diverted to the waste to prevent clogging

of capillaries by organic or inorganic compounds present in the injected samples or build up of salts on the optics in the mass spectrometer. The sample injection volume of the autosampler was set at 400  $\mu\text{l}$ . Since the injection loop had a volume of 250  $\mu\text{l}$ , the effective sample injection volume was 250  $\mu\text{l}$ .

The QTOF-MS was equipped with two orthogonal ESI probes for the eluent and lock mass solution ionization, respectively, a linear quadrupole and a T-wave collision cell. Nitrogen from a nitrogen generator (Nitroflow, Parker, Cleveland, USA) was used as drying and nebulizing gas in the ESI source. The quadrupole was turned off letting through all  $m/z$  values without fragmentation. The mass spectrometer was operated at a resolving power of 20 000 at full width at half maximum (FWHM) (defined at  $m/z$  400) acquiring profile data over an  $m/z$  range of 50-1200 Da. The ESI parameters were optimized for both positive and negative ion mode by injection of analytical standard mixtures (Table 4.1). The used ESI mode for each pharmaceutical compound as well as the respective exact ion mass are listed in Table A.2.

Leucine enkephalin (2 mg/l in water/acetonitrile 50:50 with 0.1% (v/v) formic acid) was used as lock mass and was continuously infused via the lock mass probe at a flow rate of 50  $\mu\text{l min}^{-1}$ . The optimized parameter values specific for the lock mass ESI source and the collision cell are also included in Table 4.1. Each 10 seconds, a lock mass scan was performed for automated mass calibration by following up the leucine enkephalin ion and its most abundant fragment ion at the respective  $m/z$  values of 556.2761 Da and 278.1142 Da in ESI positive ion mode, and at

**Table 4.1** Optimized ESI source parameters<sup>a</sup>.

ESI source parameter	ESI positive mode	ESI negative mode
Sample probe specific parameters		
Capillary voltage (kV)	2.5	2.5
Sample cone voltage (V)	25	20
Collision energy: low energy acquisition function (eV)	6	3
Collision energy: ramped energy acquisition function (eV)	10-30	5-25
Lock mass probe specific parameter		
Capillary voltage (kV)	3.5	3.5
Sample cone voltage (V)	20	30
Collision energy (eV)	20	30
General parameters		
Extraction cone voltage (V)	4	4
Source temperature (°C)	120	80
Desolvation gas temperature (°C)	550	550
Cone gas flow (l h <sup>-1</sup> )	20	20
Desolvation gas flow (l h <sup>-1</sup> )	1100	1100

<sup>a</sup> The ESI parameters were optimized by injection of 10 µg l<sup>-1</sup> analytical standard mixtures containing each 5 to 10 pharmaceuticals.

554.2616 Da and 236.1047 Da in ESI negative mode. The mass used for calibration is the averaged mass of the lock mass ions over 4 subsequent scans. Daily, the calibration of the mass axis was performed over a mass range of 100-1200 Da by infusion of a sodium formate solution (0.1% v/v formic acid and 0.5 mM NaOH in acetonitrile/water 80:20).

#### 4.2.4 Centroiding algorithms, accurate mass determination and measuring the full width at half maximum

Raw high-resolution data are profile data on which no post-processing is performed and where each scan in the chromatogram consists of a

profile mass spectrum. The simplest methodology for the accurate mass determination reads the accurate mass directly from the raw profile data without any post-processing and takes the mass at the maximum intensity as the accurate mass ( $m_{\max}$ ). On the other hand, on post-processing the profile data by a centroiding algorithm, sticks replace the peaks of the profile mass spectrum and the mass attributed to each stick is the centroid. The result is thus a spectrum with sticks where the resolution of the spectrum peaks is eliminated. The automated peak detection (APD) algorithm in the Masslynx software version 4.1 was used for centroiding the spectra.

First, the correctness of the accurate mass extracted from the profile data is compared to that obtained after centroiding the spectra using the APD algorithm. Second, to evaluate the performance of this APD algorithm, the mass accuracy and variability of the APD algorithm was compared with that of 6 self-defined centroiding algorithms. Therefore, spectra extracted from an assay with deionized water spiked with a set of 17 compounds with masses ranging between 152 and 916 Da (Table A.2) at a concentration of  $5 \mu\text{g l}^{-1}$  are used. For each compound, 5 scans were selected between the chromatographic peak apex and the peak tail in order to cover a wide range of signal intensities. Figure 4.1 presents a graphical interpretation of the self-defined centroiding algorithms on a spectrum of paracetamol. The  $m_{\max}$  and 6 self-defined algorithms can be ordered from low to higher complexity including an increasing number of data points of the spectrum peak:

- $m_{max}$ : The centroid is calculated as the mass for which the signal intensity is maximal i.e. at the spectrum peak apex (corresponding to the accurate mass extracted for profile data).
- $m_{HM}$ : The centroid is the mass at the center of the spectrum peak width, determined at half of the maximum intensity of the spectrum peak. First, the method locates the two nearest data points at half of the maximum intensity at both the right and left side of the spectrum peak. Then, for each side an interpolated mass is calculated at half of the maximum intensity. The centroid is then equal to the mean of the interpolated masses.
- $m_{50\%}$ ,  $m_{25\%}$ ,  $m_{10\%}$  and  $m_{5\%}$ : The centroid is calculated as the arithmetic mean of the data points of a spectrum peak with a signal intensity larger than a certain percentile  $f$  (5, 10, 25 and 50 %) of the maximum spectrum peak height.  $m_f$  is then calculated as  $\frac{\sum h_i \times m_i}{\sum h_i}$  for  $h_i > f$  where  $h_i$  is the intensity and  $m_i$  is the mass of the data points in the spectrum peak.
- $m_{gauss}$ : The centroid is calculated by least squares fitting of a Gaussian curve with mean  $m_{gauss}$  and variance  $\sigma^2$  to the spectrum peak.

The FWHM equals the difference between the interpolated masses at the left and the right side of the spectrum peak resulting from the  $m_{HM}$  algorithm and the resolving power is the exact ion mass divided by the FWHM.



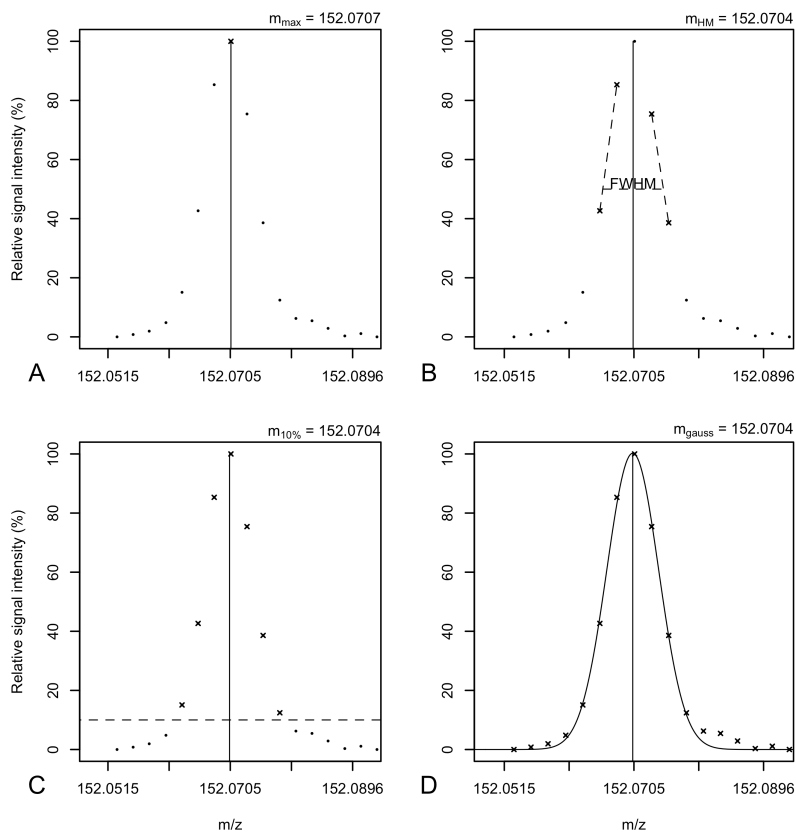


**Figure 4.1** Graphical interpretation of the centroiding algorithms (A:  $m_{max}$ , B:  $m_{HM}$ , C:  $m_{10\%}$ , D:  $m_{gauss}$ ) applied on a spectrum of paracetamol (exact ion mass:  $m/z$  152.0705 Da).

## 4.2.5 Software and statistical analyses

The data station operating software provided with the MS was Masslynx version 4.1 (Waters). Statistical tests were performed using the SPSS Statistics 20 and R 2.14.1 (R Development Core Team, 2008) software. The correlations were investigated by calculating correlation

coefficients ( $r$ ) and their associated  $p$ -values (Student's  $t$ -test). For analysis of variance (ANOVA), assumptions of homogeneity of variances and normality were evaluated on the residuals. Statistical tests were performed at the 5% level of significance.

## 4.3 Results and discussion

### 4.3.1 Accurate mass determination

To compare and evaluate the performance of the  $m_{max}$  and APD algorithm, their obtained mass accuracy and variability were compared to those of the 6 self-defined algorithms. For each centroiding algorithm, the mean mass error (ppm) was calculated for the 17 compounds with 5 scans considered per compound ( $n = 85$ ) and the variability was expressed as the standard deviation (SD) on the 85 mass errors. Table 4.2 presents the mean mass error and variability for each centroiding algorithm with the respective number of data points of the spectrum peaks that are included for the calculation of the centroids. Remark that the number of data points making up a spectrum peak increased with the ion's exact mass; therefore the whole range of number of data points over the 85 spectra is given in Table 4.2. The mean mass error for the different algorithms showed to be significantly different (two-way mixed model ANOVA,  $p < 0.001$ ) and varied between  $-1.18$  and  $0.55$  ppm. Pairwise comparison using a Scheffé test revealed that only the mass error of the  $m_{max}$  algorithm differed significantly from all the other algorithms ( $p < 0.001$ ). The variability on the mass accuracy clearly improved with increasing number of data points included in the

centroiding algorithm. The SDs on the mass error of the  $m_{max}$  and  $m_{HM}$  algorithms are significantly different from the APD algorithm (two-sided F-test,  $p < 0.001$  and  $< 0.01$ , respectively). When increasing the complexity from the  $m_{max}$  to the  $m_{gauss}$  algorithm, only 1 and all the data points, respectively, of a spectrum peak are included for the calculation of the centroid. This explains the decline of the SD from 10.15 ( $m_{max}$ ) to 4.09 ( $m_{gauss}$ ) ppm.

**Table 4.2** The mean mass error and variability (SD) obtained for each centroiding algorithm and the respective number of data points of the spectrum peaks included<sup>a</sup>.

Centroiding algorithm	Number of data points	Mean mass error (ppm)	SD on mass error (ppm)
Centroid mode			
APD	not specified	-0.66	4.33
$m_{gauss}$	8-37	-0.60	4.09
$m_{5\%}$	6-22	0.55	3.94
$m_{10\%}$	6-18	0.01	3.96
$m_{25\%}$	4-16	-0.39	4.31
$m_{50\%}$	2-10	-0.98	5.28
$m_{HM}$	4	-0.45	5.77
Profile mode			
$m_{max}$	1	-1.18	10.15

<sup>a</sup> An assay with deionized water spiked at a concentration of  $5 \mu\text{g l}^{-1}$  was used for the comparison and evaluation of the different algorithms.

As an answer to the first research question, these results demonstrate that the conversion of raw profile data to centroid data using the APD algorithm for the determination of accurate masses is necessary. If no centroiding would be applied, the Masslynx software would use, similar to the  $m_{max}$  algorithm, the mass of the spectrum peak for which the signal intensity is maximal. Table 4.2 clearly shows that the  $m_{max}$  algorithm is less precise than the APD algorithm. Indeed, the APD

algorithm was shown as good as the best self-defined algorithm ( $m_{gauss}$ ) and its variability increased by a factor of 2.3 compared to that of the  $m_{max}$  algorithm.

Next, the correlation between the mass error and the ion's exact mass and intensity was investigated. The mass error of the centroids (APD algorithm) for the 17 compounds considering the 5 selected scans per compound showed to be uncorrelated with the exact mass (Figure 4.2A,  $r = -0.10$ ,  $p > 0.1$ ,  $n = 85$ ). However, larger deviations were observed at lower signal intensities (Figure 4.2B). Although the average mass error showed to be uncorrelated with the signal intensity ( $r = -0.03$ ,  $p > 0.5$ ,  $n = 85$ ) of the spectrum peaks, the variability on the mass accuracy clearly rose for lower signal intensities. The variability showed a steep increase with mass errors up to 8 ppm for signal intensities lower than 1000 absolute units (a.u.). The standard deviation on the mass error was 6.31 and 1.67 ppm for signal intensities lower ( $n = 37$ ) and higher ( $n = 48$ ) than 1000 a.u., respectively. Possible reasons for the increased variability at lower signal intensities are the presence of noise or isobaric compounds and not-perfect spectrum peak shapes. Such low-intensity peaks result from a lower number of ions (i.e. low concentration). When interpreting the ion counts as repetitions of the same measurement, it is obvious that the variability will decrease with the ion intensity. We suggest taking this increased variability at low signal intensities into account in accurate mass based screening applications thereby reducing the number of false negative and/or false positive findings. An overall mass error tolerance of for example  $\pm 5$  ppm is not stringent enough at high signal intensities leading to false positives, whereas at low signal

intensities false negative findings will occur. A more in-depth study on this subject is presented in Chapter 5.

### 4.3.2 Optimizing the mass window width

In literature, different authors using TOF and Orbitrap mass spectrometers providing a resolving power between 10 000 and 50 000 FWHM (Table 4.3), applied different mass window widths for the construction of XICs for quantitative purposes. In general, wider XICs are applied for instruments providing less resolving power. In order to fairly compare these mass window widths independent of the provided resolving power, their corresponding values expressed in relative units (ppm) for a mid-range  $m/z$  value of 400 Da and a resolving power of 20 000 FWHM were calculated (Table 4.3). The corresponding mass window widths reported in literature varied over a relative wide range: from 12.5 to 187.5 ppm.

The use of HRMS such as TOF permits narrowing the mass window width for the construction of XICs, which results in an increased selectivity (Kaufmann *et al.*, 2007). However, a too narrow mass window could result in loss of signal intensity when profile data are used for the construction of XICs or interruption of the signal when centroid data are used. This effect is illustrated in Figure 4.3 with our data for carbamazepine spiked at a concentration of  $100 \text{ ng l}^{-1}$  in surface water. In the case of profile data, the signal intensity decreases when narrowing the mass window width from 80 to 20 ppm (Figure 4.3A). This is because an increasing fraction of the spectrum peak is cut off when narrowing the mass window. Theoretically, it can be calculated that the

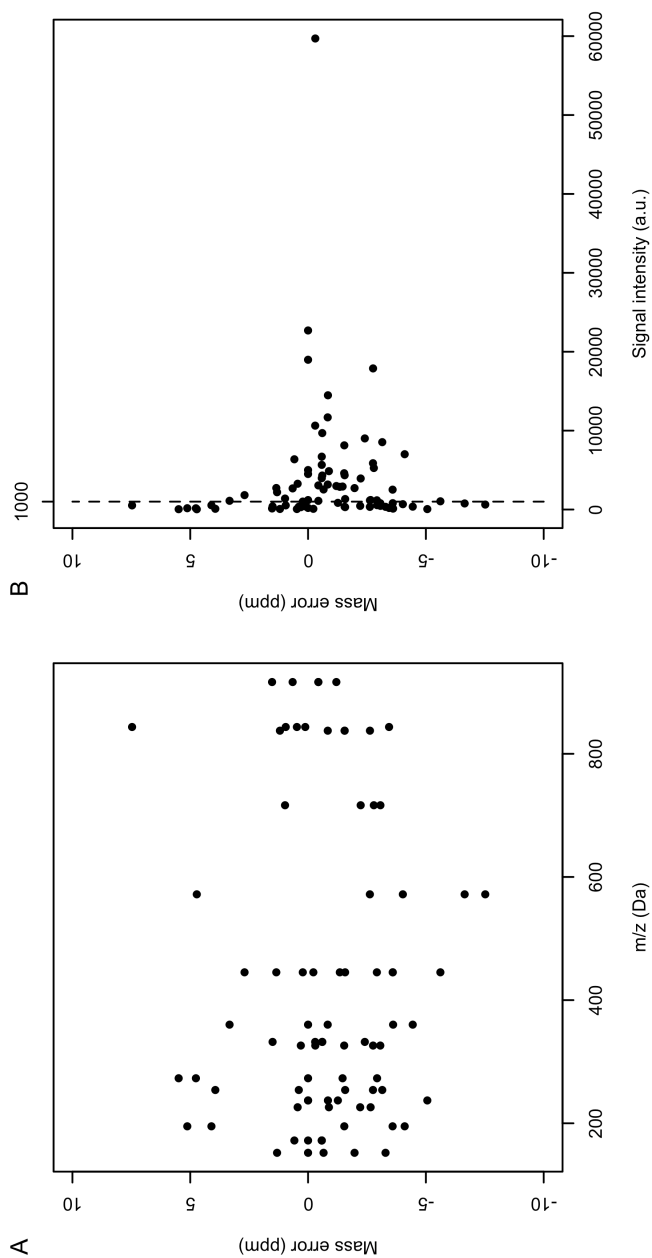


**Figure 4.2** The mass error is not correlated with the ion's exact mass (A). However, the variability on the mass error increases substantially for signal intensities lower than 1000 a.u. (B) ( $n=85$ ).

**Table 4.3** Reported and corresponding mass window widths applied by different authors for the construction of XICs.

Reported mass window width (mDa)	Mass range (Da)	Corresponding mass window width at 20 000 FWHM (mDa) <sup>a</sup>	Corresponding mass window width at 20 000 FWHM for $m/z$ 400 Da (ppm) <sup>b</sup>	Reference
TOF-MS (10 000 FWHM)				
60 <sup>c</sup>	192	30	75	
10-30 <sup>d</sup>	192	5-15	12.5-37.5	Kaufmann & Butcher (2006)
10-20 <sup>e</sup>	142-918	5-10	12.5-25	Kaufmann & Butcher (2006)
20 <sup>c</sup>	150-749	10	25	Petrović <i>et al.</i> (2006)
20 <sup>c</sup>	150-749	10	25	Farré <i>et al.</i> (2008)
TOF-MS (30 000 FWHM)				
50 <sup>d</sup>	56-916	75	187.5	Ferrer & Thurman (2012)
Orbitrap-MS (50 000 FWHM)				
10 <sup>c</sup>	202-897	25	62.5	Kaufmann <i>et al.</i> (2011)
10 <sup>c</sup>	192-716	25	62.5	Chitescu <i>et al.</i> (2012)

<sup>a</sup> Corresponding mass window width in mDa scaled to a resolving power of 20 000 FWHM.

<sup>b</sup> Corresponding mass window width in ppm. First, the corresponding mass window widths in mDa ( $\Delta m$ ) were calculated taking into account that the width of the mass window is inversely proportional to the resolving power, as stated by Kaufmann (2009):  $\Delta m$  (mDa)  $\sim$

$$\frac{1}{R}. \text{ Subsequently, the corresponding mass window width was expressed in ppm: } \Delta m$$
 (ppm)  $\sim \frac{\Delta m$  (mDa)}{400 Da} \cdot 1000.

<sup>c</sup> Raw profile data were transformed to centroid data prior to processing.

<sup>d</sup> Raw profile data were processed.

remaining fraction of the signal is 100, 98, 94, 76 and 36% for a mass window width of 150, 100, 80, 50 and 20 ppm, respectively, assuming a Gaussian spectrum peak and a resolving power of 20 000 FWHM. In the case of centroid data, there is no signal intensity loss when the mass window width decreases from 80 to 50 ppm (Figure 4.3B). However, when a too narrow mass window (Figure 4.3B, 20 ppm) is applied, it can happen that the centroid of a spectrum peak falls out of the defined mass window and that the signal is interrupted. This is the case when the mass attributed to the centroid of a spectrum peak is deviating too much from the true value so that it falls out of the defined mass window.

#### **4.3.2.1 Centroid or profile data and relative (ppm) or absolute (mDa) units for the construction of XICs?**

As shown in Figure 4.3, the use of centroid data can lead to signal interruption. Furthermore, Kaufmann (2009) observed that erroneous centroiding due to the presence of isobaric species in combination with small mass windows could result in false negative findings. They found that better quantitative results were obtained when profile data were processed, even with small mass windows. In order to avoid these unwanted effects of centroid data, the use of profile data is preferred for quantitative analysis.

Within the scope of the second sub-question, it was investigated whether the relative or absolute FWHM of a spectrum peak, expressed in ppm and mDa, respectively, was more constant over the entire investigated  $m/z$  range for TOF HRMS. The FWHM of the 17 compounds (Table A.2) ranged from 26 to 104 ppm and from 8 to



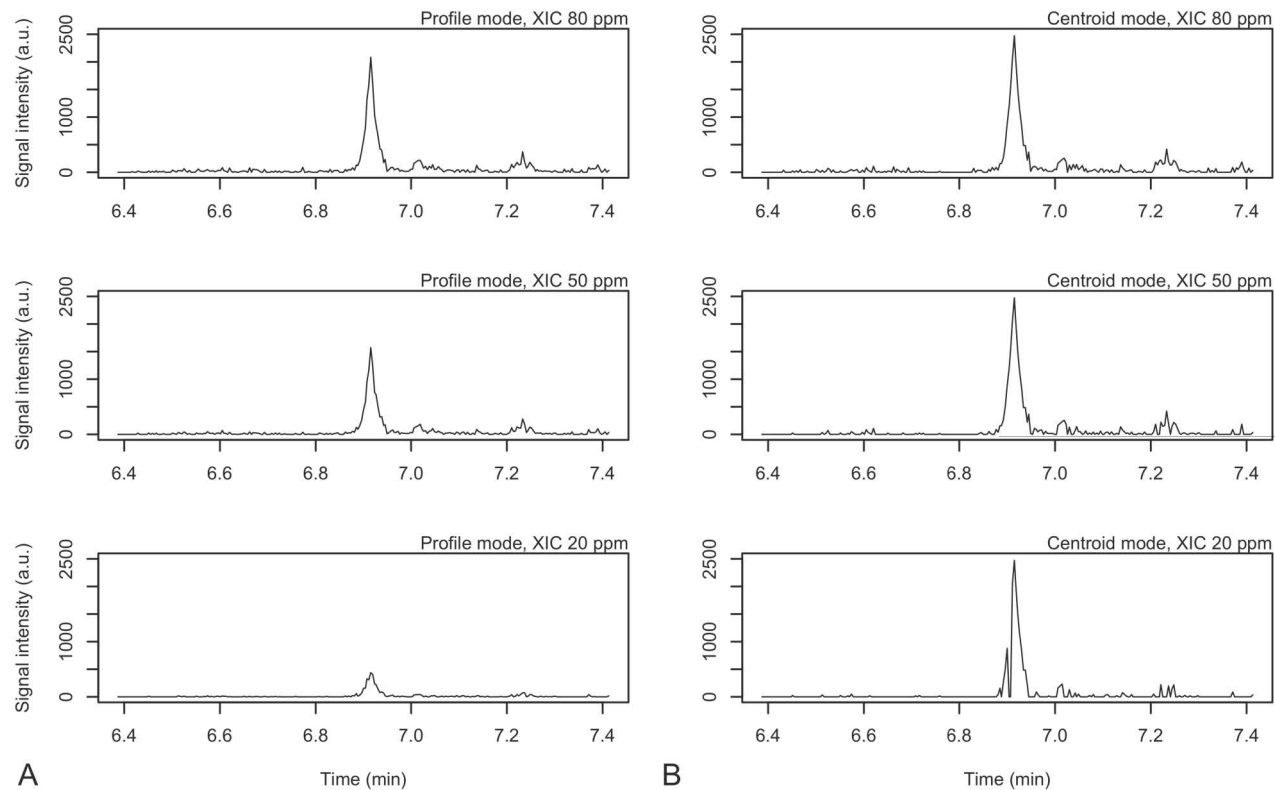


**Figure 4.3** Effect of narrowing the mass window from 80 to 20 ppm: the signal intensity of carbamazepine ( $100 \text{ ng l}^{-1}$  in surface water) decreases when profile data are used (A); the centroid of a spectrum peak falls out of the defined mass window (20 ppm) when centroid data are used causing interruption of the signal (B).

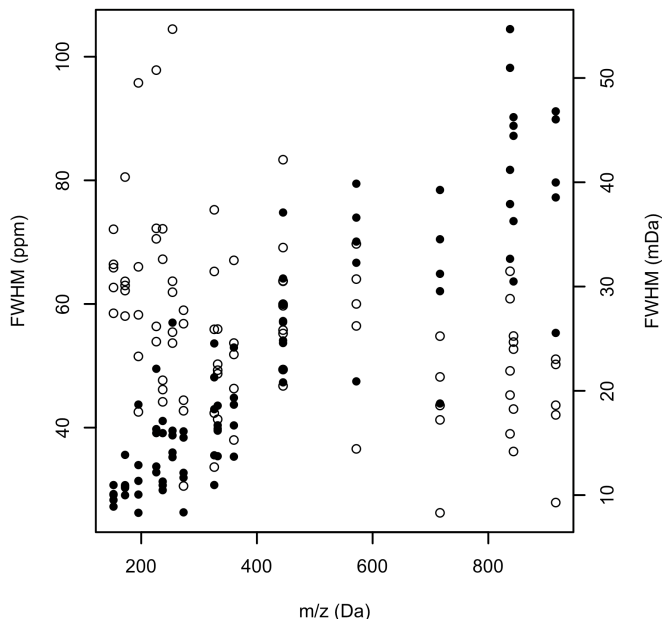


**Figure 4.4** Variability of the FWHM of a spectrum peak in ppm (○,  $r = -0.40$ ) and mDa (●,  $r = 0.89$ ) as a function of the exact mass.

55 mDa within the 152-916  $m/z$  range (Figure 4.4). The associated correlation coefficients ( $r$ ) were  $-0.40$  ( $p < 0.001$ ,  $n = 85$ ) and  $0.89$  ( $p < 0.001$ ,  $n = 85$ ), respectively, indicating that the relative FWHM (ppm) varied less over the whole mass range than the absolute FWHM (mDa). Therefore, defining the mass window width in relative units (ppm) is preferable in order to integrate ion's peaks over the whole mass range in a similar way.

### 4.3.2.2 Sensitivity versus selectivity

The optimal width of the mass window must reflect an optimal sensitivity and selectivity. Yet, it is not known how much both parameters change in function of the mass window width. Here, a way of assessing both parameters is presented. Sensitivity is defined here as the ability to detect lower concentration levels, and selectivity is the ability to distinguish the signal from a compound of interest from that from other compounds (European Union, 2002, Commission Decision 2002/657/EC).

The sensitivity of an analytical method can be assessed by the t-value of a two-sided t-test comparing the integrated area of 5 unspiked and 5 spiked samples. An increasing t-value expresses a stronger statistical difference between the response of the unspiked and spiked samples and is therefore a reliable measure for the sensitivity. An analogue concept was also applied for the calculation of the decision limit (Section 3.3). Therefore, 5 series consisting of an unspiked and 6 spiked deionized water assays (0.01, 0.05, 0.1, 0.5, 1 and 5  $\mu\text{g l}^{-1}$ ) analyzed on one day were processed using different mass window widths for the construction of XICs for 17 compounds (Table A.2). In profile mode 20, 50, 80, 100 and 150 ppm wide mass windows were utilized and additionally – for comprehension purposes – XICs were also constructed from the centroid data utilizing 20, 50 and 80 ppm wide mass windows. For each compound, a concentration close to the instrumental detection limit (10-500  $\text{ng l}^{-1}$ ) was selected for the comparison.

For each of the 17 compounds, the t-value at the selected concentration level was calculated and the results are presented in Figure 4.5A. In both centroid and profile mode, the t-values increase with increasing mass window width from on average 4.8 to 14.4 and from 6.6 to 11.4, respectively, meaning that also the sensitivity of the method increases. Additionally, the relative standard deviation (RSD) on the integrated area of the 17 compounds ( $n = 5$  per compound) at the selected concentration level was calculated. A wider mass window had a positive effect on the RSD (Figure 4.5B). The RSD decreased from on average 51 to 17 % in centroid mode and 46 to 19 % in profile mode. The effect of the mass window width was significant for both the t-value and the RSD (two-way mixed model ANOVA,  $p < 0.001$ ). Although some compounds obtained a stronger increase in sensitivity, i.e. t-value, using the centroid mode for XICs of 80 ppm, the profile mode is preferred because of the reasons given in Section 3.2. Furthermore, comparable results were obtained for the profile and centroid mode applying XICs of 20 and 50 ppm.

The selectivity is, in contrast to the sensitivity, difficult to measure because the presence of isobaric co-eluting matrix compounds is only sporadic (Kaufmann, 2009). Therefore, the selectivity is assessed theoretically as the effect that a matrix ion induces on the integrated peak area of an ion of interest. To quantify this matrix effect given a certain mass window width (profile mode), two ions (i.e. a matrix ion and the ion of interest), which are only partially resolved are considered. It can be calculated that at a resolving power of 20 000 FWHM two ions with equal intensity that are partially resolved by a valley of 50 % have a

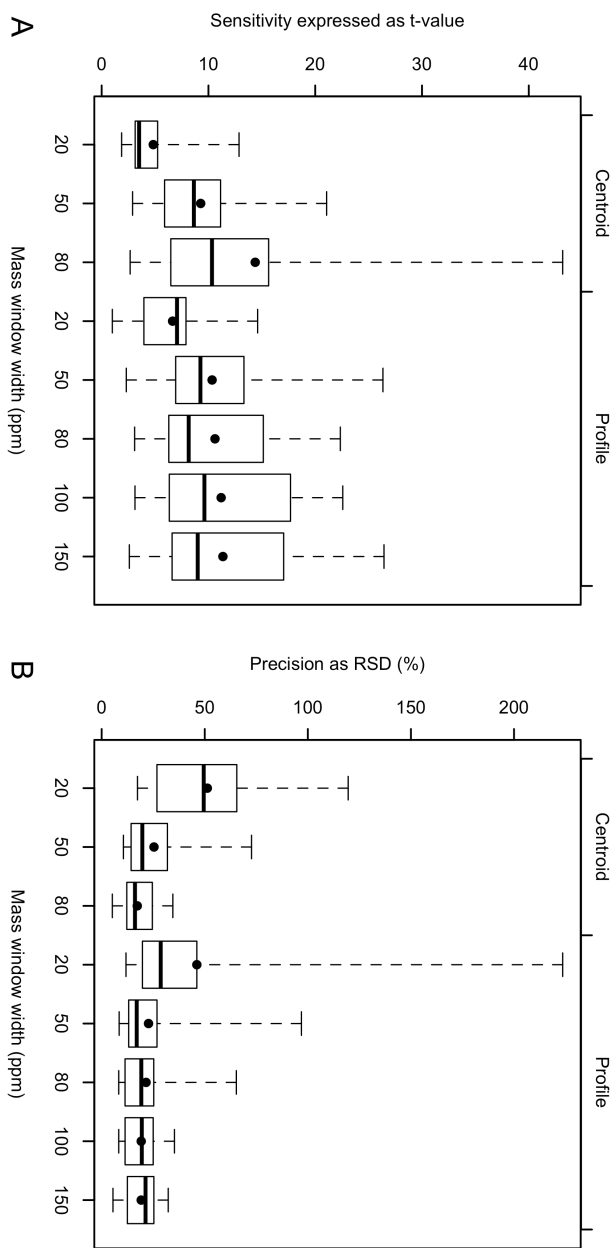


**Figure 4.5** Boxplot of (A) the sensitivity (t-value) and (B) the precision on the integrated peak areas (RSD) as function of the mass window width. The boxplots show the average (●), minimal, and maximal values and the 25, 50 and 75% percentile for the 17 compounds.

mass difference of 71 ppm supposing their spectrum peaks fit a Gaussian curve. This mass difference of 71 ppm is independent of the  $m/z$  value of the ion. The matrix effect can then be assessed as the theoretical ratio of the individual integrated areas in the spectrum within the defined mass window around the ion of interest (Figure 4.6). Maximal selectivity is reached at 0% matrix effect meaning that there is no effect of the matrix compound. The matrix effect amounts 0.6 and 2.1% at 20 and 50 ppm and increases strongly to 8, 17 and 58% at 80, 100 and 150 ppm, respectively.

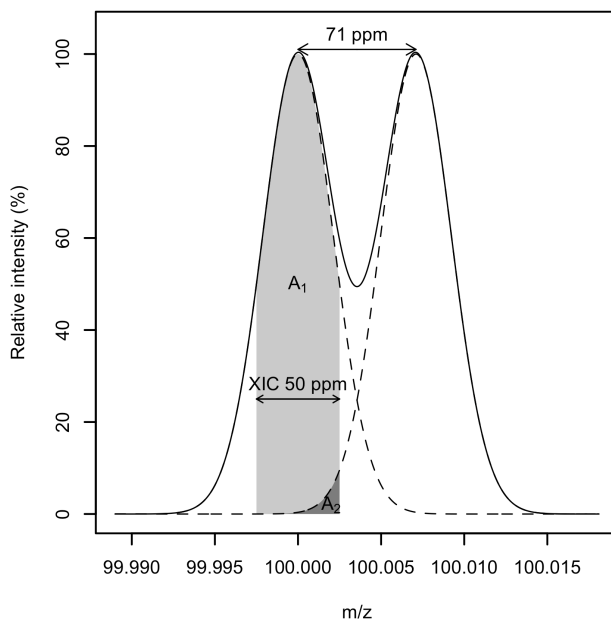


**Figure 4.6** Graphical representation of a spectrum to illustrate the calculation of the matrix effect  $\frac{A_2}{A_1} \cdot 100\%$  due to the presence of a matrix compound that is partially resolved with a valley of 50% and thus 71 ppm apart from an ion of interest ( $R = 20\,000$  FWHM).

The measured sensitivity (average t-value) is plotted as a function of the calculated selectivity (matrix effect) for the different mass window widths (20, 50, 80, 100 and 150 ppm) in profile mode in Figure 4.7. For narrow mass windows (20-50 ppm), the slope of the curve is steep meaning that the sensitivity increases substantially for only a small loss in selectivity. For wider mass windows (50-150 ppm), the sensitivity levels off, whereas the matrix effect increases substantially from 2.1 % to a maximum value of 58 %. From this figure, it can be concluded that an optimal trade-off between sensitivity and selectivity is reached for a mass window width of 50 ppm.

As an answer to the second research question, it is demonstrated that an optimal trade-off is obtained when profile data were processed with a mass window width of 50 ppm utilizing a TOF-MS providing a resolving power of 20 000 FWHM. Complementary to our results, Kaufmann & Butcher (2006) concluded from experiments with an artificially reduced resolving power that the mass window width should be inversely proportional to the resolving power. Therefore, for quantitative purposes, it is advised to utilize the following mass window widths for the construction of XICs from the profile spectra: 10 000 FWHM: 100 ppm; 20 000 FWHM: 50 ppm; 50 000 FWHM: 20 ppm; and 100 000 FWHM: 10 ppm.

### **4.3.3 Calculation of the decision limit and detection capability**

It has been stated in Section 4.1 that the S/N ratio concept for the determination of the detection and quantification limits is in some cases

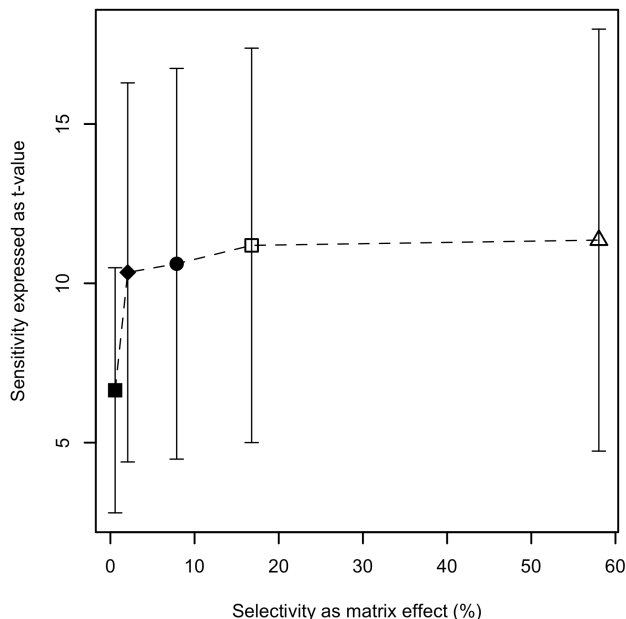


**Figure 4.7** Trade-off between the average sensitivity and the selectivity for mass window widths of 20 (■), 50 (◆), 80 (●), 100 (□) and 150 (△) ppm, calculated from profile spectra. The error bars represent one standard deviation calculated over the 17 compounds.

not applicable for HRMS data. Using narrow mass windows in HRMS can lead to the situation where almost no noise can be detected anymore. This effect is illustrated in Figure 4.8. In particular for ions in the higher mass region, such as spiramycin (Figure 4.8A), almost no noise can be detected leading to questionable S/N ratios. Moreover, this effect will be enhanced when cleaner matrices (Figure 4.8B versus C) are analyzed or when even smaller mass windows are applied for instruments providing an increased resolving power (Kaufmann, 2009). Although determining the S/N ratio from the chromatograms in Figure 4.8 is still possible,



the formulated issue will be of even more importance when using mass spectrometers with an enhanced resolving power (e.g.  $> 100\,000$  FWHM in modern HRMS).

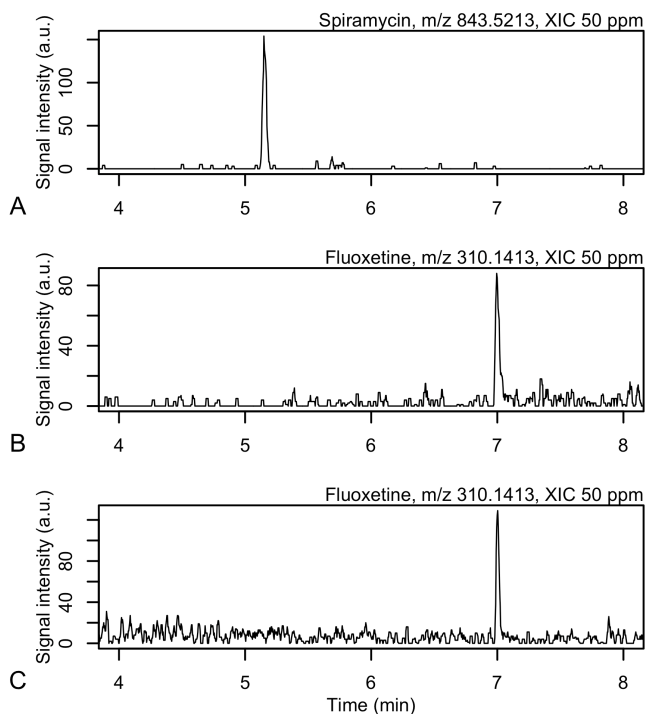


**Figure 4.8** Almost no noise can be detected anymore in XICs for ions in the higher mass region such as spiramycin (surface water, A). For fluoxetine, less noise is found when deionized water (B) is analyzed than in surface water (C). Spiramycin and fluoxetine were spiked at 500 and 50  $\text{ng l}^{-1}$ , respectively.

Therefore, new validation concepts for the determination of performance limits are needed in order to anticipate the named issue. Taking the Commission Decision 2002/657/EC (European Union, 2002)

as a guideline, an equivalent measures for the detection ( $S/N = 3$ ) limit is the decision limit ( $CC\alpha$ ). The  $CC\alpha$  represents the concentration at and above which it can be concluded with an error probability of  $\alpha$  (5 %) that a sample contains the analyte of interest. This means that a detected peak corresponding to a concentration level of at least the  $CC\alpha$  differs significantly from noise and background peaks. Next, the detection capability ( $CC\beta$ ) is the lowest concentration at which the response exceeds the decision limit with a statistical certainty of  $1 - \beta$  ( $\beta = 5\%$ ) meaning that in 95 % of the cases a positive conclusion ( $> CC\alpha$ ) will result from the analysis of a sample containing the analyte of interest at a concentration equal to the  $CC\beta$ .

In practice, the  $CC\alpha$  should be calculated as the mean response of 20 unspiked samples that are considered to be blank plus 2.33 times the standard deviation from the integration of noise or background peaks (Antignac *et al.*, 2003). However, this methodology requests the labor-intensive analysis of a large amount of truly blank matrix samples that are sometimes hard to find for the validation of ng to  $\mu\text{g l}^{-1}$  trace analytical methods due to the ubiquitous presence of trace quantities of some compounds. Furthermore, it can occur that no noise at all can be found in truly blank samples leading to a  $CC\alpha$  equal to zero. Kaufmann (2009) addressed this issue by estimating the standard deviation from a limited number ( $n = 5$ ) of samples spiked to concentrations close to  $CC\alpha$  and  $CC\beta$ . This strategy is extended by taking into account also the number of analyzed spiked samples in a reliable statistical approach.

An unspiked and 6 spiked surface water samples (0.01, 0.05, 0.1, 0.5, 1 and  $5 \mu\text{g l}^{-1}$ ) were analyzed under reproducibility conditions on

5 days within two weeks. After daily external calibration, the mean concentration and variance for each of the spiking levels are calculated. The  $CC\alpha$  is calculated by a one-sided one-sample t-test assuming normality in which the expression

$$\overline{X}_i - \overline{X}_0 \geq t_{1-\alpha, n_i-1} \cdot \sigma_i \quad (4.1)$$

is tested at the 5% ( $\alpha$ ) level of significance (t-value = 2.132).  $\overline{X}_0$  is the mean calculated concentration of the unspiked assays ( $n_0 = 5$ ) and  $\overline{X}_i$  and  $\sigma_i^2$  are the mean calculated concentration and variance of the  $i^{th}$  spiking level ( $n_i = 5$ ). The  $CC\alpha$  is the lowest calculated concentration for which this expression holds. Remark that the obtained  $CC\alpha$  can be an overestimation of the true  $CC\alpha$  because Equation 4.1 is only evaluated for a limited number of spiking levels (i.e. 0.01, 0.05, 0.1, 0.5, 1 and 5  $\mu\text{g l}^{-1}$ ) and the value of the true  $CC\alpha$  can be between two spiking levels. Subsequently, the  $CC\beta$  is calculated by a one-sided one-sample t-test assuming normality in which the expression

$$\overline{X}_i - CC\alpha \geq t_{1-\beta, n_i-1} \cdot \sigma_i \quad (4.2)$$

is tested at the 5% ( $\beta$ ) level of significance (t-value = 2.132). In order to correct for the possible overestimation of the true  $CC\alpha$ , the  $CC\alpha$  used in Equation 4.2 is the value calculated by estimating the term  $\overline{X}_i$  assuming equality in Equation 4.1.

The proposed methodology has been applied for the 17 pharmaceuticals in surface water. For reasons of comparison, also the average S/N ratio has been calculated over the five repeated analysis at the determined  $CC\alpha$  level. The  $CC\alpha$  can be considered as an equivalent measure for the detection limit, which is commonly calculated at S/N

= 3. It appears that the calculated  $CC\alpha$ s tend to exceed the S/N based detection limit, since for 10 out of 17 compounds S/N ratios at the determined  $CC\alpha$  levels range between 10 and 50 (Table 4.4). This could be related to the presence of trace quantities of the substances of interest in the unspiked surface water, resulting in a possible overestimation of the true  $CC\alpha$ .  $CC\alpha$ s calculated from Equation 4.1 are by definition at least the concentration level present in the unspiked matrix sample ( $\overline{X_0}$ ). In order to overcome this overestimation, blank deionized water samples replaced the unspiked surface water samples for the calculation of  $CC\alpha$ :  $\overline{X_0}$  in Equation 4.1 (adjusted decision limit ( $CC\alpha_{adjusted}$ ) in Table 4.4). For 8 compounds (marked in bold), the  $CC\alpha_{adjusted}$  clearly decreased in comparison with the initial  $CC\alpha$  without having a  $S/N < 3$ . Visual inspection of the chromatograms showed that the compounds were still clearly present at their  $CC\alpha_{adjusted}$ . Therefore, the  $CC\alpha_{adjusted}$  is considered to be a more realistic methodology to calculate decision limits. The  $CC\beta$ s presented in Table 4.4 are calculated based on the obtained  $CC\alpha_{adjusted}$ . It should be denoted that the calculated  $CC\alpha_{adjusted}$  values cannot be lower than the concentration present in the unspiked samples, since  $\overline{X_i}$  in equation 4.1 represents the sum of the concentration in the unspiked sample and the spiked concentration. As a consequence, unspiked matrix samples having as low as possible trace concentrations remain necessary for the validation of analytical methods.

As an answer to the third research question, an extension of the methodology presented by Kaufmann (2009) for the determination of  $CC\alpha$  and  $CC\beta$  is developed taking into account also the number of

spiked matrix samples. The methodology was successfully applied and was shown to minimize the overestimation of the true  $CC\alpha$  due to the presence of trace amounts of compounds of interest in matrix samples. This methodology is a reliable and practical alternative in the case the widespread S/N ratio concept is questionable or not applicable anymore for the validation of HRMS instruments.

**Table 4.4** Overview of obtained  $CC\alpha$  and  $CC\alpha_{adjusted}$  with the corresponding S/N and  $CC\beta$  ( $\text{ng l}^{-1}$ )<sup>a</sup>.  $CC\beta$  is calculated starting from  $CC\alpha_{adjusted}$ .

Compound	$CC\alpha$ (S/N)	$CC\alpha_{adjusted}$ (S/N)	$CC\beta$
Bisoprolol	10 (6)	10 (6)	10
Caffeine	<b>500 (52)</b>	10 (14)	500
Carbamazepine	<b>100 (21)</b>	10 (9)	100
Ciprofloxacin	50 (6)	50 (6)	100
Doxycycline	500 (14)	500 (14)	500
Enrofloxacin	<b>50 (7)</b>	10 (3)	50
Erythromycin-H <sub>2</sub> O	<b>50 (20)</b>	10 (16)	50
Furazolidone	10 (2)	10 (2)	50
Iopanoic acid	500 (14)	500 (14)	500
Metronidazole	50 (6)	50 (6)	100
Paracetamol	500 (12)	500 (12)	500
Roxithromycin	<b>100 (49)</b>	50 (15)	100
Sotalol	<b>100 (9)</b>	10 (4)	100
Spiramycin	500 (15)	500 (15)	5000
Sulfamethoxazole	<b>50 (16)</b>	10 (6)	100
Tetracycline	50 (4)	50 (4)	100
Tylosin	<b>100 (17)</b>	50 (14)	50

<sup>a</sup> The reported concentration levels represent the spiked concentration level.

## 4.4 Conclusions

In HRMS, a better performance can be obtained for qualitative and quantitative purposes by refining the data processing. Transforming the raw profile spectra to centroid is recommended for the determination of

accurate masses in qualitative analysis, resulting in a 2.3 fold improved precision on the accurate mass. However, XIC peak integration should be performed on the raw profile data. An optimal mass window width, being a trade-off between sensitivity and selectivity, of 50 ppm was determined for a TOF instrument providing a resolving power of 20 000 FWHM. The optimal mass window width can be easily calculated for instruments providing a lower or higher resolving power taking into account that it is inversely proportional to the resolving power: 10 000 FWHM: 100 ppm; 20 000 FWHM: 50 ppm; 50 000 FWHM: 20 ppm; and 100 000 FWHM: 10 ppm. As an alternative for the widely applied S/N ratio, the methodology for the calculation of the  $CC\alpha$  and  $CC\beta$  developed by Kaufmann (2009) has been extended by taking into account also the number of analyzed spiked samples in a reliable statistical approach. The methodology resulted in comparable decision limits as obtained from a S/N ratio of 3. It can be concluded that this methodology is a reliable and practical alternative for the widespread S/N ratio concept, which will be of utmost importance in most modern HRMS.



# 5

## Suspect screening and quantification of pharmaceuticals in drinking and surface water using large-volume injection - UHPLC - Time-Of-Flight mass spectrometry

*Redrafted from:*

*L. Vergeynst, H. Van Langenhove, P. Joos & K. Demeestere (2014). Suspect screening and target quantification of multi-class pharmaceuticals in surface water based on large-volume injection liquid chromatography and Time-Of-Flight mass spectrometry. Analytical and bioanalytical chemistry, 406(11):2533-2547.*



## 5.1 Introduction

Recently, different accurate mass based screening strategies were developed and applied for suspect screening towards pharmaceuticals and other micropollutants in surface waters (Section 2.5). Avoiding numerous false negative findings and reducing the number of false positive findings is a main challenge, and the performance and optimization of such screening strategies is not yet systematically investigated.

Apart from multi-residue screening, achieving quantification of trace amounts is a second challenge in environmental analysis. Usually, samples are preconcentrated using an enrichment step such as solid-phase extraction (SPE) (which is investigated in Chapter 3) and a clean-up of interfering matrix compounds is necessary to enhance the method's performance limits. However, a recent review discussed the applicability of large-volume injection (LVI) as an alternative for the widely applied but labor-intensive SPE techniques for trace analysis of environmental matrices thereby speeding up the analytical procedure (Busetti *et al.*, 2012).

Hence, the aim in this chapter is to investigate and improve the potential of LVI - ultra-high performance liquid chromatography (UHPLC) in combination with QTOF high-resolution mass spectrometry (HRMS) for both fast screening and target quantification of traces of pharmaceuticals. An optimized and validated novel analytical method for a broad variety of multi-class pharmaceuticals is presented, hereby

aiming to screen and quantify traces of pharmaceuticals in drinking and surface water.

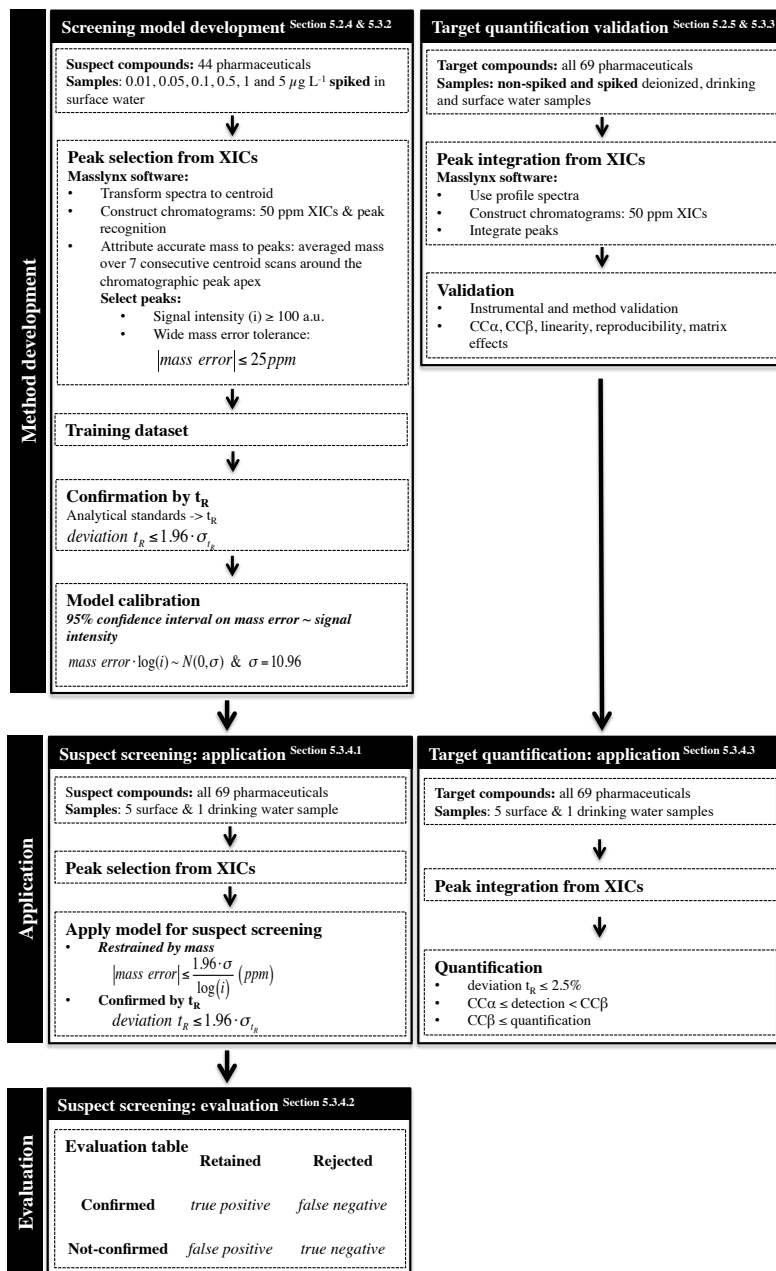
In a first part, a suspect screening strategy was developed applying a novel signal intensity-dependent mass error tolerance, which contrasts with the currently applied fixed mass error tolerance (Table 2.2). The aim is a suspect screening towards 69 pharmaceuticals without the a priori availability of standards, hereby keeping the false negative rate at 5% and simultaneously minimizing the number of false positive findings (Section 5.3.2). In a second part, both not-spiked and spiked drinking and surface water samples were analyzed and the results of a full validation for target quantification of the 69 pharmaceuticals are presented (Section 5.3.3). Finally, the results of both the suspect screening and target quantification study on a drinking water and five Belgian surface water samples are presented (Section 5.3.4). These results are to be interpreted as a first application of the new method and a proof of concept without aiming to set up an extended monitoring campaign. The applicability and advantages of LVI-UHPLC in combination with full-spectrum HRMS for rapid screening are discussed in Section 5.3.5. A comprehensive scheme representing the workflow for this chapter is presented in Figure 5.1.

## **5.2 Experimental section**

### **5.2.1 Chemicals**

The 69 pharmaceutical standards and their respective suppliers are listed in Table A.2. The masses of the pharmaceuticals cover the whole

**Figure 5.1** Comprehensive scheme representing the workflow for the development of the signal-intensity based screening approach and for its application and evaluation prior to target quantification.



mass range (151 to 1240 Da) and have a wide range of octanol-water partition coefficient ( $K_{ow}$ ) values (e.g.  $\log K_{ow}$  -2.8 for iohexol; 4.2 for diclofenac; 4.7 for fluoxetine). Chemicals and procedure for the preparation of standard and matrix-matched calibration curves (0.01, 0.05, 0.1, 0.5, 1 and 5  $\mu\text{g l}^{-1}$  in deionized, and drinking and surface water) are specified in Section 4.2.

### **5.2.2 Sampling and sample pretreatment**

Drinking water was taken from a drinking water production center (Antwerpse Waterwerken) in Rumst, Belgium. Five surface water samples were collected in prerinsed amber glass bottles on five different locations along the river Maas and the Albert channel, Belgium, and stored at 4 °C in the dark for no longer than 24 hours prior to analysis. For the method validation, a drinking water sample and a surface water sample from the Albert channel, Belgium, were stored for a one-month period (at 4 °C in the dark) and used for all the validation experiments. Prior to standard addition, surface water samples were filtered through 1.5  $\mu\text{m}$  glass microfiber filters (934-AH, Whatman) and subsequently 0.1 % and 0.02 % (v/v) formic acid was added to all samples for analysis in electrospray ionization (ESI) positive and negative ion mode, respectively.

### **5.2.3 Instrumental analysis**

A detailed overview of the chromatographic and mass spectrometric conditions is given in Section 4.2.

Briefly, the analysis were performed using an UHPLC system equipped with an autosampler with 250  $\mu$ l loop for large-volume injection and coupled to a Xevo G2 QTOF mass spectrometer with an orthogonal ESI probe.

For analysis in ESI positive ion mode, the mobile phase used was (A) water/acetonitrile 98:2 (v/v) with 0.1 % formic acid and (B) acetonitrile with 0.1 % formic acid. In ESI negative ion mode, the mobile phase used was (A) water/acetonitrile 98:2 (v/v) with 0.01 % formic acid and (B) acetonitrile. The total time for the chromatographic analysis was 19 min. The sample injection volume was 250  $\mu$ l. Even without SPE, avoiding highly polar organic and inorganic (salts) compounds in the MS can be achieved by starting the chromatographic gradient with aqueous eluent, which can be diverted to the waste by installing a post-column valve. This ‘wash step’ is highly recommended in LVI-LC (Busetti *et al.*, 2012). The chromatographic gradient used in our method started by 1 min isocratic with a mixture of aqueous solvent with 4.94 % acetonitrile. The 69 analytes that were targeted in this study eluted within 1.94 and 11.49 min. Therefore, the first 1.6 min of the eluent could be diverted to the waste without compromising the screening capability of our method even for the most polar compounds (e.g. iohexol:  $\log K_{ow}$  -2.8) of our suspect set.

The QTOF mass spectrometer was operated at a resolving power of 20 000 full width at half maximum (FWHM) acquiring profile data over an  $m/z$  range of 50-1200 Da. Data were acquired in MS<sup>E</sup> mode in which two acquisition functions with a low collision energy (LE) and a high collision energy (HE) (i.e. ramped from low to high) acquire

alternating parent and fragment ions, respectively. The data station operating software was Masslynx version 4.1 (Waters).

## **5.2.4 Development of the suspect screening methodology**

### **5.2.4.1 Investigation of the relation between the accurate mass error and the ion's signal intensity**

For screening and accurate mass determination, the chromatograms were converted to centroid data by the automated peak detection (APD) algorithm provided with the Masslynx software version 4.1 (Waters) in agreement with the recommendation in Section 4.3.2. Extracted ion chromatograms (XICs) were constructed utilizing an optimized mass window width of 50 ppm (exact mass  $\pm 25$  ppm) around the exact masses of the  $[M+H]^+$  and  $[M-H]^-$  ion for the positive and negative ion mode, respectively, and the accurate mass attributed to a chromatographic peak is determined as the averaged mass over 7 consecutive centroid scans around the chromatographic peak apex.

To develop the screening strategy, a model describing the relation between the accurate mass error and the ion's signal intensity has been defined and calibrated. Therefore, a surface water sample spiked with analytical standards (0.01, 0.05, 0.1, 0.5, 1 and 5  $\mu\text{g l}^{-1}$ ) of a subselection of 44 pharmaceuticals (Table A.2) was analyzed and used as training dataset. The model calibration was performed using the R 2.14.1 (R Development Core Team, 2008) software.

#### 5.2.4.2 Retention time and fragments for confirmation

Analytical standard mixtures of 5 to 10 pharmaceuticals with a concentration of  $10\ \mu\text{g l}^{-1}$  in deionized water were injected and analyzed in ESI positive and negative mode for the determination of the retention time ( $t_R$ ) and for the identification of the most abundant fragment ion for confirmation. The pharmaceuticals in the standard mixtures were selected so that their peaks were well separated in the chromatogram. A mass difference of at least 18 Da was preferred for the selection of a fragment ion to avoid the non-specific loss of water or ammonia. The retention time and most representative fragment ion are presented in Table A.2. The selected ionization mode for each pharmaceutical was the ionization mode for which the lowest instrumental decision limit (Section 5.2.5.1 and 5.3.3.1) was obtained.

#### 5.2.5 Validation strategy for target quantification

For quantification purposes, the extracted ion chromatograms were generated and manually integrated from the raw profile data utilizing an optimized mass window width of 50 ppm (Section 4.3.2). The validation was performed taking the Commission Decision 2002/657/EC (European Union, 2002) as a guideline. The method validation was performed for drinking and surface water, and deionized water was used for the instrumental validation. Only peaks deviating not more than 2.5% from the retention time listed in Table A.2 are considered (European Union, 2002).

### **5.2.5.1 Instrumental validation**

For the intraday and interday instrumental validation, 5 repetitions of a standard calibration curve (blank, 0.01, 0.05, 0.1, 0.5, 1 and 5  $\mu\text{g l}^{-1}$  in deionized water) were performed on one day and on 5 days in a time period of two weeks, respectively. Instrumental intraday and interday repeatability are expressed as the relative standard deviation (RSD) of the integrated peak areas of 5 repeated injections of analytical standards on one and 5 days, respectively. The instrumental decision limit ( $CC\alpha$ ) and instrumental detection capability ( $CC\beta$ ) are determined from the repeatability following the methodology recently proposed in Section 4.3.3. Linearity is tested based on the F-test for lack of fit (Kutner *et al.*, 1996) in the regression for the standard calibration curve under repeatability conditions ( $n = 5$  for each concentration level). This F-test calculates the significance of the reduction in the sum of squares of the relative errors (SSRE) in progression from a linear to a quadratic calibration curve. In other words, this F-test takes into account the applied weighting and evaluates whether a quadratic model  $j$  with 3 parameters ( $p_j$ ) describes significantly better the data than a linear model  $i$  with 2 parameters ( $p_i$ ). The test statistic  $f = \frac{SSRE_i - SSRE_j / p_j - p_i}{SSRE_j / n - p_j}$  is compared to  $F_{p_j - p_i, n - p_j}$  ( $n$  is the number of data points) at the 5 % level of significance. If non-linearity is concluded, linearity is tested again after contracting the working range by omitting the highest concentration level.



### 5.2.5.2 Calibration and quantification

Daily external calibration was performed to account for the interday variability of the analytical sequence. The parameters of the standard calibration curve are estimated by weighted least squares with the weights for the squared residuals estimated as the reciprocal of the squared concentration ( $1/x^2$ ).

For quantification in both drinking and surface water samples, matrix effects have to be determined. Therefore, the calculated concentrations of a matrix-matched calibration curve were plotted as a function of the theoretical concentration ( $n = 5$  per concentration level, interday repeatability conditions). The slope of this curve equals the extent of the matrix effects. A slope = 1 (expressed as 100 %) is obtained when no matrix effects are present; and slopes  $> 1$  and  $< 1$  represent signal enhancement and suppression, respectively. When quantifying pharmaceuticals in drinking and surface water (Section 5.3.4.3) the calculated concentrations were corrected for the matrix effects, which were calculated on samples sampled at the same locations.

### 5.2.5.3 Method validation

The method validation for both the drinking and surface water consisted of a matrix-matched calibration curve (not-spiked, 0.01, 0.05, 0.1, 0.5, 1 and  $5 \mu\text{g l}^{-1}$ ), which was repeated on 5 days within two weeks. Daily, a standard calibration curve (blank, 0.01, 0.05, 0.1, 0.5, 1 and  $5 \mu\text{g l}^{-1}$  in deionized water) was analyzed for external calibration. Each series was followed by a blank assay to prevent cross-contamination. The method

interday repeatability expresses the precision over 5 days as the RSD of the calculated concentrations after calibration.

The method  $CC\alpha$  and method  $CC\beta$  were determined as explained in section 2.5.1, considering that here, the peak areas are replaced by calculated concentrations in the matrix sample. The mass error was determined for all the compounds in deionized, drinking and surface water at the concentration level corresponding to the respective  $CC\alpha$ s and  $CC\beta$ s, and at  $5\ \mu\text{g l}^{-1}$ . The mass error was determined under interday repeatability conditions ( $n = 5$ ) and its precision was determined by calculating the 95% confidence limit ( $\pm 1.96 \times$  standard deviation).

## **5.3 Results and discussion**

### **5.3.1 Large-volume injection ultra-high performance liquid chromatography**

The applied gradient allowed sufficient retention and separation of the targeted analytes on a UHPLC column. The 69 analytes elute within a retention time ranging from 1.94 to 11.49 min. A chromatogram of an analytical standard is presented in Figure 5.2. During the optimization process, particular efforts were made to improve the chromatography of early eluting analytes, which can be affected by the LVI. The length of the initial isocratic gradient was increased to 1 min, which allowed better column focusing and improved the peak shape of fast eluting compounds. The injected solvent water, which has an elution strength lower than the starting gradient, enabled sufficient retention and good-

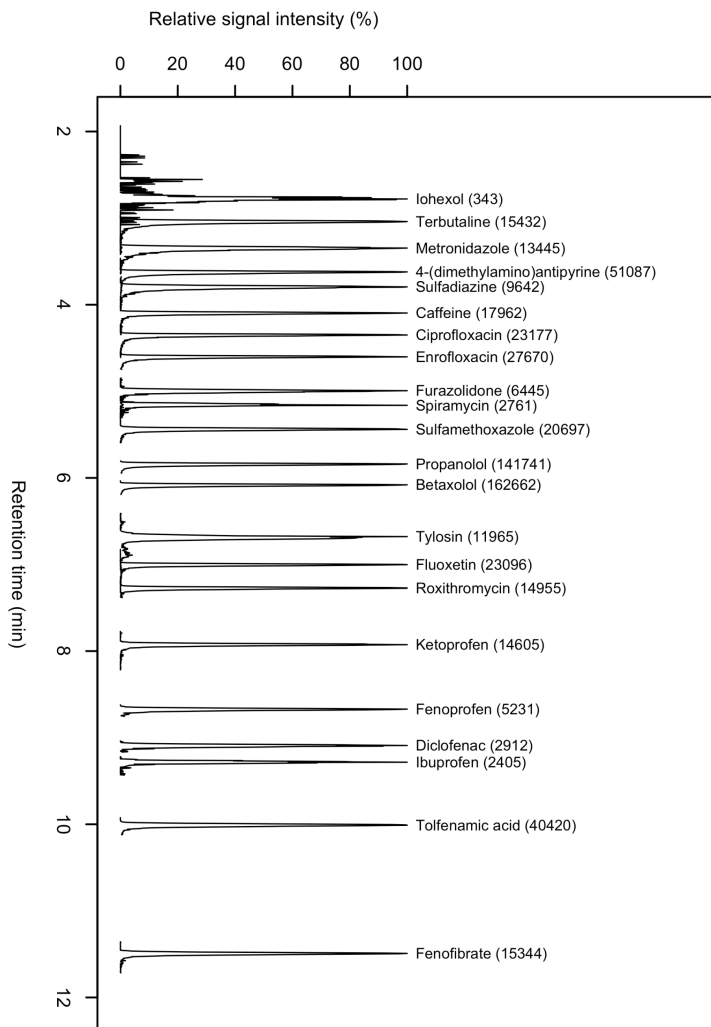


**Figure 5.2** Extracted ion chromatogram (XIC 50 ppm) of an analytical standard ( $5 \mu\text{g l}^{-1}$ ) showing the good peak shape of 23 selected analytes having retention times distributed over the whole chromatographic analysis. Relative signal intensities are used for the y-axis in order to assure that the peak shape of low as well as high signal intensity peaks can be evaluated and the absolute signal intensity (a.u.) is given for each peak.

quality peak shapes. Addition of formic acid (0.1% and 0.02% in ESI positive and negative mode, respectively) to the samples improved the peak shapes (reduced double peaks, sharper peaks, less tailing) for early eluting ( $t_R < 6$  min) compounds (sulfadiazine, sulfamerazine, sulfamethoxazole and salicylic acid).

### **5.3.2 Development of the signal intensity-dependent suspect screening model**

In a first stage, in order to create the training dataset, the obtained chromatograms of the spiked surface water samples were searched for the exact masses of a sub-selection of 44 pharmaceuticals (Table A.2). The mass error tolerance was initially set at  $\pm 25$  ppm as such that all the peaks present in the constructed extracted ion chromatograms (XICs) are found; and a reasonably low minimal signal intensity (i.e. chromatographic peak height) of 100 absolute units (a.u.) was chosen avoiding the detection of numerous noise peaks. For the given set of pharmaceuticals, the lowest concentration corresponding to a signal intensity of at least 100 a.u. in surface water is given in Table A.2. The aim was to investigate to which extent the mass error tolerance could be narrowed assuring a false negative rate of 5% and avoiding numerous false positive findings. To label a peak as confirmed, its retention time can not deviate more than  $1.96 \times$  standard deviation, i.e. within the 95% confidence interval, from the retention time listed in Table A.2 (deviation  $t_R \leq 1.96 \cdot \sigma_{t_R}$ ). The sub-selection of 44 pharmaceuticals provided enough data for the model development and the resulting training dataset consisted of a total of 208 observations (208 traces with a signal intensity  $> 100$  a.u.).

The variability of the accurate mass error obtained with the applied TOF-MS showed to strongly decrease with increasing signal intensity, being in agreement with the observations in Figure 4.2 and of Wolff *et al.* (2003). The variability on the mass error ( $e_{m/z}$ ) and the log-transformed signal intensities ( $i$ ) are inversely related: variability  $e_{m/z} \sim \frac{1}{\log(i)}$  (Figure 5.3). Hence, the distribution of the mass error can be described as:  $e_{m/z} \cdot \log(i) \sim N(0, \sigma^2)$  and a value of 10.96 was obtained for the standard deviation ( $\sigma$ ) after fitting the distribution to the training dataset. The modeled variability showed good normality as evaluated from a Q-Q plot (Figure 5.4) from which a good fit within the two first quantiles can be concluded.

This model permitted to draw the 95 % confidence limits of the mass error as a function of the signal intensity for which holds that  $|e_{m/z}| \leq \frac{1.96 \cdot \sigma}{\log(i)}$  with  $\sigma = 10.96$  ppm. From the 208 confirmed observations in the training dataset, 8 observations fell out of the 95 % confidence limits resulting in an effective false negative rate of 4 %. As an important outcome of the newly developed screening model, a mass error tolerance of 10.7, 7.2 and 5.4 ppm will be applied for the positive conclusion of peaks with signal intensities of 100, 1000 and 10 000 a.u., respectively or, in other words, the observations should fall within the 95 % confidence limits in Figure 5.3 to be retained.

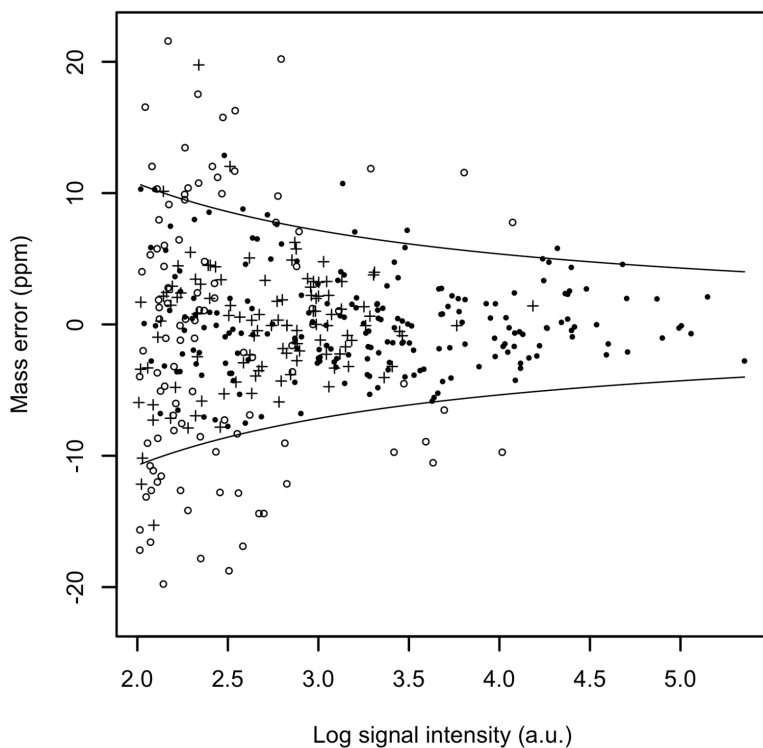


**Figure 5.3** The variability of the mass error (line: 95 % confidence limits of the training dataset (●) described in Section 5.3.2) decreases inversely with the log-transformed signal intensity. Screening results of one drinking water and five surface water samples of the confirmed (+) and non-confirmed (○) suspects based on the retention time are also presented (Section 5.3.4.1).

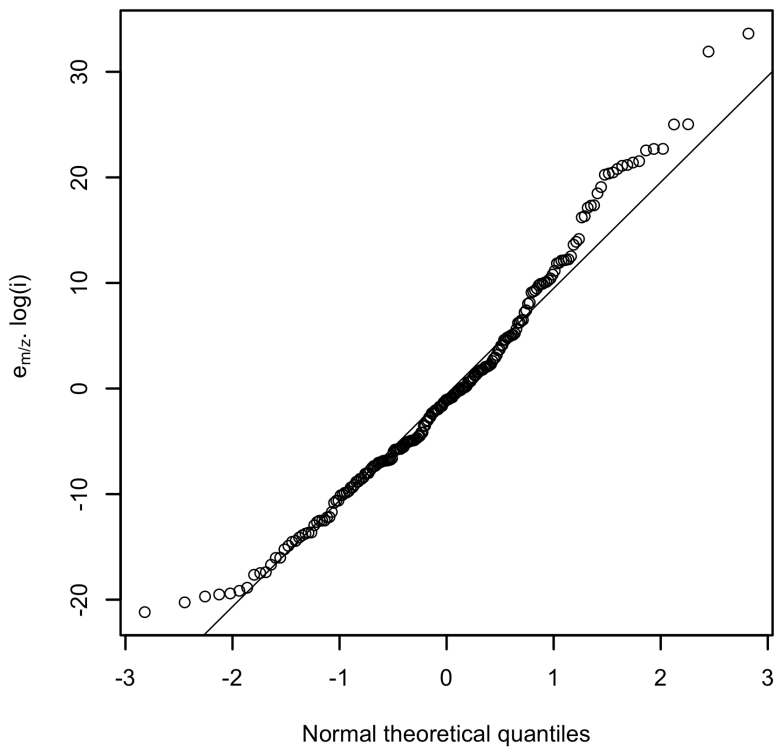


**Figure 5.4**  $e_{m/z} \cdot \log(i)$  shows good normality as evaluated from a Q-Q plot from which a good fit within the first two quantiles of a theoretical normal distribution can be concluded.

### 5.3.3 Validation for target quantification

#### 5.3.3.1 Instrumental validation

The results of the instrumental validation are given in Table 5.1 (intraday repeatability, interday repeatability, instrumental  $CC\alpha$  and  $CC\beta$ , and linear range). For a majority of the compounds, the

instrumental intraday repeatability and interday repeatability are in general more or less constant in the upper concentration range and increase for concentrations close to the instrumental  $CC\alpha$ . This is illustrated in Figure 5.5 for diclofenac. The standard deviation increases linearly with the concentration whereas the RSD increases at lower concentrations, i.e. close to  $CC\alpha$  and  $CC\beta$ , and leveled off for higher concentrations. These findings are in agreement with CMA/6/A (2012) and confirm the validity of the applied weighted least squares methodology ( $1/x^2$  weighting) for the linear calibration (Section 5.2.5.2). For more information on the weighted least square theory, the reader is referred to Kutner *et al.* (1996). The intraday variability was better than 20 % for most of the analytes over the whole concentration range. Higher interday RSDs are noticed with some values  $> 40\%$  for concentrations at or close to the instrumental  $CC\alpha$  occur when no trace was found for at least one out of the 5 repeated injections (e.g. clenbuterol, cyclophosphamide, fluoxetine, furazolidone and ketoprofen). Daily external calibration is performed in order to take interday instrumental variations into account.



**Table 5.1** Parameters of the instrumental validation indicating the performance of the analytical method for analytical standards (Concentrations in  $\mu\text{g l}^{-1}$ ).

Pharmaceutical compound	Intraday repeatability as					Interday repeatability as					CC $\alpha$	CC $\beta$	Highest Number concentrations <sup>a</sup>				
	RSD (% $_n$ , $n = 5$ ) for each spiking level					RSD (% $_n$ , $n = 5$ ) for each spiking level											
4-(dimethylamino)antipyrine	30	25	27	24	32	22	36	26	32	27	30	30	0.01	2.5	0.05	5.00	6
Atenolol	18	6	4	3	5	2	19	29	31	29	26	28	0.01	2.5	0.01	5.00	6
Betaxolol	9	5	5	3	5	2	22	25	34	29	31	27	0.01	2.5	0.01	5.00	6
Bezafibrate	8	18	9	6	7	5	35	20	20	19	17	14	0.01	2.5	0.01	5.00	6
Bisoprolol	7	5	5	3	8	2	23	23	33	24	24	23	0.01	2.5	0.01	5.00	6
Caffeine	c	17	8	8	12	9	c	19	31	25	26	31	0.05	12.5	0.05	5.00	5
Carbamazepine	14	6	5	4	7	6	31	23	34	35	36	32	0.01	2.5	0.01	0.50	6
Chlorotetracycline	c	c	35	12	10	7	c	69	50	54	59	0.10	0.10	25	0.50	1.00	3
Ciprofloxacin	c	14	15	9	2	3	c	33	38	25	32	31	0.05	12.5	0.10	5.00	5
Clenbuterol	19	10	8	6	2	5	48	27	38	35	33	35	0.01	2.5	0.01	0.50	4
Cloxacillin	b	b	b	b	b	b	c	70	56	72	65	68	0.05 <sup>e</sup>	12.5	b	b	a
Cyclophosphamide	26	7	4	6	11	10	94	41	42	42	40	36	0.01	2.5	0.05	1.00	5
Dapsone	17	13	4	10	18	17	16	28	30	26	23	28	0.01	2.5	0.01	0.50	4
Diazotric acid	c	c	c	14	5	3	c	c	59	28	32	0.50	0.50	12.5	0.50	5.00	2
Diclofenac	29	18	10	10	7	7	31	31	22	15	14	17	0.01	2.5	0.05	5.00	6
Doxycycline	c	c	c	20	15	12	c	c	35	25	34	0.50	0.50	12.5	0.50	1.00	2
Enoxacin	c	c	12	8	5	9	c	c	45	30	35	29	0.10	2.5	0.50	1.00	2
Enrofloxacin	c	c	19	8	7	5	c	c	46	29	36	27	0.10	2.5	0.50	1.00	2
Erythromycin-H <sub>2</sub> O	c	10	13	6	4	8	c	43	46	32	38	35	0.05	12.5	0.05	1.00	3
Fenofibrate	c	10	20	12	18	19	c	146	65	52	48	57	0.05	12.5	0.05	5.00	5
Fenoprofen	c	13	10	14	13	13	c	34	30	27	19	22	0.05	12.5	0.05	5.00	5
Fluoxetine	19	5	12	2	7	7	94	29	44	34	42	33	0.01	2.5	0.01	5.00	6
Furazolidone	22	9	18	14	26	19	142	45	61	49	42	40	0.01	2.5	0.01	5.00	6
Gemfibrozil	c	21	7	5	8	11	c	21	10	16	16	21	0.05	12.5	0.05	1.00	4

**Table 5.1** (continued)

Pharmaceutical compound	Intraday repeatability as RSD (% , n = 5) for each spiking level					Interday repeatability as RSD (% , n = 5) for each spiking level					C/C $\alpha$	C/C $\beta$	Highest Number of levels				
	0.01	0.05	0.10	0.50	1.00	5.00	0.01	0.05	0.10	0.50				1.00	5.00	( $\mu\text{g l}^{-1}$ )	( $\mu\text{g l}^{-1}$ )
Ibuprofen	c	27	31	9	12	4	c	92	12	11	19	14	0.05	12.5	0.10	5.00	5
Ifosfamide	23	11	9	3	10	9	141	31	47	40	39	38	0.01	2.5	0.01	1.00	4
Indometacin	c	22	24	5	17	8	c	71	69	71	64	77	0.05	12.5	0.50	5.00	5
Iodipamide	c	c	c	20	13	14	c	c	c	63	27	38	0.50	125	0.50	5.00	3
Iohexol	c	c	c	8	19	10	c	c	c	28	37	33	0.50	125	0.50	5.00	3
Iomeprol	c	c	c	20	9	13	c	c	c	27	34	38	0.50	125	0.50	5.00	3
Iopamidol	c	c	c	23	28	16	c	c	c	71	35	43	0.50	125	0.50	5.00	3
Iopanoic acid	c	c	c	11	20	13	c	c	c	18	23	17	0.50	125	0.50	5.00	3
Iopromide	c	c	c	24	30	32	22	c	c	38	34	28	0.10	25	0.50	5.00	4
Iotalamic acid	c	c	c	13	5	4	c	c	c	21	27	35	0.50	125	0.50	1.00	3
Ketoprofen	27	14	9	1	5	8	96	38	41	31	31	33	0.01	2.5	0.05	5.00	6
Lincomycin	32	6	10	6	3	2	43	26	31	23	21	23	0.01	2.5	0.05	5.00	6
Metoprolol	10	5	3	3	3	3	28	22	33	26	27	28	0.01	2.5	0.01	0.50	4
Metronidazole	c	10	17	12	6	5	c	29	31	26	27	32	0.05	12.5	0.05	5.00	5
Nafcillin	b	b	b	b	b	b	c	c	45	51	50	37	0.10 <sup>e</sup>	25	b	b	b
Naproxen	c	c	c	20	6	15	c	c	c	21	20	16	0.50	125	0.50	5.00	3
Norfloracin	c	14	2	3	3	3	c	c	c	49	24	27	0.10	25	0.50	5.00	4
Ofloxacin	c	17	11	9	7	2	c	39	43	27	28	27	0.05	12.5	0.10	5.00	5
Oleandromycin	b	b	b	b	b	b	c	c	c	41	32	40	0.10 <sup>e</sup>	25	b	b	a
Oxacillin	c	c	c	17	31	26	c	c	c	58	51	53	0.50	125	0.50	5.00	3
Oxytetracycline	c	c	20	16	10	6	c	c	c	18	29	22	0.10	25	0.10	1.00	3
Paracetamol	33	15	10	12	16	10	d	37	66	31	19	23	0.01	2.5	0.05	5.00	6
Penicillin G	b	b	b	b	b	b	c	c	c	58	45	71	0.50 <sup>e</sup>	125	b	a	a
Penicillin V	b	b	b	b	b	b	c	c	c	75	76	75	0.50 <sup>e</sup>	125	b	a	a
Pentoxifyline	2	10	9	8	7	6	84	25	29	30	31	29	0.01	2.5	0.01	0.50	4

Table 5.1 (continued)

Pharmaceutical compound	Intraday repeatability as RSD (% , n = 5) for each spiking level					Interday repeatability as RSD (% , n = 5) for each spiking level					CC $\alpha$	CC $\beta$	Highest concentration <sup>a</sup> of levels	Number of levels			
	0.01	0.05	0.10	0.50	1.00	5.00	0.01	0.05	0.10	0.50					1.00	5.00	( $\mu\text{g l}^{-1}$ )
Phenazone	11	3	5	2	1	2	33	24	28	25	24	28	0.01	2.5	0.01	1.00	5
Pindolol	6	6	3	3	5	2	35	31	33	35	27	30	0.01	2.5	0.01	0.10	3
Prindon	c	c	17	10	11	11	c	33	35	34	37	0.10	25	0.10	5.00	4	
Propranolol	7	5	5	4	4	2	22	26	29	30	30	25	0.01	2.5	0.01	1.00	5
Propyphenazone	8	4	2	1	2	3	12	22	24	26	27	25	0.01	2.5	0.01	5.00	6
Ronidazole	c	c	23	15	16	12	c	74	45	66	42	0.10	25	0.10	5.00	4	
Roxithromycin	c	9	4	8	8	9	c	32	51	23	30	22	0.05	12.5	0.05	1.00	4
Salbutamol	19	14	7	2	3	4	116	43	45	42	41	36	0.01	2.5	0.01	0.10	3
Salicylic acid	c	13	12	13	13	6	c	16	26	24	19	22	0.05	12.5	0.10	5.00	5
Sotalol	c	13	17	5	5	2	c	49	49	46	38	39	0.05	12.5	0.05	5.00	5
Spiramycin	c	c	30	12	9	c	c	47	25	66	66	0.50	125	1.00	1.00	2	
Sulfadiazine	31	16	6	7	13	12	224	34	31	24	30	25	0.01	2.5	0.05	5.00	6
Sulfamerazine	36	5	11	4	12	6	64	24	27	22	23	24	0.01	2.5	0.05	5.00	6
Sulfamethoxazole	c	9	9	9	8	8	c	23	22	24	26	29	0.05	12.5	0.05	5.00	5
Terbutaline	c	10	15	8	5	3	c	37	40	42	43	33	0.05	12.5	0.05	1.00	4
Tetracycline	c	c	29	12	7	9	c	44	28	28	34	0.10	25	0.50	1.00	2	
Tolfenamic acid	23	9	7	7	5	8	7	19	14	18	19	20	0.01	2.5	0.05	5.00	6
Trimethoprim	7	7	7	4	4	1	47	32	37	28	25	26	0.01	2.5	0.01	0.50	4
Tylosin	c	19	9	8	4	13	19	c	18	38	22	34	0.05	12.5	0.05	1.00	4
Ventilaxine	9	4	3	4	2	4	24	31	31	28	28	27	0.01	2.5	0.01	5.00	6

<sup>a</sup> Highest concentration and number of concentration levels in linear range. <sup>b</sup> Values not determined. <sup>c</sup> Values was not calculated because calculated concentration (i.e. result of the concentration present in the not-spiked sample and the spiking level) is below CC $\alpha$ . <sup>d</sup> No trace found at the concentration level. <sup>e</sup> CC $\alpha$  estimated from reproducibility data.

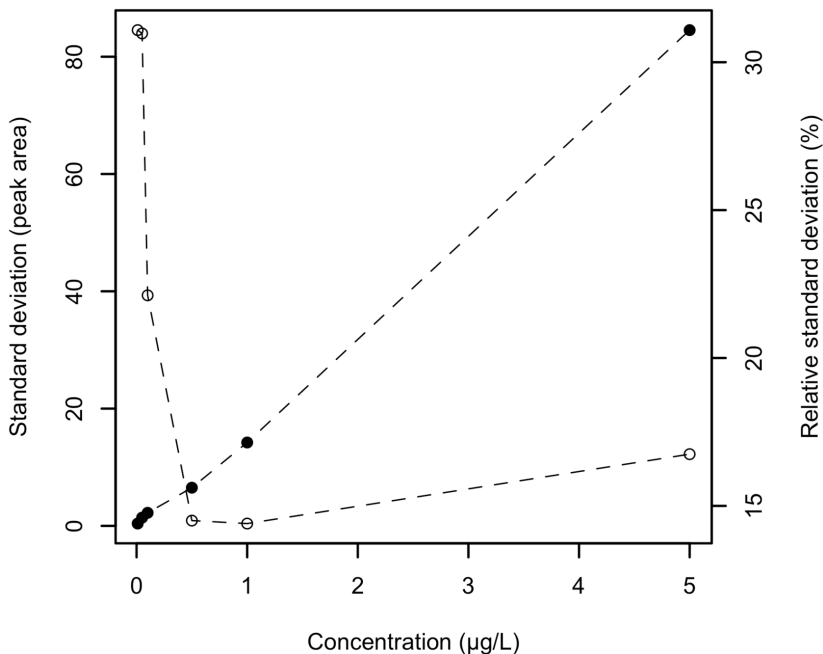


**Figure 5.5** The standard deviation (●) on the integrated peak area measured under interday repeatability conditions increases proportionally with the concentration of diclofenac in deionized water. The relative standard deviation (○) shows a steep decrease at low concentrations ( $< 0.5 \mu\text{g l}^{-1}$ ) and subsequently levels off.

The instrumental decision limits ranged from 2.5 to 125 pg injected for all compounds. For some compounds, the peak intensity indicates that even CCAs lower than 2.5 pg ( $0.01 \mu\text{g l}^{-1}$ ) could be reached with the TOF-MS used in this study, but this could not be confirmed because the lowest tested concentration level was  $0.01 \mu\text{g l}^{-1}$ . Comparable (i.e. between 10-fold higher and 10-fold lower) instrumental detection limits (IDLs) were found in literature for multi-residue methods for the

analysis of the same pharmaceuticals using TOF and triple quadrupole mass spectrometers (Figure 5.6) (Baker & Kasprzyk-Hordern, 2011; Farré *et al.*, 2008; Gros *et al.*, 2006, 2009; Ibáñez *et al.*, 2009; Petrović *et al.*, 2006; Nurmi & Pellinen, 2011; Ferrer *et al.*, 2010). On the other hand, up to 100-fold lower instrumental detection limits were found for quadrupole linear-ion trap tandem mass spectrometers (Gros *et al.*, 2012).

For a majority of the compounds, linearity was demonstrated for a range of at least 2 orders of magnitude (i.e. up to 1 or 5  $\mu\text{g l}^{-1}$ ). However, for 9 compounds a significant deviation from linearity was observed and limited up to 0.1 or 0.5  $\mu\text{g l}^{-1}$ . These results suggest that linear ranges of 2 orders of magnitude for most compounds are to be expected for the utilized TOF-MS, which is in general at least one order of magnitude less than the linearity of triple quadrupole and quadrupole linear-ion trap tandem mass spectrometers. These findings are in agreement with the findings of other authors (Nurmi & Pellinen, 2011; Ferrer & Thurman, 2012; Petrović *et al.*, 2006; Farré *et al.*, 2008) using TOF-MS.

### 5.3.3.2 Method validation

The results for the method validation for surface and drinking water are given in Table 5.2 and Table 5.3, respectively. Retention time deviations between the analytes in matrix and analytical standards were < 2.5% for all analytes. The interday repeatability for drinking and surface water barely increased compared to the RSDs of the instrumental intraday repeatability (Table 5.1) indicating that the daily external calibration was effective to reduce the day-to-day

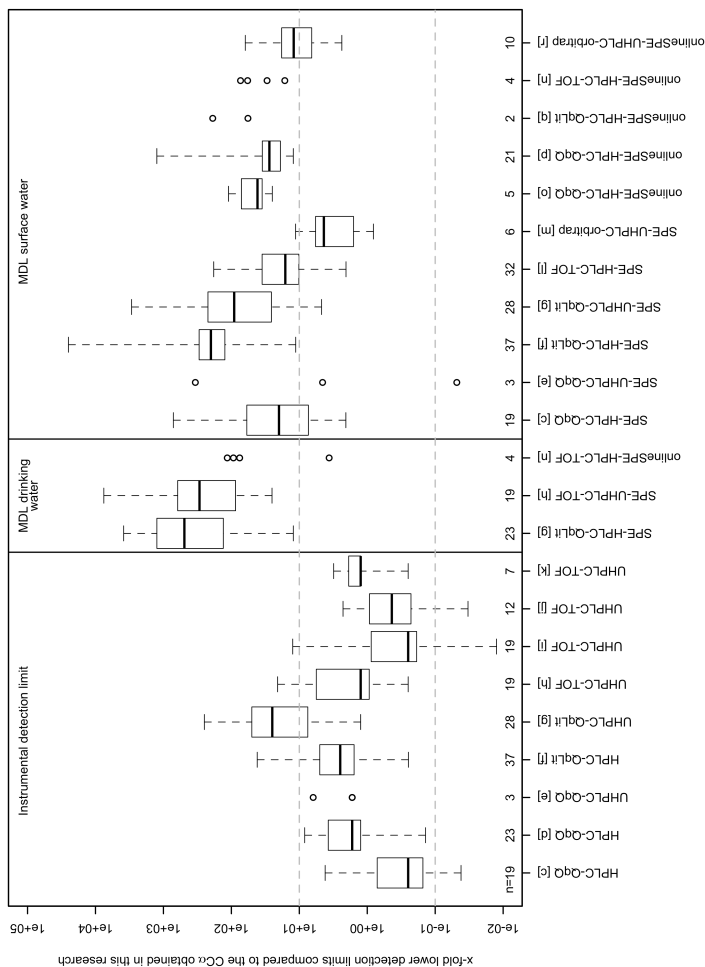


**Figure 5.6** Comparison of the instrumental (pg on column) and method detection limits (MDL, concentration in matrix) of multi-residue methods for pharmaceuticals in drinking and surface water using SPE and online-SPE combined with different MS instruments. Only the pharmaceuticals being the same as those used in this research are considered, and the number of corresponding compounds is given ( $n$ ). The boxplots show the minimal and maximal values, and the 25, 50 and 75 % percentile. The references [c-r] are given in Table 5.4.

variability. At a concentration of  $0.5 \mu\text{g l}^{-1}$ , the average RSDs of the interday repeatability are 14 and 15 % for surface and drinking water, respectively, which is only a small increase compared to the instrumental intraday repeatability of on average 9 %.

The method  $CC\alpha$  and  $CC\beta$  ranged from  $0.01 \mu\text{g l}^{-1}$  to concentrations higher than  $5 \mu\text{g l}^{-1}$  for drinking and surface water.  $CC\alpha$ s lower than 0.1 and  $0.5 \mu\text{g l}^{-1}$  were obtained for 35 (50 %) and 51 (74 %) out of the 69 compounds in surface water, and for 30 (43 %) and 52 (75 %) out of the 69 compounds in drinking water. For some chemically related pharmaceuticals, such as the iodated X-ray contrast media, typically less good performance limits were obtained. Their short retention time (e.g. iohexol in Figure 5.2) and therefore the quite aqueous composition of their elution solvent, which negatively influences the ESI efficiency, may explain these poorer performance limits. Less good performance limits for some outlying compounds such as the iodated X-ray contrast media are, however, to be expected in multi-residue methods for a broad variety of compounds.

Other authors (Gros *et al.*, 2012; Chitescu *et al.*, 2012; Farré *et al.*, 2008; Gros *et al.*, 2006; Garcia-Ac *et al.*, 2009; Gómez *et al.*, 2010; Wode *et al.*, 2012; Idder *et al.*, 2013; García-Galán *et al.*, 2010a; Pozo *et al.*, 2006) reported 10 to 100 times lower method detection limits (MDLs) for the same compounds using triple quadrupole, quadrupole linear-ion trap tandem MS, and orbitrap and TOF-HRMS (Figure 5.6). These authors all applied (online) SPE as enrichment step to increase the method performance limits and reached 100- to 1000-fold preconcentration factors (Table 5.4). By applying SPE and online SPE, the equivalent

**Table 5.2** Parameters of the method validation indicating the performance of the analytical method for surface water.

Pharmaceutical compound	CC $\alpha$ ( $\mu\text{g l}^{-1}$ )	CC $\beta$ ( $\mu\text{g l}^{-1}$ )	Interday repeatability as RSD (% , n = 5) at different spiking levels ( $\mu\text{g l}^{-1}$ )					Matrix effect (%)	
			0.01	0.05	0.1	0.5	1		5
4-(dimethylamino)antipyrine	0.14	0.54	a	a	24	17	11	7	67
Atenolol	0.07	0.12	a	43	17	17	14	6	91
Betaxolol	0.02	0.05	27	14	10	7	4	4	101
Bezafibrate	0.06	0.06	a	11	14	9	10	6	93
Bisoprolol	0.02	0.02	14	10	3	5	5	7	86
Caffeine	0.23	0.67	a	44	40	18	15	8	87
Carbamazepine	0.06	0.15	43	32	17	10	12	2	107
Chlorotetracycline	0.51	0.51	a	a	a	20	24	18	116
Ciprofloxacin	0.08	0.12	a	22	20	13	14	13	80
Clenbuterol	0.06	0.06	a	24	18	6	8	2	82
Cloxacillin	0.14	0.14	a	a	19	20	21	20	103
Cyclophosphamide	0.07	0.07	a	20	16	6	6	8	92
Dapsone	0.05	0.05	a	6	11	13	15	10	84
Diatrizoic acid	1.04	5.04	a	a	a	a	30	18	69
Diclofenac	0.04	0.07	31	16	12	9	3	4	95
Doxycycline	0.56	0.56	a	a	a	14	12	16	88
Enoxacin	0.08	0.12	a	26	18	11	15	9	94
Enrofloxacin	0.10	0.15	a	15	16	6	14	8	103
Erythromycin-H <sub>2</sub> O	0.08	0.12	a	21	11	11	10	9	99
Fenofibrate	0.06	0.48	a	19	34	13	6	19	97
Fenoprofen	0.11	0.49	a	a	27	6	9	9	93
Fluoxetin	0.05	0.05	a	12	11	13	12	18	108
Furazolidone	0.01	0.06	23	30	19	20	30	29	95
Gemfibrozil	0.12	0.12	a	a	19	4	5	5	98
Ibuprofen	0.17	0.5	a	a	30	18	14	5	93
Ifosfamide	0.11	0.55	a	44	35	9	11	7	96



**Table 5.2** (continued)

Pharmaceutical compound	CC $\alpha$ ( $\mu\text{g l}^{-1}$ )	CC $\beta$ ( $\mu\text{g l}^{-1}$ )	Interday repeatability as RSD (%) at					Matrix effect (%)		
			0.01	0.05	0.1	0.5	1		5	
Indometacin	>5.00	>5.00	a	a	a	a	a	a	a	110
Iodipamide	0.41	0.83	a	a	a	20	12	28	a	110
Iohexol	1.49	1.49	a	a	a	a	20	31	a	48
Ioprepol	1.24	1.24	a	a	a	a	18	24	a	61
Iopamidol	3.66	>5.00	a	a	a	a	24	52	a	15
Iopanoic acid	0.73	0.73	a	a	a	14	15	9	a	78
Iopromide	0.34	0.77	a	a	28	15	12	20	a	48
Iotalamic acid	0.87	4.87	a	a	a	a	30	27	a	79
Ketoprofen	0.06	0.06	a	17	16	11	9	6	a	86
Lincomycin	0.50	0.50	a	a	a	18	19	5	a	120
Metoprolol	0.15	0.55	a	a	29	13	8	4	a	93
Metronidazole	0.06	0.11	a	35	22	9	15	7	a	89
Nafillin	0.41	0.41	a	a	a	17	15	13	a	183
Naproxen	0.55	0.55	a	a	a	10	11	11	a	85
Norflloxacin	0.09	0.50	a	31	24	12	13	12	a	86
Ofloxacin	0.07	0.12	a	19	12	7	11	9	a	86
Oleandromycin	0.05	0.09	a	36	17	12	10	8	a	103
Oxacillin	0.14	0.55	a	a	16	31	20	17	a	104
Oxytetracycline	0.57	0.57	a	a	a	21	18	19	a	99
Paracetamol	0.59	0.59	a	a	a	6	13	10	a	73
Penicillin G	0.56	0.56	a	a	a	18	28	40	a	61
Penicillin V	0.53	1.02	a	a	a	28	25	18	a	97
Pentoxifylline	0.03	0.07	a	38	13	6	8	5	a	90
Phenazone	0.02	0.06	a	42	16	11	3	6	a	83
Pindolol	0.02	0.06	a	39	20	12	10	5	a	68

**Table 5.2** (continued)

Pharmaceutical compound	CC $\alpha$ ( $\mu\text{g l}^{-1}$ )	CC $\beta$ ( $\mu\text{g l}^{-1}$ )	Interday repeatability as RSD (%; $n = 5$ ) at different spiking levels ( $\mu\text{g l}^{-1}$ )					Matrix effect (%)	
			0.01	0.05	0.1	0.5	1		
Primidon	0.18	0.56	a	a	32	11	9	11	80
Propranolol	0.50	0.50	a	a	a	23	11	3	106
Propyphenazone	0.05	0.09	a	36	20	5	5	7	101
Ronidazole	0.13	1.01	a	a	29	47	40	26	99
Roxithromycin	0.06	0.11	a	28	19	20	20	20	148
Salbutamol	0.09	0.55	a	46	27	18	6	8	96
Salicylic acid	0.54	0.54	a	a	a	20	15	8	85
Sotalol	0.12	0.18	a	33	20	21	7	7	93
Spiramycin	0.55	5.04	a	a	a	31	34	37	242
Sulfadiazine	0.06	0.11	a	30	9	11	11	8	110
Sulfamerazine	0.06	0.13	a	29	19	9	9	9	132
Sulfamethoxazole	0.05	0.14	46	29	14	4	11	6	89
Terbutaline	0.55	0.55	a	a	a	18	14	9	104
Tetracycline	0.06	0.10	a	33	12	10	24	20	130
Tofenaminic acid	0.02	0.05	37	9	5	7	3	4	100
Trimethoprim	0.06	0.06	a	18	14	8	7	8	93
Tylosin	0.08	0.49	a	25	27	15	13	13	111
Venlafaxine	0.03	0.07	42	18	12	4	5	3	93

<sup>a</sup> Value was not calculated because calculated concentration (i.e. result of the concentration present in the not-spiked sample and the spiking level) is below CC $\alpha$ .

**Table 5.3** Parameters of the method validation indicating the performance of the analytical method for drinking water.

Pharmaceutical compound	CC $\alpha$ ( $\mu\text{g l}^{-1}$ )	CC $\beta$ ( $\mu\text{g l}^{-1}$ )	Intraday repeatability as RSD (%; $n = 5$ ) at different spiking levels ( $\mu\text{g l}^{-1}$ )					Matrix effect (%)	
			0.01	0.05	0.1	0.5	1		
4-(dimethylamino)antipyrine	0.05	0.05	a	9	6	9	3	7	85
Atenolol	0.13	0.13	a	a	a	12	10	3	95
Betaxolol	0.1	0.1	a	a	27	8	3	7	109
Bezafibrate	0.05	0.05	a	13	12	6	6	5	98
Bisoprolol	0.01	0.01	33	11	12	5	7	7	96
Caffeine	0.49	0.49	a	a	a	20	15	3	97
Carbamazepine	0.07	0.07	a	a	21	9	8	3	101
Chlorotetracycline	0.55	0.55	a	a	a	29	24	10	93
Ciprofloxacin	0.07	0.07	a	21	17	8	11	1	90
Clenbuterol	0.05	0.05	a	43	21	17	13	4	81
Cloxacillin	1.02	1.02	a	a	a	a	40	39	69
Cyclophosphamide	0.08	0.08	a	a	13	10	10	4	93
Dapsone	0.04	0.04	a	16	12	11	11	4	92
Diazizotic acid	1.05	1.05	a	a	a	a	32	23	72
Diclofenac	0.48	0.48	a	a	a	11	9	5	107
Doxycycline	0.49	0.49	a	a	a	18	22	23	77
Enoxacin	0.13	0.13	a	a	a	11	11	18	97
Enrofloxacin	0.09	0.09	a	a	12	13	10	22	115
Erythromycin-H <sub>2</sub> O	0.06	0.06	a	29	20	11	15	15	99
Fenofibrate	0.13	0.13	a	a	35	11	8	25	99
Fenoprofen	0.49	0.49	a	a	a	10	3	4	103
Fluoxetine	0.05	0.05	a	13	4	25	14	33	120
Furazolidone	0.06	0.06	a	15	16	24	19	16	99
Gemfibrozil	0.07	0.07	a	29	11	6	5	8	93
Ibuprofen	0.17	0.17	a	a	a	9	13	7	98
Ifosfamide	0.15	0.15	a	a	a	10	7	8	96

Table 5.3 (continued)

Pharmaceutical compound	CC $\alpha$ ( $\mu\text{g l}^{-1}$ )	CC $\beta$ ( $\mu\text{g l}^{-1}$ )	Interday repeatability as RSD (%; $n = 5$ ) at different spiking levels ( $\mu\text{g l}^{-1}$ )					Matrix effect (%)
			0.01	0.05	0.1	0.5	1	
Indomethacine	>5.00	>5.00	a	a	a	a	a	a
Iodipamide	>5.00	>5.00	a	a	a	a	a	a
Iohexol	0.46	0.46	a	a	a	28	23	37
Iomeprol	0.57	0.57	a	a	a	37	29	26
Iopamidol	>5.00	>5.00	a	a	a	a	a	a
Iopanoic acid	0.13	0.13	a	a	20	9	10	12
Iopromide	0.53	0.53	a	a	a	17	23	41
Totalamic acid	0.9	0.9	a	a	a	a	25	32
Ketoprofen	0.05	0.05	a	28	17	3	7	6
Lincomycin	0.05	0.05	a	21	16	22	21	12
Metoprolol	0.56	0.56	a	a	a	20	8	2
Metronidazole	0.06	0.06	a	22	12	10	12	7
Nafcillin	0.1	0.1	a	a	45	27	27	28
Naproxene	0.39	0.39	a	a	a	25	16	13
Norflaxacin	0.08	0.08	a	a	21	13	13	12
Ofloxacin	0.07	0.07	a	13	16	8	9	8
Oleandomycin	0.1	0.1	a	a	38	10	16	16
Oxacillin	0.63	0.63	a	a	a	24	25	22
Oxytetracycline	0.11	0.11	a	a	37	20	27	13
Paracetamol	0.12	0.12	a	a	26	14	11	7
Penicillin G	>5.00	>5.00	a	a	a	a	a	a
Penicillin V	0.51	0.51	a	a	a	40	74	39
Pentoxifylline	0.06	0.06	a	21	10	6	5	8
Phenazone	0.01	0.01	30	14	20	15	12	8
Pindolol	0.01	0.01	26	18	19	16	12	2

Table 5.3 (continued)

Pharmaceutical compound	CC $\alpha$ ( $\mu\text{g l}^{-1}$ )	CC $\beta$ ( $\mu\text{g l}^{-1}$ )	Interday repeatability as RSD (%; $n = 5$ ) at different spiking levels ( $\mu\text{g l}^{-1}$ )						Matrix effect (%)
			0.01	0.05	0.1	0.5	1	5	
Primidon	0.53	0.53	a	a	a	11	8	5	88
Propranolol	0.45	0.45	a	a	a	14	6	6	109
Propyphenazone	0.01	0.01	a	5	11	5	4	2	84
Rondazole	0.51	0.51	a	a	a	34	33	25	104
Roxithromycin	0.38	0.38	a	a	a	a	16	40	172
Salbutamol	0.13	0.13	a	a	a	7	8	11	102
Salicylic acid	0.05	0.05	a	30	27	10	11	11	89
Sotalol	0.58	0.58	a	a	a	17	8	7	95
Spiramycin	1.02	1.02	a	a	a	a	34	54	310
Sulfadiazine	0.11	0.11	a	a	a	20	10	12	114
Sulfamerazine	0.05	0.05	a	23	16	18	22	2	134
Sulfamethoxazole	0.11	0.11	a	a	a	25	5	4	97
Terbutaline	0.06	0.06	a	27	10	10	8	10	108
Tetracycline	0.12	0.12	a	a	a	33	36	37	94
Tolfanamic acid	0.01	0.01	a	10	11	11	2	2	99
Trimethoprim	0.01	0.01	46	10	12	10	10	9	97
Tylosin	0.11	0.11	a	a	a	22	17	15	108
Venlafaxine	0.06	0.06	a	27	17	4	3	6	97

<sup>a</sup> Value was not calculated because calculated concentration (i.e. result of the concentration present in the not-spiked sample and the spiking level) is below CC $\alpha$ .

sample volume ( $ESIV = \text{preconcentration factor} \times \text{volume injected}$ , assuming 100% recovery) was a factor of 2 to 80 larger compared to a 250- $\mu\text{l}$  large-volume injection without SPE enrichment, which may, explain the lower obtained performance limits in this study.

Matrix effects are a known drawback related to the use of ESI sources in LC-MS. Co-eluting organic and inorganic matrix compounds can induce signal suppression or, less frequently, enhancement and therefore affect the sensitivity of the analytical method, lead to decreased reproducibility or affect linearity (Demeestere *et al.*, 2010). Calculated matrix effects ranged from 58 to 310% for drinking water and from 15 to 242% for surface water for all compounds. Similar values for signal suppression and signal enhancement were found in literature even when applying a SPE clean-up step (Ferrer *et al.*, 2010; Gómez *et al.*, 2010; Chitescu *et al.*, 2012). These results confirm that, as stated by (Busetti *et al.*, 2012), widespread applied clean-up strategies such as SPE are less effective in removing interfering matrix compounds than commonly thought in multi-residue analysis of water samples, where washing protocols are rather simple.

The mean mass error (Table 5.5) was independent of both the matrix of the sample and the concentration level and between  $-0.5$  and  $0.5$  ppm. However, the variability clearly rose at low concentrations: the 95% confidence limits doubled at  $CC\alpha$  and  $CC\beta$  compared to  $5\ \mu\text{g l}^{-1}$ . At  $5\ \mu\text{g l}^{-1}$  the 95% confidence limit of the mass error was about 5 ppm for all matrices, which is a typical value that can be found in literature for TOF mass spectrometers.

**Table 5.4** Comparison of the injection volume and the preconcentration factor applied by various authors for the analysis of pharmaceuticals in drinking (dw) and surface (sw) water using different MS instruments.

Analytical technique	Number of corresponding compounds	Injection volume (µl)	Preconcentration factor	Reference
SPE-HPLC-QqQ	19	10	500 (sw)	(Gros <i>et al.</i> , 2006) <sup>c</sup>
SPE-HPLC-QqQ	23	15	<sup>a</sup>	(Ferrer <i>et al.</i> , 2010) <sup>d</sup>
SPE-UHPLC-QqQ	3	20	1000 (sw)	(Baker & Kasprzyk-Hordern, 2011) <sup>e</sup>
SPE-HPLC-QqLit	37	20	500 (sw)	(Gros <i>et al.</i> , 2009) <sup>f</sup>
SPE-UHPLC-QqLit	28	5	500 (dw), 100 (sw)	(Gros <i>et al.</i> , 2012) <sup>g</sup>
SPE-UHPLC-TOF	19	10	500 (dw)	(Farré <i>et al.</i> , 2008) <sup>h</sup>
SPE-UHPLC-TOF	19	10	100 (sw)	(Petrović <i>et al.</i> , 2006) <sup>i</sup>
SPE-UHPLC-TOF	12	5	<sup>a</sup>	(Nurmi & Pellinen, 2011) <sup>j</sup>
SPE-UHPLC-TOF	7	10	200 (sw)	(Ibáñez <i>et al.</i> , 2009) <sup>k</sup>
SPE-HPLC-TOF	32	20	400 (sw)	(Gómez <i>et al.</i> , 2010) <sup>l</sup>
SPE-UHPLC-Orbitrap	6	<sup>a</sup>	400 (sw)	(Gómez <i>et al.</i> , 2010) <sup>l</sup>
online SPE-HPLC-TOF	4	10 000 (dw, sw)	-	(Chitescu <i>et al.</i> , 2012) <sup>m</sup>
online SPE-HPLC-QqQ	5	9800 (sw)	-	(García-Ac <i>et al.</i> , 2009) <sup>n</sup>
online SPE-HPLC-QqQ	21	1000 (sw)	-	(Poza <i>et al.</i> , 2006) <sup>o</sup>
online SPE-HPLC-QqLit	2	15 000 (sw)	-	(Idder <i>et al.</i> , 2013) <sup>p</sup>
online SPE-UHPLC-Orbitrap	10	1000 (sw)	sample 1:2 diluted	(García-Galán <i>et al.</i> , 2010a) <sup>q</sup>
IVI-UHPLC-TOF	<sup>b</sup>	250	-	(Wode <i>et al.</i> , 2012) <sup>r</sup>

<sup>a</sup> Data not available.<sup>b</sup> This research is the reference.<sup>c-r</sup> The labels refer to the references in Figure 5.6.

**Table 5.5** Mean mass error and mass precision ( $n = 5$  observations  $\times$  69 pharmaceuticals) of the TOF-MS at the  $CC\alpha$  and  $CC\beta$  (for each of the individual compounds), and at  $5 \mu\text{g l}^{-1}$  for deionized, drinking and surface water.

Concentration level	Mean mass error (ppm)	95% confidence limit (ppm)
Deionized water		
$CC\alpha$	0.3	$\pm 11.0$
$CC\beta$	0.3	$\pm 11.0$
$5 \mu\text{g l}^{-1}$	0.5	$\pm 4.0$
Drinking water		
$CC\alpha$	0.2	$\pm 9.1$
$CC\beta$	0.5	$\pm 8.0$
$5 \mu\text{g l}^{-1}$	0.1	$\pm 4.6$
Surface water		
$CC\alpha$	0.5	$\pm 9.3$
$CC\beta$	-0.3	$\pm 7.0$
$5 \mu\text{g l}^{-1}$	-0.5	$\pm 5.6$

### 5.3.4 Application in surface and drinking water

#### 5.3.4.1 Application of the suspect screening methodology

The developed suspect screening strategy was applied on one drinking water sample and five surface water samples. First, the obtained chromatograms were screened for the presence of peaks having a minimal signal intensity ( $i$ ) of 100 a.u. and a mass error for which holds that  $|e_{m/z}| \leq \frac{1.96 \cdot \sigma}{\log(i)}$  with  $\sigma = 10.96$  ppm. Second, the resulting retained peaks were tentatively confirmed when their retention time deviates not more than  $1.96 \times$  standard deviation, i.e. within the 95% confidence interval, from the retention time listed in Table A.2.

In the drinking water sample, 4 pharmaceutical compounds (bisoprolol, enoxacin, propranolol and propyphenazone) were retained



by the signal intensity-dependent suspect screening and subsequently confirmed based on the retention time. In the 5 surface water samples, 30 pharmaceuticals (105 hits) were retained by the screening strategy in at least one sample and confirmed based on the retention time (Table 5.6). As an additional confirmation, the signal intensity-dependent screening strategy (minimal signal intensity of 100 a.u. and  $|e_{m/z}| \leq \frac{1.96 \cdot \sigma}{\log(i)}$  with  $\sigma = 10.96$  ppm) was also applied for searching the HE chromatograms for the presence of fragment ions of the respective parent ions. A fragment ion was confirmed when its retention time was within a window of 0.05 min around the retention time of its found parent ion's peak. For 14 compounds in the 5 surface water samples, also the fragment ions were retained. However, the sensitivity of the instrument in the MS<sup>E</sup> approach (HE function with ramped collision energy) seems to be not sufficient enough to obtain signal intensity  $i > 100$  a.u. for fragment ions of a wide range of analytes at real environmental concentrations. Confirmation based on fragments was only possible for 32 of the 105 hits. In Figure 5.7, LE and HE chromatograms for atenolol and metoprolol are presented illustrating cases where confirmation based on fragments was successful and not successful, respectively.

**Table 5.6** Results from the suspect screening and target quantification for the five surface water samples.

Pharmaceutical compound	Screening: Number of retained and confirmed parent (fragment) ions	Quantification: Concentration range in ng l <sup>-1</sup> (Number of detected and/or quantified peaks)
<i>Adrenergics</i>		
Salbutamol	2 (2)	> 94 <sup>a</sup> (1)
<i>Analgesics</i>		
4-(dimethylamino)antipyrine	5 (4)	≤ CC $\alpha$
Phenazone	4 (0)	> 19 <sup>a</sup> (1)
Propyphenazone	5 (1)	≤ CC $\alpha$
Salicylic acid	5 (2)	≤ CC $\alpha$
<i>Antibiotics</i>		
Enrofloxacin	1 (1)	≤ CC $\alpha$
Erythromycin-H <sub>2</sub> O	3 (1)	> 80 <sup>a</sup> (3)
Lincomycin	2 (1)	≤ CC $\alpha$
Metronidazole	1 (0)	≤ CC $\alpha$
Nafcillin	1 (0)	≤ CC $\alpha$
Norfloxacin	1 (0)	≤ CC $\alpha$
Roxithromycin	3 (1)	> 56 <sup>a</sup> - 155 (3)
Sulfamethoxazole	3 (0)	> 49 <sup>a</sup> (2)
Trimethoprim	3 (0)	≤ CC $\alpha$
<i>Antidepressant</i>		
Venlafaxine	5 (3)	>34 <sup>a</sup> (4)
<i>Antiepileptic</i>		
Carbamazepine	5 (5)	> 58 <sup>a</sup> (5)
<i>Antiinfective</i>		
Furazolidone	0 (0)	> 11a - 62 (2)
<i>Alkylating agents</i>		
Cyclophosphamide	2 (0)	≤ CC $\alpha$
Ifosfamide	5 (0)	> 106 <sup>a</sup> (2)

**Table 5.6** (continued)

Pharmaceutical compound	Screening: Number of retained and confirmed parent (fragment) ions	Quantification: Concentration range in ng l <sup>-1</sup> (Number of detected and/or quantified peaks)
<i>β-blockers</i>		
Atenolol	5 (1)	> 73 <sup>a</sup> - 425 (4)
Betaxolol	4 (0)	> 20 <sup>a</sup> (2)
Bisoprolol	5 (0)	17 - 23 (4)
Metoprolol	5 (0)	≤ CC <sub>α</sub>
Pindolol	1 (0)	≤ CC <sub>α</sub>
Propranolol	5 (0)	≤ CC <sub>α</sub>
Sotalol	5 (4)	240 - 280 (5)
<i>Anti-inflammatory drugs</i>		
Diclofenac	5 (4)	> 38 <sup>a</sup> - 76 (5)
Ibuprofen	5 (0)	> 175 <sup>a</sup> - 1391 (4)
<i>Peripheral vasodilators</i>		
Pentoxifylline	3 (0)	> 30 <sup>a</sup> (1)
Terbutaline	1 (1)	≤ CC <sub>α</sub>
<i>Psychoanaleptic</i>		
Caffeine	5 (5)	> 227 <sup>a</sup> - 3109 (4)

<sup>a</sup> Value > CC<sub>α</sub> and ≤ CC<sub>β</sub>, i.e. detected but not quantified.

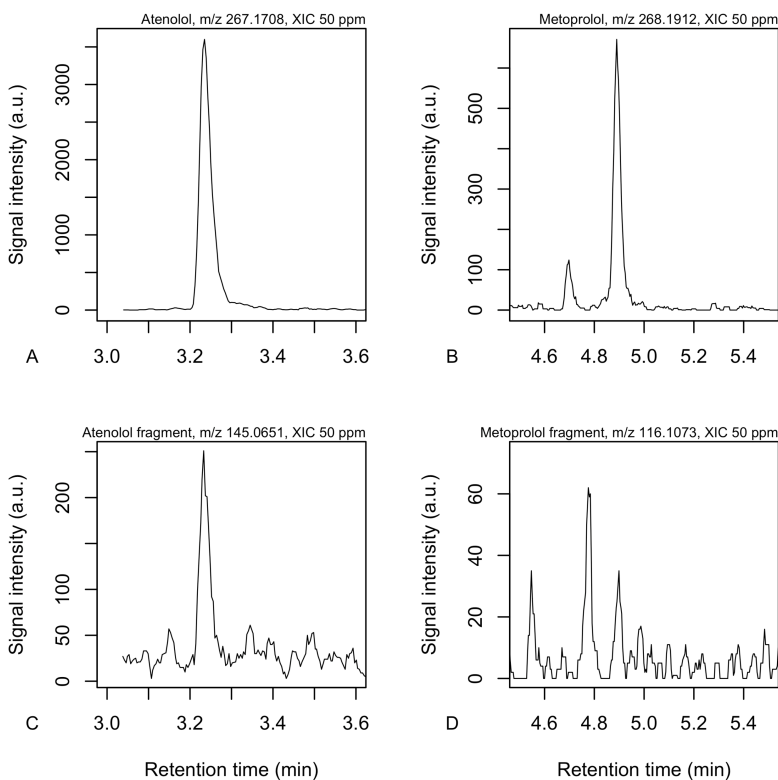


**Figure 5.7** LE and HE chromatograms for atenolol (A, C) and metoprolol (B, D) illustrating cases where confirmation based on fragments was successful and not successful, respectively.

#### 5.3.4.2 Evaluation of the screening performance

In order to evaluate the performance of the applied suspect screening strategy, all found peaks in the surface water samples within a wider mass error tolerance of  $\pm 25$  ppm are considered. For these peaks, the confirmed (+) and non-confirmed ( $\circ$ ) peaks based on the retention time

are presented in Figure 5.3. The retained peaks (157 hits related to 37 different suspect compounds) by the suspect screening fall within the 95 % confidence limits. The signal intensity based screening showed a good performance with a false negative rate (i.e. peaks not-retained by the suspect screening but confirmed by retention time) of 4.6 %. Out of the 157 retained hits, 52 hits could not be confirmed by retention time and thus labeled as false positive hits. Taking into account that these 52 hits were retained in 5 samples analyzed towards 69 pharmaceuticals, the false positive rate is about 15 % ( $\frac{52}{5 \times 69}$ ). On the other hand, the false discovery rate, which is the number of false positives (52 hits) divided by the total number of positives (157 hits), is about 33 %. The latter is specific for a certain sample and depends on the number of contaminants truly present in the measured samples (in this case  $157 - 52 = 105$  hits). Consequently, the false positive rate (15 %) is preferred instead of the false discovery rate (33 %) because this value is independent of the contamination level of the sample and will allow an unbiased comparing of future (improved) screening methods.

The importance of the signal-intensity based mass error is emphasized when a more general and often applied mass error tolerance of  $\pm 5$  ppm is applied. In that case, the false negative rate would account for 19 % of the compounds confirmed by retention time. These false negatives had signal intensities below 800 a.u.; which is in the lower intensity range of Figure 5.3. The use of a signal-intensity based mass error is therefore of utmost importance in multi-residue screening at trace levels.

### **5.3.4.3 Target quantification**

Target quantification was performed on one drinking water sample and five surface water samples following the validated analytical method. In the drinking water sample, no traces exceeding the decision limit were measured. The presence of the 4 pharmaceutical compounds retained and confirmed by the suspect screening could not be validated because their concentrations were below the decision limit. In order to be able to quantify drinking water relevant concentrations, at about 100-fold lower decision limits are required (Farré *et al.*, 2008; Gros *et al.*, 2012).

In the five surface water samples, detection and/or quantification was achieved for 17 pharmaceutical compounds in at least one out of the five samples at concentrations ranging from 17 ng l<sup>-1</sup> to 3.1 µg l<sup>-1</sup> (Table 5.6). For 5 compounds (atenolol, caffeine, ibuprofen, roxithromycin and sotalol) the concentration range exceeded the level of 100 ng l<sup>-1</sup> at least once.

All the detected and/or quantified observations in the five surface water samples were also found by the suspect screening except for 3 hits. Furazolidone, which was detected twice at a concentration above the decision limit, was not retained once by the suspect screening strategy due to its low signal intensity (< 100 a.u.) indicating that the signal intensity limit of 100 a.u. might be too stringent in some cases resulting in not-retained truly present compounds. Only one quantified observation of sulfamethoxazole was not retained by the screening due to its too erroneous accurate mass.

Only limited studies reported concentrations of pharmaceuticals in Belgian surface waters. Loos *et al.* (2009) conducted an EU-wide survey (including the river Scheldt, Belgium) of pharmaceuticals. Wille *et al.* (2010, 2011b) detected and quantified 8 pharmaceuticals in seawater ( $1\text{-}855\text{ ng l}^{-1}$ ) and marine organisms from the Belgian coastal zone from which 5 pharmaceuticals were also identified in this study (atenolol, carbamazepine, propranolol, salicylic acid and sulfamethoxazole). Although for most pharmaceuticals concentration levels found in surface waters in this study are similar to those found in other European countries (Zuccato *et al.*, 2010; Morasch *et al.*, 2010; Gros *et al.*, 2012), only limited studies revealed the occurrence of alkylating agents (cyclophosphamide and ifosfamide) in surface waters (Kosjek & Heath, 2011).

### 5.3.5 Evaluation of large-volume injection UHPLC and HRMS for rapid screening and quantification: pros and cons

Large-volume injection showed to be an important advantage of the presented rapid analytical screening and quantification technique. Good and stable (deviation  $t_R \leq 1.96 \cdot \sigma_{t_R}$ ) chromatography was obtained in a 19 min UHPLC separation and the analytical method requires no sample pretreatment (except for filtering the sample). This is in contrast with most published analytical methods for the analysis of micropollutants in surface water applying laborious and time-consuming SPE enrichment steps. Besides, sample enrichment techniques such as SPE preconcentrate compounds selectively and, as highlighted by Busetto *et al.* (2012), achieving acceptable recoveries for all compounds

is unlikely in multi-residue applications. On the other hand, SPE enables a clean-up of the sample which can be important to prevent contamination of the LC system and to reduce matrix effects for heavily polluted or salty samples. However, the drinking and surface water samples analyzed in this research did not affect the LC system and acceptable matrix effects were calculated. It still needs investigation, however, to point out what will be the potential of LVI-based analysis for a broader variety of environmental (waste)water samples.

Omitting selectivity through sample preparation for multi-residue screening is very relevant to assure a more reliable suspect screening. However, it should be denoted that, as shown in Figure 5.6, less good method performance limits are obtained compared to other analytical methods using HRMS mass spectrometers due to the lower amount of analyte injected as a result of both the injection volume and the SPE preconcentration factor. By consequence, validation of LVI-based screening methods is necessary to assure that sufficiently low performance limits are obtained for a broad variety of contaminants. Chitescu *et al.* (2012) recently discussed how low method performance limits should be for multi-residue monitoring of surface waters towards micropollutants, ensuring sufficient protection to the environment. Although the environmental impact of pharmaceuticals is still far from fully understood, a general limit of  $100 \text{ ng l}^{-1}$ , derived from ecotoxicity data, is mentioned for pharmaceuticals in surface water (Chitescu *et al.*, 2012), which is similar to the  $100 \text{ ng l}^{-1}$  limit for pesticides in drinking water, as regulated by the EU Council Directive 98/83/E. Besides,  $100 \text{ ng l}^{-1}$  is also the proposed maximum annual average concentration



for diclofenac in surface waters as found in the revision of the list of priority substances for the EU Water Framework Directive 2000/60/EC. The method development in this study showed the potential to detect 35 (50%) pharmaceuticals at a concentration of  $100 \text{ ng l}^{-1}$  or lower, and for 51 (74%) pharmaceuticals a decision limit of  $500 \text{ ng l}^{-1}$  and lower is reached. Although this is a promising result, more work is needed to further improve the sensitivity in order to be able to screen at a general level of  $100 \text{ ng l}^{-1}$  or lower for a broad range of contaminants. Additionally, an improved sensitivity is also needed for unequivocal confirmation based on fragments and their ion ratio (European Union, 2002, Commission Decision 2002/657/EC) at environmental relevant concentrations, because in this study only for 32 out of the 105 hits fragment ions were found in the HE chromatogram.

A second important advantage of the developed suspect screening strategy is that there is no a priori need for analytical standards. For confirmation of the suspect screening results, only analytical standards of the retained compounds are necessary and if the aim is also quantification, the validation of only the retained and confirmed compounds will be sufficient for a reliable quantification. Considering the 5 surface water samples, mass traces related to 37 different suspect compounds were retained in the chromatograms (Section 5.3.4.2). Analyzing only these 37 compounds as analytical standards would allow the confirmation based on the retention time. Finally, 30 out of the 37 compounds were confirmed by retention time. This means that for 10% of the suspect compounds, false positive hits occurred. The application of the developed screening approach prior to target analysis has thus the

advantage that less analytical standards (37 instead of 69) are needed and that the workload for the validation can be reduced (30 instead of 69).

## 5.4 Conclusions

A methodology for suspect screening towards a broad variety of 69 multi-class pharmaceuticals in drinking and surface water based on an innovative analytical method combining 250- $\mu$ l LVI-UHPLC and QTOF-HRMS has been investigated. The signal intensity-dependent accurate mass error in TOF-MS was taken into account in a novel screening model. The results show that a false positive rate not higher than 15% was obtained for surface water. Suspect screening in five Belgian surface water samples revealed the occurrence of 30 pharmaceuticals. The validated target quantification enabled the detection of 17 pharmaceuticals in a concentration range of 17 ng l<sup>-1</sup> up to 3.1  $\mu$ g l<sup>-1</sup> in five Belgian river water samples.

LVI-UHPLC combined with full-spectrum HRMS is a rapid and promising complement for the widely applied SPE combined with MS/MS for screening and quantification of micropollutants in environmental waters. Therefore, further research and application of LVI in combination with the newest-generation and more sensitive full-spectrum HRMS are encouraged.



# 6

## Balancing the false negative and positive rates for suspect screening in wastewater using solid-phase extraction and Orbitrap mass spectrometry

*Redrafted from:*

*L. Vergeynst, H. Van Langenhove & K. Demeestere. Balancing the false negative and positive rates in suspect screening with high-resolution Orbitrap mass spectrometry using multivariate statistics. Submitted to Analytical Chemistry.*

## 6.1 Introduction

In the suspect screening strategy presented in Chapter 5, chromatograms are searched for the presence of the exact masses of the mono isotopic ions of a list of suspect compounds for which only the molecular formulae are a priori known. This workflow diverges from the traditional target analysis where analytical standards are a priori available.

Preventing false negatives relies in a powerful screening algorithm, which is able to automatically detect peaks (Müller *et al.*, 2011; Moschet *et al.*, 2013) and for which the acceptance thresholds, such as the maximal allowed mass error, are set not too stringent (Chapter 5; Mol *et al.*, 2012). On the other hand, in order to avoid numerous false positives, the maximal allowed mass error should be stringent enough and additional confirmation parameters, such as the accurate mass of the isotopes and isotope ratios (Kaufmann & Walker, 2012b; Moschet *et al.*, 2013), retention time (Kern *et al.*, 2010; Ulrich *et al.*, 2011; Nurmi *et al.*, 2012) and fragmentation prediction (Wolf *et al.*, 2010), could improve the confidence of the identification. In addition, incorporating a peak/noise filter has shown to reduce the number of false positives (Mol *et al.*, 2012; Moschet *et al.*, 2013; Hug *et al.*, 2014). With this purpose, different peak parameters such as the signal-to-noise ratio (Moschet *et al.*, 2013), peak area (Moschet *et al.*, 2013, Chapter 5;), peak area-to-height ratio (Hug *et al.*, 2014) and peak symmetry (Moschet *et al.*, 2013) have been applied to distinguish noise from ‘true’ peaks. However, in each of these studies, an increased false negative rate (FNR) was reported upon choosing the mass error, peak/noise or

other thresholds more stringent, and an acceptable balance between the false positive and negative rate must be found.

In recently published suspect screening studies (K'oreje *et al.*, 2012; Moschet *et al.*, 2013; Hug *et al.*, 2014; Schymanski & Singer, 2014) the results are typically evaluated through a decision tree considering successively different decision criteria including the mass error, isotope fit and a peak/noise filter. Even when the tolerance on the mass error, isotope ratio error and peak/noise filter are well chosen, controlling the FNR is not obvious because a detected analyte has to pass for each of the criteria successively. As such, the FNR accumulates upon advancing through the decision tree and the overall FNR will amount to approximately  $1 - \prod(1 - \alpha_i)$ , with  $\alpha_i$  the FNR of the  $i^{th}$  criterion. For example, the overall FNR can theoretically increase to 30% supposing a decision tree with 7 criteria having each a 5% FNR. In addition, methodologies to appropriately choose the optimal tolerance for each of the decision criteria are still lacking, potentially resulting in a not well-balanced screening, which can be more stringent for some of the criteria than for others.

In this chapter, the aim is to develop a balanced screening for UHPLC-Orbitrap HRMS chromatograms towards a list of 77 suspects based on accurate mass, and taking into account isotope accurate masses and ratios in a holistic approach. Hereby, the goal is to control the overall FNR of the screening algorithm to a challenging level of only 5%. Investigated is to which extent information retrieved from the full-spectrum (without MS/MS), such as the isotope fit, can improve the indicative identification of compounds and how noise peaks can

be omitted in order to reduce the number of false positives, without compromising the false negative rate. In first instance, standards were a priori available for 40 target pharmaceuticals (set A), which were spiked in wastewater treatment plant (WWTP) effluent to construct a training dataset for the suspect screening method development. Subsequently, the same 40 pharmaceuticals (set A) were treated as artificial suspects to perform a hypothetical suspect screening in order to evaluate the screening performance and to estimate the false positive rate (FPR). As proof of concept, 7 WWTP effluents were screened for the whole set of 77 (set A + B) suspect pharmaceuticals.

## 6.2 Material and methods

### 6.2.1 Chemicals

The analyzed pharmaceuticals in Chapters 3 and 5, which are amendable to electrospray ionization (ESI) positive, are selected as suspect compounds in this chapter. For the set A and the retained set B pharmaceuticals, individual stock solutions were prepared on weight basis to a concentration of about  $1 \text{ mg l}^{-1}$  (suppliers and solvents in Table A.1). A standard mix of the pharmaceuticals was prepared at a concentration of  $2 \text{ mg l}^{-1}$ . Standard and matrix-matched solutions were prepared by diluting a standard mix in (i) 10:90 methanol/water with 0.1% (v/v) formic acid and  $0.1 \text{ g l}^{-1} \text{ Na}_2\text{EDTA} \cdot 2 \text{ H}_2\text{O}$  ( $0.01\text{--}1000 \text{ } \mu\text{g l}^{-1}$ ), and (ii) in WWTP effluent ( $0.2\text{--}20\,000 \text{ ng l}^{-1}$ ), respectively. Other chemicals are specified in Section 3.2.1.

## **6.2.2 Sampling, sample pretreatment and solid-phase extraction**

Automatic samplers (50 ml sample each 20 min, Sigma 900 or ISCO 4700, Elscolab, Belgium) collected 24 h time integrated effluent samples from 7 WWTPs in Aalst, Destelbergen, Gent, Geraardsbergen, Harelbeke, Leuven and Tessenderlo (Belgium) in February 2014. Briefly, according to the slightly modified protocol for solid-phase extraction (SPE) described in Section 3.2.3, 50 ml of sample was filtered and enriched through Oasis HLB cartridges. After washing the SPE cartridge with 6 ml, the compounds were eluted with 5 ml methanol, the eluent evaporated and reconstituted in 1 ml of 10:90 methanol/water with 0.1 % (v/v) formic acid and  $0.1 \text{ g l}^{-1} \text{ Na}_2\text{EDTA} \cdot 2 \text{ H}_2\text{O}$ .

## **6.2.3 Instrumental analysis**

Ten  $\mu\text{l}$  of the extract were injected and separated on a UHPLC reversed phase column (Hypersil Gold column,  $1.9 \mu\text{m}$  particle diameter,  $2.1 \times 50 \text{ mm}$ , Thermo Scientific). The following gradient of (A) water, (B) methanol, both acidified with 0.1 % formic acid, and (C) a mixture of equal amounts of water, methanol, acetonitrile and isopropanol acidified with 0.5 % formic acid at a flow rate of  $350 \mu\text{l min}^{-1}$  (Accela 1250 pump, Thermo Scientific) was used: 0-1.5 min 10 % B, 1.5-15 min linear gradient to 100 % B, 15-16 min 100 % B, 16-21 min 100 % C, 21-26 min 10 % B.

Mass spectrometric analysis was performed on an Orbitrap HRMS (Q-Exactive, Thermo Scientific) equipped with a heated ESI (HESI-II,



positive ion mode) source and operated in full scan (150-500  $m/z$ ) at a resolving power of 70 000 at full width at half maximum (FWHM) at 200 Da. Online mass calibration using diisooctyl phthalate ( $C_{24}H_{38}O_4$ ) as a lock mass was enabled. The optimized HESI-II parameters were: spray voltage: 3.5 kV; sheath gas flow rate: 45 a u; auxiliary gas flow rate: 10 a u; capillary temperature: 350 °C; heater temperature: 375 °C; S-lens RF-level: 60 %. The automatic gain control (AGC) target was set at 3 000 000 with a maximal injection time of 200 ms. No MS/MS scans were performed.

## 6.2.4 Suspect screening

### 6.2.4.1 Suspect library

The R-package *enviPat* was used to model the isotopic fine structure of all the suspect compounds in order to determine for each compound the exact mass of the mono isotopic ion  $[M+H]^+$ , the theoretical mass of the first three (by intensity) isotopes and their isotope ratios. The actual resolving power of the Orbitrap MS, which is proportional to  $\frac{1}{\sqrt{m/z}}$  (Zubarev & Makarov, 2013) (Figure 6.1), was taken into account and pointed out that not all isotopes are sufficiently resolved, especially with respect to the  $^{15}N$  and  $^{13}C$  isotopes in some high molecular weight compounds. It was proposed that two isotopes should be resolved by a valley of at least 50 % in order to be considered. This is illustrated in Figure 6.2 for zidovudine ( $m/z$  268.10403). Its  $^{15}N$  and  $^{13}C$  isotopes are only partially resolved. The valley between the isotopes is < 50 % of the abundance of the  $^{13}C$  isotope, however, > 50 % of the abundance

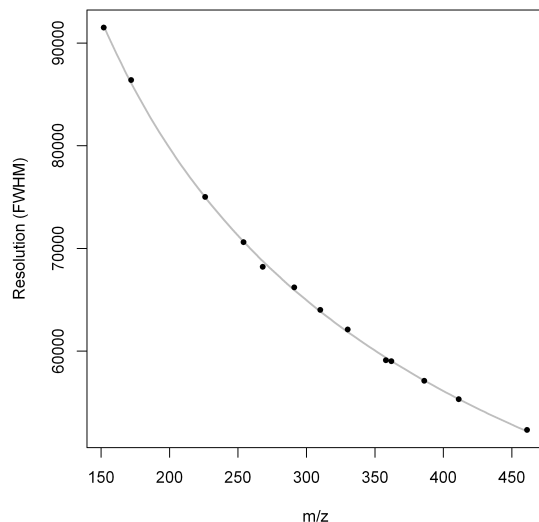


**Figure 6.1** Least squares regression for the measured resolving power ( $R$ ) versus  $m/z$ ,  $R = \frac{1125975}{\sqrt{m/z}}$ , for 13 compounds over a mass range of 150 to 450 Da.

of the  $^{15}\text{N}$  isotope. Thus, only the  $^{13}\text{C}$  isotope is added to the suspect library.

The first three (by intensity) isotopes are used. As such, for chlorinated compounds, the  $^{37}\text{Cl}$ -isotope is the first isotope and for all other compounds (containing N, O, F, I or S heteroatoms) the  $^{13}\text{C}$ -isotope is the first isotope. The selected second and third isotope depend on the number of C- and heteroatoms in each compound and are specified in Table A.3. A selected isotope of the modeled isotopic fine structure must be partially resolved from a nearby isotope by a valley of at least 50%. For compounds with N-atoms, an actual resolving

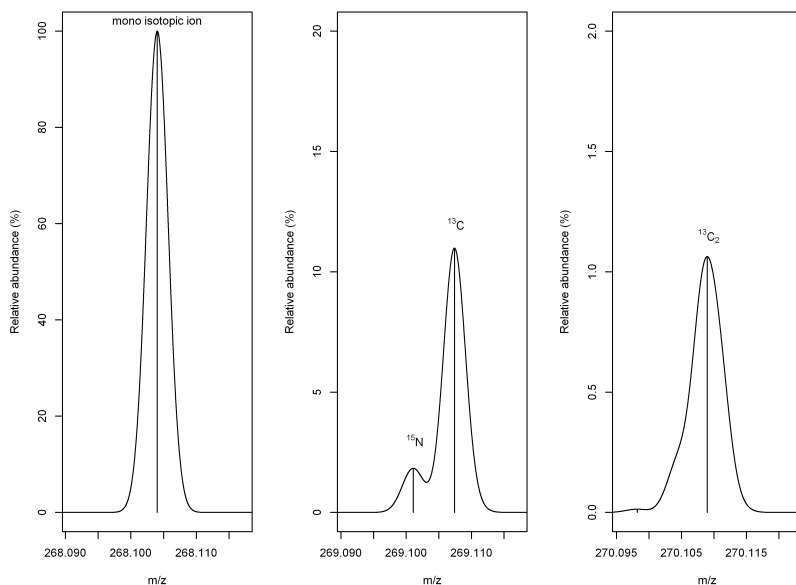


**Figure 6.2** Modelled isotopic fine structure of zidovudine (268.10403  $m/z$ , 68 766 FWHM). The mono isotopic ion (left),  $^{15}\text{N}$  and  $^{13}\text{C}$  (middle), and  $^{13}\text{C}_2$  (right) isotopes are annotated.

power of at least 70 000 FWHM showed to be necessary for a well-resolved  $^{15}\text{N}$  isotope. The suspect library (Table A.3) holds the following information: the compound names, the exact mass of the protonated mono isotopic ion  $[\text{M}+\text{H}]^+$  ( $m/z_{th,0}$ ), the theoretical masses of the three selected isotopes ( $m/z_{th,1}$ ,  $m/z_{th,2}$  and  $m/z_{th,3}$ ), and their theoretical isotopic ratios ( $ir_{th,1}$ ,  $ir_{th,2}$  and  $ir_{th,3}$ ).

#### 6.2.4.2 Non-target peak picking

A non-target peak picking algorithm designed for Orbitrap HRMS is applied on each MS data file and lists up all peaks that are found in

the chromatograms. Therefore, the raw profile MS data files (.raw format) were converted to centroid MS data files (.mzxml format) using ProteoWizard (the Thermo centroiding algorithm was selected) (Chambers *et al.*, 2012). Subsequently, the centWave feature detection algorithm (Tautenhahn *et al.*, 2008) incorporated in the R-package xcms was applied for non-targeted peak picking. Basically, first, region of interests (ROIs) are detected after which the centWave algorithm is applied to the ROIs for peak detection resulting in the detected features. A ROI is a  $m/z$  and retention time domain in which at least  $k = 5$  centroids are found with a signal intensity of at least  $I = 1000$  having a maximal mass deviation of  $\pm 3$  ppm around the mean mass of all centroids in the ROI. Subsequently, for each ROI an extracted ion chromatogram is constructed. For the subsequent peak detection, the continuous wavelet transform (CWT) is used, which reliably detects peaks assuming a Gaussian peak shape. The CWT needs as parameters a minimal and maximal expected peak width (5 and 15 s, respectively) and a minimal signal-to-noise (S/N) ratio ( $S/N > 3$ ). The peak picking process is slow (1-2 h per 15 min LC-MS data file) and therefore, the method was parallelized using the R-package doMC. The Ghent University Supercomputer Infrastructure was used to perform this task in parallel.

The algorithm calculates for each picked peak a set of parameters including accurate mass ( $m/z$ ), retention time ( $t_R$ ), baseline corrected peak area ( $PA$ ), the fit of the chromatographic peak to a Gaussian curve (root-mean-square error of Gaussian fit:  $e_{gauss}$ ), and the width of the Gaussian curve ( $sigma$ -parameter). The accurate mass ( $m/z$ ) and

retention time ( $t_R$ ) are calculated as the intensity weighted average mass and retention time of the centroids in the feature, respectively. For each processed chromatogram, the calculated parameters of the picked peaks are stored in a peak list in which each peak gets a unique ID number. Even in suspect screening - when the molecular formulae and thus the exact masses are a priori known - such a non-target peak picking is advantageous because the 2-dimensional chromatograms (retention time -  $m/z$ ) are reduced to an easily searchable list of peaks, facilitating the subsequent data processing.

### 6.2.4.3 Method development based on a training dataset

The development of the suspect screening methodology relies on the 40 target compounds (set A) spiked in WWTP effluent samples. The aim is to assemble a training dataset containing the measured accurate mass of the mono isotopic ion and its isotopes, isotope ratios, together with the Gaussian fit ( $e_{gauss,i}$ ) and width ( $sigma_i$ ) of each ion. Therefore, non-spiked and spiked (0.2, 2, 20, 200, 2000, 20 000  $ng\ l^{-1}$ ) 24 h composite samples collected at the effluent of the WWTP of Aalst (Belgium) were analyzed in triplicate on 3 different days and the data for the 40 target analytes were manually processed using ExactFinder V1.4 (Thermo Scientific) using a mass extraction window of  $\pm 5$  ppm around the mono isotopic ion. The retention time was compared with a reference standard (maximum retention time deviation of 6 s).

The same chromatograms were in parallel processed through the non-target peak picking algorithm. Then, first, the peak lists were manually searched for the peaks corresponding to the 40 target

compounds. All peaks that were manually processed were also found by the non-target peak picking. Second, the peaks being part of the isotopic pattern of the target compounds were grouped as a component (i.e. manual componentization). Third, for each component (mono isotopic ion and its attributed isotopes), the number of isotopes was counted. A total of 708 mono isotopic ions were obtained of which 573, 440 and 310 had at least 1, 2 and 3 isotopes, respectively. Finally, the mass error of the mono isotopic ion for each component is calculated ( $\Delta m/z_0 = \frac{m/z_0 - m/z_{0,th}}{m/z_{0,th}} \cdot 10^6 ppm$ ) with  $m/z_0$  the accurate mass of the mono isotopic ion as calculated by the non-target peak picking algorithm. For the isotopes ( $i = 1, 2, 3$ ) in each component, the accurate mass ( $m/z_i$ ), retention time ( $t_{Ri}$ ) and the measured isotope ratio based on the peak area ( $ir_i = \frac{PA_i}{PA_0}$ ) are used to calculate the mass error ( $\Delta m/z_i = \frac{m/z_i - m/z_{i,th}}{m/z_{i,th}} \cdot 10^6 ppm$ ), the isotopic retention time shift taking the mono isotopic ion as reference ( $\Delta t_{Ri} = t_{Ri} - t_{R0}$ ), and the relative difference of the isotope ratio ( $\Delta ir_i = \frac{ir_i - ir_0}{ir_{th,i}}$ ), respectively.

#### **6.2.4.4 Multivariate discrimination of noise and peaks**

To discriminate 'true' peaks from noise, the peak parameters which are best fit-for-purpose are selected using multivariate discrimination. The spiked WWTP effluent samples (Section 6.2.4.3) are used for the optimization of a peak/noise filter. In first instance, a dataset was generated containing sufficiently noise and 'true' peaks. Therefore, after non-target peak picking of the MS data files, a mass error filter of  $\pm 5$  ppm is applied on the peak lists for the mono isotopic masses of the 40 target (set A) compounds resulting in a data set containing a total of 1264

peaks. Subsequently, the peaks were visually inspected and 466 peaks were evaluated as being well shaped. These peaks include the peaks of the 40 target compounds but also other peaks of unknown compounds. A well-shaped peak should be a quasi-symmetrical Gaussian shaped and stand out above the surrounding noise. The other 798 peaks were labelled as noise. For the 1264 peaks a total of 12 peak parameters were calculated.

Eight parameters calculated by the centWave feature detection algorithm were used:

- Peak width at base ( $PWB = \text{maximal} - \text{minimal } t_R \text{ of a peak}$ ), as  $\log(PWB)$
- Base line corrected peak area, as  $\log(PA')$
- Peak area, as  $\log(PA)$
- Signal intensity of the peak, as  $\log(I)$
- Signal-to-noise ratio, as  $\log(S/N)$
- Goodness-of-fit of a peak to a Gaussian curve, as  $\log(e_{gauss})$
- Width of the fitted Gaussian curve, as  $\log(\sigma)$
- Height of the fitted Gaussian curve, as  $\log(h)$

Four additional parameters were calculated:

- Inter-scan mass variability, calculated as the intensity weighted standard deviation on the masses of the centroids in a feature, as  $\log(sd(m/z))$

- Area-to-height ratio, as  $\log(\frac{PA}{h})$
- Peak symmetry calculated as the weighted skewness according to Rimoldini (2014), as  $\log(skewness^2)$
- Peak sharpness calculated as the weighted kurtosis according to Rimoldini (2014), as  $\log(kurtosis^2)$

Subsequently, quadratic discriminant analysis (as provided by the MASS packing in R) was amended to evaluate which combination of peak parameters amongst the 12 defined peak parameters resulted in an optimal classification of noise and ‘true’ peaks. A variable selection algorithm adapted from Raftery & Dean (2006) was applied to search for the peak parameter combination having a minimal misclassification error (sum of misclassified peaks/ total number of peaks). The misclassification error was calculated by leave-one-out cross-validation. The selection algorithm consists of the following steps:

1. The peak parameter having the minimal misclassification error is selected.
2. Propose a next peak parameter, which results in the lowest misclassification error.
3. Determine if any selected peak parameters can be dropped without increasing the misclassification error.
4. Repeat step 2 and 3 until no improvement of the misclassification error is possible.



#### 6.2.4.5 Applied computational techniques

All computations were performed using the R software (R Development Core Team, 2008). The *enviPat*, *xcms* and *doMC*, *QRM*, and *MASS* R-packages provided the required functions for the exact mass and theoretical isotope ratio calculations (Section 6.2.4.1), the non-target peak picking (Section 6.2.4.2), calibration of the parameters of the multivariate t-distribution (Sections 6.3.2.2 and 6.3.2.3), and the discriminant analysis (Section 6.2.4.4), respectively.

### 6.3 Results and discussion

#### 6.3.1 Qualitative evaluation of the analytical method (set A)

The average mass error and precision (as standard deviation) of the mono isotopic ion and the three isotopes in the training dataset were  $0.50 \pm 1.18$ ,  $-0.93 \pm 2.57$ ,  $-0.07 \pm 2.36$  and  $-0.92 \pm 3.04$  ppm with  $n = 708$ ,  $573$ ,  $440$  and  $310$ , respectively. The boxplots in Figure 6.3A show that larger mass errors are related to outliers and that the median values are very close to zero ( $0.48$ ,  $-0.25$ ,  $-0.14$  and  $-0.44$  ppm, respectively), showing that no bias is present on the mass accuracy. The accuracy and precision of the isotope ratios is evaluated as the relative difference of the isotope ratio based on the baseline corrected peak area ( $\Delta ir$ , data from the training dataset). On average,  $\Delta ir_i$  amounted to  $-0.02 \pm 0.15$ ,  $-0.10 \pm 0.14$  and  $-0.16 \pm 0.18$  for the  $i^{th}$ , respectively. From these data, and also from the boxplot in Figure 6.3B, it can be seen that the isotope ratios are slightly underestimated in at least 75 % of the cases, especially

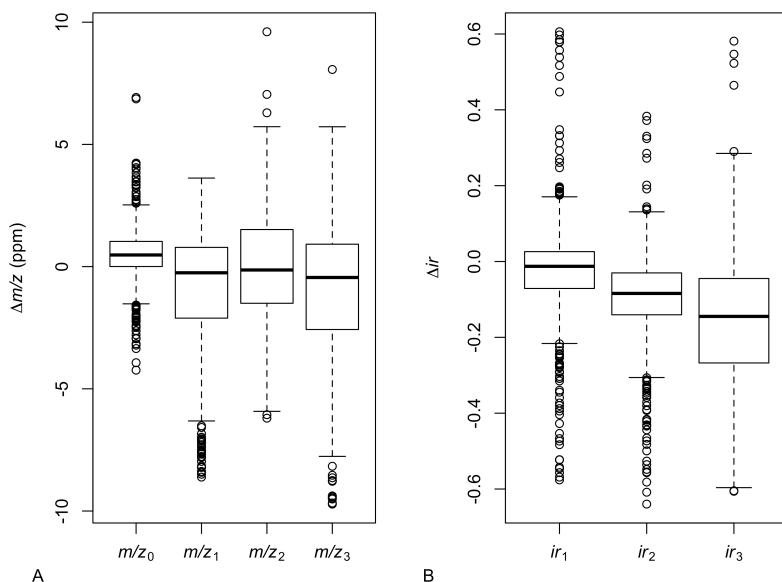


**Figure 6.3** The mass error ( $\Delta m/z$ ) and isotope ratio error ( $\Delta ir$ ) for the mono isotopic ion and the first three isotopes for the 40 target (set A) compounds ( $n = 708, 573, 440$  and  $310$ , respectively), represented as boxplots (the whiskers extend to the most extreme data point within 1.5 times the interquartile range from the box).

for lower intensity isotopes. Other authors observed the same bias and concluded that Orbitrap technology discriminates low (isotopes) against high (mono isotopic ion) intensity ions (Erve *et al.*, 2009; Kaufmann & Walker, 2012a).

### 6.3.2 Development of the suspect screening

The suspect screening workflow is schematically presented in Figure 6.4: suspect library building (Section 6.2.4.1), non-target peak picking (Section 6.2.4.2), automated componentization (Section 6.3.2.1)

followed by multivariate hypothesis testing (Section 6.3.2.2 and 6.3.2.3) after which the retained analytes are confirmed based on retention time.

### 6.3.2.1 Componentization: automated grouping of mono isotopic ions and their isotopes

In order to develop an efficient screening method, the grouping of the mono isotopic ions and their isotopes into components, which has been done manually for the construction of the training dataset, is automated. First, the picked peaks in the peak list are filtered with a wide mass error tolerance filter ( $\pm 10$  ppm) for the mono isotopic exact mass of the suspect compounds ( $|\Delta m/z_0| < 10$  ppm). In this step, a wide mass error tolerance filter of  $\pm 10$  ppm is applied to assure that no peaks, being potentially of interest, are omitted. Note that multiple peaks are possible per suspect compound. Second, for each retained mono isotopic ion, the best matching isotope peak  $i$  is extracted from the peak list. Therefore, the peak list is searched for the peak having a minimal normalized squared error ( $NSE$ ). This is repeated for 2 more isotopes.  $NSE_i$  is calculated as the sum of the normalized squared mass error and the normalized squared isotopic retention time shift:  $NSE_i = \frac{\Delta m/z_i^2}{\sigma_{\Delta m/z}^2} + \frac{\Delta t_{R_i}^2}{\sigma_{\Delta t_R}^2}$  where  $i$  refers to isotope 1 to 3 in Table A.3.  $\sigma_{\Delta m/z}^2$  and  $\sigma_{\Delta t_R}^2$  are the average standard deviations of the observed mass error and isotopic retention time shift of the three isotopes in the training dataset ( $n = 573 + 440 + 310$ ) and amounted to 2.66 ppm and 0.30 s, respectively. The grouped mono isotopic ion and isotope peaks are combined in a component list, in which  $ID_0$  and  $ID_i$  refer to the peak  $ID$  of the mono isotopic ion and its  $i^{th}$  isotope, respectively. Finally,  $\Delta m/z_0$  and  $\Delta m/z_i$ ,  $\Delta t_{R_0}$  and  $\Delta t_{R_i}$  for the mono isotopic ion

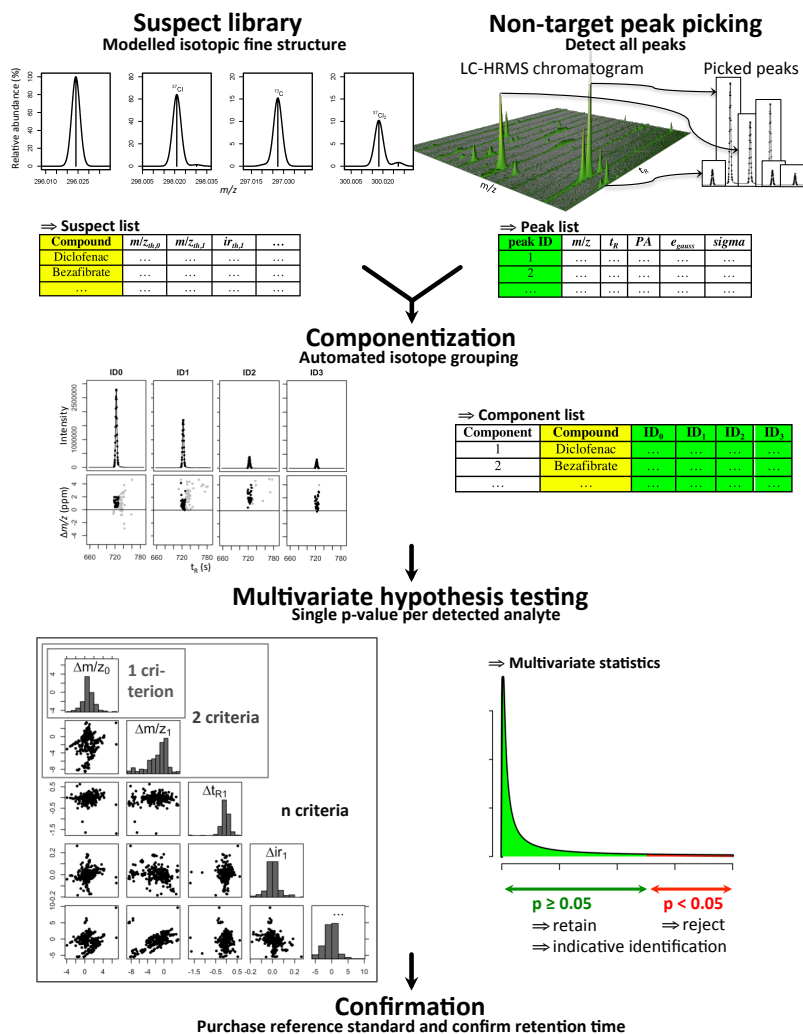


**Figure 6.4** In suspect screening, a suspect library is built; non-target peak picking is performed on the LC-HRMS chromatograms; and componentization aims to automatically group peaks belonging to the same analyte. The identification decision is based on multivariate hypothesis testing after which the retained analytes must be confirmed.

and its  $i^{th}$  isotope, respectively, are calculated using the equations given in Section 6.2.4.3.

### 6.3.2.2 Multivariate hypothesis testing for a holistic screening approach

Milman & Konopelko (2000) discussed how statistical hypothesis testing can be applied for the identification of analytes for which the null hypothesis is  $H_0$ : *detected analyte*  $\equiv$  *suspect compound of interest*. Hypothesis testing is in many screening methods the underlying idea of checking if the mass error of the mono isotopic ion ( $\Delta m/z_0$ ) of a detected analyte is within a predefined mass error tolerance. The mass error tolerance should be based on the expected variability of the mass accuracy of the MS (such as in Chapter 5). When taking additional ions into account, such as the isotopes, multiple hypotheses could be tested simultaneously (e.g. both the mono isotopic mass error and the isotope mass error). In this case, in order to test the whole at a global level of significance  $\alpha$  (e.g. 5%), multivariate hypothesis testing will be more efficient in identification than the univariate tests (Milman & Konopelko, 2000). When supposing 2 ions, i.e. the mono isotopic ion and the first isotope, a total of 4 variates can be tested simultaneously:  $\Delta m/z_0$ ,  $\Delta m/z_1$ ,  $\Delta t_{R1}$  and  $\Delta ir_1$ . Subsequently, incorporating additional isotopes adds on the variates  $\Delta m/z_i$ ,  $\Delta t_{Ri}$  and  $\Delta ir_i$  for the  $i^{th}$  isotope ( $i = 1, 2, 3$  in this study). As such, the number of variates ( $d$ ) is 1, and 4, 7 or 10 when only the mono isotopic ion is considered, and when 1, 2 or 3 isotopes are added, respectively.

The multivariate distribution of the named variates is investigated from the training dataset, and showed to fit well a multivariate Student t-distribution with heavier tails than expected from the multivariate normal distribution. The multivariate Student t-distribution is described by 3 parameters (Roth, 2013): the vector of means  $\mu$  of the  $d$  variates; a symmetric matrix  $\Sigma$  (dimension  $d \times d$ ), and the degrees of freedom  $\nu$ . In the case of the multivariate Student t-distribution, the suitable multivariate hypothesis can be tested by use of the F-distribution (Roth, 2013). For a multivariate Student t random variable with  $d$  variates  $X \sim t(\mu, \Sigma, \nu)$  the quadratic form (or squared Mahalanobis distance)  $\Delta^2 = (X - \mu)^T \Sigma^{-1} (X - \mu)$  admits a F-distribution:  $\frac{1}{d} \Delta^2 \sim F(d, \nu)$ . Figure 6.5 presents QQ-plots for the F-distributions of the different hypothesis tests showing that the data fit well the multivariate Student t distributions.

As such, for each of the detected analytes,  $H_0$  is rejected (i.e. no identification) when the  $p$ -value, calculated as  $pF(\frac{1}{d} \Delta^2, d, \nu)$ , turns out to be less than the desired significance level  $\alpha$ . If not ( $p \geq \alpha$ ), the identification is accepted and the peak is retained.

The 3 parameters  $\mu$ ,  $\Sigma$  and  $\nu$  of the Student t-distribution were estimated from the training dataset for the case where only the mono isotopic ion is used, and for the case where 1, 2 and 3 isotopes are added, respectively.  $H_{1.1}$ ,  $H_{2.4}$ ,  $H_{3.7}$  and  $H_{4.10}$  are introduced as notations for the respective hypothesis tests: only the mono isotopic ion taking into account 1 variate, the mono isotopic ion + 1 isotope taking into account a total of 4 variates, etc. (Table 6.1). The actual FNR at significance levels  $\alpha$  of 5% (FNR = fraction of the analytes in the

training dataset with  $p$ -value  $< 0.05$ ) are 5.5, 3.7, 4.8 and 4.2% for  $H_{1.1}$ ,  $H_{2.4}$ ,  $H_{3.7}$  and  $H_{4.10}$ , respectively, showing the overall good fit of the applied multivariate Student t-distributions.

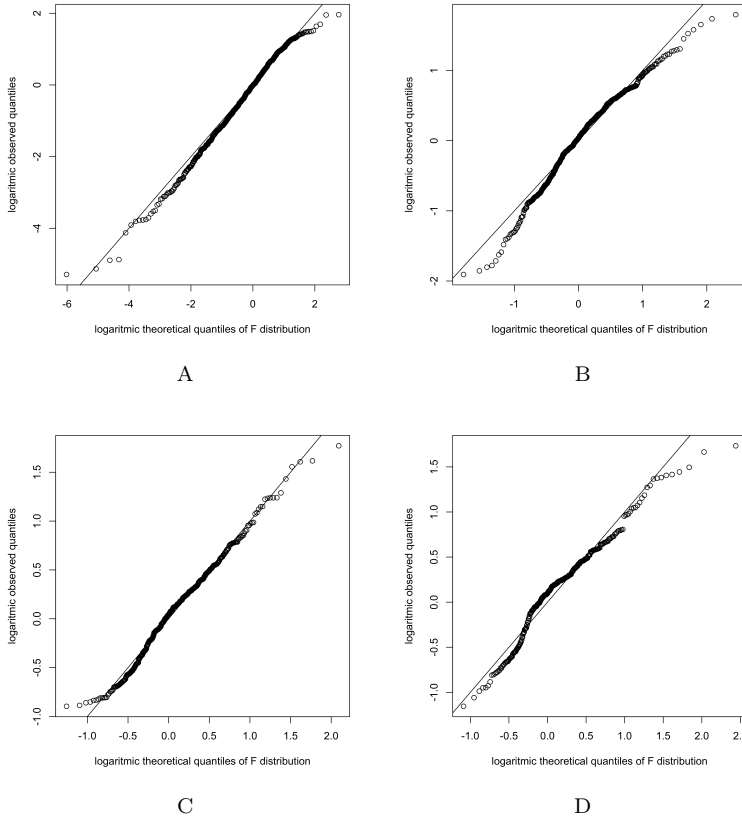


**Figure 6.5** The logarithmic observed quantiles showed to fit well the logarithmic theoretical quantiles of the F-distribution in a QQ-plot (A:  $H_{1.1}$ , B:  $H_{2.4}$ , C:  $H_{3.7}$ , D:  $H_{4.10}$ ).

### **6.3.2.3 Including a peak/noise filter in the holistic screening approach**

A new peak/noise filter concept is included in the multivariate screening. Therefore, in a first step, the multivariate discrimination is applied to select the peak parameters performing the best to discriminate noise from ‘true’ peaks. The results of the variable selection process are given in Figure 6.6. In step 1, the misclassification error was minimal (17.8%) for  $\log(e_{gauss})$  and decreased to 12.8% by inclusion of  $\log(\sigma)$  in step 2a. In step 2b,  $\log(sd(m/z))$  was added, reducing the misclassification error to 11.1%. In subsequent steps, no improvement was obtained anymore. Finally, it was decided that an optimal discrimination (minimal classification error versus model complexity) was obtained for the combination of  $\log(e_{gauss})$  and  $\log(\sigma)$  because addition of  $\log(sd(m/z))$  only marginally reduced the misclassification error.

The goodness of fit of a peak to a Gaussian curve, as  $\log(e_{gauss})$ , together with the width of the fitted Gaussian curve, as  $\log(\sigma)$ , had thus the best discriminating power amongst a set of 12 parameters. ‘True’ peaks showed overall to be better Gaussian shaped (95%  $e_{gauss} < 0.13$ ) with a Gaussian sigma parameter between 3.7 s and 15.7 s (95% interval).

In a second step, the two selected variates  $\log(e_{gauss})$  and  $\log(\sigma)$  are added on to the multivariate screening. Thus, the screening hypothesis tests  $H_{1.1}$ ,  $H_{2.4}$ ,  $H_{3.7}$  and  $H_{4.10}$  are extended with the selected parameter combination  $\log(e_{gauss})$  and  $\log(\sigma)$  per ion. As such,  $H_{1.1}$  becomes  $H_{1.3}$  and includes  $\Delta m/z_0$ ,  $\log(e_{gauss,0})$



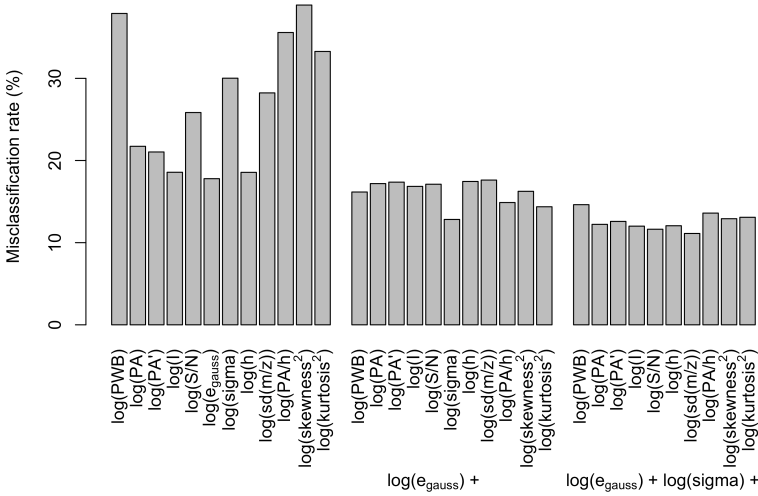


**Figure 6.6** Misclassification error of the peak parameter combinations for the peak/noise discrimination evaluated during the variable selection procedure (from left to right: step 1, 2a and 2b).

and  $\log(\sigma_0)$ , similarly  $H_{2.4}$ ,  $H_{3.7}$  and  $H_{4.10}$  are extended to  $H_{2.8}$ ,  $H_{3.13}$  and  $H_{4.18}$ , respectively, taking into account  $e_{gauss,i}$  and  $\sigma_i$  for each  $i^{th}$  ion (Table 6.1). The distributions of  $H_{1.3}$ ,  $H_{2.8}$ ,  $H_{3.13}$  and  $H_{4.18}$  showed to fit well the multivariate Student t-distribution (Figures 6.7) and their parameter values  $\mu$ ,  $\Sigma$  and  $\nu$  were estimated from the training dataset. The actual FNRs at a significance level  $\alpha$  of 5% are 5.3, 6.9, 5.0 and 6.7% for  $H_{1.3}$ ,  $H_{2.8}$ ,  $H_{3.13}$  and  $H_{4.18}$ , respectively, showing that the overall false negative rate was not compromised by inclusion of the peak/noise filter.

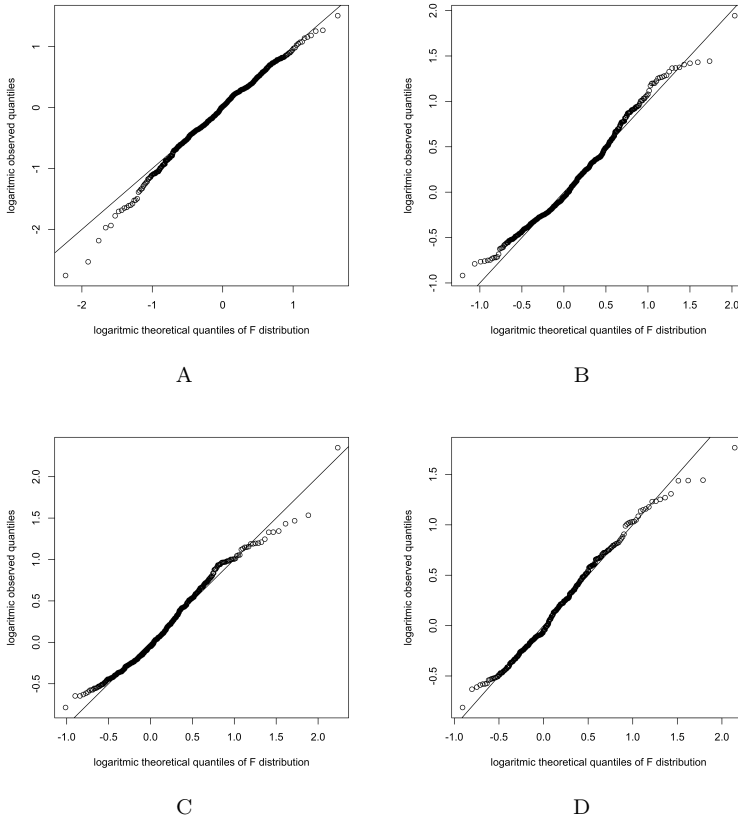


**Figure 6.7** The logarithmic observed quantiles showed to fit well the logarithmic theoretical quantiles of the F-distribution in a QQ-plot (A:  $H_{1.3}$ , B:  $H_{2.8}$ , C:  $H_{3.13}$ , D:  $H_{4.18}$ ).

Additionally, in order to be able to evaluate the effectiveness of the isotope ratios for identification, reduced models were calculated for  $H_{2.8}$ ,  $H_{3.13}$  and  $H_{4.18}$ , which leave out the isotope ratios  $\Delta ir_i$ . As such,  $H_{2.7}$ ,  $H_{3.11}$  and  $H_{4.15}$  were obtained, respectively (Table 6.1).

**Table 6.1** Variates used for the different screening hypothesis and false positive rates for the 40 artificial suspect compounds (set A).

<i>H</i>	Variates <sup>a</sup>			<i>e<sub>gauss,i</sub></i> & <i>sigma<sub>t</sub></i>	FPR (%) ( <i>n</i> =40)	Isotope specific FPR (%) <sup>b</sup>						
	$\Delta m/z_i$	$\Delta t_{R_i}$	$\Delta i r_i$			$^{37}\text{Cl}/^{13}\text{C}$ / $^{37}\text{Cl}^{13}\text{C}$	$^{13}\text{C}/^{13}\text{C}_2$ / $^{13}\text{C}/^{13}\text{C}_2$	$^{13}\text{C}/^{13}\text{C}_2$ / $^{15}\text{N}$ ( <i>n</i> =5)	$^{13}\text{C}/^{34}\text{S}$ / $^{13}\text{C}/^{15}\text{N}$	$^{13}\text{C}/^{15}\text{N}$ / $^{13}\text{C}_3$ ( <i>n</i> =20)	$^{15}\text{N}$ ( <i>n</i> =5)	$^{13}\text{C}_2$ ( <i>n</i> =2)
<i>H</i> <sub>1,1</sub>	0	-	-	0	202							
<i>H</i> <sub>1,3</sub>	0	-	-	0	131							
<i>H</i> <sub>2,4</sub>	0,1	1	1	-	28							
<i>H</i> <sub>2,7</sub>	0,1	1	-	0,1	24							
<i>H</i> <sub>2,8</sub>	0,1	1	1	0,1	22							
<i>H</i> <sub>3,7</sub>	0,1,2	1,2	1,2	-	4,7	<1.4 ( <i>n</i> =8)						
<i>H</i> <sub>3,11</sub>	0,1,2	1,2	-	0,1,2	3,9							
<i>H</i> <sub>3,13</sub>	0,1,2	1,2	1,2	0,1,2	2,8							
<i>H</i> <sub>4,10</sub>	0,1,2,3	1,2,3	1,2,3	-	<0.3	<1.4 ( <i>n</i> =8)						
<i>H</i> <sub>4,15</sub>	0,1,2,3	1,2,3	-	0,1,2,3	<0.3							
<i>H</i> <sub>4,18</sub>	0,1,2,3	1,2,3	1,2,3	0,1,2,3	<0.3	<1.4 ( <i>n</i> =8)						

<sup>a</sup> *i* = 0 for the mono isotopic ion and *i* = 1, 2 or 3 for the 1<sup>st</sup>, 2<sup>nd</sup> or 3<sup>rd</sup> isotope, respectively.

<sup>b</sup> FPR split up for the different isotope combinations (number of compounds).

- Not applicable.

### **6.3.3 Evaluation of the suspect screening performance based on artificial suspects (set A)**

#### **6.3.3.1 Screening limits of identification**

The screening limit of identification (LOI) is defined as the lowest spiking level at which at least two out of the triplicates were retained by the suspect screening algorithm. The LOIs are evaluated for the suspect screening hypothesis  $H_{1,3}$ ,  $H_{2,8}$ ,  $H_{3,13}$  and  $H_{4,18}$ , which include the peak/noise filter; and the LOIs for  $H_{1,3}$  (including only the mono isotopic ion) are compared to the decision limits ( $CC\alpha$ s). In Table 6.2, both the reported LOI and  $CC\alpha$  levels refer to the spiking levels in the samples and represent  $C_{spike} + C_{sample}$ : the spiked concentration (0.2, 2, 20, 200, 2000 or 20000  $\text{ng l}^{-1}$ ) plus the eventually measured concentration in the non-spiked sample. Thus, the reported LOI and  $CC\alpha$  values are equal to at least the measured concentration in the non-spiked sample and can therefore be an overestimation of the true LOI and  $CC\alpha$ , respectively. To estimate the concentration in the non-spiked sample, on each day, an external calibration curve (0.01, 0.03, 0.1, 0.3, 1, 3, 10, 30, 100, 300, 1000  $\mu\text{g l}^{-1}$ ) was performed to convert the obtained peak areas to concentrations and to correct for the recovery and matrix effects.

The LOI for  $H_{1,3}$  and the  $CC\alpha$  had both median values of 42  $\text{ng l}^{-1}$ . It was observed that all the peaks having a signal intensity of at least the  $CC\alpha$  were found by the non-target peak picking algorithm. Moreover, the LOI was equal to or lower than the  $CC\alpha$  for 24 and 8 out of the 40 compounds, respectively. However, for 8 other compounds, the LOI was higher than the  $CC\alpha$ . These compounds

**Table 6.2** Concentration in the non-spiked sample (effluent WWTP Aalst),  $CC\alpha$ , and the screening LOI for the 40 artificial suspect compounds (Set A). Concentrations in  $\text{ng l}^{-1}$ .

Compound	$C_{\text{sample}}$	$CC\alpha^{\text{a}}$	$H_{1.3}$	$H_{2.8}$	$H_{3.13}$	$H_{4.18}$
Acyclovir	312	312	312	312	2312	20 312
Alprazolam	6	6	7	206	206	206
Amantadine	42	42	42	42	2042	2042
Amitriptyline	26	26	2026	2026	2026	2026
Amoxicillin	63	63	63	263	2063	2063
Besifloxacin	n.d.	2000	2000	20 000	20 000	20 000
Carbamazepine	405	405	405	405	405	405
Chlortetracycline	n.d.	200	2000	200	2000	2000
Ciprofloxacin	82	82	82	2082	2082	20082
Diazepam	2	2	2	4	4	22
Diclofenac	583	583	583	583	583	583
Efavirenz	n.d.	20	20	200	200	200
Enrofloxacin	n.d.	20	20	200	2000	20 000
Flumequine	n.d.	20	0.2	2000	2000	2000
Fluoxetine	22	22	22	2022	2022	20 022
Gatifloxacin	n.d.	20	20	200	200	20 000
Indomethacin	n.d.	20	0.2	200	200	2000
Lamivudine	n.d.	2	0.2	200	200	2000
Levofloxacin	42	42	42	242	242	20 042
Metronidazole	39	40	40	40	2039	20 000
Moxifloxacin	n.d.	200	20 000	2000	20 000	>20 000
Nalidixic acid	4	4	4	24	204	2004
Nevirapine	21	21	21	21	221	2021
Oseltamivir acid	n.d.	200	200	200	2000	20 000
Oseltamivir ethylester	n.d.	20	20	200	2000	20 000
Oxytetracycline	n.d.	2	2	200	2000	2000
Paracetamol	23	43	43	43	2023	20 023
Paroxetine	n.d.	2000	2000	20 000	20 000	>20 000
Pleconaril	n.d.	200	200	2000	20 000	20 000
Rimantadine	n.d.	20	20	20	2000	20 000
Risperidone	n.d.	2000	2000	2000	20 000	20 000
Sarafloxacin	n.d.	20	20	2000	2000	20 000
Sulfadoxin	n.d.	0.2	0.2	200	200	200
Sulfamethazine	n.d.	2	0.2	20	20	2000
Sulfamethoxazole	100	100	100	100	100	100
Temazepam	17	17	17	17	17	17
Tetracycline	160	160	160	160	2160	2160
Trimethoprim	61	61	61	61	261	2061
Venlafaxine	332	332	332	332	332	2332
Zidovudine	n.d.	20	200	20 000	20 000	20 000

<sup>a</sup>  $CC\alpha$  values are calculated from the interday repeatability (as standard deviation of the concentrations obtained after external calibration) using the method elaborated in Chapter 4.

n.d. Not detected.

(e.g. amitriptyline, chlortetracycline, moxifloxacin and risperidone) showed typically relatively wide tailed chromatographic peaks and were therefore excluded by the peak/noise filter of  $H_{1.3}$ . Upon including the most intense isotope ( $H_{2.8}$ ), the median LOI was  $200 \text{ ng l}^{-1}$  and increased drastically to  $2000 \text{ ng l}^{-1}$  and  $2062 \text{ ng l}^{-1}$  for a second ( $H_{3.13}$ ) and third ( $H_{4.18}$ ), respectively. The LOIs were lower than  $2.5 \mu\text{g l}^{-1}$  for 98, 93, 85 and 55 % of the compounds for the  $H_{1.3}$ ,  $H_{2.8}$ ,  $H_{3.13}$  and  $H_{4.18}$  screening hypothesis, respectively.

### **6.3.3.2 False positive versus false negative rate**

A hypothetical suspect screening (as schematically presented in Figure 6.4) was conducted on seven non-spiked WWTP effluent samples for the 40 set A compounds treated as artificial suspects in order to evaluate the false positive rate. A false positive is a peak retained by the screening algorithm (thus with  $p$ -value  $> 0.05$ , i.e. the accepted false negative rate  $\alpha$ ) but having a retention time deviating more than 6 s from the retention time of an analytical standard. This maximal allowed retention time error was also used for the construction of the training dataset. Subsequently, the FPR was calculated as the false positive count divided by the number (40) of screened suspects, with this ratio averaged over the seven WWTP effluent samples, being in agreement with Ellison & Fearn (2005) and Chapter 5.

There was one exception. For amoxicillin ( $t_R = 1.60 \text{ min}$ ), analytes having the same accurate mass and isotopic pattern were retained at  $t_R$  4.98 and 5.67 min by all screening hypothesis (confirming thereby the  $^{34}\text{S}$  and  $^{15}\text{N}$  isotope). However, these ions also occurred at low abundance

in the chromatograms of the  $1000\ \mu\text{g l}^{-1}$  analytical standards. These analytes might be rearrangements products having the same chemical formula as amoxicillin such as amoxicillin-diketopiperazine-2',5' being identified as both an analytical impurity (US Medicines Compendium) and a major degradation product in wastewater (Lamm *et al.*, 2009). Although the exact nature of these ions could not be confirmed (MS/MS experiments would be required), they were not counted as false positives.

The FPRs for the different screening hypothesis are presented in Table 6.1. Decreased FPRs were observed when adding the peak/noise filter (e.g.  $H_{1.3}$  vs.  $H_{1.1}$ ), when adding the isotope ratios (e.g.  $H_{2.8}$  vs.  $H_{2.7}$  and  $H_{3.13}$  vs.  $H_{3.11}$ ), and when taking into account additional isotopes ( $H_{1.3}$  vs.  $H_{2.8}$  vs.  $H_{3.13}$  vs.  $H_{4.18}$ ). A FPR of about 131% was calculated for  $H_{1.3}$ . Such elevated FPRs, higher than 100%, were observed when multiple false positive hits are found per compound in a chromatogram. In addition, when screening towards only the accurate mass of the mono isotopic ion, also isotopes, having in general lower abundance, can be seen as mono isotopic ions. This is exemplified in Figure 6.8A. From high to low peak area, the number of false positives for  $H_{1.3}$  increased clearly to a maximum for ions with peak areas of about 100 000 - 500 000. However, the FPR decreased sharply for even lower abundance ions because the LOI is reached at peak areas of about 50 000.

The FPR strongly reduced to 22, 2.8 and  $< 0.3\%$  (i.e. less than 1 false positive) for  $H_{2.8}$ ,  $H_{3.13}$  and  $H_{4.18}$ , respectively, upon taking into account isotopes, which can be explained by two reasons. First, the LOI increased when progressing from  $H_{1.3}$  to  $H_{2.8}$ ,  $H_{3.13}$  and  $H_{4.18}$

due to the relatively low abundance of isotopes as compared to their mono isotopic ion. When progressing from  $H_{1.3}$  to  $H_{2.8}$ , the FPR is reduced from 131 to 22%. This reduction, illustrated in Figure 6.8A, is clearly stronger for low abundance ions ( $PA_0 < 1\,000\,000$ ) than for higher abundance ions ( $PA_0 > 1\,000\,000$ ). The reason why almost no false positives occurred for  $H_{2.8}$  having  $PA_0 < 1\,000\,000$  is thus related to the LOI (2.5% FPR with  $PA_0 < 1\,000\,000$  versus overall 21.7% FPR for  $H_{2.8}$ ). Second, progressing from  $H_{2.8}$  to  $H_{3.13}$  and  $H_{4.18}$  clearly further reduced the FPR, showing that additional isotopes improved the identification effectiveness of the screening. This reduced FPR is obtained at the cost of increasing LOI values due to the lower abundance (and thus signal intensity) of higher isotopes. Figure 6.8B presents the FPR as a function of the FNR ( $p > \alpha$ ) for  $H_{1.3}$ ,  $H_{2.8}$ ,  $H_{3.13}$  and  $H_{4.18}$ . If the goal is to obtain a FPR of 5%,  $\alpha$  (= FNR) can be set to 2% and 0.01% for  $H_{3.13}$  and  $H_{4.18}$ , respectively, which is the intersection of the curves in Figure 6.8B and the horizontal at FPR = 5%. Upon accepting an increased FNR (increasing  $\alpha$ ), the FPR reduces. At a FNR of 5%, i.e. the aim in this research, the FPR was lower than 5% for  $H_{3.13}$  (FPR = 2.8%) and  $H_{4.18}$  (FPR < 0.3%), which are thus the preferred screening hypothesis for application in this study.

### **6.3.3.3 Specificity of carbon and heteroatom isotopes**

The presence of  $^{37}\text{Cl}$  isotopes has been used in different studies for confirmation (Picó *et al.*, 2007; Ibáñez *et al.*, 2008; Kern *et al.*, 2009; Nurmi *et al.*, 2012; Li *et al.*, 2013). However, it is of particular interest to evaluate their specificity and to value also the use of other isotopes



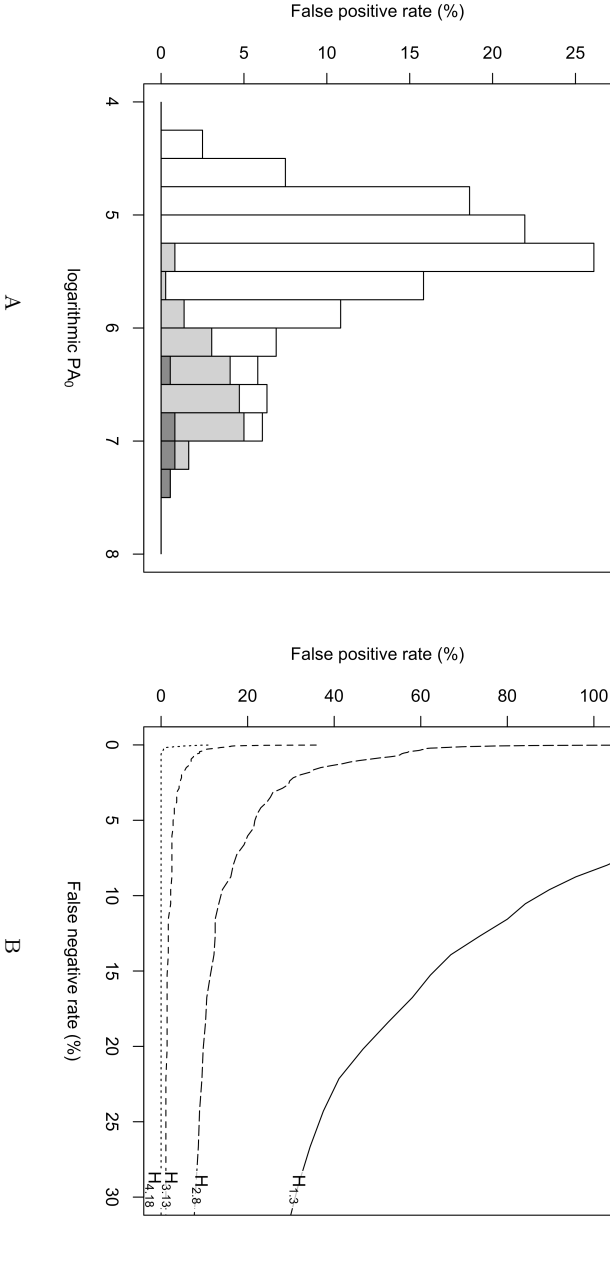


**Figure 6.8** The false positive rate decreases (A) upon taking into account additional isotopes (white:  $H_{1,3}$ , light gray:  $H_{2,8}$ , gray:  $H_{3,13}$ ) and (B) upon allowing an increased false negative rate.

such as  $^{13}\text{C}$ ,  $^{15}\text{N}$  and  $^{34}\text{S}$ . In this study, up to three isotopes - ordered from high to low abundance - were considered. As a result, the following isotope combinations were present among the 40 artificial suspect compounds (set A):  $20 \times ^{13}\text{C}/^{13}\text{C}_2/^{13}\text{C}_3$ ,  $5 \times ^{13}\text{C}/^{13}\text{C}_2/^{15}\text{N}$ ,  $2 \times ^{13}\text{C}/^{15}\text{N}/^{13}\text{C}_2$ ,  $5 \times ^{13}\text{C}/^{34}\text{S}/^{15}\text{N}$ ,  $7 \times ^{37}\text{Cl}/^{13}\text{C}/^{37}\text{Cl}^{13}\text{C}$ ,  $1 \times ^{37}\text{Cl}/^{13}\text{C}/^{37}\text{Cl}_2$ . Table 6.1 presents the FPRs for the individual isotope combinations evaluated for  $H_{2.8}$ ,  $H_{3.13}$  and  $H_{4.18}$ . As such, the specificity of different isotope combinations can be opposed. For the 8 chlorinated compounds, no false positives (FPR for  $H_{2.8} < 1.4\%$ , i.e. less than 1 false positive) were observed in the seven WWTP effluent samples when taking into account at least the  $^{37}\text{Cl}$  isotope. For the other 32 compounds, a 24% FPR was calculated for  $H_{2.8}$  when taking into account only the  $^{13}\text{C}$  isotope, showing that this isotope is less specific. The FPR reduced to 3.6% ( $H_{3.13}$ ) considering the  $^{13}\text{C}/^{13}\text{C}_2$  isotope combination for 25 compounds. For 5 compounds for which the  $^{13}\text{C}/^{34}\text{S}$  isotope combination was considered, the FPR at  $H_{3.13}$  was 4.4%. When taking into account the  $^{13}\text{C}/^{15}\text{N}$  isotope combination for 2 compounds, no false positives occurred (FPR for  $H_{3.13} < 5.6\%$ , i.e. less than 1 false positive). Thus, the isotope combinations  $^{13}\text{C}/^{34}\text{S}$ ,  $^{13}\text{C}/^{15}\text{N}$  and  $^{13}\text{C}/^{13}\text{C}_2$  resulted in similar FPRs, and more research is required to investigate the specificity of heteroatoms such as S and N isotopes versus C isotopes.

The 20 compounds (set A) for which only the  $^{13}\text{C}/^{13}\text{C}_2/^{13}\text{C}_3$  isotopes were evaluated also consist N atoms. However, these compounds had masses of at least about 260 Da, at which the actual resolving power is lower than 70 000 FWHM (the resolving power is

proportional to  $\frac{1}{\sqrt{m/z}}$  for Orbitrap MS (Zubarev & Makarov, 2013)). As a result, the  $^{15}\text{N}$  isotope would be insufficiently resolved from the  $^{13}\text{C}$  isotope and was therefore not selected for the suspect library. In contrast, the 12 compounds (set A), for which the  $^{15}\text{N}$  isotope was taken into account, had masses ranging from 152 to 237 Da, for which the resolving power was at least 70 000 FWHM. Thus, a resolving power of at least 70 000 FWHM over the whole mass range would allow screening for the  $^{15}\text{N}$  isotope for much more suspect compounds.

### 6.3.4 Application of the suspect screening (set A + B)

As proof of concept, the seven WWTP effluent samples were screened for the whole set of 77 suspect compounds (set A + B) using the screening hypothesis  $H_{3,13}$  and  $H_{4,18}$ . For chlorinated compounds also  $H_{2,8}$  was used because the  $^{37}\text{Cl}$  isotope showed to be specific with no observed false positives. No a priori knowledge about the retention time was available for set B suspects, whereas for the set A compounds the retention time is supposed to be unknown. The suspect screening results are presented in Table 6.3. For the three screening hypothesis together, a total of 25 suspect pharmaceuticals could be indicatively identified in the 7 effluent samples. Finally, for confirmation, the missing reference standards for the retained compounds of set B were purchased, their standards prepared and analyzed. As such, confirmation based on accurate mass of the mono isotopic ion and 1, 2 or 3 isotopes (depending on the screening hypothesis) and retention time was reached for 19 pharmaceuticals (i.e. true positives).

**Table 6.3** True positive and false positive screening results for the 77 suspect pharmaceuticals in 7 WWTP effluents.

Compound	$t_R$ (min)	Nature of isotopes	Detection frequency <sup>a</sup>		
			$H_{4.18}$	$H_{3.13}$	$H_{2.8}$
<i>True positives: confirmed analytes (<math>\Delta t_R \leq 6</math> s)</i>					
Amoxicillin <sup>b</sup>	5.67	$^{13}\text{C}/^{34}\text{S}/^{15}\text{N}$	1	4	-
Amoxicillin <sup>b</sup>	4.98	$^{13}\text{C}/^{34}\text{S}/^{15}\text{N}$	5	7	-
Atenolol	1.42	$^{13}\text{C}/^{13}\text{C}_2/^{13}\text{C}_3$	5	9	-
Bezafibrate	10.83	$^{37}\text{Cl}/^{13}\text{C}/^{37}\text{Cl}^{13}\text{C}$	0	0	5
Bisoprolol	7.52	$^{13}\text{C}/^{13}\text{C}_2/^{13}\text{C}_3$	6	9	-
Caffeine	4.17	$^{13}\text{C}/^{15}\text{N}/^{13}\text{C}_2$	0	7	-
Carbamazepine	8.98	$^{13}\text{C}/^{13}\text{C}_2/^{15}\text{N}$	6	8	-
Diazepam	10.50	$^{37}\text{Cl}/^{13}\text{C}/^{37}\text{Cl}^{13}\text{C}$	0	0	1
Diclofenac	12.03	$^{37}\text{Cl}/^{13}\text{C}/^{37}\text{Cl}_2$	9	9	9
Ifosfamide	6.62	$^{37}\text{Cl}/^{37}\text{Cl}_2/^{13}\text{C}_2$	1	1	2
<i>(Cyclophosphamide<sup>c</sup>)</i>					
Ketoprofen	10.35	$^{13}\text{C}/^{13}\text{C}_2/^{13}\text{C}_3$	0	2	-
Levofloxacin	4.95	$^{13}\text{C}/^{13}\text{C}_2/^{13}\text{C}_3$	0	1	-
Lincomycin	3.83	$^{13}\text{C}/^{34}\text{S}/^{13}\text{C}_2$	0	1	-
Metoprolol	6.03	$^{13}\text{C}/^{13}\text{C}_2/^{13}\text{C}_3$	2	9	-
Oxytetracycline	4.83	$^{13}\text{C}/^{13}\text{C}_2/^{13}\text{C}_3$	0	1	-
Propranolol	8.17	$^{13}\text{C}/^{13}\text{C}_2/^{13}\text{C}_3$	0	3	-
Sotalol	1.15	$^{13}\text{C}/^{34}\text{S}/^{13}\text{C}_2$	9	9	-
Sulfamethoxazole	5.05	$^{13}\text{C}/^{34}\text{S}/^{15}\text{N}$	1	4	-
Temazepam	10.10	$^{37}\text{Cl}/^{13}\text{C}/^{37}\text{Cl}^{13}\text{C}$	5	8	9
Venlafaxine	7.63	$^{13}\text{C}/^{13}\text{C}_2/^{13}\text{C}_3$	0	9	-
<i>False positives: not-confirmed analytes (<math>\Delta t_R &gt; 6</math> s)</i>					
Amoxicillin	4.00	$^{13}\text{C}/^{34}\text{S}/^{15}\text{N}$	0	2	-
Atenolol	3.79	$^{13}\text{C}/^{13}\text{C}_2/^{13}\text{C}_3$	2	9	-
Bisoprolol	8.73	$^{13}\text{C}/^{13}\text{C}_2/^{13}\text{C}_3$	0	2	-
Cloxacillin	8.65	$^{37}\text{Cl}/^{13}\text{C}/^{37}\text{Cl}^{13}\text{C}$	0	2	5
Flumequine	10.12	$^{13}\text{C}/^{13}\text{C}_2/^{13}\text{C}_3$	0	1	-
Moxifloxacin	9.92	$^{13}\text{C}/^{13}\text{C}_2/^{13}\text{C}_3$	0	6	-
Simvastatine	14.18	$^{13}\text{C}/^{13}\text{C}_2/^{13}\text{C}_3$	1	3	-
Tolfenamic acid	3.67	$^{37}\text{Cl}/^{13}\text{C}/^{37}\text{Cl}^{13}\text{C}$	0	0	8
Tolfenamic acid	8.00	$^{37}\text{Cl}/^{13}\text{C}/^{37}\text{Cl}^{13}\text{C}$	3	8	9
Venlafaxine	6.35	$^{13}\text{C}/^{13}\text{C}_2/^{13}\text{C}_3$	0	1	-

<sup>a</sup> Number of retained analytes for  $H_{4.18}$  and  $H_{3.13}$  (and also  $H_{2.8}$  for chlorinated compounds);  $n = 1$  per WWTP, except for the sample of WWTP Aalst, which was analyzed in triplicate, making a total of 9 samples analyzed.

<sup>b</sup> These detected compounds are probably rearrangements products of amoxicillin with the same chemical formula.

<sup>c</sup> Because there is no possibility that the structural isomers ifosfamide and cyclophosphamide are differentiated using the presented screening algorithm, cyclophosphamide was not counted as a false positive.

For the chlorinated compounds, false positives occurred for cloxacillin and tolfenamic acid showing that Cl isotopes are not always sufficiently specific for confirmation. For a total of 16 chlorinated compounds in set A + B, the recalculated FPR was 15 %, 6.9 % and 2.1 % for  $H_{2.8}$ ,  $H_{3.13}$  and  $H_{4.18}$ , respectively.

More in general for  $H_{3.13}$  and  $H_{4.18}$ , a total of 9 and 3 falsely identified compounds were obtained resulting in an overall recalculated false positive rate of 4.9 % and 0.9 %, respectively, for the total set of 77 suspect compounds (set A + B). The reduction in FPR of  $H_{4.18}$  versus  $H_{3.13}$  has as consequence that fewer compounds are correctly identified: 18 for  $H_{3.13}$  versus 11 for  $H_{4.18}$ . This is clearly related to the lower LOI of  $H_{3.13}$  versus  $H_{4.18}$ .

For amoxicillin, atenolol, bisoprolol and venlafaxine both true positives and false positives were retained in the same samples at different retention times. For example, for atenolol true positives were found at 1.42 min and false positives at 3.79 min (Table 6.3).

The structural isomers ifosfamide and cyclophosphamide were both retained at a retention time of 6.6 min (Table 6.3). Ifosfamide could finally be confirmed by an analytical standard. There is no possibility that the presented screening would be able to differentiate isomers because the exact masses and isotopic pattern of isomers are the same, therefore, cyclophosphamide was not counted as a false positive.

## 6.4 Conclusions

A novel suspect screening strategy using ultra-high performance liquid chromatography (UHPLC) Orbitrap HRMS is presented. For the first time, the false negative rate of the screening algorithm can be controlled to a desired level (5 % in this study) and a well-balanced identification decision (i.e. all criteria are equally stringent) is guaranteed taking the mass error, isotope fit and peak/noise filter in a holistic approach. The aim of this study was achieved through a multivariate statistical model, which was estimated from a training dataset and reflects the expected analytical variability. As such, for each detected analyte, the decision (retain or reject) is based on a hypothesis test resulting in a single  $p$ -value.

In this study, three distinct mechanisms have shown to reduce the number of false positive findings. First, incorporating a peak/noise filter can reduce the finding of noise peaks and should be included in order to prevent that noise is used to identify analytes. Second, at least one isotope should be taken into account in order to better distinguish mono isotopic ions from isotopes. Third, taking into account both the accurate mass and isotope ratio of additional isotopes has shown to reduce the FPR. With this respect, both carbon ( $^{13}\text{C}$ ) and heteroatom ( $^{15}\text{N}$ ,  $^{34}\text{S}$  or  $^{37}\text{Cl}$ ) isotopes showed to be valuable to improve the identification confidence and reduce the FPR.

A false positive rate of 4.9 % and 0.9 % was obtained when taking into account 2 and 3 isotopes, respectively. If a FPR of 5 % is acceptable, the screening using 2 isotopes yields the lowest LOIs with a median value of  $2000 \text{ ng l}^{-1}$  and resulted in 19 confirmed compounds out of 23 retained

suspects when screening towards 77 pharmaceuticals. The effectiveness of the screening can be even improved when considering three isotopes, but this implies a lower number of retained (13) and confirmed (11) pharmaceuticals because of the method sensitivity in terms of lowest measurable concentration.

# 7

## General discussion, conclusions and perspectives

The achievements in this work are twofold. First, different analytical aspects as steppingstones of the screening-to-quantification approach were investigated for multi-residue high-resolution mass spectrometry (HRMS) of pharmaceuticals in the aquatic environment. The methods were developed for 4 different matrices, namely drinking water, surface water, wastewater and biologically treated wastewater using 3 different HRMS technologies, namely double-focussing sector, Time-of-Flight (TOF) and Orbitrap HRMS. Second, the developed methods were applied on the named matrices resulting in one of the first occurrence and concentration data of pharmaceuticals in the Belgian aquatic environment.



In Section 7.1, the entire procedure for multi-residue analysis is overviewed in the context of screening-to-quantification HRMS and in the light of current scientific progress. The overall idea is that full-spectrum HRMS has the potential to identify and quantify a virtually unlimited number of analytes based on accurate mass. With this, the whole analytical train from sampling, over sample storage and pretreatment till chromatographic separation and mass spectrometric detection must adopt this multi-residue challenge. In this Chapter, 4 topics related with these current challenges are discussed: (i) sample collection and storage procedures, (ii) the performance of a solid-phase extraction (SPE) method as sample pretreatment for analysis of (treated) wastewater versus a large-volume injection (LVI)-based method for drinking and surface water analysis, (iii) the selectivity in quantitative full-spectrum HRMS and qualitative aspects of suspect screening using full-spectrum HRMS, and (iv) quantitative and qualitative validation and measurement variability in the context of multi-residue analysis.

In Section 7.2, the main outcomes of the application of the developed methods on wastewater (wastewater treatment plant (WWTP) influent), biologically treated wastewater (WWTP effluent), surface water and drinking water are summarized and the results of the occurrence and concentration profiles of pharmaceuticals in the Belgian aquatic environment are discussed.

In Section 7.3, future perspectives for screening-to-quantification of environmentally relevant contaminants and its potential to answer current research questions about micropollutants are highlighted.

## 7.1 Multi-residue analysis of pharmaceuticals in aquatic environments

Analytical methods are often developed for a particular group of compounds with typical chemical characteristics like antidepressants (Demeestere *et al.*, 2010),  $\beta$ -blockers (Galera *et al.*, 2011), cytostatic drugs (Kovalova *et al.*, 2009), sulfonamide antibiotics (García-Galán *et al.*, 2010b), quinolone antibiotics (Xiao *et al.*, 2008), and tetracycline antibiotics (Skrášková *et al.*, 2013). However, developing methods for a wide range of compounds from different classes (i.e. multi-residue) with diverse chemical characteristics is a more recent goal in environmental chemistry and makes sense for two reasons. First, analyses are expensive, and labor and time intensive. Combining different analytical methods in a single multi-residue method can thus reduce the costs. Second, many contaminants occur as a mixture in the environment. Using a targeted approach, such as MS/MS, has as disadvantage that only a selected group of contaminants can be studied. With the screening-to-quantification approach, this focus can, in first instance, be widened to much more contaminants by multi-residue screening with full-spectrum HRMS. In second instance, a more targeted approach (using analytical standards) can be applied to quantify the most relevant compounds.

However, multi-residue analysis is challenging because throughout the whole analytical procedure, losses of analytes can occur due to compound instability, biodegradation and sorptive effects. With this respect, pharmaceuticals are a good case study because they have a wide range of chemical characteristics: from hydrophilic to lipophilic

and from neutral, cationic, anionic to zwitterionic speciation depending on the solution pH (Section 1.1).

### 7.1.1 Sample collection and storage

A first step in the analytical sequence is sample collection and storage. Mompelat *et al.* (2013) reviewed the stability of pharmaceuticals during sample collection and storage and categorized losses of analytes into sorptive effects, degradation (photo- and biodegradation and hydrolysis), and other abiotic transformations (e.g. complexation with cations). They observed that in multi-residue analysis, the best conditions were not always complementary for the different pharmaceuticals and thus a compromise must be reached. Overall, glass bottles and darkness for transport and storage are recommended. In addition, for antibiotics, sorptive losses may be reduced by silanization of glassware to inactivate silanol groups, and addition of chelating agents such as ethylenediaminetetraacetic acid (EDTA) may prevent their complexation with metal cations. Filtration of the samples should be performed as soon as possible to remove particulate matter to minimize sorptive effects and biodegradation. Different filter materials such as glass fibre or membranes showed no considerable sorption of pharmaceuticals. With respect to temperature, they concluded that it was not possible to universally preserve all analytes at the same temperature. As well by freezing ( $-20\text{ }^{\circ}\text{C}$ ), cooling ( $4\text{ }^{\circ}\text{C}$ ) or at ambient temperatures some pharmaceuticals showed to be stable and others unstable. Limited data is available on the effect of addition of chemical preservation agents such as sodium azide, formaldehyde or acidification.

These conditions could at the same time enhance the stability of some compounds due to inactivation of microorganisms or be detrimental for other compounds (e.g. tetracyclines hydrolyze at  $\text{pH} < 2$ ).

In this study, in order to prevent losses of the analytes during sample collection and storage, different precautions were taken, which in general correspond well with the given recommendations. Drinking and surface water samples were collected in prerinsed amber glass bottles and stored at  $4\text{ }^{\circ}\text{C}$  in the dark for no longer than 24 hours. Wastewater samples were automatically sampled at the WWTP influent and effluent to obtain 24 h composite samples. Formic acid was subsequently added to the samples ( $\text{pH } 3$ ) to prevent microbial activity during sample storage at  $4\text{ }^{\circ}\text{C}$  in the dark for  $\leq 4$  days. The effectiveness of acidification of the wastewater samples to prevent microbial degradation should be investigated in future research. In addition, adding EDTA to the sampling bottles, which showed to prevent potential cation complexation of antibiotics when added prior to SPE extraction, merits investigation. Prior to analysis, the drinking and surface water samples were filtered through  $1.5\text{ }\mu\text{m}$  glass microfiber filters and wastewater samples were filtered through subsequently a  $1.0\text{ }\mu\text{m}$  glass fiber filter and a  $0.45\text{ }\mu\text{m}$  nylon membrane. Taking into account the recommendations of Mompelat *et al.* (2013), samples should be filtered as soon as possible after sample collection to remove particulate matter and minimize sorptive effects and biodegradation.

For the validation of quantitative methods and evaluation of screening methods, stability issues should be investigated. On the one hand, the stability of analytical standards, which are used for the

calibration curve or for spiking, should be investigated. In Chapters 4 and 5, the working solutions for the calibration curves and for spiking experiments were prepared daily and thus stability issues are expected to be less relevant. In contrast, in Chapters 3 and 6, working solutions were stored for about 2 months at 4°C in the dark. Compounds undergoing hydrolysis, such as amoxicillin, might be unstable under these conditions. If analytical standards undergo abiotic transformations, erroneous process efficiencies and matrix effects might be calculated and the quantitative results could be biased. Although instability issues have fewer consequences for the development of suspect screening techniques, the limit of identifications (LOIs) might be overestimated. On the other hand, the stability of investigated compounds during sample storage should be investigated. For target quantification, spiking experiments before and after sample storage should therefore be performed. With respect to screening, data about stability of certain compounds (or groups of compounds) could allow marking out the applicability contours of analytical screening methods.

### **7.1.2 Sample pretreatment by solid-phase extraction versus large-volume injection**

After sample collection and storage, the sample must be pretreated for instrumental analysis. This includes sample enrichment and purification.

In Chapter 3, a SPE method was optimized and validated for the analysis of 43 pharmaceuticals in WWTP influent and effluent. As an alternative for SPE, in Chapter 5, LVI has been investigated for the

analysis of 69 pharmaceuticals in drinking and surface water. Although SPE and LVI are very different, the aim of both techniques is to finally inject sufficient amounts of analyte into the liquid chromatography (LC) column in order to reach low detection limits. In SPE, this is achieved by sample enrichment, while a larger volume of sample is injected in LVI. Both techniques have advantages and disadvantages.

First, recovery is clearly no issue for LVI and can be assumed 100% for all compounds. On the other hand, in SPE most compounds had recoveries  $> 80\%$ , however, for some very hydrophilic or lipophilic compounds, recoveries  $< 30\%$  were obtained, even after a thorough method optimisation. For hydrophilic compounds (e.g. acyclovir, amoxicillin and lamivudine,  $\log K_{ow}$  from -1.59 to 0.06), breakthrough might occur and loading lower sample volumes might increase the recovery values. Very lipophilic compounds (e.g. pleconaril,  $\log K_{ow} > 5$ ), on the other hand, might not be eluted from the cartridge or might sorb onto the glass tube and vial used for evaporation and reconstitution. Using less polar solvents or larger elution volumes might result in better recoveries for lipophilic compounds. However, still a compromise on the final method must be reached in order to obtain acceptable results for a broad range of compounds.

Second, matrix effect, which are an important drawback of electrospray ionization (ESI) in LC, were in general less pronounced for the LVI method for drinking and surface water than for the SPE method for wastewater. Matrix suppression (matrix effect (ME)  $< 80\%$ ) or enhancement (ME  $> 120\%$ ) was obtained for 23 and 13 out of 43 compounds in effluent and influent water, respectively, and

for 12 and 15 out of 69 compounds for drinking water and surface water. Although for the latter cleaner matrices, less matrix effects were obtained, they remain an important drawback in both methods. These results illustrate that clean-up, to reduce matrix effect, by performing SPE in multi-residue analysis is difficult to achieve when the mechanism of extraction in SPE and separation in LC are the same: reversed phase. This can be explained by the observation of Bonfiglio *et al.* (1999) and Stahnke *et al.* (2009) that matrix effects are rather retention time dependent with regions in the chromatogram with strong or weak matrix effects. Clean-up of interfering matrix compounds when the same reversed phase mechanism for both extraction and separation is applied, is thus limited because interfering matrix compounds and analytes having similar retention times will behave similar during SPE.

However, purification of the extract such as removing salts can be necessary to prevent clogging of capillaries or build-up of salts or non-volatile compounds on optics in the mass spectrometer, whereas very lipophilic compounds might accumulate on the LC column (Busetti *et al.*, 2012). These matrix constituents could deteriorate the instrumental performance on the long term. In this research, clean-up of very hydrophilic compounds or salts was achieved by washing the SPE cartridges with water. In addition, elution of very lipophilic compounds ( $\log k_{ow} > 5$ ) was avoided by choosing 5 ml of methanol as optimal elution solvent and volume, as such, they will probably not or only partially elute from the cartridge. For the LVI-based method, the first 1.6 min of the LC eluent was diverted to the waste to prevent salts or very hydrophilic compounds to reach the MS. However, very lipophilic compounds were not removed.

Third, the LVI method is less expensive (no SPE cartridges), and less time and labor intensive both with respect to method development and for method application. The cost for only the Oasis HLB SPE cartridges is 5€ per piece and it takes about 4 hours to extract 10 samples simultaneously, not taking into account the filtration steps before SPE. Whereas in this PhD study the method development, optimisation and validation took about 1 year for the SPE method, this could be achieved in about 4 months for the LVI method. During the LVI method development, only small adjustments of the LC conditions, such as adding an initial isocratic phase of 1 min and the addition of small amounts ( $< 0.1\%$  v/v) of formic acid to the sample were necessary and enabled good peak shapes and stable chromatography.

Fourth, a drawback of the presented LVI method was that 10 to 100 times higher method detection limits were obtained as compared to other techniques published in literature using (online-)SPE (Figure 5.6). The method showed the potential to detect 50 and 74% of the pharmaceuticals at a concentration of 100 and 500 ng l<sup>-1</sup> or lower, respectively. These detection limits are close to the 100 ng l<sup>-1</sup>, which has been suggested as a lower performance limit for multi-residue screening by Chitescu *et al.* (2012). The lower sensitivity of the LVI method could be related to the lower equivalent sample injection volume (ESIV) (i.e. the enrichment factor  $\times$  injection volume) or thus the lower amount of substance that is directly (LVI) or indirectly (SPE) injected onto the LC column. The ESIV amounts to 250  $\mu$ l for the LVI method for drinking and surface water versus 500  $\mu$ l and 1000  $\mu$ l for the SPE method for influent and effluent water, respectively. Taking into



consideration that less polluted samples allow in general larger ESIVs (Chapter 2), the ESIV of drinking and surface water is relatively small as compared to the ESIVs of effluent and influent water.

Overall, both methods have merits in an analytical multi-residue analysis. On the one hand, LVI allows a faster analysis and almost no losses occur during sample pretreatment and therefore fits well for fast screening. On the other hand, SPE allows to enrich the sample and reach as such lower detection limits but always introduces some selectivity. The most important challenge for future developments for LVI is thus to be able to measure lower concentration levels, whereas for SPE, an optimal recovery for a wide range of hydrophilic and lipophilic compounds must be reached.

### **7.1.3 Quantitative and qualitative analysis with full-spectrum HRMS**

HRMS (TOF and Orbitrap) is a relatively new mass spectrometric technique and became suitable for trace analysis in environmental science thanks to its gains in sensitivity since the early 2000's. With its ability to measure a wide range of masses at once (i.e. full-spectrum), this technique fits well in the screening-to-quantification multi-residue analytical goals. However, uniform guidelines for data processing in quantitative and qualitative multi-residue analysis using full-spectrum HRMS are scarce and obtaining both a low number of false negatives and false positives in screening is challenging.

In this research, advances are made on both issues. In this Section, guidelines (i) for the construction of extracted ion chromatograms

(XICs) for proper quantitative data processing, and (ii) for accurate mass determination and the development and evaluation of screening procedures are formulated.

### **7.1.3.1 Selective quantification**

For selective peak integration and quantification in HRMS, XICs are constructed from the total ion chromatogram (TIC) by defining a mass tolerance around the exact ion mass of interest (i.e. mass window width). In Chapter 4, the relationship between selectivity and sensitivity as a function of the mass window width is investigated and specific guidelines are formulated.

First, peak integration should be performed on the raw profile data. It was shown that especially the use of centroid data can lead to signal interruption of the signal when the accurate mass of an ion is shifted out of the XIC mass window. These findings correspond with those of Kaufmann & Butcher (2006), which have also been discussed in Section 2.6.

Second, when constructing XICs from profile data, the signal intensity of a chromatographic peak will decrease upon narrowing the mass window because an increasing fraction of the mass peak is cut off. As such, the sensitivity might reduce. An optimal value for the XIC width using profile data, being a trade-off between sensitivity and selectivity, has shown to be about the FWHM, thus 100, 50, 20 and 10 ppm for a resolving power of 10 000, 20 000, 50 000 and 100 000 FWHM, respectively. In other words, the recommended mass window width (in ppm) can be calculated as  $\frac{10^6}{R}$ , with  $R$  the provided

resolving power.

With respect to 27 validated HRMS methods summarized in Table 2.1, narrower mass windows were often applied: about half of the authors applied a mass window of 2 to 5 times narrower than the recommended value in this PhD research (for this comparison, corresponding mass windows for  $m/z$  400 Da were calculated, as explained in Table 4.3). Although such narrow mass windows assure more selective XICs and are thus not per se problematic, HRMS users should take in mind that false negative results might occur when multiple signals fall out of the defined mass window in the case centroid data is integrated or that, in the case of profile data, the method sensitivity will decrease.

However, recent research has shown that signal interruption in XICs from centroid data can be avoided using an algorithm which automatically chooses the optimal mass window width for peak integration (Wei *et al.*, 2014). As such, centroid data can be used, and the decreased signal intensity when integrating profile data with too narrow mass windows can be avoided. Using centroid data can be advantageous because it requires less storage capacity and centroiding is a necessary step for qualitative analysis. This approach merits thus further investigation and application.

### **7.1.3.2 Qualitative analysis and suspect screening**

An inherent first step in qualitative analysis with HRMS is to determine the accurate mass from the spectrum peaks. In Chapter 4, transforming the profile spectra to centroid was recommended for the determination of accurate masses for qualitative analysis. Taking into account all the

data points of a mass peak instead of only the data point at the top resulted in a 2.3 fold improved precision on the accurate mass.

Two novel suspect screening strategies are presented in this PhD study. In Chapter 5, suspect screening was performed for a set of 69 pharmaceuticals in surface water using LVI-UHPLC and TOF-HRMS. The novelty in this suspect screening technique is that a statistical model takes into account the signal intensity-dependent accurate mass error of the mono isotopic ion, which is typical for TOF-MS. This allowed to control the false negative rate (FNR) at 5%, with a false positive rate (FPR) not higher than 15%.

In Chapter 6, an extended suspect screening method for 77 pharmaceuticals in WWTP effluent using SPE-UHPLC and Orbitrap HRMS was presented. In order to further improve the screening performance and reduce the FPR, the accurate mass error of the mono isotopic ion and up to three isotopes, isotope ratios and a peak/noise filter were taken into account. However, when setting up a conventional screening identification train based on successively different identification criteria, the FNR typically accumulates upon advancing through the decision tree. The challenge to elaborate a well-balanced screening was accomplished by introducing a multivariate statistical model. As such, the different criteria are equally stringent and the overall FNR could be controlled to 5%. This resulted in a strongly improved identification success with FPRs decreasing from 131, 22, 2.8 to < 0.3% upon taking into account only the mono isotopic ion and 1, 2 or 3 isotopes, respectively. Whereas the FPR reduced with additional isotopes, the LOI increased with median values of 42, 200, 2000 and

2062 ng l<sup>-1</sup> upon taking into account only the mono isotopic ion, and 1, 2, or 3 isotopes, respectively. In future research, incorporating also retention time prediction and fragmentation pattern verification in the suspect screening concept should be investigated as complement to reduce the FPR with less increasing LOI values.

In both strategies, for the first time, controlling the overall FNR to a desired level (5 %) is achieved by using statistical models. As such, for each detected analyte, the identification decision (retain or reject) is based on a hypothesis test resulting in a single  $p$ -value.

When taking into account only the mono isotopic ion and a peak/noise filter for screening, the FPR was clearly higher for  $H_{1,3}$  in Chapter 6 (131 %) than in Chapter 5 (15 %). Although the peak picking algorithm and peak/noise filter were different for both screening methods, the higher FPR in effluent water is most probably due to the generally higher contamination level of effluent water. More complex water matrices seem thus to require most advanced screening algorithms in order to maintain a feasible FPR.

In this research, an effective screening method development, evaluation and application workflow was followed for both screening methods, which is recommended for future research. The generalized workflow is schematized in Figure 7.1. First, a training dataset was constructed based on samples spiked at different concentrations with target compounds having a wide range of chemical characteristics (e.g. with masses over the whole mass range). This training data set contains information such as accurate mass, retention time, peak area and signal intensity of the ions of interest (e.g. mono isotopic ion, isotopes, adducts

and fragments) related to the spiked analytes. To confirm the identity of the peaks in the training dataset, their a priori determined retention time was used. This dataset was used to develop and optimize the statistical screening methods based on different identification refinement techniques. Mass error, peak/noise filter and isotopic pattern have been considered in this research, but other researchers have applied other complementary techniques including retention time prediction and fragmentation pattern matching (Section 2.5). The novelty in Chapter 6 is that a well-balanced identification decision is guaranteed taking the mass error, isotope fit and peak/noise filter in a holistic multivariate approach. This contrasts with the currently applied screening approaches using decision trees, which are potentially not-well balanced, leading to an increasing number of false negatives when advancing through the decision tree.

Second, the performance of the developed suspect screening methodology must be evaluated. Therefore, 3 particular parameters can be assessed for qualitative suspect screening: (i) screening LOI, (ii) FNR, and (iii) FPR. (i) The LOI is the concentration level at which a predefined fraction ( $2/3$  in Chapter 6) is correctly retained (Ellison & Fearn, 2005) and (ii) the FNR is the fraction of analytes not retained by the screening algorithm, but present in the training dataset. These parameters should be evaluated from the training dataset. (iii) A false positive is a peak retained by the screening but having a non-matching retention time with an analytical standard. The FPR is calculated as the false positive count divided by the number of screened suspects, with this ratio averaged over the considered samples, being in agreement

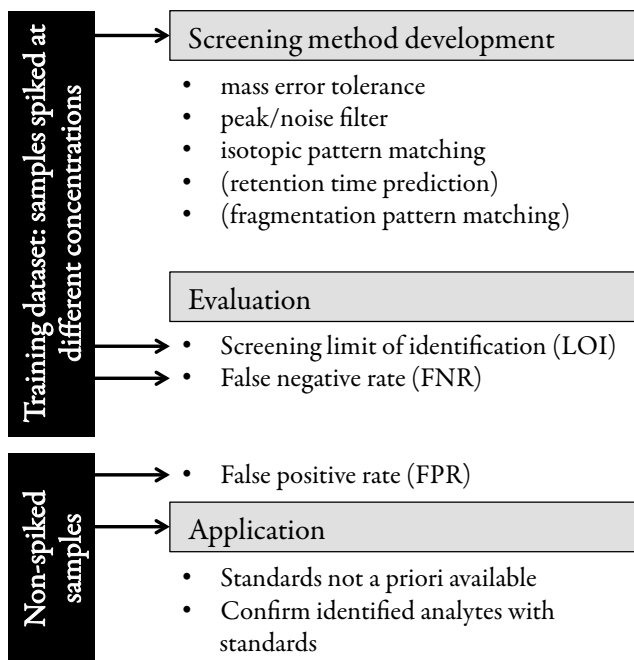


**Figure 7.1** General workflow applied in Chapters 5 and 6 and suggested for the development, evaluation and application of suspect screening strategies. Between brackets: these parameters were not considered in this research but could be valuable for future improvement.

with Ellison & Fearn (2005). This parameter should be evaluated from non-spiked samples. The latter to avoid overestimating the FPR due to the presence of double peaks of some compounds (e.g. tetracycline antibiotics) or impurities in the spiked standards with the same chemical formula (e.g. amoxicillin, Chapter 6), which could all be retained by the screening but classified as false positives. Although such false positives can also be present in non-spiked samples, in spiked samples they can be much more abundant. The FPR should not be confused with the

false discovery rate (FDR), which is the false positive count divided by the total number of (false + true) positive findings. The FPR is preferred instead of the FDR because the former value is independent of the number of true positive findings or, in other words, independent of the contamination level of a sample. This is an important distinction and allows a more unbiased comparison of screening methods.

Application of the suspect screening typically leads to indicatively identified compounds. For these suspects, no standards are a priori available and the retention time and eventually also fragmentation pattern must be experimentally confirmed. Therefore, analytical standards must be obtained for confirmation and, in the light of the screening-to-quantification approach, the analytical method can be validated for quantification of the confirmed and relevant compounds.

#### **7.1.4 Quantitative and qualitative validation of multi-residue methods**

Reliable quantification requires a thorough method validation. Therefore, different instrumental and method validation parameters such as linearity, detection and quantification limits, repeatability and reproducibility, and mass accuracy have been investigated in this research. Validation of multi-residue methods showed to be challenging and four particular issues have been investigated over the different chapters of this work. Guidelines are formulated for each issue.



#### 7.1.4.1 Precise determination of the analytical process efficiency

A precise determination of the process efficiency (PE) value of an analytical method is crucial because this value is used as a correction factor, as elaborated in Chapter 3. However, this can be problematic for compounds being ubiquitously present in environmental matrices such as wastewater. Very elevated RSDs were obtained for the determination of the PE for compounds which were present in the non-spiked sample at concentrations close to or higher than the spiking level. Therefore, the concentration of the spiking level must be high enough to allow a precise determination of the PE value (e.g. < 20% relative standard deviation). To enable this, the highest spiking concentration should be at least 3 to 5 times higher than the concentration in the non-spiked sample.

In this work, PE (Chapter 3) or ME (Chapter 5) values were always calculated from a representative sample used for method validation. Subsequently, this PE/ME value was used as correction factor for new samples. However, sample-to-sample variability of the PE/ME due to, for example, sample-dependent matrix effects, has not been considered. Future research should thus also investigate to what extent the PE/ME values change from sample to sample. Alternatively, internal standard calibration or standard addition can be applied to correct for recovery and matrix effects for each individual sample. However, internal standard calibration requires the availability of isotopically labeled standards, which are in general more expensive or sometimes hard to

find, and the standard addition method requires to analyze the sample twice; once with and once without standard addition.

#### **7.1.4.2 Determination of decision/detection limits**

For the validation of HRMS analytical methods, widespread concepts such as the signal-to-noise (S/N) ratios for the determination of detection and quantification limits have shown to be not always applicable because in some cases almost no noise can be detected anymore, as illustrated in Chapter 4. As an alternative for the widely applied S/N ratio, the methodology for the calculation of the decision limit ( $CC\alpha$ ) developed by Kaufmann (2009) has been extended by taking into account also the number of analyzed spiked samples into a statistical approach. The instrumental characteristics of the TOF instrument used in this research enabled comparison of both approaches because noise could still be observed for different compounds. The methodology resulted in comparable decision limits as obtained from a S/N ratio of 3. It can be concluded that this methodology is a reliable and practical alternative for the widespread S/N ratio concept, which will be of utmost importance in most modern HRMS.

However, the ubiquitous presence of some micropollutants in environmental matrices can be problematic for the determination of method detection limits (MDLs) ( $S/N = 3$ ) or  $CC\alpha$ s. In both (treated) wastewater (Chapter 3) and surface water (Chapter 5) some compounds were clearly present in the non-spiked validation samples. Validating the method for such compounds at lower concentrations is not possible using the standard addition (spiking) technique because truly blank

matrix samples are hard to find. As a consequence, also the correct determination of the MDL or  $CC\alpha$ , which should be performed by analysing samples at concentrations close to the MDL or  $CC\alpha$ , is not possible. As a result, the reported  $CC\alpha$  values are equal to at least the measured concentration in the non-spiked sample, which can be an overestimation of the true  $CC\alpha$ . Although for the S/N technique, extrapolation to a S/N level of 3 is possible for the estimation of the MDL, the uncertainty on these values is expected to be high.

#### 7.1.4.3 Response linearity

The relevant – to be validated – concentration range in the environment is very wide. This is illustrated in Chapter 1: concentrations of pharmaceuticals range from the  $\text{ng l}^{-1}$  for drinking water and ground water over  $\mu\text{g l}^{-1}$  for surface water and treated wastewater to the low  $\text{mg l}^{-1}$  for wastewater. This requires wide linear working ranges. The lowest concentration of the linear working range is normally the method quantification limit (MQL). The upper quantification limit (UQL) is the highest concentration level within the instrumental linear range.

For the determination of the linear regression equation, a first aspect is that the assumption of homoscedasticity of variance must be fulfilled. However, in analytical chemistry the variance of the residuals are normally unequal, i.e. heteroscedastic. This has been illustrated in Figure 5.5 for diclofenac: the standard deviation ( $\sigma$ ) increased with the concentration level. However, the precision expressed as relative standard deviation (RSD) is in general more or less constant in the upper concentration range and increases only for concentrations close

to the quantification limit. Therefore, weighted least squares regression should be applied with the reciprocal of the variances as weights:  $1/\sigma^2$ . Considering that  $\sigma$  linearly increases with the concentration level  $x$ , the weights are proportional to  $1/x^2$  (Kutner *et al.*, 1996).

A second aspect is the evaluation of the linearity of the detector response. In most publications, and for the majority of the validated methods in Table 2.1, the coefficient of determination,  $R^2 > 0.99$ , was used as the criterion for linearity. As  $R^2$  is calculated from the sum of squares of the non-weighted residuals, large residuals have the strongest impact on  $R^2$ . The increasing standard deviation with concentration of analytical data has as a consequence that in particular non-linearity at the highest concentration levels will contribute to the  $R^2$ , whereas the contribution of even strong non-linearity in the lower concentration range will be marginal. The  $R^2$  is therefore not a good measure to evaluate the linearity over the whole concentration range (Peters *et al.*, 2007). An appropriate statistical test for linearity is the F-test for lack of fit as described in Section 5.2.5.1. If non-linearity was concluded in this research, linearity can be tested again after contracting the working range by omitting the highest concentration level (Chapter 3) or a non-linear calibration curve can be used (Chapter 5).

#### **7.1.4.4 Mass measurement uncertainty**

Taking into account the variety of sources of mass error discussed in Section 2.4.1, a thorough HRMS method validation should include a characterization of the mass measurement uncertainty. Similar to the concept of uncertainty in quantitative analysis (2002/657/EC, European

Union, 2002), the mass measurement accuracy can be statistically described by the average mass error ( $\overline{\Delta m/z}$ , Equation 2.1b) and the standard deviation on the mass error ( $\sigma_{m/z}$ ), as demonstrated by Brenton & Godfrey (2010). Experimental data, acquired under reproducibility conditions (over time and per matrices of interest) on a set of analytes covering the molecular mass and concentration range of interest, should be the basis for a qualitative validation. The mass measurement accuracy can be expressed as  $\overline{\Delta m/z} \pm 1.96 \cdot \sigma_{m/z}$  or  $\pm 2.58 \cdot \sigma_{m/z}$  which are approximately the 95% or 99% confidence limits, respectively (Brenton & Godfrey, 2010).

The bias on the mass accuracy (i.e.  $\overline{\Delta m/z}$ ) was less than 0.5 ppm for both the TOF and Orbitrap HRMS. The mass precision (95% confidence interval) was about  $\pm 5$  ppm at  $5 \mu\text{g l}^{-1}$  and increased to about  $\pm 10$  ppm close to the CC $\alpha$  level independent of the analyzed matrix (deionized, drinking or surface water) for the TOF HRMS (Chapter 5). For the Orbitrap HRMS (Chapter 6), the mass precision was about  $\pm 2.3$  ppm for the mono isotopic ions in effluent water. Although a more complex matrix was analyzed with the latter, the mass precision doubled, which can be related to its improved resolving power of 70 000 FWHM versus 20 000 FWHM for the TOF HRMS.

Moreover, this mass accuracy data can be used to set the mass error tolerance for confirmation of the identity of target analytes. Although a mass error tolerance of 5 ppm has been widely applied (Ibáñez *et al.*, 2008; Kern *et al.*, 2009; Gerssen *et al.*, 2011; Nurmi & Pellinen, 2011; Martínez Bueno *et al.*, 2012), it can be of importance to reconsider (widen or narrow) this value in order not to omit truly present analytes

(i.e. false negatives) and, at the same time, be stringent enough to avoid false positives. As such, setting the mass error tolerance to the experimentally determined mass measurement accuracy (i.e.  $\pm 1.96 \cdot \sigma_{m/z}$  or  $\pm 2.58 \cdot \sigma_{m/z}$ , supposing  $\overline{\Delta m/z} \approx 0$ ) will result in approximately only 5% or 1% false negatives, respectively.

## 7.2 Occurrence of pharmaceuticals in wastewater and surface water

One of the first data on the occurrence, concentrations and removal efficiencies of pharmaceuticals in the Belgian aquatic environment has been reported in this research.

WWTPs are seen as one of the major pathways of pharmaceutical residues to the environment. In Chapter 3, the occurrence and fate of 43 pharmaceuticals has been studied in a conventional active sludge (CAS) system (Aalst, Belgium) and in a parallel CAS and membrane bioreactor (MBR) (Schilde, Belgium) WWTP. In the influent, concentrations ranging from the MQL ( $50\text{-}500 \text{ ng l}^{-1}$  for most of the compounds) to about  $50 \text{ } \mu\text{g l}^{-1}$  were measured. For the most concentrated compounds, i.e. paracetamol and ibuprofen in the influent ( $5\text{-}50 \text{ } \mu\text{g l}^{-1}$ ), loads in the effluent were at least 50 times lower than in the influent for both CAS and MBR. For all the other compounds with concentrations up to about  $1 \text{ } \mu\text{g l}^{-1}$  in the influent, the removal strongly varied with effluent loads from 17 times lower to 2 times higher than the influent load. These concentrations and reduction factors have a similar wide range as those reported by Verlicchi *et al.* (2012) in a recent review. However, although

they concluded that even for the same compounds reduction factors can strongly vary for different WWTPs, in this research, comparable reduction factors were obtained for the three studied systems (e.g. almost no reduction for venlafaxine, factor 1.5-2 for sulfamethoxazole,  $> 50$  for ibuprofen and  $> 1000$  for paracetamol). Also for moxifloxacin comparable reduction (factor 2.3-4) was observed under dry weather condition, whereas effluent loads were 2.6 times higher as compared to the influent during a rainfall event, which could be due to desorption from solids in the influent.

Although the concentrations of the most concentrated compounds reduced drastically in the effluent as compared to the influent, comparable influent and effluent concentrations (up to  $\mu\text{g l}^{-1}$ ) were observed for many pharmaceuticals. As a consequence, pharmaceutical residues enter the environment. In the river Maas and the Albert Channel (Belgium), concentrations ranging from about  $10 \text{ ng l}^{-1}$  to about  $1 \mu\text{g l}^{-1}$  were measured (Chapter 5). A first tier environmental risk assessment for the river Dender (Belgium) impacted by the WWTP of Aalst indicated that the anti-inflammatory drug diclofenac and the antidepressant venlafaxine posed a potential 'high' risk (risk quotient  $> 1$ ). For these compounds, a more intensive second tier risk investigation is required. No ecotoxicological data were found in open literature for alprazolam, amantadine and risperidone, which established the need for more research in order to better assess the risk of pharmaceutical residues in the environment. In the analyzed drinking water, concentrations of all pharmaceuticals were below the MDL (i.e.  $< 500 \text{ ng l}^{-1}$  for 75 % of the compounds).

### **7.3 Perspectives for screening-to-quantification of environmentally relevant contaminants**

The screening-to-quantification workflow elaborated in this work is a piece of the large puzzle of microcontamination of the environment which scientist are dealing with nowadays.

On the short term, suspect screening can facilitate the analytical workflow and lead to the identification of an increasing number of contaminants. With HRMS, a rather untargeted analysis can be performed and no (often expensive) analytical standards are a priori required in order to screen the acquired full-spectrum chromatograms for the presence of large lists of suspects. Analytical standards are only required in a second phase for confirmation of the indicatively identified compounds. In a third phase, the laborious method validation for target quantification can be restricted to the most relevant contaminants. As such, a cost and work reduction can be achieved.

A full non-targeted analysis and compound screening is still very challenging and requires an integrated approach. This is because, in first instance, the whole analytical procedure must reflect the multi-residue non-target idea, starting from sampling, over sample storage, sample pretreatment and purification, chromatographic separation and finally HRMS analysis. The challenge is that the entire analytical procedure must suit a variety of substances having a broad range of chemical characteristics. Therefore, it is crucial that once the different steps of the analytical procedure are optimized for a well-thought selection



of target compounds having a broad range of chemical characteristics, the applicability contours of the chemical-analytical method must be defined. Data from literature together with well-designed experimental approaches must as such allow defining the suitable domain of chemical characteristics where a certain analytical method meets the requested performance criteria. These chemical characteristics include the polarity, charge and stability of the compounds, and whether the compounds are amendable for the applied chromatographic and ionization technique. At the same time, the developed methods need to be sufficiently sensitive assuring that relevant concentrations, typically in the  $\text{ng l}^{-1}$  to  $\mu\text{g l}^{-1}$  range, are measurable with the non-target analytical screening method.

The selection of relevant pharmaceuticals in this research was not based on screening but on the available scientific knowledge. In addition, some compounds of scarcely measured pharmaceutical classes such as antiviral drugs and antidepressants were also selected as target compounds. This resulted in the measurement of relatively elevated concentrations of the antiviral drugs amantadine ( $50 \text{ ng l}^{-1}$  to  $1 \mu\text{g l}^{-1}$ ) and lamivudine ( $400$  to  $600 \text{ ng l}^{-1}$ ), and of the antidepressant risperidone ( $150$  to  $400 \text{ ng l}^{-1}$ ) in WWTP effluent. These results suggest that screening in aquatic environments might reveal the presence of even more and yet unknown contaminants. For example, the presence of the drug amantadine has been observed for the first time in treated wastewater by Ghosh *et al.* (2010) and was detected by non-target screening in treated wastewater by Hug *et al.* (2014) and in drinking water by Müller *et al.* (2011). The list of known target compounds

nowadays might thus change drastically in the near future when HRMS-based screening techniques are used more frequently.

To exemplify the potential of suspect screening for the identification of 'new' contaminants, the effluent of 7 Belgian WWTPs was screened for the presence of 77 pharmaceuticals (Chapter 6). When taking into account 2 or 3 isotopes for identification, the presence of a total of 19 out of 25 retained compounds could be confirmed. The concentration of these compounds was probably relatively high because the LOI of the screening method was  $\geq 500 \text{ ng l}^{-1}$  for 62 (2 isotopes) and 82% (3 isotopes) of the compounds. Suspect screening can thus lead to the detection of environmentally relevant contaminants.

One step further is non-target screening, which has been discussed and illustrated in Section 2.5 and Figure 2.8. In this screening concept, one of the main challenges is to prioritize the most relevant peaks for identification and propose chemical formulae and structures. From that point, similar identification refinement procedures can be performed as in suspect screening. The difficulty is that one or more chemical formulae and structures might be proposed for a given group of peaks.

In all cases of suspect and non-target screening, the challenge is to minimize the number of false negative and false positive detections. In this dissertation, it is shown that controlling the false negative rate to a desired level is possible by applying multivariate statistics (Chapter 6). Future research should focus on reducing the number of false positives by taking into account also other identification refinement criteria such as retention time prediction and fragmentation pattern matching in similar statistical approaches. This requires a systematic optimization

and evaluation of the screening methods. For this task, the general workflow as proposed in Figure 7.1 was applied in Chapters 5 and 6 and has shown to be effective. Future screening techniques could adopt this approach in order to be able to improve and compare their performance on a scientific basis.

On the longer term, screening has the potential to initiate a new way of looking to the challenges related to emerging micropollutants such as linking their presence with (eco)toxicological effects, smart design of advanced water purification technologies, and effective water quality policy establishment.

An important but unanswered question is which chemicals amongst the variety of micropollutants can be linked with ecological effects. Nowadays, researchers have been able to assess the effects of some selected contaminants. However, this rather targeted approach does not allow to assess which chemicals are actually causing effects in a complex environment. The combined use of analytical screening techniques and ecotoxicological assessment has an interesting potential to reveal these links.

Current biological wastewater treatment technology is insufficient to eliminate micropollutants from wastewater and to prevent their release in the environment. Therefore, advanced water purification technologies need to be developed and implemented. Switzerland has a leading position in this and decided recently to implement a combination of ozonation, biofiltration and powdered activated carbon as post-treatment on 100 out of its 700 WWTPs over the next 20 years (Eggen *et al.*, 2014). The aim is to reduce the load of indicator

substances such as benzotriazole, carbamazepine, diclofenac, mecoprop and sulfamethoxazole by 80% and to reduce the effluent toxicity. Although these selected indicator substances have shown to pose an ecological threat (e.g. Table 1.1), their selection is based on the current knowledge acquired by target analysis and many other ecotoxic or recalcitrant chemicals, including transformation products formed during ozonation, might be overseen. Therefore, for a smart design, optimization and control of advanced treatment technologies, analytical screening techniques will be a valuable tool to study the technology and to identify the most relevant indicator substances and transformation products.

Finally, policy must come to action and develop a legislative framework in order to ensure a good ecological status of waterbodies and healthy drinking water. Whereas currently some emerging micropollutants are incorporated in watch lists and legislation of Switzerland, the EU and the US EPA (Section 1.5), the most priority contaminants should be incorporated in future legislation. Hence, in addition to targeted analytical approaches, screening approaches should become more mainstream. Screening can be a valuable tool for example to monitor water quality, to identify accidental chemical water pollution, or to warn for unexpected contamination of drinking water resources.



## Summary

An increasing number of anthropogenic emerging organic contaminants has been discovered over the last decades in the aquatic environment. Pharmaceuticals are a particular group of emerging micropollutants. These chemicals are designed with the intention of performing a curing effect. Paradoxically, they are now seen as pollutants which might have toxic effects in our environment. Intermediate barriers such as wastewater treatment plants (WWTPs) intended for purification of anthropogenic waste streams seem to be insufficient to eliminate these micropollutants. As a result, pharmaceuticals are continuously discharged in the environment leading to concentrations in the  $\text{ng l}^{-1}$  to  $\mu\text{g l}^{-1}$  range. The occurrence, fate and (eco)toxicity of pharmaceuticals in the environment is concisely overviewed in Chapter 1.

To assure a good chemical status of water, increasing efforts should go to measuring as prerequisite for studying the occurrence, fate and risks of these organic micropollutants passing between wastewater, surface water, groundwater and drinking water.

The state-of-the-art for target analysis of polar water contaminants such as pharmaceuticals, is tandem mass spectrometry (MS/MS),

coupled to liquid chromatography and solid-phase extraction (SPE). However, since the early 2000's, new and advanced high-resolution mass spectrometry (HRMS) technologies became a viable alternative. With these instruments, wide MS spectra are continuously acquired over the entire chromatogram allowing a quasi untargeted analysis, without the requirement to define a priori which compounds should be measured. The full-spectrum HRMS approach has therefore the potential to both identify and quantify a virtually unlimited number of analytes based on accurate mass measurement and offers the ability for screening towards new (un)known contaminants. The basic principles of HRMS and the achievements of full spectrum HRMS for screening and quantification of emerging organic micropollutants in the aquatic environment are reviewed in Chapter 2.

Developing innovative HRMS-based analytical methods as stepping-stones of an innovative screening-to-quantification workflow is the general aim throughout this PhD dissertation. Different techniques using double focussing magnetic sector, Time-of-Flight (TOF) and Orbitrap HRMS are developed and their applicability is investigated for the analysis of pharmaceuticals in drinking water, surface water and (biologically treated) wastewater.

In Chapter 3, a novel analytical method using SPE and liquid chromatography magnetic sector HRMS is presented for the measurement of 43 pharmaceuticals in (biologically treated) wastewater. A thorough method validation quantified the contribution of both the extraction recovery and matrix effects in the overall method process efficiency, and a detailed variability analysis was performed to

elaborate a quality labelling strategy to be used in data interpretation. Compounds for which a precise (relative standard deviation <20 %) process efficiency between 60 % and 140 % was determined, were labelled as ‘quantitative’ whereas the results for other compounds should be interpreted as ‘indicative’. Method application on influent and effluent samples of (i) a conventional active sludge system and (ii) a parallel membrane bioreactor/conventional active sludge wastewater treatment plant in Belgium revealed the occurrence of 22 pharmaceuticals. The anti-inflammatory drug diclofenac and the antidepressant venlafaxine were measured in the effluents at concentrations ranging from 0.5 to 1.8  $\mu\text{g l}^{-1}$  and 0.2 to 0.5  $\mu\text{g l}^{-1}$ , respectively, which indicated to be of high potential environmental risk for the receiving river Dender, Belgium.

Uniform guidelines for the data processing and validation of qualitative and quantitative multi-residue analysis using full-spectrum HRMS are scarce. In Chapter 4, it is investigated how optimal mass accuracy and sensitivity can be obtained after refining the post-processing of the HRMS data. For qualitative analysis, transforming the raw profile spectra to centroid spectra is recommended resulting in a 2.3 fold improved precision on the accurate mass determination of spectrum peaks. However, processing centroid data for quantitative purposes could lead to signal interruption when too narrow mass windows are applied for the construction of extracted ion chromatograms. Therefore, peak integration on the raw profile data is recommended. An optimal width of the mass window of 50 ppm, which is a trade-off between sensitivity and selectivity, was obtained for a TOF instrument providing a resolving power of 20 000 at full width at half maximum (FWHM). For



the validation of HRMS analytical methods, widespread concepts such as the signal-to-noise ratios for the determination of decision limits and detection capabilities have shown to be not always applicable because in some cases almost no noise can be detected anymore. A statistical methodology providing a reliable alternative is extended and applied.

The ever-growing number of emerging micropollutants such as pharmaceuticals requests rapid and sensitive full-spectrum analytical techniques. In Chapter 5, a suspect screening strategy is presented, which minimizes the false negative rate (FNR) without retaining numerous false positives. At the same time, omitting laborious sample enrichment through large-volume injection (LVI) ultra-high performance liquid chromatography (UHPLC) avoids selective preconcentration. A suspect screening strategy was developed using TOF-MS aiming the detection of 69 pharmaceuticals in surface water without the a priori availability of analytical standards. As a novel approach, the screening takes into account the signal-intensity-dependent accurate mass error of TOF-MS, hereby retaining 95 % of the measured suspect pharmaceuticals present in surface water. Application on five Belgian river water samples showed the potential of the suspect screening approach, as exemplified by a false positive rate (FPR) not higher than 15 % and given that 30 out of 37 restrained suspect compounds were confirmed by the retention time of analytical standards. Subsequently, the validation and applicability of the LVI-UHPLC full-spectrum HRMS method for target quantification of the 69 pharmaceuticals in surface water is discussed. Analysis of five Belgian

river water samples revealed the occurrence of 17 pharmaceuticals in a concentration range of  $17 \text{ ng l}^{-1}$  up to  $3.1 \text{ } \mu\text{g l}^{-1}$ .

In Chapter 6, the suspect screening concept is extended. When setting up a conventional screening identification train based on successively different identification criteria including mass error and isotope fit, the FNR typically accumulates upon advancing through the decision tree. The challenge is thus to elaborate a well-balanced screening, in which the different criteria are equally stringent, leading to a controllable number of false negatives. Presented is a novel suspect screening approach using UHPLC Orbitrap HRMS. Based on a multivariate statistical model, the screening takes into account the accurate mass error of the mono isotopic ion and up to three isotopes, isotope ratios and a peak/noise filter. As such, for the first time, controlling the overall false negative rate of the screening algorithm to a desired level (5% in this study) is achieved. Simultaneously, a well-balanced identification decision is guaranteed taking the different identification criteria as a whole in a holistic statistical approach. Taking into account 1, 2 and 3 isotopes decreased the false positive rates from 22, 2.8 to  $< 0.3\%$  at the cost of increasing the median limits of identification from 200, 2000 to  $2062 \text{ ng l}^{-1}$ , respectively. As proof of concept, 7 biologically treated waste waters were screened towards 77 suspect pharmaceuticals resulting in the indicative identification of 25 suspects. Subsequently obtained reference standards allowed confirmation for 19 out of these 25 pharmaceutical contaminants.

## *Summary*

An overall discussion focusing on the scientific results and perspectives with respect to the screening-to-quantification workflow using HRMS is given in Chapter 7.

## Samenvatting

Gedurende de laatste tiental jaren werd een toenemend aantal antropogene organische contaminanten waargenomen in het aquatische milieu. Geneesmiddelen zijn hierbij een bijzondere groep van micropolluenten die recent in de belangstelling kwamen. Hoewel deze stoffen ontwikkeld zijn omwille van hun geneeskrachtige werking, is de paradox dat ze nu gezien worden als potentieel schadelijke stoffen voor ons milieu. Barrières zoals waterzuiveringsinstallaties blijken onvoldoende om hun residu's te verwijderen waardoor ze continu in the milieu geloosd worden. Het voorkomen van lage concentraties (in de grootte orde van  $\text{ng l}^{-1}$  tot  $\mu\text{g l}^{-1}$ ), het gedrag en de (eco)toxiciteit van geneesmiddelen in het milieu wordt bondig samengevat in Hoofdstuk 1.

Om een goede chemische waterkwaliteit te garanderen, zijn inspanningen nodig om de diversiteit aan organische micropolluenten nauwgezet te analyseren. Analyse is onmisbaar voor de studie naar het voorkomen, het gedrag en de risico's van deze micropolluenten die getransporteerd worden tussen afvalwater, oppervlaktewater, grondwater en uiteindelijk ook drinkwater.

De state-of-the-art voor de doelgerichte analyse van polaire watercontaminanten zoals geneesmiddelen is tandem massa spectrometrie gekoppeld aan vloeistofchromatografie en vaste fase extractie. Echter, sinds de jaren 2000 werden nieuwe en geavanceerde technologieën voor hoge-resolutie massa spectrometrie (HRMS) een interessant alternatief. Met deze instrumenten kan een breed massabereik continue geanalyseerd worden gedurende de chromatografische scheiding. Dit laat een niet-gerichte analyse toe waarbij het a priori vastleggen van doelverbindingen overbodig wordt. Daardoor heeft deze breed spectrum HRMS benadering het potentieel om een quasi ongelimiteerd aantal componenten te identificeren en te kwantificeren. Tegelijkertijd laat dit toe om te screenen naar nieuwe (on)bekende contaminanten. De basisbeginselen en de mogelijkheden van breed spectrum HRMS voor het screenen en kwantificeren van micropolluenten in het aquatisch milieu worden behandeld in Hoofdstuk 2.

De algemene doelstelling doorheen deze doctoraatsverhandeling is het ontwikkelen van innovatieve analytische methoden gebaseerd op HRMS als stapstenen voor een innovatief screenen-tot-kwantificatie concept. Verschillende technieken op basis van dubbel-focuserende magnetische sector, Time-Of-Flight (TOF) en Orbitrap HRMS worden ontwikkeld, en hun toepasbaarheid wordt onderzocht voor de analyse van geneesmiddelen in drinkwater, oppervlaktewater, en (biologisch gezuiverd) afvalwater.

In Hoofdstuk 3 wordt een nieuwe analytische methode voor het meten van 43 geneesmiddelen in (biologisch gezuiverd) afvalwater gepresenteerd. Deze methode is gebaseerd op vaste fase extractie,

vloeistofchromatografie en magnetische sector HRMS. De bijdrage van de extractie-efficiëntie en de matrix effecten, die samen de globale procesefficiëntie bepalen, wordt grondig onderzocht aan de hand van een methodevalidatie. Vervolgens worden kwaliteitslabels toegekend op basis van een gedetailleerde onzekerheidsanalyse om de data-interpretatie te vereenvoudigen. Componenten met een nauwkeurig bepaalde (relatieve standaard afwijking  $< 20\%$ ) procesefficiëntie tussen  $60\%$  en  $140\%$  worden gelabeld als kwantitatief. De resultaten van de andere componenten moeten eerder als indicatief beschouwd worden. Een totaal van 22 geneesmiddelen werd gemeten in het influent en effluent van (i) een conventioneel actiefslib systeem en (ii) een parallel systeem bestaande uit een membraanbioreactor en een conventioneel actiefslib systeem. De effluent concentraties van de ontstekingsremmer diclofenac en het antidepressivum venlafaxine varieerden respectievelijk van  $0.5$  tot  $1.8 \mu\text{g l}^{-1}$  en van  $0.2$  tot  $0.5 \mu\text{g l}^{-1}$ . Het lozen van dit effluent in de rivier De Dender zorgt mogelijks voor een verhoogd milieurisico omwille van de relatief hoge concentraties van sommige geneesmiddelen.

Uniforme richtlijnen voor de dataverwerking en voor de kwalitatieve en kwantitatieve validatie van breedspectrum HRMS zijn schaars. In Hoofdstuk 4 wordt onderzocht hoe een optimale massa-accuraatheid en gevoeligheid bekomen kan worden door het optimaliseren van de dataverwerking. Voor kwalitatieve analyse wordt het omzetten van de gemeten spectra naar staafspectra aangeraden. Op die manier kan de massaprecisie met een factor 2.3 verbeterd worden. Echter, voor kwantitatieve doeleinden kan het gebruik van staafspectra leiden tot signaalonderbreking indien ionenchromatogrammen geëxtraheerd

worden met te smalle massavensters. Daarom wordt aangeraden om de piekintegratie uit te voeren op de oorspronkelijk gemeten spectra. Op basis van een nauwkeurige afweging tussen gevoeligheid en selectiviteit werd een optimaal massavenster van 50 ppm aangeraden voor een TOF instrument met een massa-onderscheidend vermogen van 20 000.

Wijdverspreide concepten voor het bepalen van detectielimieten op basis van de signaal-ruisverhouding blijken niet altijd toepasbaar meer bij HRMS omdat soms geen ruis meer gedetecteerd wordt. As alternatief werd een statistische methode verbeterd en toegepast.

Het steeds toenemend aantal micropolluenten zoals geneesmiddelen vergt snelle en gevoelige breedspectrum HRMS technieken. In Hoofdstuk 5 wordt een gerichte screeningstrategie gepresenteerd die in staat is om het aantal valse negatieven te minimaliseren zonder al te veel vals positieve waarnemingen te weerhouden. De gebruikte analytische methode vermijdt het gebruik van de traditionele staalopzuiveringstechnieken door een groot volume te injecteren in een ultrahoog performante vloeistofchromatograaf. De gerichte screeningstrategie is ontwikkeld voor een TOF-HRMS voor de detectie van 69 geneesmiddelen in oppervlaktewater. De screening houdt rekening met de signaal-afhankelijkheid van de accurate massafout door middel van een vernieuwende statistische benadering. Op die manier kan gegarandeerd worden dat 95% van de gemeten geneesmiddelen ook weerhouden wordt. De methode is toegepast op 5 waterstalen van Belgische rivieren. Minder dan 15% vals positieve werden weerhouden, wat de toepasbaarheid van de methode illustreert. Uiteindelijk konden 30 van de 37 weerhouden componenten bevestigd worden

door het experimenteel verifiëren van de retentietijd met analytische standaarden. De kwantitatieve validatieresultaten en toepasbaarheid van de ontwikkelde methode die gebruik maakt van groot-volume injectie wordt bediscussieerd. Concentraties variërend van  $17 \text{ ng l}^{-1}$  tot  $3.1 \text{ } \mu\text{g l}^{-1}$  werden gekwantificeerd in de 5 rivierwaterstalen.

In Hoofdstuk 6 wordt het concept van gerichte screening uitgebreid. In conventionele screeningprocedures worden verschillende identificatiecriteria, zoals de massafout en het isotopenpatroon, één na één afgelopen. Hierbij loopt het aantal vals negatieven typische op. De uitdaging is om een goed uitgebalanceerde screening te bedenken waarbij de verschillende criteria even streng zijn, zodat het globaal aantal vals negatieven controleerbaar is. Daarom wordt een innovatieve gerichte screening voorgesteld die gebruik maakt van ultrahoog performante vloeistofchromatografie en Orbitrap HRMS. Op basis van een multivariaat statistisch model is het mogelijk om zowel de accurate massafout van het mono-isotopisch ion, 3 isotopen en hun isotoopabundantie, en een piek/ruis filter in rekening te brengen. Op die manier kon voor de eerste keer het aantal vals negatieven beperkt worden tot het gewenste niveau van 5%. Tegelijkertijd wordt een uitgebalanceerde identificatiebeslissing gegarandeerd door de verschillende identificatiecriteria op een holistische manier te evalueren. Indien 1, 2 en 3 isotopen in rekening gebracht worden, daalt het aantal vals positieven van 22, 2.8 tot  $< 0.3\%$  terwijl de mediane identificatie limiet toeneemt van 200, 2000 tot  $2062 \text{ ng l}^{-1}$ , respectievelijk. Om de effectiviteit van dit concept aan te tonen werden 7 biologisch gezuiverde afvalwaters gescreend naar het voorkomen van 77 geneesmiddelen. Dit



### *Samenvatting*

resulteerde in de indicatieve identificatie van 25 componenten waarvan, na het aankopen van analytische standaarden om hun retentietijd te verifiëren, 19 componenten geconfirmeerd werden.

De wetenschappelijke vooruitgang en perspectieven voor screenen-tot-kwantificatie met HRMS worden bediscussieerd in Hoofdstuk 7.

# Addenda

**Table A.1** Specifications of the analytical standards of the pharmaceutical compounds used in Chapters 3 and 6 (therapeutic group, chemical formula, solvent en concentration of analytical stock solution).

Substance (salt)	Therapeutic group	Formula	Solvent	Concentration (g l <sup>-1</sup> )
Acyclovir <sup>a</sup>	Antiviral	C <sub>8</sub> H <sub>11</sub> N <sub>5</sub> O <sub>3</sub>	Dimethyl sulfoxide	1.06
Alprazolam <sup>b</sup>	Tranquillizer	C <sub>17</sub> H <sub>13</sub> ClN <sub>4</sub>	Water	1.05
Amantadine (HCl) <sup>a</sup>	Antiviral, antiparkinson	C <sub>10</sub> H <sub>17</sub> N	Water	1.03
Amiripryline (HCl) <sup>a</sup>	Anti-depressant	C <sub>20</sub> H <sub>23</sub> N <sub>1</sub>	Water	1.06
Amoxicillin (3H <sub>2</sub> O) <sup>c</sup>	Antibiotic: penicilline	C <sub>16</sub> H <sub>19</sub> N <sub>3</sub> O <sub>5</sub> S	Water	1.14
Atenolol <sup>h</sup>	$\beta$ -blocker	C <sub>14</sub> H <sub>22</sub> N <sub>2</sub> O <sub>3</sub>	Methanol	0.70
Besifloxacin <sup>d</sup>	Antibiotic: quinolone	C <sub>19</sub> H <sub>21</sub> Cl <sub>1</sub> FN <sub>3</sub> O <sub>3</sub>	Water	1.16
Bezafibrate <sup>a</sup>	Lipid regulator	C <sub>19</sub> H <sub>20</sub> ClNO <sub>4</sub>	Methanol	1.00
Bisoprolol (fumarate) <sup>h</sup>	$\beta$ blocker	C <sub>18</sub> H <sub>31</sub> NO <sub>4</sub>	Acetonitril	0.0085
Caffeine <sup>a</sup>	Psychoanaaleptic	C <sub>8</sub> H <sub>10</sub> N <sub>4</sub> O <sub>2</sub>	Methanol	1.00
Carbamazepine <sup>e</sup>	Anti-epilepticum	C <sub>15</sub> H <sub>12</sub> N <sub>2</sub> O	Methanol	1.01
Chloramphenicol <sup>a</sup>	Desinfektant	C <sub>11</sub> H <sub>12</sub> Cl <sub>2</sub> N <sub>2</sub> O <sub>5</sub>	Acetonitril	1.06
Chlorotetracycline (HCl) <sup>c</sup>	Antibiotic: tetracycline	C <sub>22</sub> H <sub>23</sub> ClN <sub>2</sub> O <sub>8</sub>	Water	0.90
Ciprofloxacin (HCl) <sup>e</sup>	Antibiotic: quinolone	C <sub>17</sub> H <sub>18</sub> FN <sub>3</sub> O <sub>3</sub>	Water	1.04
Cloxacillin (NaOH) <sup>a</sup>	Antibiotic: penicillin	C <sub>19</sub> H <sub>18</sub> Cl <sub>2</sub> N <sub>2</sub> O <sub>5</sub> S	Methanol	1.00
Cyclophosphamide <sup>a</sup>	Alkylating agent	C <sub>7</sub> H <sub>15</sub> Cl <sub>2</sub> N <sub>2</sub> O <sub>2</sub> P	Methanol	1.00
Diazepam <sup>e</sup>	Tranquillizer	C <sub>16</sub> H <sub>13</sub> ClN <sub>2</sub> O	Methanol	1.03
Diclofenac <sup>a</sup>	Anti-inflammatorij drug	C <sub>14</sub> H <sub>11</sub> Cl <sub>2</sub> NO <sub>2</sub>	Methanol	1.22
Enfluranc <sup>d</sup>	Antiviral	C <sub>14</sub> H <sub>9</sub> ClF <sub>3</sub> NO <sub>2</sub>	Methanol	1.14
Enrofloxacin <sup>c</sup>	Antibiotic: quinolone	C <sub>19</sub> H <sub>22</sub> FN <sub>3</sub> O <sub>3</sub>	Acetonitril	1.04
Flumequine <sup>e</sup>	Antibiotic: quinolone	C <sub>14</sub> H <sub>12</sub> FN <sub>3</sub> O <sub>3</sub>	Acetonitril	0.96
Fluoxetine (HCl) <sup>c</sup>	Anti-depressant	C <sub>17</sub> H <sub>18</sub> F <sub>3</sub> NO	Methanol	0.85
Gatifloxacin <sup>d</sup>	Antibiotic: quinolone	C <sub>19</sub> H <sub>22</sub> FN <sub>3</sub> O <sub>4</sub>	10mM NaOH in water	1.02
Ibuprofen <sup>a</sup>	Anti-inflammatorij drug	C <sub>13</sub> H <sub>18</sub> O <sub>2</sub>	Methanol	1.04
Ifosfamid <sup>a</sup>	Alkylating agent	C <sub>7</sub> H <sub>15</sub> Cl <sub>2</sub> N <sub>2</sub> O <sub>2</sub> P	Methanol	1.00
Indomethacin <sup>a</sup>	Anti-inflammatorij drug	C <sub>19</sub> H <sub>16</sub> ClNO <sub>4</sub>	Acetonitril	0.98
Ketoprofen <sup>h</sup>	Anti-inflammatorij drug	C <sub>16</sub> H <sub>14</sub> O <sub>3</sub>	Methanol	1.30
Lamivudine <sup>a</sup>	Antiviral	C <sub>8</sub> H <sub>11</sub> N <sub>3</sub> O <sub>3</sub> S	Dimethyl sulfoxide	0.74
Levofloxacin <sup>c</sup>	Antibiotic: quinolone	C <sub>18</sub> H <sub>20</sub> FN <sub>3</sub> O <sub>4</sub>	Acetonitril	1.05
Lincomycin (HCl · H <sub>2</sub> O) <sup>h</sup>	Antibiotic	C <sub>18</sub> H <sub>34</sub> N <sub>2</sub> O <sub>6</sub> S	Methanol	0.80
Metoprolol <sup>h</sup>	$\beta$ -blocker	C <sub>15</sub> H <sub>25</sub> NO <sub>3</sub>	Methanol	1.30

Table A.1 (continued)

Substance (salt)	Therapeutic group	Formula	Solvent	Concentration (g l <sup>-1</sup> )
Metronidazole <sup>c</sup>	Antibiotic	C <sub>6</sub> H <sub>9</sub> N <sub>3</sub> O <sub>3</sub>	Acetonitril	1.31
Moxifloxacin (HCl) <sup>f</sup>	Antibiotic: quinolone	C <sub>21</sub> H <sub>24</sub> FN <sub>3</sub> O <sub>4</sub>	Water	0.99
Nalidixic Acid <sup>c</sup>	Antibiotic: quinolone	C <sub>12</sub> H <sub>12</sub> N <sub>2</sub> O <sub>3</sub>	Acetonitril	1.02
Naproxen <sup>c</sup>	Anti-inflammatory drug	C <sub>14</sub> H <sub>14</sub> O <sub>3</sub>	Methanol	1.20
Nevirapine <sup>d</sup>	Antiviral	C <sub>15</sub> H <sub>14</sub> N <sub>4</sub> O	Methanol	0.90
Oseltamivir acid <sup>d</sup>	Antiviral	C <sub>14</sub> H <sub>24</sub> N <sub>2</sub> O <sub>4</sub>	Water	0.47
Oseltamivir ethylester <sup>d</sup>	Antiviral	C <sub>16</sub> H <sub>28</sub> N <sub>2</sub> O <sub>4</sub>	Water	0.61
Oxytetracycline (HCl) <sup>c</sup>	Antibiotic: tetracycline	C <sub>22</sub> H <sub>24</sub> N <sub>2</sub> O <sub>9</sub>	10mM NaOH in water	0.77
Paracetamol <sup>c</sup>	Anti-inflammatory drug	C <sub>8</sub> H <sub>9</sub> NO <sub>2</sub>	Methanol	0.95
Paroxetine (HCl · 5 H <sub>2</sub> O) <sup>a</sup>	Antidepressant	C <sub>19</sub> H <sub>20</sub> F <sub>1</sub> NO <sub>3</sub>	Methanol	0.72
Pleconaril <sup>d</sup>	Antiviral	C <sub>18</sub> H <sub>18</sub> F <sub>3</sub> N <sub>3</sub> O <sub>3</sub>	Methanol	0.97
Propranolol (HCl) <sup>a</sup>	β-blocker	C <sub>16</sub> H <sub>21</sub> NO <sub>2</sub>	Methanol	1.00
Rimantadine (HCl) <sup>a</sup>	Antiviral, antiparkinson	C <sub>12</sub> H <sub>21</sub> N	Water	0.90
Risperidone <sup>a</sup>	Antidepressant	C <sub>23</sub> H <sub>27</sub> FN <sub>4</sub> O <sub>2</sub>	Methanol	0.94
Sarafloxacin (HCl · 3 H <sub>2</sub> O) <sup>c</sup>	Antibiotic: quinolone	C <sub>20</sub> H <sub>17</sub> F <sub>2</sub> N <sub>3</sub> O <sub>3</sub>	10mM NaOH in water	1.01
Simvastatine <sup>a</sup>	Statin	C <sub>25</sub> H <sub>38</sub> O <sub>5</sub>	Acetonitril	1.10
Sotalol (HCl) <sup>h</sup>	β-blocker	C <sub>12</sub> H <sub>20</sub> N <sub>2</sub> O <sub>3</sub> S	Methanol	0.80
Sulfadoxin <sup>a</sup>	Antibiotic: sulfonamide	C <sub>12</sub> H <sub>14</sub> N <sub>4</sub> O <sub>4</sub> S	Acetonitril	1.02
Sulfamethazine <sup>a</sup>	Antibiotic: sulfonamide	C <sub>12</sub> H <sub>14</sub> N <sub>4</sub> O <sub>2</sub> S	Acetonitril	1.13
Sulfamethoxazole <sup>c</sup>	Antibiotic: sulfonamide	C <sub>10</sub> H <sub>11</sub> N <sub>3</sub> O <sub>3</sub> S	Acetonitril	1.10
Temazepam <sup>b</sup>	Tranquilizer	C <sub>16</sub> H <sub>13</sub> ClN <sub>2</sub> O <sub>2</sub>	Methanol	1.01
Tetracycline (HCl) <sup>c</sup>	Antibiotic: tetracycline	C <sub>22</sub> H <sub>24</sub> N <sub>5</sub> O <sub>8</sub>	10mM NaOH in water	1.05
Tolfenamic acid <sup>a</sup>	Anti-inflammatory drug	C <sub>14</sub> H <sub>12</sub> ClNO <sub>2</sub>	Methanol	1.10
Triclosan <sup>a</sup>	Desinfektant	C <sub>12</sub> H <sub>7</sub> Cl <sub>3</sub> O <sub>2</sub>	Acetonitril	1.12
Trimethoprim <sup>c</sup>	Antibiotic	C <sub>14</sub> H <sub>18</sub> N <sub>4</sub> O <sub>3</sub>	Acetonitril	1.14
Venlafaxine (HCl) <sup>a</sup>	Antidepressant	C <sub>17</sub> H <sub>27</sub> N <sub>1</sub> O <sub>2</sub>	Methanol	0.73
Zidovudine <sup>a</sup>	Antiviral	C <sub>10</sub> H <sub>13</sub> N <sub>5</sub> O <sub>4</sub>	Methanol	0.84

<sup>a</sup> Supplier: Sigma-Aldrich, Belgium <sup>b</sup> Supplier: Lipomed GmbH, Germany <sup>c</sup> Supplier: Fluka, Belgium <sup>d</sup> Supplier: TRC, Canada <sup>e</sup> Supplier: MpBio, Belgium <sup>f</sup> Supplier: Bayer, Germany <sup>g</sup> Supplier: Dr. Ehrenstorfer GmbH, Germany <sup>h</sup> Supplier: Bayer, Germany

**Table A.2** Overview of the 69 pharmaceutical compounds and their therapeutic groups, suppliers of the analytical standards, solvent used for the individual stock solutions, chemical formula, ESI mode, exact ion mass, accurate mass of fragment ion, retention time and the lowest concentration > 100 a.u. in surface water.

Compounds <sup>a</sup>	Therapeutic group	Formula	Solvent of standard	Exact mass (Da), ESI mode	Average mass error $\pm$ SD (ppm) over 5 days <sup>b</sup>	Fragment ion: accurate mass (Da) $\pm$ SD [M $\pm$ H] <sup>±</sup> ( $n=5$ )	Retention time $\pm$ SD (min) ( $n=5$ )	Lowest concentration > 100 a.u. (pg l <sup>-1</sup> ) <sup>c</sup>
4-(dimethylamino)-antipyrine (S44) <sup>d</sup>	Analgesics	C <sub>13</sub> H <sub>17</sub> N <sub>3</sub> O	MeOH	231.1372 <sup>+</sup>	-0.6 $\pm$ 2.2	113.1072 $\pm$ 0.6	3.59 $\pm$ 0.03	0.01
Atenolol (S44) <sup>e</sup>	$\beta$ -blockers	C <sub>14</sub> H <sub>22</sub> N <sub>2</sub> O <sub>3</sub>	MeOH	266.1630 <sup>+</sup>	0.4 $\pm$ 2.8	145.0651 $\pm$ 1.0	3.21 $\pm$ 0.05	0.01
Betaxolol (S44) <sup>f</sup>	$\beta$ -blockers	C <sub>18</sub> H <sub>29</sub> NO <sub>3</sub>	MeOH	307.2147 <sup>+</sup>	0.4 $\pm$ 1.5	116.1070 $\pm$ 0.9	6.08 $\pm$ 0.01	0.01
Bezafibrate (S44) <sup>e</sup>	Lipid regulators	C <sub>19</sub> H <sub>20</sub> ClNO <sub>4</sub>	MeOH	361.1081 <sup>-</sup>	0.1 $\pm$ 0.9	274.0642 $\pm$ 0.2	8.06 $\pm$ 0.01	0.01
Bisoprolol (S44, S17) <sup>e</sup>	$\beta$ -blockers	C <sub>18</sub> H <sub>31</sub> NO <sub>4</sub>	MeOH	325.2253 <sup>+</sup>	1.5 $\pm$ 0.7	116.1075 $\pm$ 0.3	5.67 $\pm$ 0.01	0.01
Caffeine (S17) <sup>g</sup>	Psychoanaleptics	C <sub>8</sub> H <sub>10</sub> N <sub>4</sub> O <sub>2</sub>	MeOH	194.0804 <sup>+</sup>	1.2 $\pm$ 3.1	138.0666 $\pm$ 0.5	4.07 $\pm$ 0.02	0.01
Carbamazepine (S44, S17) <sup>g</sup>	Antiepileptics	C <sub>15</sub> H <sub>12</sub> N <sub>2</sub> O	MeOH	236.0950 <sup>+</sup>	2.4 $\pm$ 2.3	194.0969 $\pm$ 0.6	6.91 $\pm$ 0.01	0.01
Chlorotetracycline (S44) <sup>e</sup>	Tetracycline antibiotics	C <sub>22</sub> H <sub>23</sub> ClN <sub>2</sub> O <sub>8</sub>	MeOH	478.1143 <sup>+</sup>	0.3 $\pm$ 2.1	462.0952 $\pm$ 0.8	4.79 $\pm$ 0.01	0.5
Ciprofloxacin (S44) <sup>h</sup>	Quinolone antibiotics	C <sub>17</sub> H <sub>18</sub> FN <sub>3</sub> O <sub>3</sub>	MeOH	331.1332 <sup>+</sup>	1.8 $\pm$ 2.3	288.1512 $\pm$ 0.7	4.34 $\pm$ 0.01	0.05
Clenbuterol (S44) <sup>h</sup>	Adrenergics	C <sub>12</sub> H <sub>18</sub> Cl <sub>2</sub> N <sub>2</sub> O	MeOH	276.0796 <sup>+</sup>	0.6 $\pm$ 2.0	203.0140 $\pm$ 0.7	4.90 $\pm$ 0.01	0.05
Cloxacillin (S44) <sup>e</sup>	Penicillin antibiotics	C <sub>16</sub> H <sub>18</sub> ClN <sub>3</sub> O <sub>5</sub> S	MeOH	435.0656 <sup>-</sup>	0.5 $\pm$ 1.8	293.0154 $\pm$ 1.4	7.70 $\pm$ 0.01	0.05
Cyclophosphamide (S44) <sup>e</sup>	Alkylating agents	C <sub>7</sub> H <sub>15</sub> Cl <sub>2</sub> N <sub>2</sub> O <sub>2</sub> P	MeOH	260.0248 <sup>+</sup>	1.3 $\pm$ 0.4	140.0031 $\pm$ 0.2	5.86 $\pm$ 0.01	0.05
Dapsone (S44) <sup>h</sup>	Other antibiotics	C <sub>12</sub> H <sub>12</sub> N <sub>2</sub> O <sub>2</sub> S	MeOH	248.0619 <sup>+</sup>	0.4 $\pm$ 1.8	156.0117 $\pm$ 0.5	5.04 $\pm$ 0.02	0.05
Diatrizoic acid <sup>e</sup>	Iodated X-ray contrast media	C <sub>11</sub> H <sub>9</sub> I <sub>3</sub> N <sub>2</sub> O <sub>4</sub>	H <sub>2</sub> O / MeOH	613.7696 <sup>+</sup>	-3.4 $\pm$ 1.8	360.9687 $\pm$ 3.7	2.62 $\pm$ 0.19	5
Diclofenac (S44) <sup>g</sup>	Anti-inflammatory drugs	C <sub>14</sub> H <sub>11</sub> Cl <sub>2</sub> NO <sub>2</sub>	MeOH	295.0167 <sup>-</sup>	-0.1 $\pm$ 0.5	250.0196 $\pm$ 0.2	9.07 $\pm$ 0.01	0.01
Doxycycline (S44, S17) <sup>e</sup>	Tetracycline antibiotics	C <sub>22</sub> H <sub>24</sub> N <sub>2</sub> O <sub>8</sub>	MeOH	444.1533 <sup>+</sup>	-0.1 $\pm$ 1.5	428.1336 $\pm$ 0.8	5.47 $\pm$ 0.01	0.5

Table A.2 (continued)

Compounds <sup>a</sup>	Therapeutic group	Formula	Solvent of standard	Exact mass (Da), ESI mode	Average mass error $\pm$ SD (ppm) over 5 days <sup>b</sup>	Fragment ion: accurate mass (Da) $\pm$ SD (mDa) [M $\pm$ H] <sup>±</sup> (n=5)	Retention time $\pm$ SD (min) (n=5)	Lowest concentration > 100 a.u. ( $\mu\text{g L}^{-1}$ ) <sup>c</sup>
Enoxacin (S44) <sup>e</sup>	Quinolone antibiotics	C <sub>15</sub> H <sub>17</sub> FN <sub>4</sub> O <sub>3</sub>	MeOH	320.1285 <sup>+</sup>	0.6 $\pm$ 1.7	234.1040 $\pm$ 0.8	4.16 $\pm$ 0.01	0.05
Erofloxacin (S44, S17) <sup>h</sup>	Quinolone antibiotics	C <sub>19</sub> H <sub>22</sub> FN <sub>3</sub> O <sub>3</sub>	MeOH	359.1645 <sup>+</sup>	0.8 $\pm$ 1.3	316.1824 $\pm$ 0.3	4.59 $\pm$ 0.01	0.05
Erythromycin-H <sub>2</sub> O (S17) <sup>h</sup>	Macrolide antibiotics	C <sub>37</sub> H <sub>67</sub> NO <sub>13</sub>	MeOH	715.451 <sup>+</sup>	-0.9 $\pm$ 2.0	158.1182 $\pm$ 0.6	6.95 $\pm$ 0.01	0.05
Fenofibrate <sup>e</sup>	Lipid regulators	C <sub>20</sub> H <sub>21</sub> ClO <sub>4</sub>	MeOH	360.1128 <sup>+</sup>	0.2 $\pm$ 2.5	233.0364 $\pm$ 0.3	11.49 $\pm$ 0.01	0.5
Fenopropfen (S44) <sup>e</sup>	Anti-inflammatory drugs	C <sub>15</sub> H <sub>14</sub> O <sub>3</sub>	MeOH	242.0943 <sup>-</sup>	-1.6 $\pm$ 1.2	93.0345 $\pm$ 0.2	8.66 $\pm$ 0.01	1
Fluoxetine <sup>e</sup>	Antidepressants	C <sub>17</sub> H <sub>18</sub> F <sub>3</sub> NO	MeOH	309.1340 <sup>+</sup>	0.8 $\pm$ 1.1	148.1121 $\pm$ 1.2	7.00 $\pm$ 0.01	0.05
Furazolidone (S17) <sup>h</sup>	Other antibiotics	C <sub>8</sub> H <sub>7</sub> N <sub>3</sub> O <sub>5</sub>	MeOH	225.0386 <sup>+</sup>	0.3 $\pm$ 2.7	122.0116 $\pm$ 0.8	4.97 $\pm$ 0.02	0.05
Gemfibrozil (S44) <sup>e</sup>	Lipid regulators	C <sub>13</sub> H <sub>22</sub> O <sub>3</sub>	MeOH	250.1569 <sup>-</sup>	0.1 $\pm$ 1.4	121.0659 $\pm$ 0.3	9.94 $\pm$ 0.01	0.05
Ibuprofen (S44) <sup>g</sup>	Anti-inflammatory drugs	C <sub>13</sub> H <sub>18</sub> O <sub>2</sub>	MeOH	206.1307 <sup>-</sup>	0.2 $\pm$ 1.6	161.1334 $\pm$ 0.4	9.27 $\pm$ 0.01	0.5
Ifosfamide (S44) <sup>e</sup>	Alkylating agents	C <sub>7</sub> H <sub>15</sub> Cl <sub>2</sub> N <sub>2</sub> O <sub>2</sub> P	MeOH	260.0248 <sup>+</sup>	1.2 $\pm$ 1.3	153.9825 $\pm$ 0.4	5.72 $\pm$ 0.01	0.01
Indometacin <sup>e</sup>	Anti-inflammatory drugs	C <sub>19</sub> H <sub>16</sub> ClNO <sub>4</sub>	MeOH	357.0768 <sup>+</sup>	0.2 $\pm$ 1.8	138.9946 $\pm$ 0.4	9.14 $\pm$ 0.01	0.5
Iodipamide (S44) <sup>e</sup>	Iodated X-ray contrast media	C <sub>20</sub> H <sub>14</sub> I <sub>6</sub> N <sub>2</sub> O <sub>6</sub>	MeOH	1139.5120 <sup>-</sup>	1.3 $\pm$ 1.1	j	6.40 $\pm$ 0.02	1
Iohexol <sup>e</sup>	Iodated X-ray contrast media	C <sub>19</sub> H <sub>26</sub> I <sub>3</sub> N <sub>3</sub> O <sub>9</sub>	H <sub>2</sub> O/ MeOH 20:80	820.8803 <sup>+</sup>	-2.9 $\pm$ 0.5	803.8750 $\pm$ 7.9	2.49 $\pm$ 0.32	>5
Iomeprol <sup>e</sup>	Iodated X-ray contrast media	C <sub>17</sub> H <sub>22</sub> I <sub>3</sub> N <sub>3</sub> O <sub>8</sub>	H <sub>2</sub> O/ MeOH 20:80	776.8541 <sup>+</sup>	2.1 $\pm$ 1.9	531.8962 $\pm$ 4.4	2.80 $\pm$ 0.22	5

Table A.2 (continued)

Compound <sup>a</sup>	Therapeutic group	Formula	Solvent of standard	Exact mass (Da), ESI mode	Average mass error $\pm$ SD (ppm) over 5 days <sup>b</sup>	Fragment ion: accurate mass (Da) $\pm$ SD [M $\pm$ H] <sup>±</sup> (n=5)	Retention time $\pm$ SD (min) (n=5)	Lowest concentration > 100 a.u. ( $\mu\text{g l}^{-1}$ ) <sup>c</sup>
Iopamidol <sup>e</sup>	Iodated X-ray contrast media	C <sub>17</sub> H <sub>22</sub> I <sub>3</sub> N <sub>3</sub> O <sub>8</sub>	H <sub>2</sub> O/ MeOH 20:80	776.8541 <sup>+</sup>	-1.7 $\pm$ n=1	558.8899 $\pm$ 3.3	1.94 $\pm$ 0.18	5
Iopanoic acid (S44, S17) <sup>e</sup>	Iodated X-ray contrast media	C <sub>11</sub> H <sub>12</sub> I <sub>3</sub> NO <sub>2</sub>	H <sub>2</sub> O/ MeOH 20:80	570.8002 <sup>-</sup>	0.1 $\pm$ 1.7	126.9053 $\pm$ 0.1	10.03 $\pm$ 0.02	0.5
Iopronide (S44) <sup>e</sup>	Iodated X-ray contrast media	C <sub>18</sub> H <sub>24</sub> I <sub>3</sub> N <sub>3</sub> O <sub>8</sub>	H <sub>2</sub> O/ MeOH 20:80	790.8697 <sup>-</sup>	1.8 $\pm$ 1.8	126.9054 $\pm$ 0.7	3.47 $\pm$ 0.03	0.5
Iotalamic acid <sup>e</sup>	Iodated X-ray contrast media	C <sub>11</sub> H <sub>9</sub> I <sub>3</sub> N <sub>2</sub> O <sub>4</sub>	H <sub>2</sub> O/ MeOH 20:80	613.7696 <sup>-</sup>	-3.4 $\pm$ 1.8	360.9687 $\pm$ 3.7	2.62 $\pm$ 0.19	5
Ketoprofen <sup>e</sup>	Anti-inflammatory drugs	C <sub>16</sub> H <sub>14</sub> O <sub>3</sub>	MeOH	254.0943 <sup>+</sup>	0.6 $\pm$ 2.3	209.0963 $\pm$ 0.6	7.92 $\pm$ 0.01	0.1
Lincomycin <sup>h</sup>	Other antibiotics	C <sub>18</sub> H <sub>34</sub> N <sub>2</sub> O <sub>6</sub> S	MeOH	406.2138 <sup>+</sup>	-0.3 $\pm$ 1.1	126.1278 $\pm$ 0.8	3.91 $\pm$ 0.02	0.01
Metoprolol (S44) <sup>e</sup>	$\beta$ -blockers	C <sub>15</sub> H <sub>25</sub> NO <sub>3</sub>	MeOH	267.1834 <sup>+</sup>	1.7 $\pm$ 2.3	116.1073 $\pm$ 0.5	4.90 $\pm$ 0.01	0.01
Metronidazole (S17) <sup>h</sup>	Other antibiotics	C <sub>6</sub> H <sub>9</sub> N <sub>3</sub> O <sub>3</sub>	MeOH	171.0644 <sup>+</sup>	0.5 $\pm$ 5.9	128.0455 $\pm$ 1.0	3.29 $\pm$ 0.05	0.1
Nafcillin (S44) <sup>e</sup>	Penicillin antibiotics	C <sub>21</sub> H <sub>22</sub> N <sub>2</sub> O <sub>5</sub> S	MeOH	414.1249 <sup>-</sup>	0.7 $\pm$ 0.9	272.0754 $\pm$ 0.3	7.93 $\pm$ 0.01	0.5
Naproxen (S44) <sup>e</sup>	Anti-inflammatory drugs	C <sub>14</sub> H <sub>14</sub> O <sub>3</sub>	MeOH	230.0943 <sup>-</sup>	0.2 $\pm$ 1.7	170.0733 $\pm$ 0.2	7.94 $\pm$ 0.01	0.5
Norfloxacin <sup>h</sup>	Quinolone antibiotics	C <sub>16</sub> H <sub>18</sub> FN <sub>3</sub> O <sub>3</sub>	MeOH	319.1332 <sup>+</sup>	1.4 $\pm$ 1.5	276.1510 $\pm$ 0.5	4.24 $\pm$ 0.01	0.1
Ofloxacin <sup>e</sup>	Quinolone antibiotics	C <sub>18</sub> H <sub>20</sub> FN <sub>3</sub> O <sub>4</sub>	H <sub>2</sub> O/ MeOH 20:80	361.1438 <sup>+</sup>	0.6 $\pm$ 1.6	318.1616 $\pm$ 0.5	4.28 $\pm$ 0.01	0.05
Oleandomycin <sup>e</sup>	Macrolide antibiotics	C <sub>35</sub> H <sub>61</sub> NO <sub>12</sub>	MeOH	687.4194 <sup>+</sup>	-0.6 $\pm$ 2.0	158.1174 $\pm$ 1.0	6.17 $\pm$ 0.01	0.5

Table A.2 (continued)

Compounds <sup>a</sup>	Therapeutic group	Formula	Solvent of standard	Exact mass (Da), ESI mode	Average mass error $\pm$ SD (ppm) over 5 days <sup>b</sup>	Fragment ion: accurate mass (Da) $\pm$ SD [M $\pm$ H] <sup>±</sup> ( $n=5$ )	Retention time $\pm$ SD (min) ( $n=5$ )	Lowest concentration > 100 a.u. ( $\mu\text{g L}^{-1}$ ) <sup>c</sup>
Oxacillin (S44) <sup>e</sup>	Penicillin antibiotics	C <sub>19</sub> H <sub>19</sub> N <sub>3</sub> O <sub>5</sub> S	H <sub>2</sub> O/ MeOH	401.1045 <sup>-</sup>	0.0 $\pm$ 1.7	259.0550 $\pm$ 0.5	7.30 $\pm$ 0.01	0.1
Oxytetracycline <sup>h</sup>	Tetracycline antibiotics	C <sub>22</sub> H <sub>24</sub> N <sub>2</sub> O <sub>9</sub>	MeOH	460.1482 <sup>+</sup>	0.6 $\pm$ 0.6	426.1190 $\pm$ 0.6	4.35 $\pm$ 0.01	0.1
Paracetamol (S17) <sup>e</sup>	Analgesics	C <sub>8</sub> H <sub>9</sub> NO <sub>2</sub>	MeOH	151.0633 <sup>+</sup>	4.6 $\pm$ 1.9	110.0603 $\pm$ 1.0	3.24 $\pm$ 0.06	0.1
Penicillin G (S44) <sup>e</sup>	Penicillin antibiotics	C <sub>16</sub> H <sub>18</sub> N <sub>2</sub> O <sub>4</sub> S	MeOH	334.0987 <sup>+</sup>	1.0 $\pm$ 2.2	j	4.40 $\pm$ 0.01	0.5
Penicillin V (S44) <sup>e</sup>	Penicillin antibiotics	C <sub>16</sub> H <sub>18</sub> N <sub>2</sub> O <sub>5</sub> S	MeOH	350.0936 <sup>-</sup>	-0.1 $\pm$ 1.2	208.0441 $\pm$ 0.6	6.93 $\pm$ 0.01	0.1
Pentoxifylline <sup>e</sup>	Peppiperhal vasodilators	C <sub>13</sub> H <sub>18</sub> N <sub>4</sub> O <sub>3</sub>	MeOH	278.1379 <sup>+</sup>	1.6 $\pm$ 1.2	181.0725 $\pm$ 0.5	5.26 $\pm$ 0.01	0.01
Phenazone (S44) <sup>e</sup>	Analgesics	C <sub>11</sub> H <sub>12</sub> N <sub>2</sub> O	MeOH	188.0950 <sup>+</sup>	2.6 $\pm$ 3.8	147.0916 $\pm$ 0.6	4.89 $\pm$ 0.01	0.01
Pindolol (S44) <sup>e</sup>	$\beta$ -blockers	C <sub>14</sub> H <sub>20</sub> N <sub>2</sub> O <sub>2</sub>	MeOH	248.1525 <sup>+</sup>	2.0 $\pm$ 2.7	116.1073 $\pm$ 0.6	4.16 $\pm$ 0.02	0.01
Primidon <sup>e</sup>	Antiepileptics	C <sub>12</sub> H <sub>14</sub> N <sub>2</sub> O <sub>2</sub>	MeOH	218.1055 <sup>+</sup>	0.8 $\pm$ 3.3	162.0921 $\pm$ 0.9	4.88 $\pm$ 0.02	0.5
Propranolol (S44) <sup>e</sup>	$\beta$ -blockers	C <sub>16</sub> H <sub>21</sub> NO <sub>2</sub>	MeOH	259.1572 <sup>+</sup>	1.9 $\pm$ 0.6	116.1075 $\pm$ 0.2	5.84 $\pm$ 0.01	0.01
Propyphenazone (S44) <sup>e</sup>	Analgesics	C <sub>14</sub> H <sub>18</sub> N <sub>2</sub> O	MeOH	230.1419 <sup>+</sup>	2.5 $\pm$ 2.7	189.1028 $\pm$ 0.5	7.34 $\pm$ 0.01	0.01
Ronidazole <sup>h</sup>	Other antibiotics	C <sub>6</sub> H <sub>8</sub> N <sub>4</sub> O <sub>4</sub>	MeOH	200.0546 <sup>+</sup>	-3.0 $\pm$ 3.9	140.0453 $\pm$ 0.6	3.62 $\pm$ 0.04	0.5
Roxithromycin (S17) <sup>e</sup>	Macrolide antibiotics	C <sub>41</sub> H <sub>76</sub> N <sub>2</sub> O <sub>15</sub>	MeOH	836.5246 <sup>+</sup>	-1.6 $\pm$ 1.0	158.1184 $\pm$ 0.7	7.27 $\pm$ 0.01	0.1
Salbutamol <sup>h</sup>	Adrenergics	C <sub>13</sub> H <sub>21</sub> NO <sub>3</sub>	MeOH	239.1521 <sup>+</sup>	3.1 $\pm$ 1.7	148.0760 $\pm$ 1.2	3.05 $\pm$ 0.10	0.05
Salicylic acid (S44) <sup>h</sup>	Analgesics (metabolite)	C <sub>7</sub> H <sub>6</sub> O <sub>3</sub>	MeOH	138.0317 <sup>-</sup>	-1.1 $\pm$ 8.8	93.0348 $\pm$ 0.2	5.25 $\pm$ 0.03	0.05
Sotalol (S44, S17) <sup>e</sup>	$\beta$ -blockers	C <sub>12</sub> H <sub>20</sub> N <sub>2</sub> O <sub>3</sub> S	MeOH	272.1195 <sup>+</sup>	1.5 $\pm$ 1.0	133.0759 $\pm$ 1.1	3.12 $\pm$ 0.07	0.01
Spiramycin (S44, S17) <sup>e</sup>	Macrolide antibiotics	C <sub>43</sub> H <sub>74</sub> N <sub>2</sub> O <sub>14</sub>	MeOH	842.5140 <sup>+</sup>	-0.8 $\pm$ 1.0	174.1128 $\pm$ 0.8	5.15 $\pm$ 0.01	0.5
Sulfadiazine <sup>e</sup>	Sulfonamide antibiotics	C <sub>10</sub> H <sub>10</sub> N <sub>4</sub> O <sub>2</sub> S	MeOH	250.0524 <sup>+</sup>	-1.0 $\pm$ 3.1	156.0114 $\pm$ 0.8	3.75 $\pm$ 0.03	0.05



Table A.2 (continued)

Compounds <sup>a</sup>	Therapeutic group	Formula	Solvent of standard	Exact mass (Da), ESI mode	Average mass error $\pm$ SD (ppm) over 5 days <sup>b</sup>	Fragment ion: accurate mass (Da) $\pm$ SD [M $\pm$ H] <sup>±</sup> ( $n=5$ )	Retention time $\pm$ SD (min)	Lowest concentration > 100 a.u. ( $\mu\text{g l}^{-1}$ ) <sup>c</sup>
Sulfamerazine (S44) <sup>e</sup>	Sulfonamide antibiotics	C <sub>11</sub> H <sub>12</sub> N <sub>4</sub> O <sub>2</sub> S	MeOH	264.0681 <sup>+</sup>	2.0 $\pm$ 2.9	156.0119 $\pm$ 0.6	4.32 $\pm$ 0.02	0.05
Sulfamethoxazole (S44, S17) <sup>e</sup>	Sulfonamide antibiotics	C <sub>10</sub> H <sub>11</sub> N <sub>3</sub> O <sub>3</sub> S	MeOH	253.0521 <sup>+</sup>	1.6 $\pm$ 1.5	156.0118 $\pm$ 0.4	5.42 $\pm$ 0.01	0.01
Terbutaline <sup>h</sup>	Adrenergics	C <sub>12</sub> H <sub>19</sub> NO <sub>3</sub>	MeOH	225.1365 <sup>+</sup>	2.9 $\pm$ 2.2	152.0713 $\pm$ 0.4	2.90 $\pm$ 0.16	0.05
Tetracycline (S44, S17) <sup>h</sup>	Tetracycline antibiotics	C <sub>22</sub> H <sub>24</sub> N <sub>2</sub> O <sub>8</sub>	MeOH	444.1533 <sup>+</sup>	0.2 $\pm$ 1.1	410.1235 $\pm$ 1.0	4.56 $\pm$ 0.01	0.05
Tolfenamic acid (S44) <sup>h</sup>	Anti-inflammatory drugs	C <sub>14</sub> H <sub>12</sub> ClNO <sub>2</sub>	MeOH	261.0557 <sup>-</sup>	0.2 $\pm$ 1.8	216.0585 $\pm$ 0.4	10.00 $\pm$ 0.01	0.01
Timethoprim <sup>h</sup>	Other antibiotics	C <sub>14</sub> H <sub>18</sub> N <sub>4</sub> O <sub>3</sub>	MeOH	290.1379 <sup>+</sup>	1.4 $\pm$ 1.7	230.1164 $\pm$ 0.5	4.18 $\pm$ 0.02	0.01
Tylosin (S44, S17) <sup>h</sup>	Macrolide antibiotics	C <sub>46</sub> H <sub>77</sub> NO <sub>17</sub>	MeOH	915.5192 <sup>+</sup>	0.8 $\pm$ 3.9	174.1133 $\pm$ 0.7	6.69 $\pm$ 0.01	0.1
Venlafaxine (S44) <sup>i</sup>	Antidepressants	C <sub>17</sub> H <sub>27</sub> NO <sub>2</sub>	MeOH	277.2042 <sup>+</sup>	2.2 $\pm$ 0.8	260.2012 $\pm$ 0.3	5.59 $\pm$ 0.01	0.01

<sup>a</sup> S44: subselection of 44 compounds for calibration of suspect screening model in Chapter 5; S17: subselection of 17 compounds used in Chapter 4.

<sup>b</sup> 5  $\mu\text{g l}^{-1}$  in deionized water.

<sup>c</sup> Lowest concentration having a signal intensity > 100 a.u. in surface water ( $\mu\text{g l}^{-1}$ ).

<sup>d</sup> Supplier: Alfa Aesar, USA.

<sup>e</sup> Supplier: Dr. Ehrenstorfer GmbH, Germany.

<sup>f</sup> Supplier: US pharmacopeial, USA.

<sup>g</sup> Supplier: Dr. Ehrenstorfer GmbH, Germany.

<sup>h</sup> Standards were kindly provided by Fytolab (Zwijnaarde, Belgium).

<sup>i</sup> Supplier: Molekula GmbH, Germany.

<sup>j</sup> No fragments found.

**Table A.3** Screening library and Retention time of the suspect compounds.

Compound	$t_R$ (min)	Nature of selected isotopes	$m/z_{th,0}$	$m/z_{th,1}$	$m/z_{th,2}$	$m/z_{th,3}$	$i_{r_{th,1}}$	$i_{r_{th,2}}$	$i_{r_{th,3}}$
<i>Set A: Target/artificial suspect compounds</i>									
Acyclovir	0.71	$^{13}C/^{15}N/^{13}C_2$	226.09347	227.09687	227.09047	228.09848	0.088	0.018	0.007
Alprazolam	9.81	$^{37}Cl/^{13}C/^{37}Cl^{13}C$	309.09015	311.08724	310.09307	312.09014	0.321	0.185	0.059
Amantadine	4.98	$^{13}C/^{13}C_2/^{15}N$	152.14338	153.14674	154.15010	153.14041	0.108	0.005	0.004
Amitriptyline	9.91	$^{13}C/^{13}C_2/^{13}C_3$	278.19033	279.19361	280.19690	281.20039	0.217	0.022	0.001
Amoxicillin	1.60	$^{13}C/^{34}S/^{14}N$	366.11182	367.11470	368.10779	368.11775	0.179	0.045	0.023
Besifloxacin	8.41	$^{37}Cl/^{13}C/^{37}Cl^{13}C$	394.13282	396.13060	395.13590	397.13326	0.322	0.209	0.067
Carbamazepine	9.01	$^{13}C/^{13}C_2/^{15}N$	237.10224	238.10561	239.10861	238.09910	0.163	0.013	0.007
Chlorotetracycline	6.56	$^{37}Cl/^{13}C/^{37}Cl^{13}C$	479.12157	481.11971	480.12478	482.12240	0.326	0.245	0.080
Ciprofloxacin	5.29	$^{13}C/^{13}C_2/^{13}C_3$	332.14050	333.14354	334.14613	335.14876	0.186	0.020	0.002
Diazepam	10.53	$^{37}Cl/^{13}C/^{37}Cl^{13}C$	285.07892	287.07599	286.08205	288.07912	0.320	0.174	0.056
Diclofenac	12.04	$^{37}Cl/^{13}C/^{37}Cl_2$	296.02396	298.02103	297.02720	300.01810	0.640	0.153	0.102
Efavirenz	12.12	$^{37}Cl/^{13}C/^{37}Cl^{13}C$	316.03467	318.03176	317.03790	319.03513	0.320	0.153	0.049
Enrofloxacin	5.45	$^{13}C/^{13}C_2/^{13}C_3$	360.17180	361.17488	362.17756	363.18020	0.209	0.025	0.002
Flumequine	8.66	$^{13}C/^{13}C_2/^{13}C_3$	262.08740	263.09076	264.09310	265.09581	0.153	0.013	0.001
Fluoxetine	10.28	$^{13}C/^{13}C_2/^{13}C_3$	310.14133	311.14459	312.14761	313.15064	0.185	0.017	0.001
Gatifloxacin	6.25	$^{13}C/^{13}C_2/^{13}C_3$	376.16671	377.16979	378.17238	379.17501	0.209	0.027	0.003
Indomethacin	12.03	$^{37}Cl/^{13}C/^{37}Cl^{13}C$	358.08406	360.08130	359.08734	361.08473	0.320	0.208	0.067
Lamivudine	0.76	$^{13}C/^{34}S/^{15}N$	230.05939	231.06270	232.05522	231.05682	0.088	0.045	0.013
Levofloxacin	4.92	$^{13}C/^{13}C_2/^{13}C_3$	362.15106	363.15413	364.15666	365.15929	0.198	0.024	0.002
Metronidazole	1.35	$^{13}C/^{15}N/^{13}C_2$	172.07167	173.07509	173.06870	174.07645	0.066	0.011	0.006
Moxifloxacin	6.88	$^{13}C/^{13}C_2/^{13}C_3$	402.18236	403.18547	404.18814	405.19078	0.232	0.032	0.003
Nalidixic Acid	8.28	$^{13}C/^{13}C_2/^{15}N$	233.09207	234.09546	235.09743	234.08898	0.131	0.009	0.007
Nevirapine	6.98	$^{13}C/^{13}C_2/^{13}C_3$	267.12404	268.12739	269.13038	270.13231	0.163	0.013	0.001
Osetamivir acid	5.77	$^{13}C/^{13}C_2/^{13}C_3$	285.18088	286.18402	287.18634	288.18915	0.154	0.015	0.001
Osetamivir ethylester	8.42	$^{13}C/^{13}C_2/^{13}C_3$	313.21218	314.21535	315.21781	316.22039	0.176	0.019	0.002
Oxytetracycline	4.84	$^{13}C/^{13}C_2/^{13}C_3$	461.15546	462.15867	463.16106	464.16353	0.245	0.045	0.006

**Table A.3** (continued)

Compound	$t_R$ (min)	Nature of selected isotopes	Screening library <sup>a</sup>							
			$m/z_{th,0}$	$m/z_{th,1}$	$m/z_{th,2}$	$m/z_{th,3}$	$ir_{th,1}$	$ir_{th,2}$	$ir_{th,3}$	
Paracetamol	1.49	<sup>13</sup> C/ <sup>13</sup> C <sub>2</sub> / <sup>15</sup> N	152.07061	153.07398	154.07484	153.06764	0.087	0.004	0.004	
Paroxetine	9.63	<sup>13</sup> C/ <sup>13</sup> C <sub>2</sub> / <sup>13</sup> C <sub>3</sub>	330.15000	331.15328	332.15605	333.15881	0.208	0.024	0.002	
Pleconaril	13.91	<sup>13</sup> C/ <sup>13</sup> C <sub>2</sub> / <sup>13</sup> C <sub>3</sub>	382.13730	383.14036	384.14300	385.14564	0.198	0.023	0.002	
Rimantadine	7.94	<sup>13</sup> C/ <sup>13</sup> C <sub>2</sub> / <sup>15</sup> N	180.17468	181.17809	182.18151	181.17171	0.130	0.008	0.004	
Risperidone	6.95	<sup>13</sup> C/ <sup>13</sup> C <sub>2</sub> / <sup>13</sup> C <sub>3</sub>	411.21908	412.22213	413.22499	414.22772	0.254	0.034	0.003	
Sarafloxacin	5.99	<sup>13</sup> C/ <sup>13</sup> C <sub>2</sub> / <sup>13</sup> C <sub>3</sub>	386.13107	387.13416	388.13687	389.13954	0.220	0.028	0.003	
Sulfadoxin	5.36	<sup>13</sup> C/ <sup>34</sup> S/ <sup>14</sup> N	311.08085	312.08345	313.07678	313.08629	0.133	0.045	0.014	
Sulfamethazine	3.89	<sup>13</sup> C/ <sup>34</sup> S/ <sup>14</sup> N	279.09102	280.09362	281.08694	281.09665	0.132	0.045	0.010	
Sulfamethoxazole	5.06	<sup>13</sup> C/ <sup>34</sup> S/ <sup>14</sup> N	254.05939	255.06261	256.05524	256.06455	0.110	0.045	0.009	
Temazepam	10.11	<sup>37</sup> Cl/ <sup>13</sup> C/ <sup>37</sup> Cl <sup>13</sup> C	301.07383	303.07092	302.07696	304.07406	0.320	0.174	0.056	
Tetracycline	4.68	<sup>13</sup> C/ <sup>13</sup> C <sub>2</sub> / <sup>13</sup> C <sub>3</sub>	445.16054	446.16376	447.16620	448.16867	0.244	0.043	0.006	
Trimethoprim	4.34	<sup>13</sup> C/ <sup>13</sup> C <sub>2</sub> / <sup>13</sup> C <sub>3</sub>	291.14517	292.14802	293.15044	294.15311	0.153	0.014	0.001	
Venlafaxine	7.62	<sup>13</sup> C/ <sup>13</sup> C <sub>2</sub> / <sup>13</sup> C <sub>3</sub>	278.21146	279.21474	280.21758	281.22037	0.185	0.018	0.001	
Zidovudine	4.38	<sup>13</sup> C/ <sup>13</sup> C <sub>2</sub> / <sup>13</sup> C <sub>3</sub>	268.10403	269.10740	270.10870	271.11195	0.110	0.011	0.001	
<i>Set B: Suspect compounds<sup>b</sup></i>										
4-(dimethylamino)antipyrimine	-	<sup>13</sup> C/ <sup>13</sup> C <sub>2</sub> / <sup>15</sup> N	232.14444	233.14783	234.15076	233.14138	0.141	0.010	0.011	
Atenolol	1.41	<sup>13</sup> C/ <sup>13</sup> C <sub>2</sub> / <sup>13</sup> C <sub>3</sub>	267.17032	268.17369	269.17590	270.17873	0.153	0.013	0.001	
Betaxolol	-	<sup>13</sup> C/ <sup>13</sup> C <sub>2</sub> / <sup>13</sup> C <sub>3</sub>	308.22202	309.22532	310.22805	311.23076	0.197	0.022	0.002	
Bezafibrate	10.85	<sup>37</sup> Cl/ <sup>13</sup> C/ <sup>37</sup> Cl <sup>13</sup> C	362.11536	364.11317	363.11865	365.11604	0.321	0.208	0.067	
Bisoprolol	7.52	<sup>13</sup> C/ <sup>13</sup> C <sub>2</sub> / <sup>13</sup> C <sub>3</sub>	326.23258	327.23589	328.23849	329.24115	0.198	0.024	0.002	
Caffeine	4.14	<sup>13</sup> C/ <sup>15</sup> N/ <sup>13</sup> C <sub>2</sub>	195.08763	196.09106	196.08468	197.09475	0.087	0.015	0.004	
Clenbuterol	-	<sup>37</sup> Cl/ <sup>13</sup> C/ <sup>37</sup> Cl <sub>2</sub>	277.08690	279.08396	278.09024	281.08103	0.640	0.131	0.102	
Clofibrate	-	<sup>37</sup> Cl/ <sup>13</sup> C/ <sup>37</sup> Cl <sup>13</sup> C	243.07825	245.07530	244.08165	246.07870	0.320	0.131	0.042	
Cloxacillin	9.93	<sup>37</sup> Cl/ <sup>13</sup> C/ <sup>37</sup> Cl <sup>13</sup> C	436.07285	438.07049	437.07580	439.07306	0.365	0.215	0.078	
Cyclophosphamide	7.05	<sup>37</sup> Cl/ <sup>37</sup> Cl <sub>2</sub> / <sup>13</sup> C	261.03210	263.02916	265.02622	262.03550	0.640	0.102	0.077	
Ilofamide	6.63	<sup>37</sup> Cl/ <sup>37</sup> Cl <sub>2</sub> / <sup>13</sup> C	261.03210	263.02916	265.02622	262.03550	0.640	0.102	0.077	
Dapsone	-	<sup>13</sup> C/ <sup>34</sup> S/ <sup>13</sup> C <sub>2</sub>	249.06922	250.07209	251.06507	251.07479	0.131	0.045	0.009	

Table A.3 (continued)

Compound	$t_R$ (min)	Nature of selected isotopes	Screening library <sup>a</sup>						
			$m/z_{th,0}$	$m/z_{th,1}$	$m/z_{th,2}$	$m/z_{th,3}$	$ir_{th,1}$	$ir_{th,2}$	$ir_{th,3}$
Doxycycline		- $^{13}\text{C}/^{13}\text{C}_2/^{13}\text{C}_3$	445.16054	446.16376	447.16620	448.16867	0.244	0.043	0.006
Enoxacin		- $^{13}\text{C}/^{13}\text{C}_2/^{13}\text{C}_3$	321.13575	322.13863	323.14109	324.14376	0.164	0.016	0.001
Fenofibrate		- $^{37}\text{Cl}/^{13}\text{C}/^{37}\text{Cl}^{13}\text{C}$	361.12011	363.11734	362.12351	364.12092	0.320	0.219	0.070
Furazolidone		- $^{13}\text{C}/^{13}\text{C}_2/^{15}\text{N}$	226.04585	227.04925	228.05043	227.04283	0.088	0.011	0.011
Ketoprofen	10.37	$^{13}\text{C}/^{13}\text{C}_2/^{13}\text{C}_3$	255.10157	256.10496	257.10760	258.11015	0.174	0.016	0.001
Lincomycin	3.82	$^{13}\text{C}/^{34}\text{S}/^{13}\text{C}_2$	407.22103	408.22409	409.21699	409.22726	0.204	0.048	0.030
Metoprolol	6.00	$^{13}\text{C}/^{13}\text{C}_2/^{13}\text{C}_3$	268.19072	269.19400	270.19655	271.19922	0.164	0.015	0.001
Nafticillin		- $^{13}\text{C}/^{34}\text{S}/^{13}\text{C}_2$	415.13222	416.13530	417.12813	417.13858	0.235	0.048	0.035
Norflloxacin		- $^{13}\text{C}/^{13}\text{C}_2/^{13}\text{C}_3$	320.14050	321.14352	322.14606	323.14869	0.175	0.018	0.002
Oxacillin		- $^{13}\text{C}/^{34}\text{S}/^{13}\text{C}_2$	402.11182	403.11477	404.10781	404.11808	0.214	0.046	0.030
Penicillin G		- $^{13}\text{C}/^{34}\text{S}/^{13}\text{C}_2$	335.10600	336.10900	337.10191	337.11189	0.177	0.045	0.021
Penicillin V		- $^{13}\text{C}/^{34}\text{S}/^{13}\text{C}_2$	351.10092	352.10391	353.09684	353.10676	0.178	0.045	0.023
Pentoxifylline		- $^{13}\text{C}/^{13}\text{C}_2/^{13}\text{C}_3$	279.14517	280.14851	281.15035	282.15304	0.142	0.012	0.001
Phenazone		- $^{13}\text{C}/^{13}\text{C}_2/^{15}\text{N}$	189.10224	190.10563	191.10842	190.09927	0.119	0.007	0.007
Pindolol		- $^{13}\text{C}/^{13}\text{C}_2/^{13}\text{C}_3$	249.15975	250.16314	251.16549	252.16840	0.152	0.012	0.001
Primidon		- $^{13}\text{C}/^{13}\text{C}_2/^{15}\text{N}$	219.11280	220.11620	221.11867	220.10978	0.130	0.008	0.007
Propranolol	8.15	$^{13}\text{C}/^{13}\text{C}_2/^{13}\text{C}_3$	260.16451	261.16788	262.17056	263.17334	0.174	0.016	0.001
Propylphenazone		- $^{13}\text{C}/^{13}\text{C}_2/^{15}\text{N}$	231.14919	232.15258	233.15555	232.14610	0.152	0.011	0.007
Rondazole		- $^{13}\text{C}/^{15}\text{N}/^{13}\text{C}_2$	201.06183	202.06525	202.05886	203.06647	0.066	0.015	0.008
Sinvastatine	13.74	$^{13}\text{C}/^{13}\text{C}_2/^{13}\text{C}_3$	419.27920	420.28261	421.28546	422.28817	0.275	0.044	0.005
Sotalol	1.10	$^{13}\text{C}/^{34}\text{S}/^{13}\text{C}_2$	273.12674	274.12963	275.12259	275.13224	0.132	0.045	0.011
Sulfadiazine		- $^{13}\text{C}/^{34}\text{S}/^{13}\text{C}_2$	251.05972	252.06298	253.05560	253.06499	0.109	0.045	0.007
Sulfamerazine		- $^{13}\text{C}/^{34}\text{S}/^{13}\text{C}_2$	265.07537	266.07858	267.07127	267.08082	0.120	0.045	0.008
Terbutaline		- $^{13}\text{C}/^{13}\text{C}_2/^{15}\text{N}$	226.14377	227.14718	228.14932	227.14068	0.131	0.009	0.004
Tolfenamic acid	13.28	$^{37}\text{Cl}/^{13}\text{C}/^{37}\text{Cl}^{13}\text{C}$	262.06293	264.06000	263.06629	265.06335	0.320	0.152	0.049

<sup>a</sup> Exact mass of the protonated mono isotopic ion  $[\text{M}+\text{H}]^+$  ( $m/z_{th,0}$ ), theoretical masses of the three selected isotopes ( $m/z_{th,1}$ ,  $m/z_{th,2}$  and  $m/z_{th,3}$ ), and their theoretical isotopic ratios ( $ir_{th,1}$ ,  $ir_{th,2}$  and  $ir_{th,3}$ ).

<sup>b</sup> Analytical standards for set B compounds were only purchased if the analyte was retained by the suspect screening.



# Bibliography

- V. Acuña, D. von Schiller, M. J. García-Galán, S. Rodríguez-Mozaz, L. Corominas, M. Petrović, M. Poch, D. Barceló & S. Sabater (2014). Occurrence and in-stream attenuation of wastewater-derived pharmaceuticals in Iberian rivers. *Science of the Total Environment*, (in press.).
- J.-P. Antignac, B. L. Bizec, F. Monteau & F. Andre (2003). Validation of analytical methods based on mass spectrometric detection according to the 2002/657/EC European decision: guideline and application. *Analytica Chimica Acta*, 483:325–334.
- D. R. Baker & B. Kasprzyk-Hordern (2011). Multi-residue analysis of drugs of abuse in wastewater and surface water by solid-phase extraction and liquid chromatography-positive electrospray ionisation tandem mass spectrometry. *Journal of Chromatography A*, 1218(12):1620–1631.
- D. Barceló & M. Petrović (2007). Challenges and achievements of LC-MS in environmental analysis: 25 years on. *Trends in Analytical Chemistry*, 26(1):2–11.

- M. J. Benotti, R. A. Trenholm, B. J. Vanderford, J. C. Holady, B. D. Stanford & S. A. Snyder (2009). Pharmaceuticals and Endocrine Disrupting Compounds in U. S. Drinking Water. *Environmental Science and Technology*, 43(3):597–603.
- L. Bijlsma, E. Emke, F. Hernández & P. de Voogt (2013). Performance of the linear ion trap Orbitrap mass analyzer for qualitative and quantitative analysis of drugs of abuse and relevant metabolites in sewage water. *Analytica Chimica Acta*, 768:102–110.
- K. F. Blom (2001). Estimating the precision of exact mass measurements on an orthogonal time-of-flight mass spectrometer. *Analytical Chemistry*, 73(3):715–719.
- R. Bonfiglio, R. King, T. Olah & K. Merkle (1999). The effects of sample preparation methods on the variability of the electrospray ionization response for model drug compounds. *Rapid Communications in Mass Spectrometry*, 13(12):1175–1185.
- H. Botitsi & S. Garbis (2011). Current mass spectrometry strategies for the analysis of pesticides and their metabolites in food and water matrices. *Mass Spectrometry Reviews*, 30:907–939.
- J. P. Bound & N. Voulvoulis (2005). Household disposal of pharmaceuticals as a pathway for aquatic contamination in the United Kingdom. *Environmental Health Perspectives*, 113(12):1705–1711.
- A. P. Bras, H. R. Hoff, F. Y. Aoki & D. S. Sitar (1998). Amantadine acetylation may be effected by acetyltransferases other than NAT1 or NAT2. *Canadian Journal of Physiology and Pharmacology*, 76(7-8):701–706.

- A. G. Brenton & A. R. Godfrey (2010). Accurate mass measurement: terminology and treatment of data. *Journal of the American Society for Mass Spectrometry*, 21(11):1821–1835.
- T. Brodin, J. Fick, M. Jonsson & J. Klaminder (2013). Dilute Concentrations of a Psychiatric Drug Alter Behavior of Fish from Natural Populations. *Science*, 339:814–815.
- F. Busetti, W. J. Backe, N. Bendixen, U. Maier, B. Place, W. Giger & J. A. Field (2012). Trace analysis of environmental matrices by large-volume injection and liquid chromatography-mass spectrometry. *Analytical and Bioanalytical Chemistry*, 402(1):175–186.
- M. G. Cahill, B. A. Dineen, M. A. Stack & K. J. James (2012). A critical evaluation of liquid chromatography with hybrid linear ion trap - Orbitrap mass spectrometry for the determination of acidic contaminants in wastewater effluents. *Journal of Chromatography A*, 1270:88–95.
- F. Calbiani, M. Careri, L. Elviri, A. Mangia & I. Zagoni (2006). Matrix effects on accurate mass measurements of low-molecular weight compounds using liquid chromatography-electrospray-quadrupole time-of-flight mass spectrometry. *Journal of Mass Spectrometry*, 41(3):289–294.
- O. Cardoso, J.-M. Porcher & W. Sanchez (2014). Factory-discharged pharmaceuticals could be a relevant source of aquatic environment contamination: Review of evidence and need for knowledge. *Chemosphere*, 115:20–30.



- C. Carlsson, A.-K. Johansson, G. Alvan, K. Bergman & T. Kühler (2006). Are pharmaceuticals potent environmental pollutants? Part I: environmental risk assessments of selected active pharmaceutical ingredients. *Science of the Total Environment*, 364(1-3):67–87.
- M. D. Celiz, J. Tso & D. S. Aga (2009). Pharmaceutical metabolites in the environment: analytical challenges and ecological risks. *Environmental Toxicology and Chemistry*, 28(12):2473–2484.
- H. Celle-Jeanton, D. Schemberg, N. Mohammed, F. Huneau, G. Bertrand, V. Lavastre & P. Le Coustumer (2014). Evaluation of pharmaceuticals in surface water: Reliability of PECs compared to MECs. *Environment International*, 73:10–21.
- M. C. Chambers, B. Maclean, R. Burke, D. Amodei, D. L. Ruderman, S. Neumann, L. Gatto, B. Fischer, B. Pratt, J. Egertson, K. Hoff, D. Kessner, N. Tasman, N. Shulman, B. Frewen, T. A. Baker, M.-Y. Brusniak, C. Paulse, D. Creasy, L. Flashner, K. Kani, C. Moulding, S. L. Seymour, L. M. Nuwaysir, B. Lefebvre, F. Kuhlmann, J. Roark, P. Rainer, S. Detlev, T. Hemenway, A. Huhmer, J. Langridge, B. Connolly, T. Chadick, K. Holly, J. Eckels, E. W. Deutsch, R. L. Moritz, J. E. Katz, D. B. Agus, M. MacCoss, D. L. Tabb & P. Mallick (2012). A cross-platform toolkit for mass spectrometry and proteomics. *Nature biotechnology*, 30(10):918–920.
- C. L. Chitescu, E. Oosterink, J. de Jong & A. A. M. L. Stolker (2012). Accurate mass screening of pharmaceuticals and fungicides in water by U-HPLC-Exactive Orbitrap MS. *Analytical and Bioanalytical Chemistry*, 403(10):2997–3011.

- CMA/6/A (2012). Validation: Performance Characteristics. URL <http://www.emis.vito.be>.
- E. R. Cooper, T. C. Siewicki & K. Phillips (2008). Preliminary risk assessment database and risk ranking of pharmaceuticals in the environment. *Science of the Total Environment*, 398(1-3):26–33.
- S. Coutu, L. Rossi, D. A. Barry & N. Chèvre (2012). Methodology to account for uncertainties and tradeoffs in pharmaceutical environmental hazard assessment. *Journal of Environmental Management*, 98:183–190.
- B. A. Crouse, A. J. Ghoshdastidar & A. Z. Tong (2012). The presence of acidic and neutral drugs in treated sewage effluents and receiving waters in the Cornwallis and Annapolis River watersheds and the Mill Cove Sewage Treatment Plant in Nova Scotia, Canada. *Environmental Research*, 112:92–99.
- C. G. Daughton & T. A. Ternes (1999). Pharmaceuticals and personal care products in the environment: agents of subtle change? *Environmental Health Perspectives*, 107 Suppl:907–938.
- C. M. de Jongh, P. J. F. Kooij, P. de Voogt & T. L. ter Laak (2012). Screening and human health risk assessment of pharmaceuticals and their transformation products in Dutch surface waters and drinking water. *Science of the Total Environment*, 427-428:70–77.
- K. Demeestere, M. Petrović, M. Gros, J. Dewulf, H. Van Langenhove & D. Barceló (2010). Trace analysis of antidepressants in environmental waters by molecularly imprinted polymer-based solid-phase extraction followed by ultra-performance liquid

- chromatography coupled to triple quadrupole mass spectrometry. *Analytical and Bioanalytical Chemistry*, 396(2):825–837.
- R. Díaz, M. Ibáñez, J. V. Sancho & F. Hernández (2011). Building an empirical mass spectra library for screening of organic pollutants by ultra-high-pressure liquid chromatography/hybrid quadrupole time-of-flight mass spectrometry. *Rapid Communications in Mass Spectrometry*, 25(2):355–369.
- R. Diaz, M. Ibáñez, J. V. Sancho & F. Hernández (2013). Qualitative validation of a liquid chromatography - quadrupole-time-of-flight mass spectrometry screening method for organic pollutants in waters. *Journal of Chromatography A*, 1276:47–57.
- N. Dorival-García, A. Zafra-Gómez, A. Navalón, J. González & J. L. Vílchez (2012). Removal of quinolone antibiotics from wastewaters by sorption and biological degradation in laboratory-scale membrane bioreactors. *Science of the Total Environment*, 442:317–328.
- S. E. Duirk, C. Lindell, C. C. Cornelison, J. Kormos, T. a. Ternes, M. Attene-Ramos, J. Osiol, E. D. Wagner, M. J. Plewa & S. D. Richardson (2011). Formation of toxic iodinated disinfection by-products from compounds used in medical imaging. *Environmental Science and Technology*, 45(16):6845–6854.
- R. I. L. Eggen, J. Hollender, A. Joss, M. Schärer & C. Stamm (2014). Reducing the discharge of micropollutants in the aquatic environment: the benefits of upgrading wastewater treatment plants. *Environmental Science and Technology*, 48(14):7683–7689.

- S. Ellison & T. Fearn (2005). Characterising the performance of qualitative analytical methods: Statistics and terminology. *Trends in Analytical Chemistry*, 24(6):468–476.
- J. C. L. Erve, M. Gu, Y. Wang, W. DeMaio & R. E. Talaat (2009). Spectral accuracy of molecular ions in an LTQ/Orbitrap mass spectrometer and implications for elemental composition determination. *Journal of the American Society for Mass Spectrometry*, 20(11):2058–2069.
- European Medicine Agency (2005). Guideline EMEA/CHMP/SWP/4447/00 on the environmental risk assessment of medicinal products for human use.
- European Union (2002). Commission Decision 2002/657/EC implementing Council Directive 96/23/EC concerning the performance of analytical methods and the interpretation of results. *Official Journal of the European Communities*, L221.
- European Union (2009). SANCO/10684/2009: Method validation and quality control procedures for pesticide residues analysis in food and feed. Technical report, EU Reference Laboratories for Residues of Pesticides.
- European Union (2013). Water Framework Directive 2013/39/EU amending Directives 2000/60/EC and 2008/105/EC as regards priority substances in the field of water policy. *Official Journal of the European Union*, L226.
- M. Farré, M. Gros, B. Hernández, M. Petrović, P. Hancock & D. Barceló (2008). Analysis of biologically active compounds in water by

- ultra-performance liquid chromatography quadrupole time-of-flight mass spectrometry. *Rapid Communications in Mass Spectrometry*, 22(1):41–51.
- D. Fatta-Kassinos, S. Meric & A. Nikolaou (2011). Pharmaceutical residues in environmental waters and wastewater: current state of knowledge and future research. *Analytical and Bioanalytical Chemistry*, 399(1):251–275.
- G. Fedorova, T. Randak, R. H. Lindberg & R. Grabic (2013). Comparison of the quantitative performance of a Q-Exactive high-resolution mass spectrometer with that of a triple quadrupole tandem mass spectrometer for the analysis of illicit drugs in wastewater. *Rapid Communications in Mass Spectrometry*, 27(15):1751–1762.
- K. Fent, A. a. Weston & D. Caminada (2006). Ecotoxicology of human pharmaceuticals. *Aquatic Toxicology*, 76(2):122–159.
- B. Ferrari, R. Mons, B. Vollat, B. Fraysse, N. Paxéus, R. Lo Giudice, A. Pollio & J. Garric (2004). Environmental risk assessment of six human pharmaceuticals: are the current environmental risk assessment procedures sufficient for the protection of the aquatic environment? *Environmental Toxicology and Chemistry*, 23(5):1344–1354.
- I. Ferrer & E. M. Thurman (2007). Multi-residue method for the analysis of 101 pesticides and their degradates in food and water samples by liquid chromatography/time-of-flight mass spectrometry. *Journal of Chromatography A*, 1175(1):24–37.

- I. Ferrer & E. M. Thurman (2010). Analysis of sucralose and other sweeteners in water and beverage samples by liquid chromatography/time-of-flight mass spectrometry. *Journal of Chromatography A*, 1217(25):4127–4134.
- I. Ferrer & E. M. Thurman (2012). Analysis of 100 pharmaceuticals and their degradates in water samples by liquid chromatography/quadrupole time-of-flight mass spectrometry. *Journal of Chromatography A*, 1259:148–157.
- I. Ferrer, E. M. Thurman, J. A. Zweigenbaum & P. A. Zavitsanos (2008). Comparison Of LC/TOF-MS and LC/MS-MS for the Analysis of 100 Pesticides in Food: Finding the Crossover Point Source: Liquid Chromatography Time-of-Flight Mass Spectrometry. In *Liquid Chromatography Time-of-Flight Mass Spectrometry: Principles, Tools, and Applications for Accurate Mass Analysis*, pp. 247–257. John Wiley & Sons, Inc.
- I. Ferrer, J. A. Zweigenbaum & E. M. Thurman (2010). Analysis of 70 Environmental Protection Agency priority pharmaceuticals in water by EPA Method 1694. *Journal of Chromatography A*, 1217(36):5674–5686.
- P. P. Fong & C. M. Hoy (2012). Antidepressants (venlafaxine and citalopram) cause foot detachment from the substrate in freshwater snails at environmentally relevant concentrations. *Marine and Freshwater Behaviour and Physiology*, 45(2):145–153.

- P. P. Fong & N. Molnar (2013). Antidepressants cause foot detachment from substrate in five species of marine snail. *Marine Environmental Research*, 84:24–30.
- M. M. Galera, P. P. Vázquez, M. D. M. P. Vázquez, M. D. G. García & C. F. Amate (2011). Analysis of  $\beta$ -blockers in groundwater using large-volume injection coupled-column reversed-phase liquid chromatography with fluorescence detection and liquid chromatography time-of-flight mass spectrometry. *Journal of Separation Science*, 34:1796–1804.
- M. Galus, J. Jeyaranjaan, E. Smith, H. Li, C. Metcalfe & J. Y. Wilson (2013). Chronic effects of exposure to a pharmaceutical mixture and municipal wastewater in zebrafish. *Aquatic Toxicology*, 132-133:212–22.
- P. Gao, M. Munir & I. Xagorarakis (2012). Correlation of tetracycline and sulfonamide antibiotics with corresponding resistance genes and resistant bacteria in a conventional municipal wastewater treatment plant. *Science of the Total Environment*, 421-422:173–183.
- A. Garcia-Ac, P. A. Segura, L. Viglino, A. Fürtös, C. Gagnon, M. Prévost & S. Sauvé (2009). On-line solid-phase extraction of large-volume injections coupled to liquid chromatography-tandem mass spectrometry for the quantitation and confirmation of 14 selected trace organic contaminants in drinking and surface water. *Journal of Chromatography A*, 1216(48):8518–8527.
- M. J. García-Galán, M. S. Díaz-Cruz & D. Barceló (2010a). Determination of 19 sulfonamides in environmental water samples

- by automated on-line solid-phase extraction-liquid chromatography-tandem mass spectrometry (SPE-LC-MS/MS). *Talanta*, 81(1-2):355–366.
- M. J. García-Galán, M. Villagrasa, M. S. Díaz-Cruz & D. Barceló (2010b). LC-QqLIT MS analysis of nine sulfonamides and one of their acetylated metabolites in the Llobregat River basin. Quantitative determination and qualitative evaluation by IDA experiments. *Analytical and Bioanalytical Chemistry*, 397(3):1325–1334.
- A. Gerssen, P. P. J. Mulder & J. de Boer (2011). Screening of lipophilic marine toxins in shellfish and algae: development of a library using liquid chromatography coupled to orbitrap mass spectrometry. *Analytica Chimica Acta*, 685(2):176–185.
- G. C. Ghosh, N. Nakada, N. Yamashita & H. Tanaka (2010). Occurrence and fate of oseltamivir carboxylate (Tamiflu) and amantadine in sewage treatment plants. *Chemosphere*, 81(1):13–17.
- M. Godejohann, J.-D. Berset & D. Muff (2011). Non-targeted analysis of wastewater treatment plant effluents by high performance liquid chromatography-time slice-solid phase extraction-nuclear magnetic resonance/time-of-flight-mass spectrometry. *Journal of Chromatography A*, 1218(51):9202–9209.
- A. R. Godfrey & A. G. Brenton (2012). Accurate mass measurements and their appropriate use for reliable analyte identification. *Analytical and Bioanalytical Chemistry*, 404(4):1159–1164.
- M. J. Gómez, M. D. M. Gómez-Ramos, O. Malato, M. Mezcua & A. R. Fernández-Alba (2010). Rapid automated screening, identification



- and quantification of organic micro-contaminants and their main transformation products in wastewater and river waters using liquid chromatography-quadrupole-time-of-flight mass spectrometry with an accurate-mass. *Journal of Chromatography A*, 1217(45):7038–7054.
- M. J. Gómez, O. Malato, I. Ferrer, A. Agüera & A. R. Fernández-Alba (2007). Solid-phase extraction followed by liquid chromatography-time-of-flight-mass spectrometry to evaluate pharmaceuticals in effluents. A pilot monitoring study. *Journal of Environmental Monitoring*, 9(7):718–729.
- I. González-Mariño, J. B. Quintana, I. Rodríguez, M. González-Díez & R. Cela (2012). Screening and selective quantification of illicit drugs in wastewater by mixed-mode solid-phase extraction and quadrupole-time-of-flight liquid chromatography-mass spectrometry. *Analytical Chemistry*, 84(3):1708–1717.
- M. V. Gorshkov, L. Fornelli & Y. O. Tsybin (2012). Observation of ion coalescence in Orbitrap Fourier transform mass spectrometry. *Rapid Communications in Mass Spectrometry*, 26(15):1711–1717.
- M. Gros, M. Petrović & D. Barceló (2006). Development of a multi-residue analytical methodology based on liquid chromatography-tandem mass spectrometry (LC-MS/MS) for screening and trace level determination of pharmaceuticals in surface and wastewaters. *Talanta*, 70(4):678–690.
- M. Gros, M. Petrović & D. Barceló (2009). Tracing pharmaceutical residues of different therapeutic classes in environmental waters by using liquid chromatography/quadrupole-linear ion trap mass

- spectrometry and automated library searching. *Analytical Chemistry*, 81(3):898–912.
- M. Gros, S. Rodríguez-Mozaz & D. Barceló (2012). Fast and comprehensive multi-residue analysis of a broad range of human and veterinary pharmaceuticals and some of their metabolites in surface and treated waters by ultra-high-performance liquid chromatography coupled to quadrupole-linear ion trap tandem. *Journal of Chromatography A*, 1248:104–121.
- J. H. Gross (2011). *Mass Spectrometry - A textbook*. Springer, Berlin, Heidelberg, second edition.
- M. Grung, T. Källqvist, S. Sakshaug, S. Skurtveit & K. V. Thomas (2008). Environmental assessment of Norwegian priority pharmaceuticals based on the EMEA guideline. *Ecotoxicology and Environmental Safety*, 71(2):328–340.
- B. Halling-Sørensen, S. N. Nielsen, P. F. Lanzky, F. Ingerslav, H. C. Holten Lützhøft & S. E. Jørgenson (1998). Occurrence, fate and effects of pharmaceutical substances in the environment-A review. *Chemosphere*, 36(2):357–393.
- G. Hart-Smith & S. J. Blanksby (2012). Mass analysis. In *Mass Spectrometry in Polymer Chemistry*, pp. 5–32. Wiley-VCH Verlag GmbH & Co. KGaA, Weinheim, Germany.
- T. Heberer (2002). Occurrence, fate, and removal of pharmaceutical residues in the aquatic environment: a review of recent research data. *Toxicology letters*, 131(1-2):5–17.

- M. L. Hedgespeth, Y. Sapozhnikova, P. Pennington, A. Clum, A. Fairey & E. Wirth (2012). Pharmaceuticals and personal care products (PPCPs) in treated wastewater discharges into Charleston Harbor, South Carolina. *Science of the Total Environment*, 437:1–9.
- F. Hernández, L. Bijlsma, J. V. Sancho, R. Díaz & M. Ibáñez (2011). Rapid wide-scope screening of drugs of abuse, prescription drugs with potential for abuse and their metabolites in influent and effluent urban wastewater by ultrahigh pressure liquid chromatography-quadrupole-time-of-flight-mass spectrometry. *Analytica Chimica Acta*, 684(1-2):87–97.
- F. Hernández, J. V. Sancho, M. Ibáñez, E. Abad, T. Portolés & L. Mattioli (2012). Current use of high-resolution mass spectrometry in the environmental sciences. *Analytical and Bioanalytical Chemistry*, 403(5):1251–1264.
- M. D. Hernando, M. Mezcua, A. R. Fernández-Alba & D. Barceló (2006). Environmental risk assessment of pharmaceutical residues in wastewater effluents, surface waters and sediments. *Talanta*, 69(2):334–342.
- P. T. P. Hoa, S. Managaki, N. Nakada, H. Takada, A. Shimizu, D. H. Anh, P. H. Viet & S. Suzuki (2011). Antibiotic contamination and occurrence of antibiotic-resistant bacteria in aquatic environments of northern Vietnam. *Science of the Total Environment*, 409(15):2894–2901.
- B. Hoeger, B. Köllner, D. R. Dietrich & B. Hitzfeld (2005). Water-borne diclofenac affects kidney and gill integrity and selected

- immune parameters in brown trout (*Salmo trutta* f. *fario*). *Aquatic Toxicology*, 75(1):53–64.
- A. C. Hogenboom, J. A. van Leerdam & P. de Voogt (2009). Accurate mass screening and identification of emerging contaminants in environmental samples by liquid chromatography-hybrid linear ion trap Orbitrap mass spectrometry. *Journal of Chromatography A*, 1216(3):510–519.
- C. Hug, N. Ulrich, T. Schulze, W. Brack & M. Krauss (2014). Identification of novel micropollutants in wastewater by a combination of suspect and nontarget screening. *Environmental pollution*, 184:25–32.
- M. Ibáñez, C. Guerrero, J. V. Sancho & F. Hernández (2009). Screening of antibiotics in surface and wastewater samples by ultra-high-pressure liquid chromatography coupled to hybrid quadrupole time-of-flight mass spectrometry. *Journal of Chromatography A*, 1216(12):2529–2539.
- M. Ibáñez, J. V. Sancho, F. Hernández, D. Mcmillan & R. Rao (2008). Rapid non-target screening of organic pollutants in water by ultraperformance liquid chromatography coupled to time-of-light mass spectrometry. *Trends in Analytical Chemistry*, 27(5):481–489.
- S. Idder, L. Ley, P. Mazellier & H. Budzinski (2013). Quantitative on-line preconcentration-liquid chromatography coupled with tandem mass spectrometry method for the determination of pharmaceutical compounds in water. *Analytica Chimica Acta*, 805:107–115.

- M. Isidori, M. Lavorgna, A. Nardelli, L. Pascarella & A. Parrella (2005). Toxic and genotoxic evaluation of six antibiotics on non-target organisms. *Science of the Total Environment*, 346(1-3):87–98.
- A. Jia, Y. Wan, Y. Xiao & J. Hu (2012). Occurrence and fate of quinolone and fluoroquinolone antibiotics in a municipal sewage treatment plant. *Water Research*, 46(2):387–394.
- O. A. H. Jones, N. Voulvoulis & J. N. Lester (2002). Aquatic environmental assessment of the top 25 English prescription pharmaceuticals. *Water Research*, 36(20):5013–5022.
- S. E. Jørgenson & B. Halling-Sørensen (2000). Drugs in the environment. *Chemosphere*, 40:691–699.
- B. Kasprzyk-Hordern, R. M. Dinsdale & A. J. Guwy (2007). Multi-residue method for the determination of basic/neutral pharmaceuticals and illicit drugs in surface water by solid-phase extraction and ultra performance liquid chromatography-positive electrospray ionisation tandem mass spectrometry. *Journal of Chromatography A*, 1161(1-2):132–145.
- A. Kaufmann (2009). Validation of multiresidue methods for veterinary drug residues; related problems and possible solutions. *Analytica Chimica Acta*, 637(1-2):144–155.
- A. Kaufmann & P. Butcher (2006). Strategies to avoid false negative findings in residue analysis using liquid chromatography coupled to time-of-flight mass spectrometry. *Rapid Communications in Mass Spectrometry*, 20(23):3566–3572.

- A. Kaufmann, P. Butcher, K. Maden, S. Walker & M. Widmer (2010a). Comprehensive comparison of liquid chromatography selectivity as provided by two types of liquid chromatography detectors (high resolution mass spectrometry and tandem mass spectrometry): "where is the crossover point?". *Analytica Chimica Acta*, 673(1):60–72.
- A. Kaufmann, P. Butcher, K. Maden, S. Walker & M. Widmer (2011). Quantification of anthelmintic drug residues in milk and muscle tissues by liquid chromatography coupled to Orbitrap and liquid chromatography coupled to tandem mass spectrometry. *Talanta*, 85(2):991–1000.
- A. Kaufmann, P. Butcher, K. Maden & M. Widmer (2007). Ultra-performance liquid chromatography coupled to time-of-flight mass spectrometry (UPLC-TOF): a novel tool for multiresidue screening of veterinary drugs in urine. *Analytica Chimica Acta*, 586(1-2):13–21.
- A. Kaufmann, V. Dvorak, C. Crüzer, P. Butcher, K. Maden, S. Walker, M. Widmer & A. Schürmann (2012). Study of high-resolution mass spectrometry technology as a replacement for tandem mass spectrometry in the field of quantitative pesticide residue analysis. *Journal of AOAC International*, 95(2):528–548.
- A. Kaufmann & S. Walker (2012a). Accuracy of relative isotopic abundance and mass measurements in a single-stage orbitrap mass spectrometer. *Rapid Communications in Mass Spectrometry*, 26(9):1081–1090.

- A. Kaufmann & S. Walker (2012b). Post-run target screening strategy for ultra high performance liquid chromatography coupled to Orbitrap based veterinary drug residue analysis in animal urine. *Journal of Chromatography A*, 1292:104–110.
- A. Kaufmann & S. Walker (2013). Evaluation of the interrelationship between mass resolving power and mass error tolerances for targeted bioanalysis using liquid chromatography coupled to high-resolution mass spectrometry. *Rapid Communications in Mass Spectrometry*, 27(2):347–356.
- A. Kaufmann, M. Widmer & K. Maden (2010b). Post-interface signal suppression, a phenomenon observed in a single-stage Orbitrap mass spectrometer coupled to an electrospray interfaced liquid chromatograph. *Rapid Communications in Mass Spectrometry*, 24(14):2162–2170.
- M. Kellmann, H. Muenster, P. Zomer & H. Mol (2009). Full scan MS in comprehensive qualitative and quantitative residue analysis in food and feed matrices: How much resolving power is required? *Journal of the American Society for Mass Spectrometry*, 20(8):1464–1476.
- S. Kern, R. Baumgartner, D. E. Helbling, J. Hollender, H. P. Singer, M. J. Loos, R. P. Schwarzenbach & K. Fenner (2010). A tiered procedure for assessing the formation of biotransformation products of pharmaceuticals and biocides during activated sludge treatment. *Journal of environmental management*, 12(11):2100–2111.
- S. Kern, K. Fenner, H. P. Singer, R. P. Schwarzenbach & J. Hollender (2009). Identification of transformation products of organic

- contaminants in natural waters by computer-aided prediction and high-resolution mass spectrometry. *Environmental Science and Technology*, 43(18):7039–7046.
- K. O. K'oreje, K. Demeestere, P. De Wispelaere, L. Vergeynst, J. Dewulf & H. Van Langenhove (2012). From multi-residue screening to target analysis of pharmaceuticals in water: Development of a new approach based on magnetic sector mass spectrometry and application in the Nairobi River basin, Kenya. *Science of the Total Environment*, 437:153–164.
- T. Kosjek & E. Heath (2011). Occurrence, fate and determination of cytostatic pharmaceuticals in the environment. *Trends in Analytical Chemistry*, 30(7):1065–1087.
- L. Kovalova, C. S. McArdell & J. Hollender (2009). Challenge of high polarity and low concentrations in analysis of cytostatics and metabolites in wastewater by hydrophilic interaction chromatography/tandem mass spectrometry. *Journal of Chromatography A*, 1216(7):1100–1108.
- M. Krauss & J. Hollender (2008). Analysis of nitrosamines in wastewater: exploring the trace level quantification capabilities of a hybrid linear ion trap/orbitrap mass spectrometer. *Analytical Chemistry*, 80(3):834–842.
- M. Krauss, H. P. Singer & J. Hollender (2010). LC-high resolution MS in environmental analysis: from target screening to the identification of unknowns. *Analytical and Bioanalytical Chemistry*, 397(3):943–951.



- A. Kumar & I. Xagorarakis (2010). Pharmaceuticals, personal care products and endocrine-disrupting chemicals in U.S. surface and finished drinking waters: A proposed ranking system. *Science of the Total Environment*, 408(23):5972–5989.
- K. Kümmerer (2009a). Antibiotics in the aquatic environment - a review - part I. *Chemosphere*, 75(4):417–434.
- K. Kümmerer (2009b). Antibiotics in the aquatic environment - a review - part II. *Chemosphere*, 75(4):435–441.
- K. Kümmerer & A. Henninger (2003). Promoting resistance by the emission of antibiotics from hospitals and households into effluent. *Clinical Microbiology and Infection*, 9(12):1203–1214.
- M. H. Kutner, K. Neter, C. J. Nachtsheim & W. Li (1996). *Applied linear statistical models*. Irwin, Chicago, 4th edition.
- S. Lacorte & A. R. Fernández-Alba (2006). Time-of-flight mass spectrometry applied to the liquid chromatography analysis of pesticides in water and food. *Mass Spectrometry Reviews*, pp. 866–880.
- A. Lamm, I. Gozlan, A. Rotstein & D. Avisar (2009). Detection of amoxicillin-diketopiperazine-2', 5' in wastewater samples. *Journal of Environmental Science and Health Part A*, 44(14):1512–1517.
- D. Lapworth, N. Baran, M. Stuart & R. Ward (2012). Emerging organic contaminants in groundwater: A review of sources, fate and occurrence. *Environmental Pollution*, 163:287–303.

- P. A. Lara-Martín, E. González-Mazo & B. J. Brownawell (2011). Multi-residue method for the analysis of synthetic surfactants and their degradation metabolites in aquatic systems by liquid chromatography-time-of-flight-mass spectrometry. *Journal of Chromatography A*, 1218(30):4799–4807.
- D. G. J. Larsson, C. de Pedro & N. Paxéus (2007). Effluent from drug manufactures contains extremely high levels of pharmaceuticals. *Journal of Hazardous Materials*, 148(3):751–755.
- M. Lavén, T. Alsberg, Y. Yu, M. Adolffsson-Erici & H. Sun (2009). Serial mixed-mode cation- and anion-exchange solid-phase extraction for separation of basic, neutral and acidic pharmaceuticals in wastewater and analysis by high-performance liquid chromatography-quadrupole time-of-flight mass spectrometry. *Journal of Chromatography A*, 1216(1):49–62.
- K. S. Le Corre, C. Ort, D. Kateley, B. Allen, B. I. Escher & J. Keller (2012). Consumption-based approach for assessing the contribution of hospitals towards the load of pharmaceutical residues in municipal wastewater. *Environment International*, 45C:99–111.
- Z. Li, M. P. Maier & M. Radke (2013). Screening for pharmaceutical transformation products formed in river sediment by combining ultrahigh performance liquid chromatography/high resolution mass spectrometry with a rapid data-processing method. *Analytica Chimica Acta*, 810:61–70.
- A. Lommen, G. van der Weg, M. C. van Engelen, G. Bor, L. A. P. Hoogenboom & M. W. F. Nielen (2007). An untargeted metabolomics

- approach to contaminant analysis: pinpointing potential unknown compounds. *Analytica Chimica Acta*, 584(1):43–49.
- R. Loos, B. M. Gawlik, G. Locoro, E. Rimaviciute, S. Contini & G. Bidoglio (2009). EU-wide survey of polar organic persistent pollutants in European river waters. *Environmental pollution*, 157(2):561–568.
- A. Makarov, E. Denisov, O. Lange & S. Horning (2006). Dynamic range of mass accuracy in LTQ Orbitrap hybrid mass spectrometer. *Journal of the American Society for Mass Spectrometry*, 17(7):977–982.
- R. F. Mankes & C. D. Silver (2013). Quantitative study of controlled substance bedside wasting, disposal and evaluation of potential ecologic effects. *Science of the Total Environment*, 444:298–310.
- A. G. Marshall & C. L. Hendrickson (2008). High-resolution mass spectrometers. *Annual Review of Analytical Chemistry*, 1:579–599.
- J. Martín, W. Buchberger, J. L. Santos, E. Alonso & I. Aparicio (2012). High-performance liquid chromatography quadrupole time-of-flight mass spectrometry method for the analysis of antidiabetic drugs in aqueous environmental samples. *Journal of Chromatography B*, 895-896:94–101.
- M. J. Martínez Bueno, M. M. Ulaszewska, M. J. Gomez, M. D. Hernando & A. R. Fernández-Alba (2012). Simultaneous measurement in mass and mass/mass mode for accurate qualitative and quantitative screening analysis of pharmaceuticals in river water. *Journal of Chromatography A*, 1256:80–88.

- A. Masiá, M. Ibáñez, C. Blasco, J. V. Sancho, Y. Picó & F. Hernández (2013). Combined use of liquid chromatography triple quadrupole mass spectrometry and liquid chromatography quadrupole time-of-flight mass spectrometry in systematic screening of pesticides and other contaminants in water samples. *Analytica Chimica Acta*, 761:117–127.
- B. K. Matuszewski, M. L. Constanzer & C. M. Chavez-Eng (2003). Strategies for the assessment of matrix effect in quantitative bioanalytical methods based on HPLC-MS/MS. *Analytical Chemistry*, 75(13):3019–3030.
- C. D. Metcalfe, S. Kleywegt, R. J. Letcher, E. Topp, P. Wagh, V. L. Trudeau & T. W. Moon (2013). A multi-assay screening approach for assessment of endocrine-active contaminants in wastewater effluent samples. *Science of the Total Environment*, 454-455:132–140.
- I. Michael, L. Rizzo, C. S. McArdell, C. M. Manaia, C. Merlin, T. Schwartz, C. Dagot & D. Fatta-Kassinos (2013). Urban wastewater treatment plants as hotspots for the release of antibiotics in the environment: a review. *Water Research*, 47(3):957–995.
- C. Miège, J. M. Choubert, L. Ribeiro, M. Eusèbe & M. Coquery (2008). Removal efficiency of pharmaceuticals and personal care products with varying wastewater treatment processes and operating conditions - conception of a database and first results. *Water Science and Technology*, 57(1):49–56.

- B. L. Milman & L. A. Konopelko (2000). Identification of chemical substances by testing and screening of hypotheses. I. General. *Fresenius' Journal of Analytical Chemistry*, 367(7):621–628.
- L. Minguez, E. Farcy, C. Ballandonne, A. Lepailleur, A. Serpentine, J.-M. Lebel, R. Bureau & M.-P. Halm-Lemeille (2014). Acute toxicity of 8 antidepressants: What are their modes of action? *Chemosphere*, 108:314–319.
- H. G. J. Mol, P. Zomer & M. de Koning (2012). Qualitative aspects and validation of a screening method for pesticides in vegetables and fruits based on liquid chromatography coupled to full scan high resolution (Orbitrap) mass spectrometry. *Analytical and Bioanalytical Chemistry*, 403(10):2891–2908.
- S. Mompelat, A. Jaffrezic, E. Jardé & B. Le Bot (2013). Storage of natural water samples and preservation techniques for pharmaceutical quantification. *Talanta*, 109:31–45.
- B. Morasch, F. Bonvin, H. Reiser, D. Grandjean, L. F. de Alencastro, C. Perazzolo, N. Chèvre & T. Kohn (2010). Occurrence and fate of micropollutants in the Vidy Bay of Lake Geneva, Switzerland. Part II: micropollutant removal between wastewater and raw drinking water. *Environmental Toxicology and Chemistry*, 29(8):1658–1668.
- C. Moschet, A. Piazzoli, H. P. Singer & J. Hollender (2013). Alleviating the reference standard dilemma using a systematic exact mass suspect screening approach with liquid chromatography-high resolution mass spectrometry. *Analytical Chemistry*, 85(21):10312–10320.

- A. Müller, W. Schulz, W. K. L. Ruck & W. H. Weber (2011). A new approach to data evaluation in the non-target screening of organic trace substances in water analysis. *Chemosphere*, 85:1211–1219.
- M. W. F. Nielen, M. C. van Engelen, R. Zuiderent & R. Ramaker (2007). Screening and confirmation criteria for hormone residue analysis using liquid chromatography accurate mass time-of-flight, Fourier transform ion cyclotron resonance and orbitrap mass spectrometry techniques. *Analytica Chimica Acta*, 586(1-2):122–129.
- J. Nurmi & J. Pellinen (2011). Multiresidue method for the analysis of emerging contaminants in wastewater by ultra performance liquid chromatography-time-of-flight mass spectrometry. *Journal of Chromatography A*, 1218(38):6712–6719.
- J. Nurmi, J. Pellinen & A.-L. Rantalainen (2012). Critical evaluation of screening techniques for emerging environmental contaminants based on accurate mass measurements with time-of-flight mass spectrometry. *Journal of Mass Spectrometry*, 47(3):303–312.
- T. O'Brien (2002). Emergence, spread, and environmental effect of antimicrobial resistance: How use of an antimicrobial anywhere can increase resistance to any antimicrobial anywhere else. *Clinical Infectious Diseases*, 34(Suppl 3):S78–84.
- L. P. Padhye, H. Yao, F. T. Kung'u & C.-H. Huang (2014). Year-long evaluation on the occurrence and fate of pharmaceuticals, personal care products, and endocrine disrupting chemicals in an urban drinking water treatment plant. *Water Research*, 51:266–276.

*Bibliography*

- A. Pal, Y. He, M. Jekel, M. Reinhard & K. Y.-H. Gin (2014). Emerging contaminants of public health significance as water quality indicator compounds in the urban water cycle. *Environment International*, 71:46–62.
- F. T. Peters, O. H. Drummer & F. Musshoff (2007). Validation of new methods. *Forensic Science International*, 165(2-3):216–224.
- B. Petrie, E. J. McAdam, M. D. Scrimshaw, J. N. Lester & E. Cartmell (2013). Fate of drugs during wastewater treatment. *Trends in Analytical Chemistry*, 49:145–159.
- M. Petrović & D. Barceló (2006). Application of liquid chromatography/quadrupole time-of-flight mass spectrometry ( LC-QqTOF-MS ) in the environmental analysis. *Journal of Mass Spectrometry*, pp. 1259–1267.
- M. Petrović, M. Gros & D. Barceló (2006). Multi-residue analysis of pharmaceuticals in wastewater by ultra-performance liquid chromatography-quadrupole-time-of-flight mass spectrometry. *Journal of Chromatography A*, 1124(1-2):68–81.
- Y. Picó, M. Farré, C. Soler & D. Barceló (2007). Identification of unknown pesticides in fruits using ultra-performance liquid chromatography-quadrupole time-of-flight mass spectrometry. Imazalil as a case study of quantification. *Journal of Chromatography A*, 1176(1-2):123–134.
- O. J. Pozo, C. Guerrero, J. V. Sancho, M. Ibáñez, E. Pitarch, E. A. Hogendoorn & F. Hernández (2006). Efficient approach for the

- reliable quantification and confirmation of antibiotics in water using on-line solid-phase extraction liquid chromatography/tandem mass spectrometry. *Journal of Chromatography A*, 1103(1):83–93.
- C. Prasse, M. P. Schlüsener, R. Schulz & T. A. Ternes (2010). Antiviral drugs in wastewater and surface waters: a new pharmaceutical class of environmental relevance? *Environmental Science and Technology*, 44(5):1728–1735.
- R Development Core Team (2008). *R: A Language and Environment for Statistical Computing*. R Foundation for Statistical Computing, Vienna, Austria. URL <http://www.R-project.org>.
- A. E. Raftery & N. Dean (2006). Variable selection for model-based clustering. *Journal of the American Statistical Association*, 101(473):168–178.
- S. D. Richardson (2012). Environmental mass spectrometry: emerging contaminants and current issues. *Analytical Chemistry*, 84(2):747–778.
- S. D. Richardson & T. A. Ternes (2009). Water analysis: emerging contaminants and current issues. *Analytical Chemistry*, 81:4645–4677.
- S. D. Richardson & T. A. Ternes (2011). Water analysis: emerging contaminants and current issues. *Analytical Chemistry*, 83(12):4614–4648.
- S. D. Richardson & T. A. Ternes (2014). Water analysis: emerging contaminants and current issues. *Analytical Chemistry*, 86(6):2813–2848.



- L. Rimoldini (2014). Weighted skewness and kurtosis unbiased by sample size and Gaussian uncertainties. *Astronomy and Computing*, 5:1–8.
- J. Rivera-Utrilla, M. Sánchez-Polo, M. A. Ferro-García, G. Prados-Joya & R. Ocampo-Pérez (2013). Pharmaceuticals as emerging contaminants and their removal from water. A review. *Chemosphere*, 93(7):1268–1287.
- L. Rizzo, C. Manaia, C. Merlin, T. Schwartz, C. Dagot, M. C. Ploy, I. Michael & D. Fatta-Kassinos (2013). Urban wastewater treatment plants as hotspots for antibiotic resistant bacteria and genes spread into the environment: A review. *Science of the Total Environment*, 447C:345–360.
- J. Rockström, W. Steffen & K. Noone (2009). A safe operating space for humanity. *Nature*, 461(September):472–475.
- M. Roth (2013). On the multivariate t distribution. Technical Report 3059, Linköping University Electronic Press. URL <http://liu.diva-portal.org/smash/get/diva2:618567/FULLTEXT02.pdf>.
- V. G. Samaras, A. S. Stasinakis, D. Mamais, N. S. Thomaidis & T. D. Lekkas (2013). Fate of selected pharmaceuticals and synthetic endocrine disrupting compounds during wastewater treatment and sludge anaerobic digestion. *Journal of Hazardous Materials*, 244-245:259–267.
- J. V. Sancho, O. J. Pozo, M. Ibáñez & F. Hernández (2006). Potential of liquid chromatography/time-of-flight mass spectrometry for the

- determination of pesticides and transformation products in water. *Analytical and Bioanalytical Chemistry*, 386(4):987–997.
- H. Sanderson, D. J. Johnson, T. Reitsma, R. A. Brain, C. J. Wilson & K. R. Solomon (2004). Ranking and prioritization of environmental risks of pharmaceuticals in surface waters. *Regulatory Toxicology and Pharmacology*, 39(2):158–183.
- L. H. M. L. M. Santos, A. N. Araújo, A. Fachini, A. Pena, C. Delerue-Matos & M. C. B. S. M. Montenegro (2010). Ecotoxicological aspects related to the presence of pharmaceuticals in the aquatic environment. *Journal of Hazardous Materials*, 175(1-3):45–95.
- L. H. M. L. M. Santos, M. Gros, S. Rodriguez-Mozaz, C. Delerue-Matos, A. Pena, D. Barceló & M. C. B. S. M. Montenegro (2013). Contribution of hospital effluents to the load of pharmaceuticals in urban wastewaters: Identification of ecologically relevant pharmaceuticals. *Science of the Total Environment*, 461-462:302–316.
- A. K. Sarmah, M. T. Meyer & A. B. A. Boxall (2006). A global perspective on the use, sales, exposure pathways, occurrence, fate and effects of veterinary antibiotics (VAs) in the environment. *Chemosphere*, 65(5):725–759.
- M. Schriks, M. B. Heringa, M. M. E. van der Kooi, P. de Voogt & A. P. van Wezel (2010). Toxicological relevance of emerging contaminants for drinking water quality. *Water Research*, 44(2):461–476.
- B. W. Schwab, E. P. Hayes, J. M. Fiori, F. J. Mastrocco, N. M. Roden, D. Cragin, R. D. Meyerhoff, V. J. D'Aco & P. D. Anderson (2005).

- Human pharmaceuticals in US surface waters: a human health risk assessment. *Regulatory Toxicology and Pharmacology*, 42(3):296–312.
- E. Schymanski & H. Singer (2014). Strategies to characterize polar organic contamination in wastewater: Exploring the capability of high resolution mass spectrometry. *Environmental Science and Technology*, 48:1811–1818.
- P. A. Segura, M. François, C. Gagnon & S. Sauvé (2009). Review of the occurrence of anti-infectives in contaminated wastewaters and natural and drinking waters. *Environmental Health Perspectives*, 117(5):675–684.
- B. F. D. Silva, A. Jelic, R. López-Serna, A. A. Mozeto, M. Petrović & D. Barceló (2011). Occurrence and distribution of pharmaceuticals in surface water, suspended solids and sediments of the Ebro river basin, Spain. *Chemosphere*, 85(8):1331–1339.
- W.-J. Sim, J.-W. Lee & J.-E. Oh (2010). Occurrence and fate of pharmaceuticals in wastewater treatment plants and rivers in Korea. *Environmental pollution*, 158(5):1938–1947.
- K. Skrášková, L. H. M. L. M. Santos, D. Satínský, A. Pena, M. C. B. S. M. Montenegro, P. Solich & L. Nováková (2013). Fast and sensitive UHPLC methods with fluorescence and tandem mass spectrometry detection for the determination of tetracycline antibiotics in surface waters. *Journal of Chromatography B*, 927:201–208.
- N. Sokkalingam, S. Ashrafi, L. Schneider, A. Tenderholt, W. Wright, F. Way, P. Alto, T. Cajka & O. Fiehn (2014). PeakInvestigator:

- Software to improve the precision, resolution, and sensitivity of your mass analyzer. In *American Society for Mass Spectrometry*.
- P. E. Stackelberg, E. T. Furlong, M. T. Meyer, S. D. Zaugg, A. K. Henderson & D. B. Reissman (2004). Persistence of pharmaceutical compounds and other organic wastewater contaminants in a conventional drinking-water-treatment plant. *Science of the Total Environment*, 329(1-3):99–113.
- H. Stahnke, T. Reemtsma & L. Alder (2009). Compensation of matrix effects by postcolumn infusion of a monitor substance in multiresidue analysis with LC-MS/MS. *Analytical Chemistry*, 81(6):2185–2192.
- R. Tautenhahn, C. Böttcher & S. Neumann (2008). Highly sensitive feature detection for high resolution LC/MS. *BMC Bioinformatics*, 9:504.
- T. L. ter Laak, M. van der Aa, C. J. Houtman, P. G. Stoks & A. P. van Wezel (2010). Relating environmental concentrations of pharmaceuticals to consumption: A mass balance approach for the river Rhine. *Environment International*, 36(5):403–409.
- S. Terzic & M. Ahel (2011). Nontarget analysis of polar contaminants in freshwater sediments influenced by pharmaceutical industry using ultra-high-pressure liquid chromatography-quadrupole time-of-flight mass spectrometry. *Environmental pollution*, 159(2):557–566.
- K. V. Thomas, M. R. Hurst, P. Matthiessen & M. J. Waldock (2001). Characterization of estrogenic compounds in water samples collected from United Kingdom estuaries. *Environmental Toxicology and Chemistry*, 20(10):2165–2170.

- A. Y. C. Tong, B. M. Peake & R. Braund (2011). Disposal practices for unused medications in New Zealand community pharmacies. *Journal of Primary Health Care*, 3(3):197–203.
- E. Touraud, B. Roig, J. P. Sumpter & C. Coetsier (2011). Drug residues and endocrine disruptors in drinking water: risk for humans? *International Journal of Hygiene and Environmental Health*, 214(6):437–441.
- N. Ulrich, G. Schüürmann & W. Brack (2011). Linear Solvation Energy Relationships as classifiers in non-target analysis—a capillary liquid chromatography approach. *Journal of Chromatography A*, 1218(45):8192–8196.
- United States Environmental Protection Agency (2009). Drinking Water Contaminant List 3. *Federal Register*, 74(194):51850–51862.
- Y. Valcárcel, S. González Alonso, J. L. Rodríguez-Gil, A. Gil & M. Catalá (2011). Detection of pharmaceutically active compounds in the rivers and tap water of the Madrid Region (Spain) and potential ecotoxicological risk. *Chemosphere*, 84(10):1336–1348.
- M. van der Aa, L. Bijlsma, E. Emke, E. Dijkman, A. L. N. van Nuijs, B. van de Ven, F. Hernández, A. Versteegh & P. de Voogt (2013). Risk assessment for drugs of abuse in the Dutch watercycle. *Water Research*, 47(5):1848–1857.
- E. van der Heeft, Y. J. C. Bolck, B. Beumer, A. W. J. M. Nijrolder, A. A. M. L. Stolker & M. W. F. Nielen (2009). Full-scan accurate mass selectivity of ultra-performance liquid chromatography combined

- with time-of-flight and orbitrap mass spectrometry in hormone and veterinary drug residue analysis. *Journal of the American Society for Mass Spectrometry*, 20(3):451–463.
- X. Van Doorslaer, J. Dewulf, H. Van Langenhove & K. Demeestere (2014a). Fluoroquinolone antibiotics: An emerging class of environmental micropollutants. *Science of the Total Environment*, 500-501:250–269.
- X. Van Doorslaer, I. D. Haylamicheal, J. Dewulf, H. Van Langenhove, C. R. Janssen & K. Demeestere (2014b). Heterogeneous photocatalysis of moxifloxacin in water: Chemical transformation and ecotoxicity. *Chemosphere*, (in press.).
- J. A. van Leerdam, A. C. Hogenboom, M. M. van der Kooi & P. de Voogt (2009). Determination of polar 1H-benzotriazoles and benzothiazoles in water by solid-phase extraction and liquid chromatography LTQ FT Orbitrap mass spectrometry. *International Journal of Mass Spectrometry*, 282(3):99–107.
- J. Van Loco, A. János, S. Impens, S. Fraselle, V. Cornet & J. M. Degroodt (2007). Calculation of the decision limit (CC $\alpha$ ) and the detection capability (CC $\beta$ ) for banned substances: the imperfect marriage between the quantitative and the qualitative criteria. *Analytica Chimica Acta*, 586(1-2):8–12.
- P. Vazquez-Roig, V. Andreu, C. Blasco & Y. Picó (2012). Risk assessment on the presence of pharmaceuticals in sediments, soils and waters of the Pego-Oliva Marshlands (Valencia, eastern Spain). *Science of the Total Environment*, 440:24–32.

- P. Verlicchi, M. Al Aukidy & E. Zambello (2012). Occurrence of pharmaceutical compounds in urban wastewater: Removal, mass load and environmental risk after a secondary treatment - A review. *Science of the Total Environment*, 429:123–155.
- C. Walgraeve, K. Demeestere, P. De Wispelaere, J. Dewulf, J. Lintelmann, K. Fischer & H. Van Langenhove (2012). Selective accurate-mass-based analysis of 11 oxy-PAHs on atmospheric particulate matter by pressurized liquid extraction followed by high-performance liquid chromatography and magnetic sector mass spectrometry. *Analytical and Bioanalytical Chemistry*, 402(4):1697–1711.
- H.-X. Wang, Y. Zhou & Q.-W. Jiang (2012). Simultaneous screening of estrogens, progestogens, and phenols and their metabolites in potable water and river water by ultra-performance liquid chromatography coupled with quadrupole time-of-flight mass spectrometry. *Microchemical Journal*, 100:83–94.
- X.-H. Wang & A. Y.-C. Lin (2014). Is the phototransformation of pharmaceuticals a natural purification process that decreases ecological and human health risks? *Environmental Pollution*, 186:203–215.
- Waterbouwkundig Laboratorium Belgium (2013). Hydrologisch informatiecentrum. URL [www.waterstanden.be](http://www.waterstanden.be).
- A. J. Watkinson, E. J. Murby, D. W. Kolpin & S. D. Costanzo (2009). The occurrence of antibiotics in an urban watershed: from wastewater

- to drinking water. *Science of the Total Environment*, 407(8):2711–2723.
- K. Web, T. Bristow, M. Sargent & B. Stein (2004). *Methodology for Accurate Mass Measurement of Small Molecules, Best Practice Guide*. LGC Limited.
- X. Wei, X. Shi, S. Kim, J. S. Patrick, J. Binkley, M. Kong, C. McClain & X. Zhang (2014). Data dependent peak model based spectrum deconvolution for analysis of high resolution LC-MS data. *Analytical Chemistry*, 86(4):2156–2165.
- J. M. Weiss, E. Simon, G. J. Stroomberg, R. de Boer, J. de Boer, S. C. van der Linden, P. E. G. Leonards & M. H. Lamoree (2011). Identification strategy for unknown pollutants using high-resolution mass spectrometry: androgen-disrupting compounds identified through effect-directed analysis. *Analytical and Bioanalytical Chemistry*, 400(9):3141–3149.
- K. Wille, M. Claessens, K. Rappé, E. Monteyne, C. R. Janssen, H. F. De Brabander & L. Vanhaecke (2011a). Rapid quantification of pharmaceuticals and pesticides in passive samplers using ultra high performance liquid chromatography coupled to high resolution mass spectrometry. *Journal of Chromatography A*, 1218(51):9162–9173.
- K. Wille, J. A. L. Kiebooms, M. Claessens, K. Rappé, J. Vanden Bussche, H. Noppe, N. Van Praet, E. De Wulf, P. Van Caeter, C. R. Janssen, H. F. De Brabander & L. Vanhaecke (2011b). Development of analytical strategies using U-HPLC-MS/MS and LC-ToF-MS for



- the quantification of micropollutants in marine organisms. *Analytical and Bioanalytical Chemistry*, 400(5):1459–1472.
- K. Wille, H. Noppe, K. Verheyden, J. Vanden Bussche, E. De Wulf, P. Van Caeter, C. R. Janssen, H. F. De Brabander & L. Vanhaecke (2010). Validation and application of an LC-MS/MS method for the simultaneous quantification of 13 pharmaceuticals in seawater. *Analytical and Bioanalytical Chemistry*, 397(5):1797–1808.
- F. Wode, C. Reilich, P. Van Baar, U. Dünnbier, M. Jekel & T. Reemtsma (2012). Multiresidue analytical method for the simultaneous determination of 72 micropollutants in aqueous samples with ultra high performance liquid chromatography-high resolution mass spectrometry. *Journal of Chromatography A*, 1270:118–126.
- S. Wolf, S. Schmidt, M. Müller-Hannemann & S. Neumann (2010). In silico fragmentation for computer assisted identification of metabolite mass spectra. *BMC Bioinformatics*, 11:148.
- J.-C. Wolff, T. R. Fuentes & J. Taylor (2003). Investigations into the accuracy and precision obtainable on accurate mass measurements on a quadrupole orthogonal acceleration time-of-flight mass spectrometer using liquid chromatography as sample introduction. *Rapid Communications in Mass Spectrometry*, 17(11):1216–1219.
- Y.-Q. Xia, J. Lau, T. Olah & M. Jemal (2011). Targeted quantitative bioanalysis in plasma using liquid chromatography/high-resolution accurate mass spectrometry: an evaluation of global selectivity as a function of mass resolving power and extraction window, with

- comparison of centroid and profile mo. *Rapid Communications in Mass Spectrometry*, 25(19):2863–2878.
- Y. Xiao, H. Chang, A. Jia & J. Hu (2008). Trace analysis of quinolone and fluoroquinolone antibiotics from wastewaters by liquid chromatography-electrospray tandem mass spectrometry. *Journal of Chromatography A*, 1214(1-2):100–108.
- H. Yamamoto, Y. Nakamura, S. Moriguchi, Y. Nakamura, Y. Honda, I. Tamura, Y. Hirata, A. Hayashi & J. Sekizawa (2009). Persistence and partitioning of eight selected pharmaceuticals in the aquatic environment: laboratory photolysis, biodegradation, and sorption experiments. *Water Research*, 43(2):351–362.
- Yiruhan, Q.-J. Wang, C.-H. Mo, Y.-W. Li, P. Gao, Y.-P. Tai, Y. Zhang, Z.-L. Ruan & J.-W. Xu (2010). Determination of four fluoroquinolone antibiotics in tap water in Guangzhou and Macao. *Environmental Pollution*, 158(7):2350–2358.
- M. Zedda & C. Zwiener (2012). Is nontarget screening of emerging contaminants by LC-HRMS successful? A plea for compound libraries and computer tools. *Analytical and Bioanalytical Chemistry*, 403(9):2493–2502.
- A. Zenker, M. R. Cicero, F. Prestinaci, P. Bottoni & M. Carere (2014). Bioaccumulation and biomagnification potential of pharmaceuticals with a focus to the aquatic environment. *Journal of environmental management*, 133:378–387.
- R. A. Zubarev & A. Makarov (2013). Orbitrap mass spectrometry. *Analytical Chemistry*, 85(11):5288–5296.

*Bibliography*

- E. Zuccato, S. Castiglioni, R. Bagnati, M. Melis & R. Fanelli (2010). Source, occurrence and fate of antibiotics in the Italian aquatic environment. *Journal of Hazardous Materials*, 179(1-3):1042–1048.

# Curriculum Vitae

## Personal Information

Leendert Vergeynst

Date of birth: 25<sup>th</sup> of July 1987

Place of birth: Ronse

Address: Stuivenberg 19, 9570 Lierde, Belgium

Telephone: +32 498 84 20 70

Email: Leendert.Vergeynst@ugent.be

## Areas of Expertise

- **Analytical organic chemistry:** quantitative analysis and screening towards micropollutants Keywords: high-resolution mass spectrometry, liquid chromatography, solid-phase extraction, pressurized liquid extraction
- **Environmental fate of micropollutants** in the aquatic environment and wastewater treatment plants

- **Model development** using WEST software (Word wide Engine for Simulation, Training and automation)

## Education

- 2011-2015 PhD in bioscience engineering, Screening and quantification of pharmaceutical residues in aquatic environments using high-resolution mass spectrometry, promotor: prof. dr. ir. Kristof Demeestere  
Doctoral school of bioscience engineering, Faculty of Bioscience Engineering, Ghent University, Belgium
- 2005-2010 Bachelor and master in bioscience engineering, environmental technology, Faculty of Bioscience Engineering, Ghent University, Belgium  
Thesis: Methods for measuring and modelling *Escherichia coli* in stormwater ponds. promotor: prof. dr. ir. Peter Vanrolleghem

## Scientific awards

- **Poster Presentation Prize:** Modelling pathogen fate in stormwaters by a particle-pathogen interaction model using population balances. In: Proceedings 6th IWA International Conference on Sewer Processes and Networks (SPN6). Surfers Paradise, Gold Coast, Australia, November 7-10 2010
- **Best Presentation Award:** Multi-residue analysis of pharmaceutical in Belgian surface water: a novel screening-to-quantification approach using large-volume injection liquid chromatography coupled to high-resolution mass spectrometry.

In: Proceedings 3rd Regional Conference Yong Water Professionals Benelux IWA, Belval, Luxemburg, October 2-4 2013

## **Publications**

### **First author of 4 A1 publications**

- Vergeynst L, Van Langenhove H, Demeestere K (2015) Multi-residue analysis of pharmaceuticals in wastewater treatment: method quality assessment and application in a Belgian case study. *Chemosphere* 119:S2-S8.
- Vergeynst L, Van Langenhove H, Joos P, Demeestere K (2014) Suspect screening and target quantification of multi-class pharmaceuticals in surface water based on large-volume injection liquid chromatography and time-of-flight mass spectrometry. *Analytical and Bioanalytical Chemistry* 406:2533-2547
- Vergeynst L, Van Langenhove H, Joos P, Demeestere K (2013) Accurate mass determination, quantification and determination of detection limits in liquid chromatography-high-resolution time-of-flight mass spectrometry: Challenges and practical solutions. *Analytica Chimica Acta* 789:74-82
- K'oreje KO, Demeestere K, De Wispelaere P, Vergeynst L, Dewulf J, Van Langenhove H (2012) From multi-residue screening to target analysis of pharmaceuticals in water: Development of a new approach based on magnetic sector mass spectrometry and

application in the Nairobi River basin, Kenya. *Science of the Total Environment* 437:153-164

- Vergeynst L, Vallet B, Vanrolleghem PA (2012) Modeling pathogen fate in stormwaters by a particle-pathogen interaction model using population balances. *Water Science and Technology* 65(5):823-32

## Scientific activities

### 5 conferences presentations

- 38th International Symposium on Environmental Analytical Chemistry, Lausanne, Switzerland, June 17-20 2014. (Oral contribution)
- 3rd Regional Conference Yong Water Professionals Benelux IWA, Belval, Luxemburg, October 2-4 2013. (Oral contribution)
- 13th International conference on Environmental Science and Technology, Athens, Greece, September 5-7, 2013. (Oral contribution)
- EuCheMS International Conference on Chemistry and the Environment, Barcelona, Spain, June 25-20 2013. (Oral contribution)
- 18th National symposium on Applied Biological Sciences, Ghent, Belgium, February 8 2013. (Oral contribution)

- 2nd IWA/WEF Wastewater Treatment Modelling Seminar, Mont-Sainte-Anne, Quebec, Canada, March 28-30 2010. (Passive contribution)
- CEDA Dredging Days - Dredging facing sustainability, Antwerp, Belgium, October 1-3 2008. (Passive contribution)

## Teaching activities

- Teaching 6 practical exercises of courses at the Faculty of Bioscience Engineering: Analysis and abatement of air pollution (prof. H. Van Langenhove); Environmental technology: theoretical exercises (prof. H. Van Langenhove); Analysis of organic micropollutants: practicum mass spectrometry, practicum solid-phase microextraction and advise assignment about analysis of organic micropollutants (prof. K. Demeestere); Chemical analysis techniques: practicum qualitative gas chromatography (prof. K. Demeestere)
- Tutor of 1 Master student Bio-science Engineering, 3 Master students Environmental Sanitation, 4 Bachelor students Bio-science Engineering, and 1 Bachelor student Chemistry and Environment (Kaho Sint-Lieven, Department Ghent)